Receptores Monoaminérgicos en Corteza Prefrontal: Mecanismo de Acción de Fármacos Antipsicóticos

Tesis Doctoral presentada por

Noemí Santana Ramos

Barcelona, julio de 2007

Trabajo 1

Expression of Serotonin1A and Serotonin2A Receptors in Pyramidal and GABAergic Neurons of the Rat Prefrontal Cortex.

Santana N, Bortolozzi A, Serrats J, Mengod G and Artigas F

Cerebral Cortex 14, 1100–1109 (2004)

En este trabajo se muestra que una gran proporción (entre un 40 y un 80%, dependiendo del área cortical) de neuronas glutamatérgicas de la CPF expresan el ARNm tanto del receptor serotoninérgico 5-HT_{1A} como del 5-HT_{2A}. Para la identificación inequívoca de estas neuronas se utilizó el transportador vesicular de glutamato vGluT1, considerado como marcador específico de este tipo neuronal en corteza. El presente estudio muestra asimismo que el ARNm de receptores 5-HT_{1A} y 5-HT_{2A} se encuentra presente en todas las regiones de la pared medial de la corteza prefrontal (infralímbica, prelímbica, cingulada y motora secundaria) tanto en capas superficiales como profundas, siendo el 5-HT_{1A} más abundante en capas profundas (V-VI) y el 5HT_{2A} en capas más superficiales (III-V). Nuestros datos también indican una modulación serotoninérgica de las neuronas GABAérgicas de corteza prefrontal a través de los receptores 5HT_{1A} y 5HT_{2A}. El ARNm de los receptores 5-HT_{1A} y 5-HT_{2A} se expresa en un 10-30% de las interneuronas GABAérgicas de las diferentes áreas de la corteza prefrontal medial, a excepción del 5-HT_{2A} en capa VI, donde este receptor se expresa en menor proporción.

Expression of Serotonin$_{1A}$ and Serotonin$_{2A}$ Receptors in Pyramidal and GABAergic Neurons of the Rat Prefrontal Cortex

Noemí Santana, Analía Bortolozzi, Jordi Serrats, Guadalupe Mengod and Francesc Artigas

Department of Neurochemistry, Institut d'Investigacions Biomèdiques de Barcelona (CSIC), IDIBAPS, 08036 Barcelona, Spain

Serotonergic 5-HT$_{1A}$ and 5-HT$_{2A}$ receptors are abundantly expressed in prefrontal cortex (PFC) and are targets of atypical antipsychotic drugs. They mediate, respectively, inhibitory and excitatory actions of 5-HT. The transcripts for both receptors are largely (~80%) colocalized in rat and mouse PFC, yet their quantitative distribution in pyramidal and GABAergic interneurons is unknown. We used double *in situ* hybridization histochemistry to estimate the proportion of pyramidal and GABAergic neurons expressing these receptor transcripts in rat PFC. The number of GABAergic interneurons (expressing GAD mRNA) was a 22% of glutamatergic neurons (expressing vGluT1 mRNA, considered as putative pyramidal neurons). 5-HT$_{2A}$ receptor mRNA was present in a large percentage of pyramidal neurons (from 55% in prelimbic cortex to 88% in tenia tecta), except in layer VI, where it was localized only in 30% of those neurons. 5-HT$_{2A}$ receptor mRNA was present in ~25% of GAD-containing cells except in layer VI (10%). Likewise, ~60% of glutamatergic cells contained the 5-HT$_{1A}$ receptor transcript. We also found that ~25% of GAD-expressing cells contained the 5-HT$_{1A}$ receptor mRNA. These data help to clarify the role of 5-HT in prefrontal circuits and shed new light to the cellular elements involved in the action of atypical antipsychotics.

Keywords: 5-HT$_{1A}$ receptors, 5-HT$_{2A}$ receptors, GABA interneurons, medial prefrontal cortex, pyramidal neurons

Introduction

The prefrontal cortex receives a moderate to dense serotonergic innervation from the raphe nuclei (Azmitia and Segal, 1978; Steinbusch, 1981; Blue *et al.*, 1988) and contains several serotonin (5-hydroxytryptamine, 5-HT) receptor subtypes, with a particularly high density of 5-HT$_{1A}$ and 5-HT$_{2A}$ receptors (Pazos and Palacios, 1985; Pazos *et al.*, 1985; Pompeiano *et al.*, 1992, 1994). Immunohistochemical studies have revealed the presence of 5-HT$_{1A}$ and 5-HT$_{2A}$ receptors in cortical pyramidal neurons (Kia *et al.*, 1996; Willins *et al.*, 1997; Jakab and Goldman-Rakic, 1998, 2000; Cornea-Hébert *et al.*, 1999; De Felipe *et al.*, 2001; Martín-Ruiz *et al.*, 2001) and of 5-HT$_{2A}$ receptors in GABAergic interneurons (Willins *et al.*, 1997; Jakab and Goldman-Rakic, 2000). Recent immunohistochemical studies also suggest the presence of 5-HT$_{1A}$ receptors in nearly all calbindin- and parvalbumin-positive neurons (Aznar *et al.*, 2003).

5-HT$_{1A}$ and 5-HT$_{2A}$ receptors mediate, respectively, the direct hyperpolarizing and depolarizing actions of 5-HT and selective agonists on prefrontal neurons, as assessed *in vitro* (Araneda and Andrade, 1991; Aghajanian and Marek, 1997, 1999; Zhou and Hablitz, 1999) whereas the activation of 5-HT$_{2A}$ receptors in GABAergic interneurons inhibits pyramidal neurons (Ashby *et al.*, 1990; Zhou and Hablitz, 1999). The *in vivo* physiological activation of 5-HT$_{2A}$ and 5-HT$_{1A}$ receptors excites and inhibits, respectively, pyramidal neurons in the medial prefrontal cortex (Puig *et al.*, 2003; Amargós-Bosch *et al.*, 2004), an area projecting to numerous cortical and subcortical areas (Groenewegen and Uylings, 2000). Hence, 5-HT may influence the descending excitatory input into limbic and motor structures, where the prefrontal cortex projects, through the activation of pyramidal 5-HT$_{1A}$ and 5-HT$_{2A}$ receptors.

The exact role of serotonergic transmission in prefrontal cortex is poorly known (Robbins, 2000). However, 5-HT$_{2A}$ receptors in the dorsolateral prefrontal cortex are involved in working memory (Williams *et al.*, 2002) and recent work associates allelic variants of the 5-HT$_{2A}$ receptor with memory capacity in humans (De Quervain *et al.*, 2003). Furthermore, an excessive activation of 5-HT$_{2A}$ receptors by agonists such as LSD or DOI likely underlies the hallucinogenic properties of these compounds. On the other hand, atypical antipsychotics exert their therapeutic action, at least in part, by occupying cortical 5-HT$_{2A}$ receptors and blocking 5-HT$_{2A}$-mediated responses (Kroeze and Roth, 1998; Meltzer, 1999; Nyberg *et al.*, 1999).

5-HT$_{1A}$ receptors have long been implicated in anxiety, depression and suicide (De Vry, 1995; Artigas *et al.*, 1996; Stockmeier *et al.*, 1998). Recent data suggest an association of depression and suicide with the impaired expression of a 5-HT$_{1A}$ suppressor element (NUDR), which may lead to receptor overexpression (Lemonde *et al.*, 2003). Moreover, some atypical antipsychotics are partial agonists (Newman-Tancredi *et al.*, 1996, 2001) or behave as indirect 5-HT$_{1A}$ agonists (Ichikawa *et al.*, 2001). Finally, 5-HT$_{1A}$ receptor antagonists may be useful in the treatment of age-related cognitive impairment because of their ability to reverse drug-induced cognitive deficits (Harder and Ridley, 2000; Mello e Souza *et al.*, 2001; Misane and Ögren, 2003).

Atypical antipsychotics display a preferential occupancy of 5-HT$_{2A}$ versus dopamine D2 receptors at therapeutic doses (Nordstrom *et al.*, 1995; Nyberg *et al.*, 1999). This suggests that neurons expressing 5-HT$_{2A}$ (and possibly 5-HT$_{1A}$) receptors are the primary cellular targets of these drugs, irrespectively of an additional action on D2 receptors. We therefore examined the expression of both receptor transcripts in pyramidal and GABAergic cells of the rat prefrontal cortex using double *in situ* hybridization histochemistry. The study also improves our knowledge on cortical serotonergic transmission by identifying the cell types and anatomical localization of the neurons expressing the two main 5-HT receptors present in prefrontal cortex.

Cerebral Cortex October 2004;14:1100–1109; doi:10.1093/cercor/bhh070

Materials and Methods

Tissue Preparation

Male albino Wistar rats weighing 250–320 g were used (Iffa Credo, Lyon, France). Animals were kept in a controlled environment (12 h light-dark cycle and 22 ± 2°C room temperature) with food and water provided *ad libitum*. Animal care followed the European Union regulations (O.J. of E.C. L358/1 18/12/1986) and was approved by the local Institutional Animal Care and Use Committee. The rats were killed by decapitation and the brains rapidly removed, frozen on dry ice and stored at –20°C. Tissue sections, 14 µm thick, were cut using a microtome-cryostat (HM500 OM; Microm, Walldorf, Germany), thaw-mounted onto APTS (3-aminopropyltriethoxysilane; Sigma,St Louis, MO) coated slides and kept at –20°C until use.

Hybridization Probes

The oligodeoxyribonucleotide probes used were as follows. For 5-HT_{1A} receptor mRNA four oligonucleotides were simultaneously used, complementary to bases 82–122, 123–171, 885–933 and 1341–1389 (Albert *et al.*, 1990). For the mRNA coding for 5-HT_{2A} receptor the three oligonucleotides used were complementary to bases 669–716, 1882–1520 and 1913–1960 (Pritchett *et al.*, 1988). These probes were synthesized on a 380 Applied Biosystem DNA synthesizer (Foster City Biosystem, Foster City, CA) and purified on a 20% polyacrylamide/8 M urea preparative sequencing gel.

Glutamatergic cells were identified by the presence of the vesicular glutamate transporter vGluT1 mRNA with two oligonucleotides complementary to bases 127–172 and 1756–1800 (GenBank accession No. U07609). GABAergic cells were identified by the presence of the enzyme synthesizing GABA, glutamic acid decarboxylase (GAD), that in adult brain exists as two major isoforms, GAD65 and GAD67. Two oligonucleotides for each isoform mRNA were made: bp 159–213 and 514–558 (GenBank accession No. NM_012563) and bp 191–235 and 1600–1653 (GenBank accession No. NM_017007). They were synthesized and HPLC purified by Isogen Bioscience BV (Maarsden, The Netherlands).

Each 5-HT_{1A} and 5-HT_{2A} receptor oligonucleotide was individually labeled (2 pmol) at its 3′-end with [^{33}P]-dATP (>2500 Ci/mmol; DuPont-NEN, Boston, MA) using terminal deoxynucleotidyltransferase (Roche Diagnostics GmbH, Mannheim, Germany), purified by centrifugation using QIAquick Nucleotide Removal Kit (Qiagen GmbH, Hilden, Germany). GAD and vGluT oligonucleotides (100 pmol) were non-radioactively labeled with the same enzyme and Dig-11-dUTP (Boehringer Mannheim) according to a previously described procedure (Schmitz *et al.*, 1991).

In Situ Hybridization Histochemistry Procedure

The protocols for single- and double-label *in situ* hybridization were based on previously described procedures (Tomiyama *et al.*, 1997; Landry *et al.*, 2000) and have been already published (Serrats *et al.*, 2003a). Frozen tissue sections were first brought to room temperature, fixed for 20 min at 4°C in 4% paraformaldehyde in phosphate-buffered saline (1× PBS: 8 mM Na_2HPO_4, 1.4 mM KH_2PO_4, 136 mM NaCl, 2.6 mM KCl), washed for 5 min in 3× PBS at room temperature, twice for 5 min each in 1× PBS and incubated for 2 min at 21°C in a solution of predigested pronase (Calbiochem, San Diego, CA) at a final concentration of 24 U/ml in 50 mM Tris–HCl pH 7.5, 5 mM EDTA. The enzymatic activity was stopped by immersion for 30 s in 2 mg/ml glycine in 1× PBS. Tissues were finally rinsed in 1× PBS and dehydrated through a graded series of ethanol. For hybridization, the radioactively-labeled and the non-radioactively labeled probes were diluted in a solution containing 50% formamide, 4× SSC (1× SSC: 150 mM NaCl, 15 mM sodium citrate), 1× Denhardt's solution (0.02% Ficoll, 0.02% polyvinylpyrrolidone, 0.02% bovine serum albumin), 10% dextran sulfate, 1% sarkosyl, 20 mM phosphate buffer pH 7.0, 250 µg/ml yeast tRNA and 500 µg/ml salmon sperm DNA. The final concentrations of radioactive and Dig-labeled probes in the hybridization buffer were in the same range (~1.5 nM). Tissue sections were covered with hybridization solution containing the labeled probe(s), overlaid with Nescofilm coverslips (Bando Chemical Ind., Kobe, Japan) and incubated overnight at 42°C in humid boxes. Sections were then washed four times (15 min each) in 1× SSC at 60°C and once in 1× SSC at room temperature for 30 min.

Development of Radioactive and Non-radioactive Hybridization Signal

Hybridized sections were treated as described by Landry *et al.* (2000). Briefly, after washing, the slides were immersed for 30 min in a buffer containing 0.1 M Tris–HCl pH 7.5, 1 M NaCl, 2 mM $MgCl_2$ and 0.5% bovine serum albumin (Sigma) and incubated overnight at 4°C in the same solution with alkaline-phosphate-conjugated anti-digoxigenin-F(ab) fragments (1:5000; Boehringer Mannheim). Afterwards, they were washed three times (10 min each) in the same buffer (without antibody) and twice in an alkaline buffer containing 0.1 M Tris–HCl pH 9.5, 0.1 M NaCl and 5 mM $MgCl_2$. Alkaline phosphatase activity was developed by incubating the sections with 3.3 mg nitroblue tetrazolium and 1.65 mg bromochloroindolyl phosphate (Gibco BRL, Gaithersburg, MD) diluted in 10 ml of alkaline buffer. The enzymatic reaction was blocked by extensive rinsing in the alkaline buffer containing 1 mM EDTA. The sections were then briefly dipped in 70 and 100% ethanol, air-dried and dipped into Ilford K5 nuclear emulsion (Ilford, Mobberly, Cheshire, UK) diluted 1:1 with distilled water. They were exposed in the dark at 4°C for 6 weeks and finally developed in Kodak D19 (Kodak, Rochester, NY) for 5 min and fixed in Ilford Hypam fixer (Ilford).

Specificity of the Probes

The specificity of the hybridization signals has been previously established and published (Pompeiano *et al.*, 1992, 1994; Serrats *et al.*, 2003a). These controls included the following procedures. (i) The thermal stability of the hybrids obtained was checked for every probe. (ii) For a given oligonucleotide probe, the hybridization signal was completely blocked by competition of the labeled probe in the presence of 50-fold excess of the same unlabeled oligonucleotide. (iii) Since we synthesized more than one probe for each mRNA analyzed, the hybridization signal obtained with each oligonucleotide for the same mRNA was identical at both regional and cellular levels when used independently. (iv) To assure the specificity of the non-radioactive hybridization signal, we compared the results obtained with the same probe radioactively labeled.

Analysis of the Results

Tissue sections were examined in bright- and dark-field in a Wild 420 macroscope (Leica, Heerbrugg, Germany) and in a Nikon Eclipse E1000 microscope (Nikon, Tokyo, Japan) equipped with bright- and dark-field condensers for transmitted light and with epi-illumination. Micrography was performed using a digital camera (DXM1200 3.0; Nikon) and analySIS Software (Soft Imaging System GmbH, Germany). Bright-field images were captured with transmitted light. Dark-field images were captured with Darklite illuminator (Micro Video Instruments, Avon, MA). The figures were prepared for publication using Adobe Photoshop software (Adobe Software, Mountain View, CA).

Cell counting was performed manually at the microscope with the help of analySIS Software. Dig-labeled cells were considered positive when a dark precipitate was clearly distinguished from background. Only cellular profiles showing great abundance of the corresponding 5-HT receptor mRNA and the cell type identifier (either GAD or vGluT1 mRNAs) were considered to be double-labeled. Cells with a dense Dig labeling and occasional silver grains (or vice versa) were not considered to co-express both transcripts. Analysis of variance (ANOVA) and *post hoc* Tukey's test were performed using GraphPad Prism software (GraphPad Software, San Diego, CA). $P < 0.05$ was considered statistically significant.

Results

The prefrontal cortex contains a large number of cells expressing the 5-HT_{1A} and 5-HT_{2A} receptor transcripts in various cortical fields, such as the secondary motor area (MOs), dorsal anterior cingulate area (ACAd), prelimbic (PrL) and infralimbic areas (ILA), as well as in the tenia tecta (TT) and

piriform cortex (PIR) (Fig. 1; see also Fig. 2 for the localization of these areas). A particularly high expression was noted in the latter two areas as well as in intermediate layers of the prelimbic and cingulate cortices. There was a marked overlap in the distribution of both receptor transcripts in most areas, with the exception of a lower expression of 5-HT_{2A} receptor

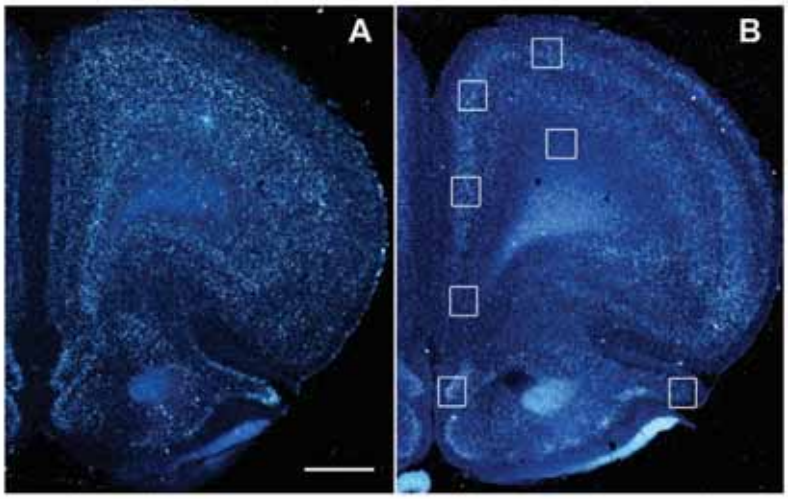

Figure 1. Dark-field photomicrographs showing the localization of (*A*) 5-HT_{1A} and (*B*) 5-HT_{2A} receptor mRNAs in the rat prefrontal cortex using *in situ* hybridization histochemistry. The sections correspond approximately to AP +3.0 mm (Paxinos and Watson, 1998). Both receptor transcripts were labeled with ^{33}P-labeled oligonucleotides. Large number of cells in superficial and middle cortical layers of the secondary motor area (MO), dorsal anterior cingulate (ACAd) and prelimbic (PrL) areas, as well as in tenia tecta (TT) and piriform cortex (PIR) expressed either receptor. Previous results revealed a very marked co-localization of both receptor mRNAs in most prefrontal areas (Amargós-Bosch *et al.*, 2004). The ventral part of the infralimbic (ILA) area and layer VI contain a lower number of cells expressing 5-HT_{2A} receptors compared with 5-HT_{1A} receptors. Open squares mark the approximate areas where cell counts were performed (see location of the corresponding areas in Fig. 2). Scale bar = 1 mm.

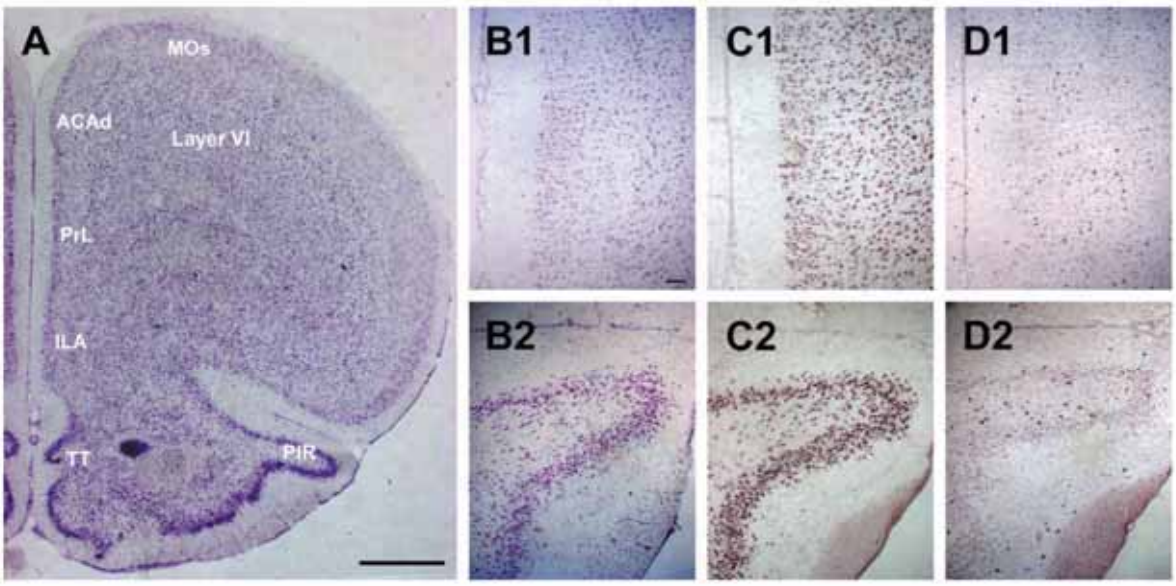

Figure 2. (*A*) Nissl-stained section of rat prefrontal cortex showing the various areas where the expression of 5-HT_{1A} and 5-HT_{2A} receptors has been studied. *B1* and *B2* show, at a higher magnification, Nissl-stained sections corresponding to the prelimbic area (see midline on the left side) and piriform cortex. *C1* and *C2* correspond to the same areas and show the presence of vGluT1-positive cells (Dig-labeled oligonucleotides). *D1* and *D2* correspond to the same areas and show the presence of GAD-positive cells (Dig-labeled oligonucleotides). Note the large abundance of pyramidal neurons, labeled with vGluT1 mRNA in intermediate and deep layers of the prelimbic area, contrasting with the total absence in layer I, near the midline. GAD mRNA-positive cells were scattered throughout the prefrontal cortex, as shown here in the prelimbic area. The observed ratio between GAD- and vGluT1-positive cells was 1:4.6. Scale bars: 1 mm (*A*), 100 μm (*B1–D2*).

mRNA in layer VI compared with that of 5-HT_{1A} receptors. In coronal sections more caudal than those shown in Figure 1, cells in layer VIb and claustrum also expressed the 5-HT_{2A} receptor mRNA (not shown). Likewise, the ventral part of the infralimbic area contained many more cells expressing 5-HT_{1A} than 5-HT_{2A} receptors.

We examined the labeling of cells in the prefrontal cortex containing the vGluT1 and GAD mRNAs (Fig. 2). High densities of pyramidal cells, as labeled by vGluT1 mRNA, were found at various cortical levels. Dense clusters of these cells were observed in the tenia tecta (not shown) and piriform cortex (Fig. 2*C2*), which also showed a greater density of label compared with that in other cortical areas, such as the prelimbic area (Fig. 2*C1*) or the anterior cingulate. In contrast, no vGluT1-expressing cells were seen in layer 1 (Fig. 2*C1*). GAD-expressing cells were scattered throughout the prefrontal cortex, including layer 1, near the midline (Fig. 2*D1*). We estimated the proportion of vGluT1 and GAD-positive cells by reference to Nissl-stained adjacent sections. The percentage of vGluT1-labeled cells was 75 ± 5% of all Nissl-stained cells whereas the corresponding value for GAD-positive cells was 16 ± 1% (data from three rats; each individual value is the average of three adjacent sections except for the Nissl-stained section, which were duplicate sections). The calculated ratio between vGluT1- and GAD-expressing cells was 4.6.

There was a remarkable co-expression of the 5-HT_{1A} receptor mRNA with vGluT1 mRNA in all areas examined (Fig. 3). As observed in panels *A* and *B*, many vGluT1-positive cells in the dorsal anterior cingulate and in the prelimbic areas, respectively, expressed the 5-HT_{1A} receptor transcript. Figure 3*C1–C2* show enlargements of a few double-labeled cells in the dorsal anterior cingulate. We also found a much more moderate proportion of GAD mRNA-containing cells which also expressed the 5-HT_{1A} receptor mRNA. These cells were found scattered throughout the various areas of the prefrontal cortex and did not follow any particular pattern of distribution. Figure 3 shows the presence of such GABAergic cells in the prelimbic area (Fig. 3*D*) and tenia tecta (Fig. 3*E*). At a higher magnification, GAD-positive cells in the prelimbic area (Fig. 3*F1*) and orbitofrontal cortex (Fig. 3*F2*) expressing 5-HT_{1A} receptors are also shown. Figure 4 shows additional GAD-positive neurons in the prelimbic area which also express the 5-HT_{1A} receptor mRNA.

As observed for 5-HT_{1A} receptors, there was also a large expression of the 5-HT_{2A} receptor transcript in vGluT1 mRNA-positive cells in most prefrontal areas (Fig. 5), such as prelimbic area (Fig. 5*A*) or tenia tecta (Fig. 5*B*). Figure 5*C1* and *C2* show, at a higher magnification, vGluT1-positive cells expressing the 5-HT_{2A} receptor transcript, which was also present in GAD-positive cells from the prelimbic area (Fig.

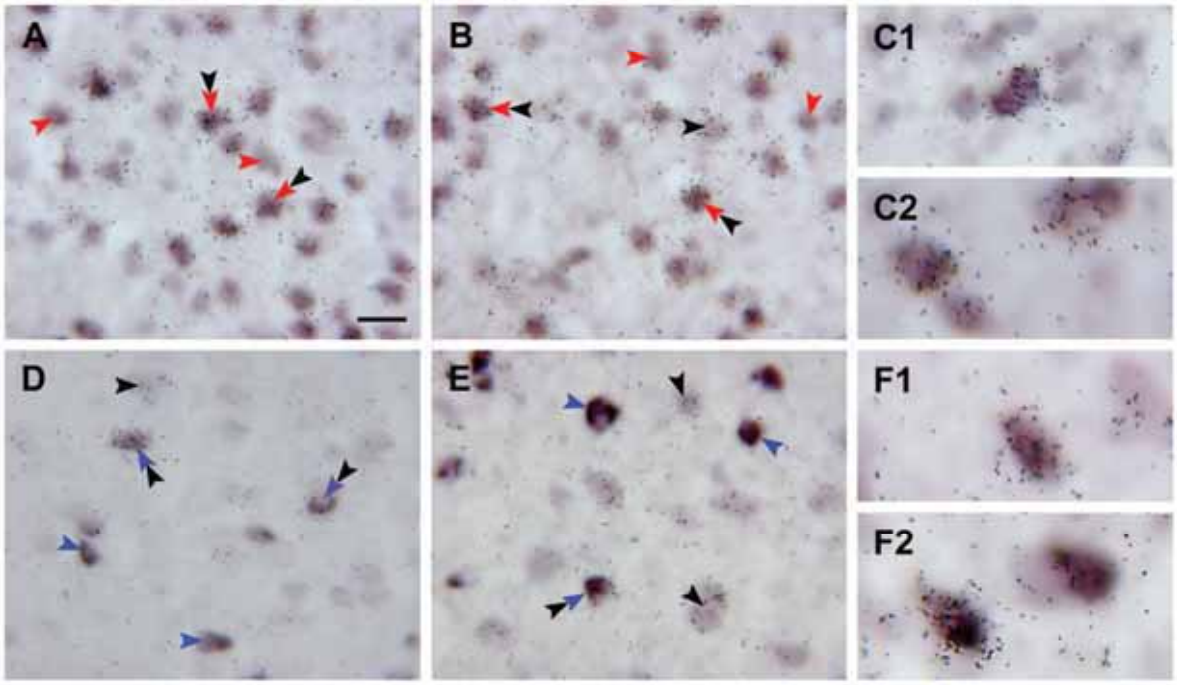

Figure 3. Upper row (*A–C*): low and high magnification photomicrographs showing the presence of 5-HT_{1A} receptor mRNA (^{33}P-labeled oligonucleotides) in pyramidal cells, identified by the presence of vGluT1 mRNA (Dig-labeled oligonucleotides). *A* and *B* show respectively, the presence of abundant cells expressing both transcripts in deep layers of the cingulate area and prelimbic area, respectively. Red arrowheads mark cells positive for vGluT1 mRNA, black arrowheads mark cells positive for 5-HT_{1A} receptor mRNA. Double labeled cells are marked by both arrowheads. For the sake of simplicity, only a few cells of each type are marked. A majority of glutamatergic cells expressed the 5-HT_{1A} receptor mRNA, as denoted by the double labeling. Note also the presence of non-glutamatergic cells expressing the 5-HT_{1A} receptor mRNA (black arrowheads). *C1* and *C2* show individual cells expressing both transcripts in the dorsal anterior cingulate. Lower row (*D–F*): the 5-HT_{1A} receptor mRNA was also found in GABAergic cells throughout the prefrontal cortex. *D* and *E* show a few double labeled cells in the prelimbic area and piriform cortex, respectively. Blue arrowheads mark cells positive for GAD mRNA and black arrowheads mark cells positive for 5-HT_{1A} receptor mRNA. Some double labeled cells are marked by both arrowheads. *F* shows, at a higher magnification, individual GABAergic cells expressing the 5-HT_{1A} receptor in the prelimbic area (*F1*) and orbitofrontal cortex (*F2*). Scale bar = 20 μm (*A, B, D, E*), 10 μm (*C, F*).

Table 1
Expression of 5-HT_{1A} and 5-HT_{2A} receptor transcripts in pyramidal (vGluT1 mRNA-positive) and GABAergic (GAD mRNA-positive) cells in rat prefrontal cortex

	vGluT1 mRNA		GAD mRNA	
	5-HT_{1A} mRNA	5-HT_{2A} mRNA	5-HT_{1A} mRNA	5-HT_{2A} mRNA
MOs	54 ± 4	60 ± 2	28 ± 6	28 ± 10
ACAd	54 ± 3	66 ± 5	22 ± 4	32 ± 2
PrL	61 ± 2	51 ± 3	20 ± 1	34 ± 1
ILA[a]	40 ± 4*	12 ± 1**	22 ± 4	22 ± 3
TT	63 ± 6	81 ± 3***	24 ± 1	24 ± 2
PIR	60 ± 2	50 ± 3	21 ± 6	24 ± 2
Layer VIa	54 ± 3	26 ± 3+	23 ± 4	11 ± 3++

Data are means of three rats (each individual measure is the mean of four consecutive sections) and represent the percentage of the counted cells expressing the mRNAs of each 5-HT receptor in pyramidal (vGluT1 mRNA-positive) and GABAergic (GAD mRNA-positive) cellular profiles. The average numbers of vGluT1 mRNA-expressing cells per field were: 30 ± 1 (MO), 32 ± 1 (ACAd), 44 ± 2 (PrL), 44 ± 2 (ILA), 56 ± 1 (TT), 85 ± 4 (PIR), 44 ± 2 (Layer VI). The respective figures for GAD mRNA-expressing cells were: 12 ± 1, 15 ± 1, 16 ± 1, 18 ± 1, 12 ± 1, 10 ± 1 and 13 ± 1 cells per field (due to the lower abundance of GABAergic cells, these were counted at a lower magnification).
Cortical areas designated according to Paxinos and Watson (1998) and Swanson (1998). MOs, secondary motor area; ACAd, dorsal anterior cingulate area; PrL, prelimbic area; ILA, infralimbic area; PIR, piriform cortex; TT, tenia tecta. Layer VIa denotes deep areas of the sensorimotor cortex at prefrontal level (Swanson, 1998). The approximate location of the counted fields is shown by small rectangles in Figure 1*B*.
[a]The data of the infralimbic area (ILA) correspond to its more ventral part, which shows a remarkable low level of 5-HT_{2A} receptor, whereas cell counts from its dorsal part are more similar to those of PrL (see Fig. 1).
*$P < 0.05$ versus PrL, TT and PIR; **$P < 0.05$ versus the rest of areas, except layer VIa ($P = 0.9$); ***$P < 0.05$ versus the rest of areas; +$P < 0.05$ versus the rest of areas except ILA; ++$P < 0.05$ versus ACAd and PrL (Tukey test post-ANOVA).

wise, layer VI (particularly VIa) showed also a lower proportion of glutamatergic cells expressing the 5-HT_{2A} receptor transcript. One-way ANOVA showed a significant effect of the region on the density of glutamatergic cells expressing one or other receptor ($P < 0.001$), with significant differences among regions (Table 1).

Twenty to twenty-five percent of GAD-positive cells expressed the 5-HT_{1A} receptor mRNA (Table 1 and Fig. 3). There was no apparent enrichment of these double-labeled cells in any of the areas examined. 5-HT_{2A} receptors were present in a similar percentage of GABAergic cells in most areas, except in layer VI, where there was a significantly lower proportion compared with some other areas (11 versus 22–34% in the rest of regions; $P < 0.03$), as observed for the 5-HT_{2A} receptors in vGluT1-positive cells.

Discussion

The present study shows that a high proportion (>50% on average) of glutamatergic cells in the rat prefrontal cortex express 5-HT_{1A} and/or 5-HT_{2A} receptors. A smaller proportion (20–25% on average) of GABAergic cells also express 5-HT_{1A} and/or 5-HT_{2A} receptor mRNAs. The percentage of GAD-expressing cells was estimated to be a 16%, a figure very similar to the percentage of GABAergic cells in various cortical areas (15%; Beaulieu, 1993) whereas the percentage of vGluT1-positive cells was 75% of all cellular profiles in Nissl-stained sections. Taking into account the ratio between GABAergic and pyramidal neurons and the proportion of cells of each type that contain 5-HT_{1A} or 5-HT_{2A} receptor mRNAs, it follows that the actual proportion of each receptor transcript in GABAergic interneurons (compared with that in pyramidal neurons) is low, close to 10%. To our knowledge, this is the first quantitative study of the expression of these receptors at cellular level in mammalian cortex. A novel finding is the occurrence of 5-HT_{1A} receptor mRNA in cortical GABAergic interneurons in a proportion similar to that of 5-HT_{2A} receptors. Collectively, these observations provide an anatomical background to interpret the complex functional effects of 5-HT on prefrontal pyramidal cells.

Methodological Considerations

The recent cloning and further characterization of three structurally related glutamate vesicular transporters, vGluT1, vGluT2 and vGluT3, in rat brain (Takamori *et al.*, 2000, 2001; Gras *et al.*, 2002) has originated a new approach to histologically identify glutamatergic phenotype in neurons (Fremeau *et al.*, 2001; Takamori *et al.*, 2001; Gras *et al.*, 2002; Oliveira *et al.*, 2003). The distributions of vGluT1 and vGluT2 mRNAs in rat brain show a complementary pattern that agrees with the localization of glutamatergic neurons as identified by previous techniques (Ziegler *et al.*, 2002). Most of the cells in rat cerebral cortex express very high levels of vGluT1 mRNA (Gras *et al.*, 2002; Ziegler *et al.*, 2002), whereas the other two transporters are found at much lower densities. VGluT1 immunoreactivity is evenly distributed in neuropil of the cerebral neocortex, being more intense in layers I-III and V (Fujiyama *et al.*, 2001). Thus, the presence of vGluT1 can be used for the identification of most cortical glutamatergic pyramidal neurons. GABAergic neurons were identified by the presence of GAD67 or GAD65 mRNA. Immunohistochemical and *in situ* hybridization histochemistry indicate that the majority of GABA-containing neurons in the brain co-express the genes encoding the two GAD isoforms (Erlander *et al.*, 1991; Esclapez *et al.*, 1993, 1994; Feldblum *et al.*, 1993).

Expression of 5-HT_{1A} and 5-HT_{2A} Receptors in Prefrontal Cortex

The present results add to previous data showing a high degree of co-expression (80%) of 5-HT_{1A} and 5-HT_{2A} receptor mRNAs in most prefrontal areas (Amargós-Bosch *et al.*, 2004). According to the present data, a very large percentage of both mRNAs are localized in glutamatergic neurons.

The distribution of cells expressing the receptor transcripts agrees well with the regional patterns of distribution of the respective mRNA and protein, as assessed autoradiographically (Pazos *et al.*, 1985; Pompeiano *et al.*, 1992, 1994). A high density of both receptor transcripts was observed in most cortical layers except for the 5-HT_{2A} receptor mRNA in layer VI and the ventral part of the infralimbic area, expressed by a considerable lower cell number. The piriform cortex and the tenia tecta displayed a very large number of cells with a high expression of both receptor transcripts, where they also co-localize extensively (Amargós-Bosch *et al.*, 2004).

The mRNAs of both receptors are effectively translated into functional proteins, as shown by previous immunohistochemical and autoradiographic studies (see introductory section). Likewise, electrophysiological reports showed that exogenously applied 5-HT and selective agonists modulate the excitability and firing rate of cortical pyramidal neurons via these receptors (see below). Furthermore, the electrical stimulation

of the raphe nuclei at physiological rates inhibits (via 5-HT_{1A} receptors) and activates (via 5-HT_{2A} receptors) pyramidal neurons in the rat prefrontal cortex (Puig *et al.*, 2003; Amargós-Bosch *et al.*, 2004). Given the connectivity of the prefrontal cortex (Groenewegen and Uylings, 2000), this indicates that 5-HT and selective ligands of these receptors may modulate the cortical excitatory output to subcortical motor and limbic structures. Of particular interest are the many neurons of the prelimbic and infralimbic areas expressing 5-HT_{2A} and/or 5-HT_{1A} receptors, since these areas project to midbrain serotonergic and dopaminergic cells and influence their activity (Thierry *et al.*, 1983; Sesack *et al.*, 1989; Hajós *et al.*, 1998; Peyron *et al.*, 1998; Carr and Sesack, 2000; Celada *et al.*, 2001). Therefore, the present results may account for the observed effects of 5-HT_{1A} and 5-HT_{2A} agonists/antagonists on monoaminergic cell firing and transmitter release (Lejeune and Millan, 1998; Celada *et al.*, 2001; Ichikawa *et al.*, 2001; Martín-Ruiz *et al.*, 2001). In support of this view is the fact that many pyramidal neurons excited through 5-HT_{2A} receptors simultaneously project to the dorsal raphe and ventral tegmental area, as assessed by antidromic activation from both areas (Puig *et al.*, 2003).

Cortical microcircuits encompass pyramidal neurons and different types of GABAergic interneurons. The latter neurons are located at various levels of the pyramidal neurons and exert a local inhibitory control through GABAergic inputs onto apical dendrites, basal dendrites and cell bodies (Somogyi *et al.*, 1998). 5-HT can modulate the activity of these microcircuits in various ways. Direct inputs onto pyramidal cells involve 5-HT_{1A} and 5-HT_{2A} receptors, expressed by these neurons, whereas indirect inputs involve GABAergic neurons expressing 5-HT_{2A} and 5-HT_3 receptors (Araneda and Andrade, 1991; Tanaka and North, 1993; Aghajanian and Marek, 1997; Morales and Bloom, 1997; Willins *et al.*, 1997; Zhou and Hablitz, 1999; Jakab and Goldman-Rakic, 2000; Férézou *et al.*, 2002; Puig *et al.*, 2003; Amargós-Bosch *et al.*, 2004).

Our data indicate that ~25% of the GABAergic interneurons express the 5-HT_{2A} receptor mRNA. These cells are possibly large perisomatic interneurons (e.g. basket cells) involved in the feed-forward control of pyramidal activity, as revealed by immunohistochemical studies (Somogyi *et al.*, 1998; Jakab and Goldman-Rakic, 1998, 2000). The lower absolute number of 5-HT_{2A} receptors in interneurons compared to that in pyramidal cells (nearly 10%) would suggest that only a minority of pyramidal neurons are under this indirect control. However, marked inhibitory effects of 5-HT_{2A} receptors on pyramidal cell activity have been reported *in vitro* and *in vivo* after local or systemic application of 5-HT or 5-HT_{2A} receptor agonists (Ashby *et al.*, 1990; Zhou and Hablitz, 1999; Puig *et al.*, 2003). A possibility to circumvent this apparent contradiction may be the presence of 5-HT_{2A} receptors in networks of fast-spiking interneurons electrically connected through connexin hemichannels (Galarreta and Hestrin, 2001). Yet, this possibility has not been tested so far.

To our knowledge, the presence of 5-HT_{1A} receptor mRNA in cortical GABAergic neurons had not been previously reported. This adds an additional complexity to the ways in which 5-HT may control pyramidal activity. Recently, 5-HT_{1A} immunoreactivity was detected in most cortical parvalbumin- and calbindin-containing neurons (85–99%) and pyramidal cells (85%; Aznar *et al.*, 2003). Methodological aspects may contribute to the difference with the present results. Indeed, the specificity of some of the antibodies used in that study was unclear (e.g. 1:10 antibody against 'pyramidal/principal cells') or was not adequately tested. Indeed, serious concerns have been raised about the specificity of immunohistochemical procedures (Saper and Sawchencko, 2003). This contrasts with the rigorous controls for mRNA probes used in the present study (see Materials and Methods).

To our knowledge, a 5-HT_{1A}-mediated disinhibitory effect of 5-HT or selective agonists in cortex has not been reported previously in prefrontal cortex. The systemic administration of 8-OH-DPAT exhibited a biphasic effect on the firing rate of prefrontal cells (increase followed by decrease at high doses; Borsini *et al.*, 1995) which may be suggestive of an action on different 5-HT_{1A} receptor populations. However, the cellular elements involved remain unidentified. In contrast, there is evidence of a 5-HT_{1A} receptor-mediated modulation of excitatory postsynaptic currents (EPSCs) recorded in putative GABAergic neurons in entorhinal cortex (Schmitz *et al.*, 1998). Interestingly, raphe GABAergic cells also express 5-HT_{1A} receptor mRNA (Serrats *et al.*, 2003a,b) and 5-HT increases EPSCs in dorsal raphe 5-HT neurons *in vitro* by a TTX- and 5-HT_{1A} receptor-mediated disinhibitory mechanism (Liu *et al.*, 2000), which might be also operant in cortex.

Functional Consequences

The present data may help to clarify the anatomical substrate for the complex actions of 5-HT and ligands of 5-HT_{1A} and 5-HT_{2A} receptors in prefrontal cortex, including the atypical antipsychotic drugs. The presence of these receptors in nearly half of glutamatergic pyramidal neurons and their high degree of colocalization in the areas examined indicates that 5-HT may finely tune the activity of prefrontal neurons. Pyramidal 5-HT_{2A} receptors in the apical dendrites of these neurons can modulate excitatory glutamate inputs (Aghajanian and Marek, 1997, 1999; Martín-Ruiz *et al.*, 2001; Puig *et al.*, 2003) whereas 5-HT_{1A} receptors (perhaps located in the axon hillock; De Felipe *et al.*, 2001; Czyrak *et al.*, 2003; David E. Lewis, unpublished observations) suppress the generation of action impulses along pyramidal axons, thus reducing glutamate release in subcortical areas.

Atypical antipsychotic drugs are preferential 5-HT_{2A} receptor antagonists (Meltzer, 1999). Some also behave as direct (aripiprazole, ziprasidone) or indirect partial 5-HT_{1A} agonists (Newman-Tancredi *et al.*, 1996, 2001; Ichikawa *et al.*, 2001). The occupancy of these pyramidal receptors by atypical antipsychotics should conceivably result in a diminished excitatory input onto mesolimbic dopaminergic neurons, innervated by prefrontal afferents (Thierry *et al.*, 1983; Carr and Sesack, 2000). This effect would attenuate the presumed hyperactivity of mesolimbic dopamine neurons in schizophrenic patients (Weinberger *et al.*, 1994; Laruelle *et al.*, 1996). This attenuation would not require the high (>80%) occupancy of postsynaptic dopamine receptors produced by conventional antipsychotics, responsible for the secondary motor effects. Further anatomical studies are required to determine the areas and cellular elements targeted by pyramidal neurons expressing 5-HT_{1A} and 5-HT_{2A} receptors.

Notes

Work supported by grants SAF2001-2133 and Fundació La Marató TV3. N.S. and J.S. are recipient of predoctoral fellowships from the Ministry of Science and Technology and IDIBAPS, respectively. A. B. is recipient of a postdoctoral fellowship from the Fundación Carolina.

Support from the CIEN network (Instituto Carlos III) and Generalitat de Catalunya (Grup de Recerca de Qualitat 2001SGR-00355) is also acknowledged.

Address correspondence to Francesc Artigas, Department of Neurochemistry, Institut d'Investigacions Biomèdiques de Barcelona (CSIC), IDIBAPS, Rosselló, 161, 6th floor, 08036 Barcelona, Spain. Email: fapnqi@iibb.csic.es.

References

Aghajanian GK, Marek GJ (1997) Serotonin induces excitatory postsynaptic potentials in apical dendrites of neocortical pyramidal cells. Neuropharmacology 36:589–599.

Aghajanian GK, Marek GJ (1999) Serotonin–glutamate interactions: a new target for antipsychotic drugs. Neuropsychopharmacology 21:S122–S133.

Albert PR, Zhou QY, Van Tol HH, Bunzow JR, Civelli O (1990) Cloning functional expression and mRNA tissue distribution of the rat 5-hydroxytryptamine1A receptor gene. J Biol Chem 265:5825–5832.

Amargós-Bosch M, Bortolozzi A, Puig MV, Serrats , Adell A, Celada P, Toth M, Mengod G, Artigas F (2004) Co-expression and *in vivo* interaction of serotonin$_{1a}$ and serotonin$_{2a}$ receptors in pyramidal neurons of prefrontal cortex. Cereb Cortex 14:281–299.

Araneda R, Andrade,R (1991) 5-Hydroxytryptamine-2 and 5-hydroxytryptamine-1A receptors mediate opposing responses on membrane excitability in rat association cortex. Neuroscience 40:399–412.

Artigas F, Romero L, de Montigny C, Blier P (1996) Acceleration of the effect of selected antidepressant drugs in major depression by 5-HT$_{1A}$ antagonists. Trends Neurosci 19:378–383.

Ashby CR, Jiang LH, Kasser RJ, Wang RY (1990) Electrophysiological characterization of 5-hydroxytryptamine-2 receptors in the rat medial prefrontal cortex. J Pharmacol Exp Ther 252:171–178.

Azmitia EC, Segal M (1978) An autoradiographic analysis of the differential ascending projections of the dorsal and median raphe nuclei in the rat. J Comp Neurol 179:641–668.

Aznar S, Qian Z, Shah R, Rahbek B, Knudsen GM (2003) The 5-HT$_{1A}$ serotonin receptor is located in calbindin- and parvalbumin-containing neurons of the rat brain. Brain Res 959:58–67.

Beaulieu C (1993) Numerical data on neocortical neurons in adult rat, with special reference to the GABA population. Brain Res 609:284–292.

Blue ME, Yagaloff KA, Mamounas LA, Hartig PR, Molliver ME (1988) Correspondence between 5-HT$_2$ receptors and serotonergic axons in rat neocortex. Brain Res 453:315–328.

Borsini F, Ceci A, Bietti G, Donetti A (1995) BIM17, a 5-HT$_{1A}$ receptor agonist/5-HT$_{2A}$ receptor antagonist directly activates postsynaptic 5-HT inhibitory responses in the rat cerebral cortex. Naunyn-Schmiederberg's Arch Pharmacol 352:283–290.

Carr DB, Sesack SR (2000) Projections from the rat prefrontal cortex to the ventral tegmental area: target specificity in the synaptic associations with mesoaccumbens and mesocortical neurons. J Neurosci 20:3864–3873.

Celada P, Puig MV, Casanovas JM, Guillazo G, Artigas F (2001) Control of dorsal raphe serotonergic neurons by the medial prefrontal cortex: involvement of serotonin-1A GABA(A) and glutamate receptors. J Neurosci 21:9917–9929.

Cornea-Hébert V, Riad M, Wu C, Singh SK, Descarries L (1999) Cellular and subcellular distribution of the serotonin 5-HT$_{2A}$ receptor in the central nervous system of adult rat. J Comp Neurol 409:187–209.

Czyrak A, Czepiel K, Mackowiak M, Chocyk A, Wedzony K (2003) Serotonin 5-HT$_{1A}$ receptors might control the output of cortical glutamatergic neurons in rat cingulate cortex. Brain Res 989:42–51.

De Felipe J, Arellano JI, Gomez A, Azmitia EC, Muñoz A (2001) Pyramidal cell axons show a local specialization for GABA and 5-HT inputs in monkey and human cerebral cortex. J Comp Neurol 433:148–155.

De Quervain DJ, Henke K, Aerni A, Coluccia D, Wollmer MA, Hock C, Nitsch RM, Papassotiropoulos A (2003) A functional genetic variation of the 5-HT$_{2A}$ receptor affects human memory. Nat Neurosci 11:1141–1142

De Vry J (1995) 5-HT$_{1A}$ receptor agonists: recent developments and controversial issues. Psychopharmacology 121:1–26.

Erlander MG, Tillakaratne NJ, Feldblum S, Patel N, Tobin AJ (1991) Two genes encode distinct glutamate decarboxylases. Neuron 7:91–100.

Esclapez M, Tillakaratne NJ, Tobin AJ, Houser CR (1993) Comparative localization of mRNAs encoding two forms of glutamic acid decarboxylase with nonradioactive *in situ* hybridization methods. J Comp Neurol 331:339–362.

Esclapez M, Tillakaratne NJ, Kaufman DL, Tobin AJ, Houser CR (1994) Comparative localization of two forms of glutamic acid decarboxylase and their mRNAs in rat brain supports the concept of functional differences between the forms. J Neurosci 14:1834–1855.

Feldblum S, Erlander MG,Tobin AJ (1993) Different distributions of GAD$_{65}$ and GAD$_{67}$ mRNAs suggest that the two glutamate decarboxylases play distinctive functional roles. J Neurosci Res 34:689–706.

Férézou I, Cauli B, Hill EL, Rossier J, Hamel E, Lambolez B (2002) 5-HT$_3$ receptors mediate serotonergic fast synaptic excitation of neocortical vasoactive intestinal peptide/cholecystokinin interneurons. J Neurosci 22:7389–7397.

Fremeau RT Jr, Troyer MD, Pahner I, Nygaard GO, Tran CH, Reimer RJ, Bellocchio EE, Fortin D, Storm-Mathisen J, Edwards RH (2001) The expression of vesicular glutamate transporters defines two classes of excitatory synapse. Neuron 31:247–260.

Fujiyama F, Furuta T, Kaneko T (2001) Immunocytochemical localization of candidates for vesicular glutamate transporters in the rat cerebral cortex. J Comp Neurol 435:379–387.

Galarreta M, Hestrin S (2001) Electrical synapses between GABA-releasing interneurons. Nat Rev Neurosci 2:425–433.

Gras C, Herzog E, Bellenchi GC, Bernard V, Ravassard P, Pohl M, Gasnier B, Giros B, El Mestikawy S (2002) A third vesicular glutamate transporter expressed by cholinergic and serotoninergic neurons. J Neurosci 22:5442–5451.

Groenewegen HJ, Uylings HB (2000) The prefrontal cortex and the integration of sensory limbic and autonomic information. Prog Brain Res 126:3–28.

Hajós M, Richards CD, Szekely AD, Sharp T (1998) An electrophysiological and neuroanatomical study of the medial prefrontal cortical projection to the midbrain raphe nuclei in the rat. Neuroscience 87:95–108.

Hajós M, Gartside SE, Varga V, Sharp T (2003) *In vivo* inhibition of neuronal activity in the rat ventromedial prefrontal cortex by midbrain-raphe nuclei: role of 5-HT$_{1A}$ receptors. Neuropharmacology 45: 72–81.

Harder JA, Ridley RM (2000) The 5-HT$_{1A}$ antagonist WAY 100 635 alleviates cognitive impairments induced by dizocilpine (MK-801) in monkeys. Neuropharmacology 39:547–552.

Heisler LK, Chu HM, Brennan TJ, Danao JA, Bajwa P, Parsons LH, Tecott LH (1998) Elevated anxiety and antidepressant-like responses in serotonin 5-HT$_{1A}$ receptor mutant mice. Proc Natl Acad Sci USA 95:15049–15054.

Ichikawa J, Ishii H, Bonaccorso S, Fowler WL, O'Laughlin IA, Meltzer HY (2001) 5-HT$_{2A}$ and D-2 receptor blockade increases cortical DA release via 5-HT$_{1A}$ receptor activation: a possible mechanism of atypical antipsychotic-induced cortical dopamine release. J Neurochem 76:1521–1531.

Jakab RL, Goldman-Rakic PS (1998) 5-Hydroxytryptamine(2A) serotonin receptors in the primate cerebral cortex: possible site of action of hallucinogenic and antipsychotic drugs in pyramidal cell apical dendrites. Proc Natl Acad Sci USA 95:735–740.

Jakab RL, Goldman-Rakic PS (2000) Segregation of serotonin 5-HT$_{2A}$ and 5-HT$_3$ receptors in inhibitory circuits of the primate cerebral cortex. J Comp Neurol 417:337–348.

Jansson A, Tinner B, Bancila M, Vergé D, Steinbusch HW, Agnati LF, Fuxe K (2001) Relationships of 5-hydroxytryptamine immunoreactive terminal-like varicosities to 5-hydroxytryptamine-2A

receptor-immunoreactive neuronal processes in the rat forebrain. J Chem Neuroanat 22:185–203.

Kia HK, Miquel MC, Brisorgueil MJ, Daval G, Riad M, Elmestikawy S, Hamon M, Vergé D (1996) Immunocytochemical localization of serotonin(1A) receptors in the rat central nervous system. J Comp Neurol 365:289–305.

Kroeze WK, Roth BL (1998) The molecular biology of serotonin receptors: therapeutic implications for the interface of mood and psychosis. Biol Psychiatry 44:1128–1142.

Landry M, Holmberg K, Zhang X, Hökfelt T (2000) Effect of axotomy on expression of NPY galanin and NPY Y1 and Y2 receptors in dorsal root ganglia and the superior cervical ganglion studied with double-labeling *in situ* hybridization and immunohistochemistry. Exp Neurol 162:361–384.

Laruelle M, Abi-Dargham A, van Dyck CH, Gil R, D'Souza CD, Erdos J, McCance E, Rosenblatt W, Fingado C, Zoghbi SS, Baldwin RM, Seibyl JP, Krystal JH, Charney DS, Innis RB (1996) Single photon emission computerized tomography imaging of amphetamine-induced dopamine release in drug-free schizophrenic subjects. Proc Natl Acad Sci USA 93:9235–9240.

Lejeune F, Millan MJ (1998) Induction of burst firing in ventral tegmental area dopaminergic neurons by activation of serotonin (5-HT)(1A) receptors: WAY 100 635-reversible actions of the highly selective ligands flesinoxan and S-15535. Synapse 30:172–180.

Lemonde S, Turecki G, Bakish D, Du L, Hrdina PD, Bown CD, Sequeira A, Kushwaha N, Morris SJ, Basak A, Ou XM, Albert PR (2003) Impaired repression at a 5-hydroxytryptamine-1A receptor gene polymorphism associated with major depression and suicide. J Neurosci 23:8788–8799.

Liu R, Jolas T, Aghajanian G (2000) Serotonin 5-HT_2 receptors activate local GABA inhibitory inputs to serotonergic neurons of the dorsal raphe nucleus. Brain Res 873:34–45.

Martín-Ruiz R, Puig MV, Celada P, Shapiro DA, Roth BL, Mengod G, Artigas F (2001) Control of serotonergic function in medial prefrontal cortex by serotonin-2A receptors through a glutamate-dependent mechanism. J Neurosci 21:9856–9866.

Mello e Souza T, Rodrigues C, Souza MM, Vinade E, Coitinho A, Choi H, Izquierdo I (2001) Involvement of the serotonergic type 1A (5-HT1A) receptor in the agranular insular cortex in the consolidation of memory for inhibitory avoidance in rats. Behav Pharmacol 12:349–353.

Misane I, Ögren SO (2003) Selective 5-HT_{1A} antagonists WAY 100635 and NAD-299 attenuate the impairment of passive avoidance caused by scopolamine in the rat. Neuropsychopharmacology 28:253–264.

Meltzer HY (1999) The role of serotonin in antipsychotic drug action. Neuropsychopharmacology 21:S106–S115.

Morales M, Bloom FE (1997) The 5-HT_3 receptor is present in different subpopulations of GABAergic neurons in the rat telencephalon. J Neurosci 17: 3157–3167.

Newman-Tancredi A, Chaput C, Verriele L, Millan MJ (1996) Clozapine is a partial agonist at cloned, human serotonin 5-HT_{1A} receptors. Neuropharmacology 35:119–121.

Newman-Tancredi A, Verriele L, Touzard M, Millan MJ (2001) Efficacy of antipsychotic agents at human 5-HT(1A) receptors determined by [3H]WAY100 635 binding affinity ratios: relationship to efficacy for G-protein activation. Eur J Pharmacol 428:177–184.

Nordstrom AL, Farde L, Nyberg S, Karlsson P, Halldin C, Sedvall G (1995) D1, D2, and 5-HT_2 receptor occupancy in relation to clozapine serum concentration: a PET study of schizophrenic patients. Am J Psychiatry 152:1444–1449.

Nyberg S, Eriksson B, Oxenstierna G, Halldin C, Farde L (1999) Suggested minimal effective dose of risperidone based on PET-measured D2 and 5-HT_{2A} receptor occupancy in schizophrenic patients. Am J Psychiatry 156:869–875.

Oliveira AL, Hydling F, Olsson E, Shi T, Edwards RH, Fujiyama F, Kaneko T, Hokfelt T, Cullheim S, Meister B (2003) Cellular localization of three vesicular glutamate transporter mRNAs and proteins in rat spinal cord and dorsal root ganglia. Synapse 50:117–129.

Paxinos G, Watson C (1998) The rat brain in stereotaxic coordinates, 4th edn. Sydney: Academic Press.

Pazos A, Palacios JM (1985) Quantitative autoradiographic mapping of serotonin receptors in the rat brain: I. Serotonin-1 receptors. Brain Res 346:205–230.

Pazos A, Cortés R, Palacios JM (1985) Quantitative autoradiographic mapping of serotonin receptors in the rat brain: II. Serotonin-2 receptors Brain Res 346:231–249.

Peyron C, Petit JM, Rampon C, Jouvet M, Luppi PH (1998) Forebrain afferents to the rat dorsal raphe nucleus demonstrated by retrograde and anterograde tracing methods. Neuroscience 82:443–468.

Pompeiano M, Palacios JM, Mengod G (1992) Distribution and cellular localization of mRNA coding for 5-HT_{1A} receptor in the rat brain: correlation with receptor binding. J Neurosci 12:440–453.

Pompeiano M, Palacios JM, Mengod G (1994) Distribution of the serotonin 5-HT_2 receptor family mRNAs: comparison between 5-HT_{2A} and 5-HT_{2C} receptors. Mol Brain Res 23:163–178.

Pritchett DB, Bach AW, Wozny M, Taleb O, Dal Toso R, Shih JC, Seeburg PH (1988) Structure and functional expression of cloned rat serotonin 5HT_2 receptor. EMBO J 7:4135–4140.

Puig MV, Celada P, Díaz-Mataix L, Artigas F (2003) *In vivo* modulation of the activity of pyramidal neurons in the rat medial prefrontal cortex by 5-HT_{2A} receptors. Relationship to thalamocortical afferents. Cereb Cortex 13:1870–1882

Robbins TW (2000) Chemical neuromodulation of frontal-executive functions in humans and other animals. Exp Brain Res 133:130–138.

Saper CB, Sawchencko PE (2003) Editorial: magic peptides, magic antibodies: guidelines for appropriate controls for immunohistochemistry. J Comp Neurol 465:161–163.

Schmitz D, Gloveli T, Empson RM, Heinemann U (1998) Serotonin reduces polysynaptic inhibition via 5-HT_{1A} receptors in the superficial entorhinal cortex. J Neurophysiol 80: 1116–1121.

Schmitz GG, Walter T, Seibl R, Kessler C (1991) Nonradioactive labeling of oligonucleotides *in vitro* with the hapten digoxigenin by tailing with terminal transferase. Anal Biochem 192:222–231.

Serrats J, Artigas F, Mengod G, Cortés R (2003a) $GABA_B$ receptor mRNA in the raphe nuclei: co-expression with serotonin transporter and glutamic acid decarboxylase. J Neurochem 84:743–752.

Serrats J, Mengod G, Cortés R (2003b) Cellular localization of 5-HT_{1A} and 5-HT_{1B} receptor mRNAs in the raphe nuclei: a double *in situ* hybridization study throughout the raphe nuclei. Eur Neuropsychopharmacol 13(Suppl. 4):S104.

Sesack SR, Deutch AY, Roth RH, Bunney BS (1989) Topographical organization of the efferent projections of the medial prefrontal cortex in the rat: an anterograde tract-tracing study with *Phaseolus vulgaris* leucoagglutinin. J Comp Neurol 290:213–242.

Somogyi P, Tanás G, Lujan R, Buhl EH (1998) Salient features of the synaptic organization in the cerebral cortex. Brain Res Rev 26:113–135.

Steinbusch HWM (1981) Distribution of serotonin-immunoreactivity in the central nervous system of the rat. Cell bodies and terminals. Neuroscience 6:557–618.

Stockmeier CA, Shapiro LA, Dilley GE, Kolli TN, Friedman L, Rajkowska G (1998) Increase in serotonin-1A autoreceptors in the midbrain of suicide victims with major depression – postmortem evidence for decreased serotonin activity. J Neurosci 18:7394–7401.

Swanson LW (1998) Brain maps: structure of the rat brain. Elsevier: Amsterdam.

Takamori S, Rhee JS, Rosenmund C, Jahn R (2000) Identification of a vesicular glutamate transporter that defines a glutamatergic phenotype in neurons. Nature 407:189–193.

Takamori S, Rhee JS, Rosenmund C, Jahn R (2001) Identification of differentiation-associated brain-specific phosphate transporter as a second vesicular glutamate transporter (VGLUT2). J Neurosci 21:193T.

Tanaka E, North RA (1993) Actions of 5 hydroxytryptamine on neurons of the rat cingulate cortex. J Neurophysiol 69:1749–1757.

Thierry AM, Deniau JM, Chevalier G, Ferron A, Glowinski J (1983) An electrophysiological analysis of some afferent and efferent pathways of the rat prefrontal cortex. Prog Brain Res 58:257–261.

Tomiyama M, Palacios JM, Cortés R, Vilaró MT, Mengod G (1997) Distribution of AMPA receptor subunit mRNAs in the human basal ganglia: an *in situ* hybridization study Brain Res Mol Brain Res 46:281–289.

Weinberger DR, Aloia MS, Goldberg TE, Berman KF (1994) The frontal lobes and schizophrenia. J Neuropsychiatry Clin Neurosci 6:419–427.

Williams GV, Rao SG, Goldman-Rakic PS (2002) The physiological role of 5-HT_{2A} receptors in working memory. J Neurosci 22:2843–2854.

Willins DL, Deutch AY, Roth BL (1997) Serotonin 5-HT_{2A} receptors are expressed on pyramidal cells and interneurons in the rat cortex. Synapse 27:79–82.

Zhou FM, Hablitz JJ (1999) Activation of serotonin receptors modulates synaptic transmission in rat cerebral cortex. J Neurophysiol 82:2989–2999.

Ziegler DR, Cullinan WE, Herman JP (2002) Distribution of vesicular glutamate transporter mRNA in rat hypothalamus. J Comp Neurol 448:217–229.

Trabajo 2

In Vivo Excitation of GABA Interneurons in the Medial Prefrontal Cortex through 5-HT_3 Receptors

Puig MV*, Santana N*, Celada P, Mengod G and Artigas F

*Authors with equal contribution to the study

Cerebral Cortex 14, 1365–1375 (2004)

Este trabajo muestra la presencia del ARNm del receptor serotoninérgico 5-HT_3 en interneuronas GABAérgicas de corteza prefrontal (CPF) de rata. Este receptor se distribuye preferentemente en capas superficiales de CPF y se encuentra presente exclusivamente en este tipo neuronal, dado que las células glutamatérgicas no lo expresan. El porcentaje de neuronas positivas para el ARNm de la enzima glutamato descarboxilasa (GAD, marcador de neuronas GABAérgicas) que expresaron el ARNm del receptor 5-HT_3 en las diferentes capas de CPF fue 40, 18, 6, 8% en capas I, II-III, V y VI, respectivamente. En este trabajo se muestra además que la estimulación fisiológica de los núcleos del rafe excita neuronas probablemente GABAérgicas en las áreas cingulada y prelímbica la la CPF de rata *in vivo*. Estas excitaciones fueron bloqueadas por la administración i.v. de los antagonistas del receptor 5-HT_3 ondansetron y tropisetron.

La autora de la presente tesis contribuyó a este trabajo con los experimentos de doble hibridación *in situ*

In Vivo Excitation of GABA Interneurons in the Medial Prefrontal Cortex through 5-HT_3 Receptors

M. Victoria Puig*, Noemí Santana*, Pau Celada, Guadalupe Mengod and Francesc Artigas

Department of Neurochemistry, Institut d'Investigacions Biomèdiques de Barcelona (CSIC), IDIBAPS, 08036 Barcelona, Spain
*The first two authors contributed equally to this study

Serotonin (5-hydroxytryptamine, 5-HT) controls pyramidal cell activity in prefrontal cortex (PFC) through various receptors, in particular, 5-HT_{1A} and 5-HT_{2A} receptors. Here we report that the physiological stimulation of the raphe nuclei excites local, putatively GABAergic neurons in the prelimbic and cingulate areas of the rat PFC *in vivo*. These excitations had a latency of 36 ± 4 ms and a duration of 69 ± 9 ms and were blocked by the i.v. administration of the 5-HT_3 receptor antagonists ondansetron and tropisetron. The latency and duration were shorter than those elicited through 5-HT_{2A} receptors in pyramidal neurons of the same areas. Double *in situ* hybridization histochemistry showed the presence of GABAergic neurons expressing 5-HT_3 receptor mRNA in PFC. These cells were more abundant in the cingulate, prelimbic and infralimbic areas, particularly in superficial layers. The percentages of GAD mRNA-positive neurons expressing 5-HT_3 receptor mRNA in prelimbic cortex were 40, 18, 6 and 8% in layers I, II–III, V and VI, respectively, a distribution complementary to that of cells expressing 5-HT_{2A} receptors. Overall, these results support an important role of 5-HT in the control of the excitability of apical dendrites of pyramidal neurons in the medial PFC through the activation of 5-HT_3 receptors in GABAergic interneurons.

Keywords: GABA interneurons, 5-HT_{2A} receptors, 5-HT_3 receptors, medial prefrontal cortex, pyramidal neurons

Introduction

The prefrontal cortex (PFC) plays a key role in higher brain functions (Fuster, 2001; Miller and Cohen, 2001) and controls, via the excitatory axons of pyramidal neurons, the activity of many subcortical motor and limbic areas (Groenewegen and Uylings, 2000). The activity of projection pyramidal neurons is controlled, among other areas, by the brainstem monoaminergic systems. In particular, the mesocortical dopaminergic system is involved in working memory and cognition through a complex control of the activity of pyramidal neurons (Williams and Goldman-Rakic, 1995; Goldman-Rakic, 1996; O'Donnell, 2003; Wang *et al.*, 2003). There is also increasing evidence that the ascending serotonergic pathways originating in the dorsal and median raphe nuclei (DR and MnR, respectively) may play an important role in prefrontal function. Indeed, prefrontal neurons in various species express several 5-HT receptor subtypes (Pompeiano *et al.*, 1992, 1994; Morales and Bloom, 1997; Hall *et al.*, 2000; Talvik-Lotfi *et al.*, 2000; Martinez *et al.*, 2001; Arango *et al.*, 2002; Amargós-Bosch *et al.*, 2004), which suggests a role for 5-HT in the function of PFC. Hence, 5-HT_{2A} receptors in dorsolateral PFC are involved in working memory (Williams *et al.*, 2002) and recent work associates allelic variants of this receptor with memory capacity in humans (De Quervain *et al.*, 2003). Hallucinogens such as LSD or DOI (1-[2,5]-dimethoxy-4-iodophenyl-2-aminopropane) are 5-HT_{2A} receptor agonists, whereas atypical antipsychotics are 5-HT_{2A} receptor antagonists (Kroeze and Roth, 1998; Meltzer, 1999). On the other hand, 5-HT_{1A} receptor antagonists reverse drug-induced cognitive deficits (Harder and Ridley, 2000; Mello e Souza *et al.*, 2001; Misane and Ögren, 2003).

5-HT_3 receptors appear also to be involved in the cortical actions of 5-HT. Hence, 5-HT_3 receptor antagonists display procognitive actions (Staubli and Zu, 1995). These agents have been also reported to display anxiolytic and antipsychotic activity in animal models (Higgins and Kilpatrick, 1999) and to improve the therapeutic action of antipsychotics in schizophrenic patients (Sirota *et al.*, 2000), perhaps through changes in dopamine release (Blandina *et al.*, 1989; Chen *et al.*, 1992; De Deurwaerdère *et al.*, 1998). Likewise, the atypical antipsychotic clozapine is an antagonist of 5-HT_3 receptors (Watling *et al.*, 1989; Edwards *et al.*, 1991).

Early microiontophoretic studies showed that 5-HT and 5-HT_3 receptor agonists suppressed pyramidal activity in rat PFC through the activation of 5-HT_3 receptors by a direct action (Ashby *et al.*, 1989, 1991, 1992). However, more recent *in vitro* studies indicate that 5-HT may increase IPSCs in cortical pyramidal neurons by activation of 5-HT_3 receptors, likely as a result of a fast synaptic excitation of local GABAergic neurons (Zhou and Hablitz, 1999; Férézou *et al.*, 2002). The latter observations are consistent with the presence of 5-HT_3 receptors in GABAergic interneurons in the rat telencephalon (Morales *et al.*, 1996; Morales and Bloom, 1997). Likewise, in macaque cortex, 5-HT_3 receptors are expressed by a subpopulation of calbindin- and calretinin-positive interneurons (Jakab and Goldman-Rakic, 2000). To gain further insight on the actions of 5-HT in PFC, we examined the localization of 5-HT_3 receptors in GABA interneurons of the rat PFC and the effects of the physiological stimulation of the DR on the activity of such neurons recorded *in vivo*.

Materials and Methods

Animals and Tissue Preparation

Male albino Wistar rats weighing 250–320 g were used (Iffa Credo, Lyon, France). These were kept in a controlled environment (12 h light–dark cycle and 22 ± 2°C room temperature) with food and water provided *ad libitum*. Animal care followed the European Union regulations (O.J. of E.C. L358/1 18/12/1986) and was approved by the local ethics committee. Stereotaxic coordinates were taken from bregma and duramater according to the atlas of Paxinos and Watson (1998). We used the brain maps of Swanson (1998) for nomenclature of cortical areas.

Tissue Preparation

Rats used in electrophysiological experiments were killed by an anesthetic overdose. The location of stimulation electrodes was verified

Cerebral Cortex December 2004;14:1365–1375; doi:10.1093/cercor/bhh097

histologically (Neutral Red staining). The rats used for *in situ* hybridization histochemistry were killed by decapitation, the brains rapidly removed, frozen on dry ice and stored at -20°C. Tissue sections, 14 µm thick, were cut using a microtome-cryostat (HM500 OM; Microm, Walldorf, Germany), thaw-mounted onto APTS (3-aminopropyltriethoxysilane; Sigma, St Louis, MO)-coated slides and kept at -20°C until use.

Electrophysiological Recordings

We assessed the effects of the electrical stimulation of the DR at physiological rates on the activity of non-pyramidal neurons in the dorsal anterior cingulate and prelimbic areas of the rat PFC. Descents were carried out at AP +3.2 to +3.4, DV -1.1 to -3.6 below the brain surface. For the recording of 5-HT_3-expressing GABAergic neurons, the lateral coordinate was adjusted between -0.2 and -0.5 mm in order to target cells in the border between layers I and II-III, which show the greater abundance of cells expressing this receptor, as observed in *in situ* hybridization experiments (see below). To this end, the sinus was retracted to allow recording near the midline. As in previous studies, pyramidal neurons were identified by antidromic activation from projection areas of the medial prefrontal cortex (mPFC), such as the DR (at two different coordinates) or the mediodorsal thalamus (AP -2.8, L -0.5, DV -5.3), up to 2 mA and collision extinction with spontaneously occurring spikes (Fuller and Schlag, 1976). Non-projecting units which were spontaneously active with a slow firing rate were considered candidates for the examination of the *in vivo* effects of 5-HT through 5-HT_3 receptors (see below). To this end, the DR (tip coordinates: AP -7.8, L -0, DV -6.5) was stimulated at 0.5-1.7 mA, 0.2 ms square pulses, 0.9 Hz. Peristimulus time histograms (PSTH) were constructed in baseline conditions and after the administration of the 5-HT_3 receptor antagonists ondansetron (gift from VITA-INVEST, Sant Joan Despí, Spain) and tropisetron (Sigma).

Single-unit extracellular recordings were performed as follows. Rats were anesthetized (chloral hydrate 400 mg/kg i.p.) and positioned in an stereotaxic apparatus (David Kopf). Additional doses of chloral hydrate (80 mg/kg) were administered i.v. through the femoral vein. Body temperature was maintained at 37°C throughout the experiment with a heating pad. All wound margins and points of contact between the animal and the stereotaxic apparatus were infiltrated with lidocaine solution (5%). In order to minimize pulsation, the atlanto-occipital membrane was punctured to release some CSF. Putative GABAergic neurons were recorded extracellularly with glass micropipettes pulled from 2.0 mm capillary glass (WPI, Sarasota, FL) on a Narishige PE-2 pipette puller (Narishige Sci. Inst., Tokyo, Japan). Microelectrodes were filled with 2M NaCl. Typically, impedance was between 4-10 MΩ. Bipolar stimulating electrodes consisted of two stainless steel enamel-coated wire (California Fine Wire, Grover Beach, CA) with a diameter of 150 µm and a tip of separation of ~100 µm and *in vitro* impedance of 10-30 KΩ. Constant current electrical stimuli were generated with a Grass stimulation unit S-48 connected to a Grass SIU 5 stimulus isolation unit. Single unit extracellular recordings were amplified with a Neurodata IR283 (Cygnus Technology Inc., Delaware Water Gap, PA), postamplified and filtered with a Cibertec amplifier (Madrid, Spain) and computed on-line using a DAT 1401plus interface system Spike2 software (Cambridge Electronic Design, Cambridge, UK).

Oligonucleotide Probes

The oligodeoxyribonucleotide probes used were complementary to the following bases: 669-716, 1482-1520 and 1913-1960 of the rat 5-HT_{2A} receptor mRNA (Pritchett *et al.*, 1988); 728-772 and 1001-1045 of the rat 5-HT_{3A} receptor subunit mRNA (GenBank Accession No. U59672); 159-213 and 514-558 of the GAD65 mRNA (GenBank Accession No. NM_012563); 191-235 and 1600-1653 of the GAD67 mRNA (GenBank Accession. N.o NM_017007); 127-172 and 1756-1800 of the vGluT1 mRNA (GenBank Accession No. U07609). The probes for 5-HT_{2A} receptor and GAD67 were synthesized on a 380 Applied Biosystem DNA synthesizer (Foster City Biosystem, Foster City, CA) and purified on a 20% polyacrylamide/8 M urea preparative sequencing gel. The rest of the probes were synthesized and HPLC purified by Isogen Bioscience BV (Maarsden, The Netherlands).

Oligonucleotides were individually labeled at the 3'-end either with [^{33}P]-dATP (>2500 Ci/mmol; DuPont-NEN, Boston, MA) or with Dig-11-dUTP (Boehringer Mannheim) using terminal deoxynucleotidyltransferase (Roche Diagnostics GmbH, Mannheim, Germany), purified by centrifugation using QIAquick Nucleotide Removal Kit (QIAGEN GmbH, Hilden, Germany).

In Situ ***Hybridization Histochemistry Procedure***

The protocols for single- and double-label *in situ* hybridization were based on previously described procedures (Tomiyama *et al.*, 1997; Landry *et al.*, 2000) and have been already published (Serrats *et al.*, 2003). Frozen tissue sections were first brought to room temperature, fixed for 20 min at 4°C in 4% paraformaldehyde in phosphate-buffered saline (1× PBS: 8 mM Na_2HPO_4, 1.4 mM KH_2PO_4, 136 mM NaCl, 2.6 mM KCl), washed for 5 min in 3× PBS at room temperature twice for 5 min each in 1× PBS, and incubated for 2 min at 21°C in a solution of predigested pronase (Calbiochem, San Diego, CA) at a final concentration of 24 U/ml in 50 mM Tris-HCl pH 7.5, 5 mM EDTA. The enzymatic activity was stopped by immersion for 30 s in 2 mg/ml glycine in 1× PBS. Tissues were finally rinsed in 1× PBS and dehydrated through a graded series of ethanol. For hybridization, the radioactively-labeled and the non-radioactively labeled probes were diluted in a solution containing 50% formamide, 4× SSC (1× SSC: 150 mM NaCl, 15 mM sodium citrate), 1× Denhardt's solution (0.02% Ficoll, 0.02% polyvinylpyrrolidone, 0.02% bovine serum albumin), 10% dextran sulfate, 1% sarkosyl, 20 mM phosphate buffer pH 7.0, 250 µg/ml yeast tRNA and 500 µg/ml salmon sperm DNA. The final concentrations of radioactive and Dig-labeled probes in the hybridization buffer were in the same range (~1.5 nM). Tissue sections were covered with hybridization solution containing the labeled probe/s, overlaid with Nescofilm coverslips (Bando Chemical Ind., Kobe, Japan) and incubated overnight at 42°C in humid boxes. Sections were then washed four times (45 min each) in a buffer containing 0.6 M NaCl and 10 mM Tris-HCl (pH 7.5) at 60°C.

Development of Radioactive and Non-radioactive Hybridization Signal

Hybridized sections were treated as described by Landry *et al.* (2000). Briefly, after washing, the slides were immersed for 30 min in a buffer containing 0.1 M Tris-HCl pH 7.5, 1 M NaCl, 2 mM $MgCl_2$ and 0.5% bovine serum albumin (Sigma) and incubated overnight at 4°C in the same solution with alkaline-phosphatase-conjugated anti-digoxigenin-F(ab) fragments (1:5000; Boehringer Mannheim). Afterwards, they were washed three times (10 min each) in the same buffer (without antibody) and twice in an alkaline buffer containing 0.1 M Tris-HCl pH 9.5, 0.1 M NaCl and 5 mM $MgCl_2$. Alkaline phosphatase activity was developed by incubating the sections with 3.3 mg nitroblue tetrazolium and 1.65 mg bromochloroindolyl phosphate (Gibco BRL, Gaithersburg, MD) diluted in 10 ml of alkaline buffer. The enzymatic reaction was blocked by extensive rinsing in the alkaline buffer containing 1 mM EDTA. The sections were then briefly dipped in 70 and 100% ethanol, air-dried and dipped into Ilford K5 nuclear emulsion (Ilford, Mobberly, Chesire, UK) diluted 1:1 with distilled water. They were exposed in, USA) for 5 min, and fixed in Ilford Hypam fixer (Ilford).

Specificity of the Probes

The specificity of the hybridization signals has been previously established and published (Pompeiano *et al.*, 1992, 1994; Serrats *et al.*, 2003). These controls included: (i) the thermal stability of the hybrids obtained was checked for every probe; (ii) for a given oligonucleotide probe, the hybridization signal was completely blocked by competition of the labeled probe in the presence of 50-fold excess of the same unlabeled oligonucleotide (iii) since we synthesized more than one probe for each mRNA analyzed, the hybridization signal obtained with each oligonucleotide for the same mRNA was identical at regional and cellular levels when used independently; and (iv) to assure the specificity of the non-radioactive hybridization signal, we compared the results obtained with the same probe radioactively labeled.

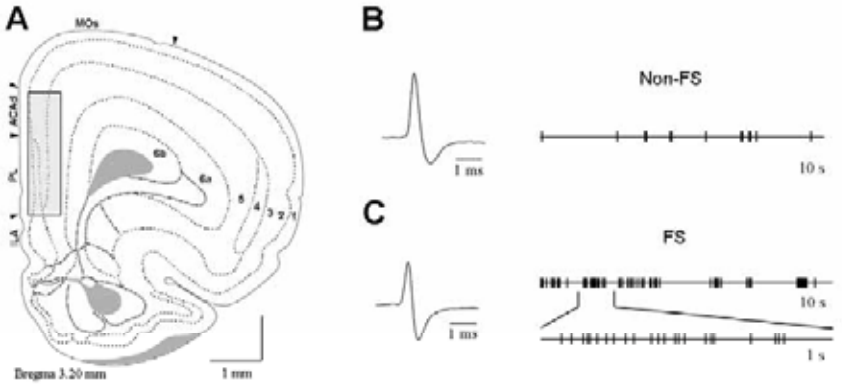

Figure 1. (*A*) Section drawing taken from Swanson (1998) showing the localization of the units recorded (shaded rectangle in the cingulate and prelimbic areas of the mPFC). These units were not antidromically activated from DR or mediodorsal thalamus and showed orthodromic activation from the DR that was blocked by the 5-HT_3 receptor antagonists. (*B*, *C*) Extracellular recordings of putative GABAergic neurons in mPFC. (*B*) Representative waveform (average of 10 sweeps) and firing pattern of a non-fast-spiking (non-FS) neuron whose orthodromic activation from the DR was blocked by 5-HT_3 receptor antagonist administration. (*C*) Representative waveform (average of 10 sweeps) and firing pattern of a spontaneously fast-spiking (FS) neuron. Firing rates of these two units were 1.3 and 10.6 spikes/s, respectively.

Analysis of the Results

The responses in putative GABAergic neurons evoked by DR stimulation were characterized by measuring the delay, magnitude and duration of excitatory responses from PSTH (4 ms bin width). Orthodromic excitations elicited spikes with short and variable latencies with a success rate greater than 10% (Celada *et al.*, 2001). Success rate in PSTHs were corrected by the pre-stimulus firing. Drug changes were assessed with paired Student's *t*-test.

Tissue sections were examined in bright- and dark-field in a Wild 420 macroscope (Leica, Heerbrugg, Germany) and in a Nikon Eclipse E1000 microscope (Nikon, Tokyo, Japan) equipped with bright- and dark-field condensers for transmitted light and with epi-illumination. Micrography was performed using a digital camera (DXM1200 3.0; Nikon) and analySIS Software (Soft Imaging System GmbH, Germany). Bright-field images were captured with transmitted light. Dark-field images were also captured with Darklite illuminator (Micro Video Instruments, Avon, MA). The figures were prepared for publication using Adobe Photoshop software (Adobe Software, Mountain View, CA).

Cell counting was performed manually at the microscope with the help of analySIS Software. Only cellular profiles showing great abundance of both transcripts were considered to co-express both mRNAs. Cells with a dense labeling of GAD mRNAs and occasional silver grains were not considered to co-express both receptors. $P < 0.05$ was considered statistically significant.

Results

5-HT_3-mediated Excitations of Local Neurons in mPFC

The present experiments were initiated in parallel to the study of the effect of DR/MnR stimulation on pyramidal neurons of mPFC mediated by 5-HT_{1A} and 5-HT_{2A} receptors (Puig *et al.*, 2003, 2004; Amargós-Bosch *et al.*, 2004). Pyramidal neurons were recorded at a lateral coordinate typically between −0.5 and −1.0 mm. During these experiments, encompassing ~230 neurons, we occasionally found cells that (i) were excited by DR/MnR stimulation but were not antidromically activated from the midbrain and thalamus and (ii) exhibited excitations with a latency and duration shorter than those typically elicited through the activation of 5-HT_{2A} receptors. Because of the presence of 5-HT_3 receptors in GABA interneurons in rat telencephalon (Morales and Bloom, 1997), we hypothesized that these excitations might be due to the activation of 5-HT_3 receptors. Five units were recorded at this location, whose excitations were reversed by 5-HT_3 receptor antagonists. Based on these initial observations, we carried out *in situ* hybridization experiments to determine the location of cells expressing the 5-HT_3 receptor mRNA. Once these results were available (see below), additional descents were systematically performed at a more central coordinate, between −0.2 and −0.5 mm, aiming at cells expressing 5-HT_3 receptors in superficial layers (I–III). In all cases, only slow-spiking neurons, not antidromically activated from the DR or the mediodorsal thalamus were considered to be potential candidates to examine the effects of DR stimulation upon 5-HT_3 receptors. A total of 14 excitations were considered to be potentially attributable to 5-HT_3 receptor activation and blockade was successfully attempted in 11 cases with the 5-HT_3 receptor antagonists ondansetron and tropisetron. Since other 5-HT receptors might potentially contribute to these excitations, here we report only the data of those cells whose excitations were reversed by these antagonists.

The electrical stimulation of the DR at a physiological rate (0.9 Hz, 0.2 ms square pulses) resulted in orthodromic excitations of slow-spiking putative GABAergic neurons. Fast-spiking neurons (>10 spikes/s) were not excited by DR stimulation (data not shown). The characteristics of the recorded neurons, as well as the latency and duration of the excitations are given in Figure 1 and Table 1. Unlike fast-spiking cells, these neurons

Table 1
Characteristics of 5-HT_3 and 5-HT_{2A} receptor-mediated excitations induced by stimulation of the DR

	5-HT_3	5-HT_{2A}
Firing rate (spikes/s)	1.7 ± 0.3	1.1 ± 0.8
Latency (ms)	36 ± 4*	71 ± 8
Duration (ms)	69 ± 9*	101 ± 8
Success rate (%)	68 ± 11*	38 ± 8
Localization (DV, mm)	2.1 ± 0.3	2.2 ± 0.1
n	11	10

*$P < 0.05$, paired Student's *t*-test.
Data from 5-HT_{2A} receptor-mediated excitations calculated from Amargós-Bosch *et al.* (2004).

exhibited a slow firing rate (<3 spikes/s), as recorded extracellularly, with a mean firing rate of 1.7 ± 0.3 spikes/s (n = 11, one neuron per rat). The latency and duration of these excitations were significantly lower than those elicited by DR stimulation, using the same parameters, in pyramidal neurons recorded in layers III–V of cingulate and prelimbic areas (Table 1 and Fig. 2). The latter excitations were mediated by 5-HT_{2A} receptor activation, since they were blocked by the i.v. administration of the 5-HT_{2A} receptor antagonist M100907 (Puig *et al.*, 2003; Amargós-Bosch *et al.*, 2004). Moreover, the success rate was significantly greater for the 5-HT_3 receptor- than for 5-HT_{2A} receptor-mediated excitations at the same current (68 ± 11% versus 38 ± 8, P < 0.04).

We used the 5-HT_3 receptor antagonists ondansetron and tropisetron to examine whether the DR-induced excitations were mediated by 5-HT_3 receptors. Considering all cases (n = 11), 5-HT_3 receptor blockade significantly blocked these excitations, reducing the success rate from 68 ± 11% to 26 ± 8% on average (P < 0.006). Ondansetron was used to reverse the excitations in seven cases (from 73 ± 16% to 29 ± 11%, P < 0.001). Typically, excitations were blocked by 0.5–2 mg/kg i.v. except in one unit which required 3 mg/kg. Tropisetron was used in four units (from 59 ± 12% to 20 ± 9% success rate, P < 0.003). Three of them were blocked at 0.5–1 mg/kg i.v., whereas one was blocked at 3 mg/kg i.v. Figure 3 shows the reversal of the excitations in two different units by ondansetron and tropisetron, respectively.

5-HT_3 receptor-mediated responses have been shown to desensitize after exposure to 5-HT and 5-HT_3 receptor agonists *in vitro* (Zhou and Hablitz, 1999). Here we examined whether physiological amounts of 5-HT released by raphe stimulation could elicit a similar desensitizing response *in vivo*. To this end, we calculated the success rate for 1 min intervals at different times after the onset of the stimulation. The corresponding values were 114 ± 14, 108 ± 16 and 101 ± 17 %, for the 2nd, 3rd and 4th minutes after beginning the raphe simulation, taking 100 % as the success rate during the first minute.

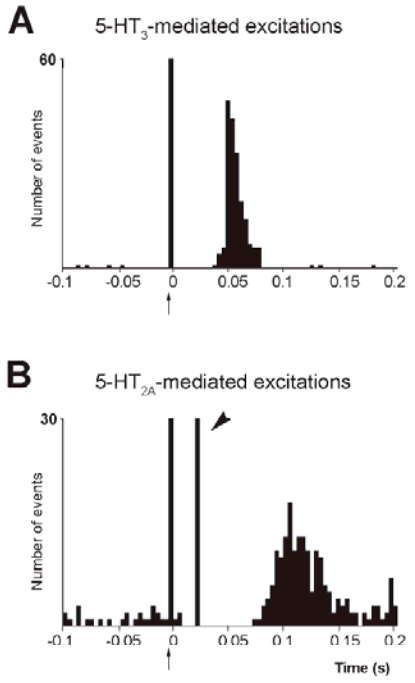

Figure 2. Peristimulus time histograms showing the orthodromic excitations elicited by the electrical stimulation of the DR on (*A*) a putatively GABAergic, 5-HT_3 receptor-containing neuron and (*B*) on a pyramidal neuron in the prelimbic PFC identified by antidromic stimulation. Both responses were selectively blocked by the administration of the respective antagonists ondansetron (*A*) and M100907 (*B*) (not shown). Note that, as many pyramidal neurons in mPFC, this unit had antidromic (arrowhead) and orthodromic responses to DR stimulation as a result of the reciprocal connectivity and functional interaction between the DR and mPFC (Puig *et al.*, 2003). The latency and duration of the 5-HT_3-mediated responses in putative GABAergic neurons was significantly lower than those evoked by 5-HT_{2A} receptor activation in pyramidal neurons. The concordances of the units shown are 85% (*A*) and 43% (*B*). Each peristimulus consists of 200 triggers; bin size is 4 ms. The arrow at zero abcissa marks the stimulus artifact.

Expression of 5-HT3 Receptors in GABA Interneurons

The presence of cells expressing the 5-HT_3 receptor transcript in various areas of the rat PFC is illustrated in Figure 4. These cells were present in all cortical layers, although they had a preferential localization in superficial layers. In particular, they were more abundant in the cingulate, prelimbic and infralimbic areas as well as in primary and secondary motor areas (Fig. 4*B*,*C*). A smaller number of cells were also present in piriform cortex and adjacent olfactory areas. Some cells were also present in layer VI of medial and motor cortices whereas layers III–V of these areas as well as the tenia tecta were almost without or with a much smaller population of neurons expressing 5-HT_3 receptors. Most cells positive for the 5-HT_3 receptor had a high level of expression, as judged from the large density of silver grains, corresponding to the ^{33}P-labeled oligonucleotides used to hybridize with the mRNA (Figs 4*D* and 5). This was more marked than that of 5-HT_{2A} receptors in GABAergic neurons in the same prefrontal areas observed using the same methodology (Santana *et al.*, 2004). This difference may indicate a higher density of 5-HT_3 receptors per cell although methodological reasons may also account (e.g. a higher hybridization of the oligonucleotides complementary to the 5-HT_3 receptor mRNA).

The vast majority of 5-HT_3 receptor-expressing cells also contained the transcript for GAD (Dig-labeled), as observed in double *in situ* experiments (Fig. 5). The estimated proportions of GAD + 5-HT_3 receptor-expressing cells versus the total of GABAergic (GAD-expressing) cells in layers I–III were 16.1 ± 0.3, 23.9 ± 3.5 and 19.1 ± 3.6% in the cingulate, prelimbic and infralimbic areas, respectively (means of three rats; each value is the average of three sections; the average number of GAD-positive cells per field was between 29 and 33). However, the localization of these cells was not homogeneous in the various fields examined and sometimes appeared as clusters (several cells per field, as shown in Figs 4*C* and 5*C*, for instance). Unlike GAD-positive cells, the number of those double-labeled cells fell rapidly at a greater lateral coordinate. Table 2 shows the number of cells expressing GAD mRNA, 5-HT_3 receptor mRNA and double-labeled cells in the various cortical layers of the prelimbic area. ANOVA showed a significant effect of the layer on the number of cells expressing GAD [F(3,8) = 88.3, P < 0.000005], 5-HT_3 receptors [F(3,8) = 14.2, P < 0.0002] and the percentage of double-labeled cells [F(3,8) = 127.7, P < 0.000001]. *Post hoc* Tukey t-test revealed significant differences between layers. Thus, the number of double-labeled cells was significantly greater in layers II–III than in the rest of

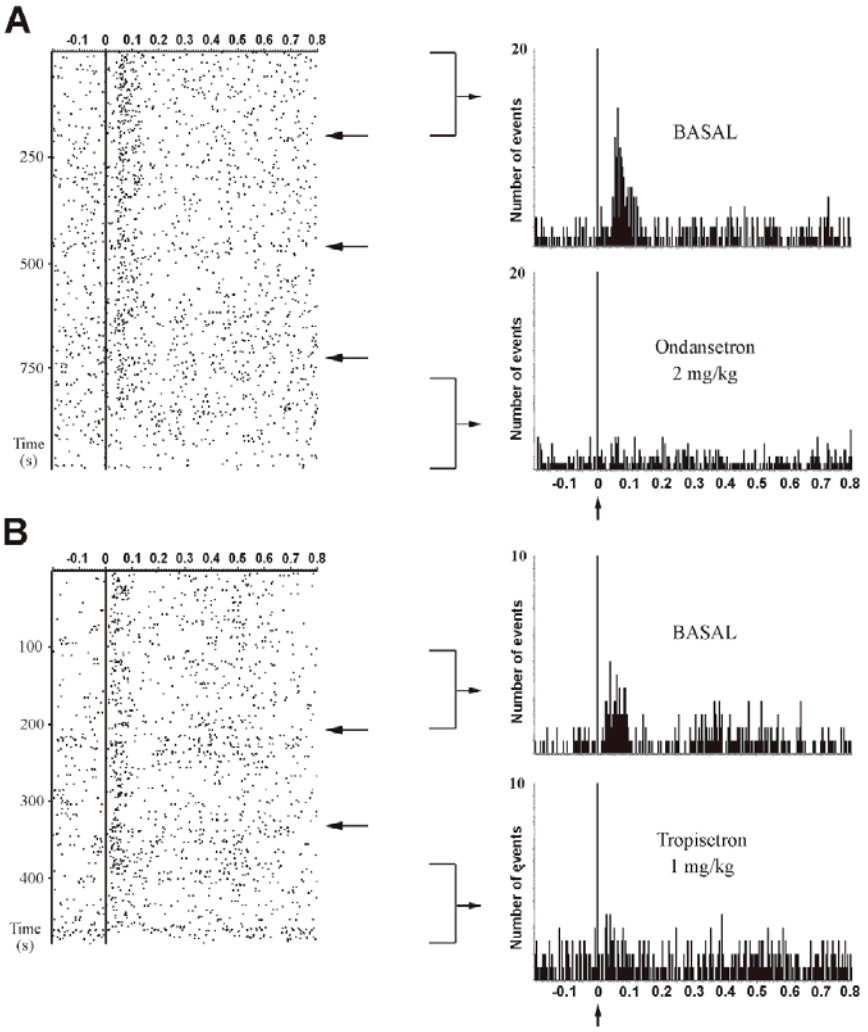

Figure 3. Blockade of the 5-HT-induced excitations in putative GABAergic neurons by the 5-HT_3 antagonists ondansetron and tropisetron. (*A*) Raster display and PSTHs of a neuron in basal conditions and after the administration of ondansetron (0.5–2 mg/kg i.v. cumulative doses; injection time shown by arrows in the raster display). Note the complete suppression of the DR-induced orthodromic excitation by ondansetron. Each PSTH corresponds to 200 triggers; bin size 4 ms. (*B*) Raster display and PSTHs of a neuron in basal conditions and after the administration of tropisetron (0.5–1 mg/kg i.v. cumulative doses; injection times shown by arrows in the raster display). Note the marked suppression of the DR-induced orthodromic excitation induced by tropisetron. Each PSTH corresponds to 100 triggers; bin size 4 ms. The brackets denote the times in the raster displays at which PSTH have been constructed. *x*-axis units are in seconds.

layers. However, due to the lower number of GABAergic neurons in layer I compared to other layers, the percentage of double-labeled cells was greater in this layer (40% in layer I versus 18% in layers II–III and 6–8% in deeper layers; Table 2).

We observed a minority of cells expressing the 5-HT_3 receptor mRNA which apparently were not positive for GAD mRNA (Table 2). This suggests that the 5-HT_3 receptor transcript may also be present in a few non-GABAergic neurons. A pilot double *in situ* hybridization experiment showed the presence of some 5-HT_3 receptor-positive cells which also contained the vGluT1 mRNA, yet these results require further confirmation. Likewise, it cannot be excluded that those are GABAergic cells with a faint labeling (e.g. poor penetration of the oligonucleotides or the antibody against digoxygenin).

5-HT_{2A} and 5-HT_3 receptors mediate direct excitatory responses of 5-HT on the cells expressing these receptors (see Introduction). A previous immunohistochemical study suggested the localization of these two 5-HT receptors in different subpopulations of GABAergic interneurons in monkey neocortex (Jakab and Goldman-Rakic, 2000). We therefore examined the localization of cells expressing these receptors in the mPFC. As observed in the prelimbic area of PFC (Fig. 6), 5-HT_3 receptor-expressing cells were located near the midline, in layers I–III. Shown in the same figure are the cells positive for vGluT1 (Fig. 6*A*) and GAD (Fig. 6*B*) mRNAs in layers I–VI of this cortical area. GAD-positive cells were present in all layers, including layer I where, as expected, pyramidal cells (vGluT1-expressing) were absent. On the other

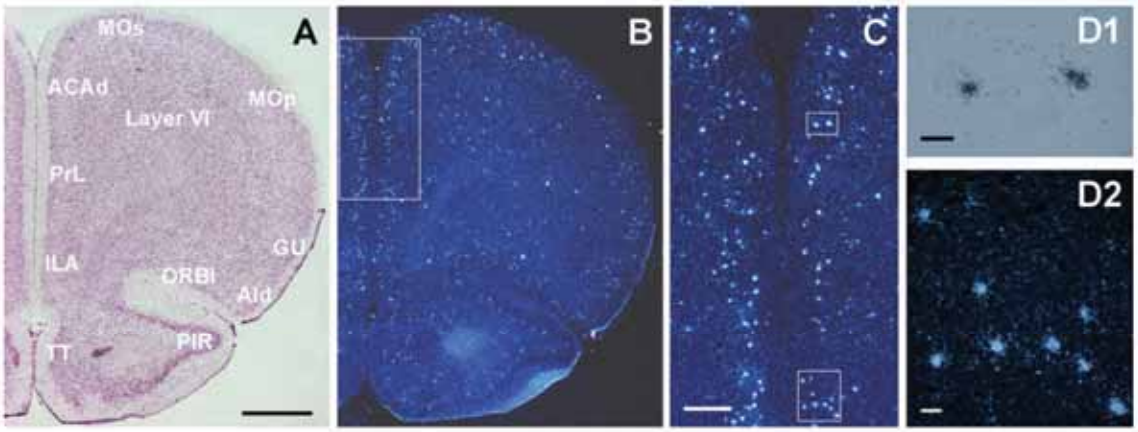

Figure 4. Visualization of 5-HT_3 receptor mRNA in the rat prefrontal cortex. (*A*) Nissl stained section consecutive to *B* used as anatomical reference for the areas where 5-HT_3 receptors are expressed. (*B*) Macroscopic dark-field image from an emulsion-dipped coronal section showing the localization of cells containing 5-HT_3 receptor mRNA. Note the preferential expression in superficial cortical layers in all cortical areas. Frame in *B* limits the approximate area shown at higher magnification in panel *C*. High magnification bright field (*D1*) and dark field (*D2*) photomicrographs of the areas marked in *C*, showing individual cells expressing 5-HT_3 receptors. Note the abundance of silver grains. ACAd, anterior cingulate (dorsal); AId, agranular insular (dorsal); GU, gustatory area; ILA, infralimbic area; MOp, primary motor area; MOs, secondary motor area, layer VI; ORBl, orbital area (lateral); PIR, piriform area; PrL, prelimbic area; TT, taenia tecta. Scale bar = 1 mm (*A, B*); 250 μm (*C*); 30 μm (*D1, D2*).

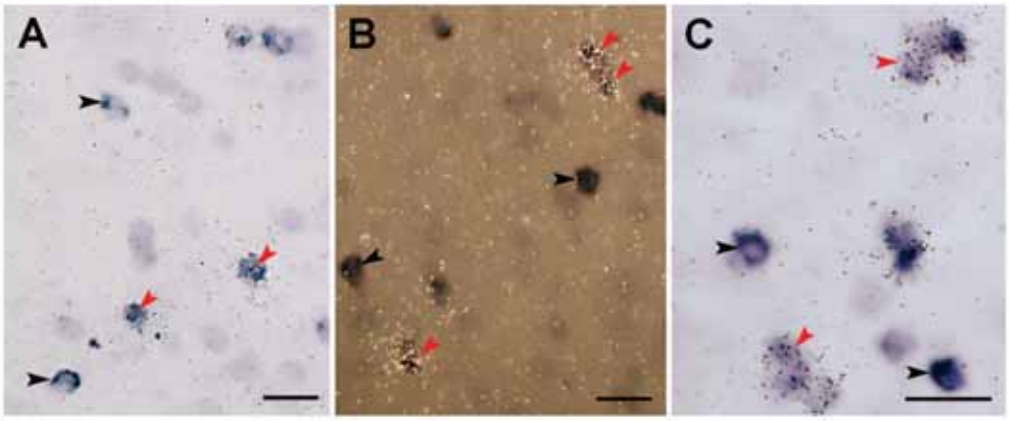

Figure 5. High magnification photomicrographs showing the detection in layers II–III of prelimbic and cingulate areas of 5-HT_3 receptor mRNA using ^{33}P-labeled oligonucleotides (silver grains) in GABAergic cells, visualized by hybridization with Dig-labeled oligonucleotides complementary to GAD mRNA (dark precipitate). (*A, C*) Bright-field photomicrographs showing the presence of several double-labeled cells (red arrowheads) as well as GABAergic cells not expressing the 5-HT_3 receptor (black arrowheads) in the infralimbic (*A*) and prelimbic (*C*) areas. (*B*) Dark-field photomicrograph showing three double-labeled cells with a very dense labeling of the 5-HT_3 receptor transcript (silver grains are seen as yellowish dots) in the dorsal anterior cingulate area. Scale bar = 20 μm.

hand, cells expressing 5-HT_{2A} receptors were located mainly in layers III–V, an area where the 5-HT_3 receptor mRNA was much less abundant (Fig. 6*C*,*D*). The 5-HT_{2A} receptor transcript is expressed by ~60% of pyramidal (vGluT1-positive) cells and by ~25% of GABAergic cells (GAD-positive; Santana *et al.*, 2004). However, the proportion between 5-HT_{2A} receptors in GAD- and vGluT1-positive cells is similar in all areas of the PFC and, therefore, the total population of cells positive for the 5-HT_{2A} receptor mRNA is representative of that in GABAergic neurons. The conspicuous absence of cells containing the 5-HT_{2A} receptor mRNA in layer I indicates that the GABAergic neurons close to the midline express 5-HT_3 but not 5-HT_{2A} receptors.

Discussion

The present study shows that (i) endogenous 5-HT excites putative GABAergic interneurons in the medial PFC through the activation of 5-HT_3 receptors and (ii) GAD- and 5-HT_3 receptor-expressing cells are mainly located in superficial layers of the PFC, a location different – but complementary – to that of GABAergic neurons expressing 5-HT_{2A} receptors. These results add to previous studies in rat PFC indicating that 5-HT modulates the activity of cortical microcircuits in various ways, either directly through the activation excitatory and inhibitory receptors in pyramidal neurons or indirectly, through the activation of excitatory receptors in selected populations of GABAergic interneurons.

Methodological Considerations

Previous studies examining the cellular phenotypes expressing 5-HT_3 receptors used GABA immunoreactivity to label GABAergic interneurons (Morales *et al.*, 1996; Morales and Bloom, 1997). Here we identified GABAergic neurons by the presence of GAD67 or GAD65 mRNAs. Immunohistochemical and *in situ* hybridization histochemistry indicate that the majority of GABA-containing neurons in the brain co-express the genes encoding the two GAD isoforms (Erlander *et al.*, 1991; Esclapez *et al.*, 1993, 1994; Feldblum *et al.*, 1993). On the other hand, the cloning and characterization of glutamate vesicular transporters, vGluT1, vGluT2 and vGluT3, in rat brain (Takamori *et al.*, 2000, 2001; Gras *et al.*, 2002) has enabled the histological identification of a glutamatergic neuronal phenotype (Fremeau *et al.*, 2001; Takamori *et al.*, 2001; Gras *et al.*, 2002; Oliveira *et al.*, 2003). In particular, most rat cortical cells express very high levels of vGluT1 mRNA (Gras *et al.*, 2002; Ziegler *et al.*, 2002), which supports the use of vGluT1 to identify cortical glutamatergic pyramidal neurons.

Several classifications of GABAergic interneurons have been made, based on their morphology, chemical neuroanatomy and electrophysiological characteristics (De Felipe, 2002; Freund, 2003). Considering their firing characteristics when

Table 2
Expression of 5-HT_3 receptors in prelimbic cortex

	Layer I	Layers II–III	Layer V	Layer VI
GAD mRNA	6.6 ± 0.4*	22.1 ± 1.2	26.7 ± 1.5	23.9 ± 0.1
GAD + 5-HT_3 receptor mRNAs	2.6 ± 0.2***	4.1 ± 0.5*	1.5 ± 0.3	2.0 ± 0.1
5-HT_3 receptor mRNA alone	0.2 ± 0.1	0.4 ± 0.1	0.1 ± 0.1	0.1 ± 0.1
% double-labeled cells	40 ± 2*	18 ± 2**	6 ± 1	8.2 ± 0.4

*$P < 0.05$ versus the rest of layers, **$P < 0.05$ versus deeper layers, *** $P < 0.05$ versus layers II–V (Tukey *t*-test).
Data are number of cells expressing the corresponding mRNAs in the various cortical layers in the prelimbic area (mean ± SEM of three rats). The values for each rat were calculated by averaging the number of cells in three consecutive fields per section (three sections per rat) as observed at ×40 magnification in a Nikon Eclipse E1000 microscope. Layer and area nomenclature are according to Swanson (1998).

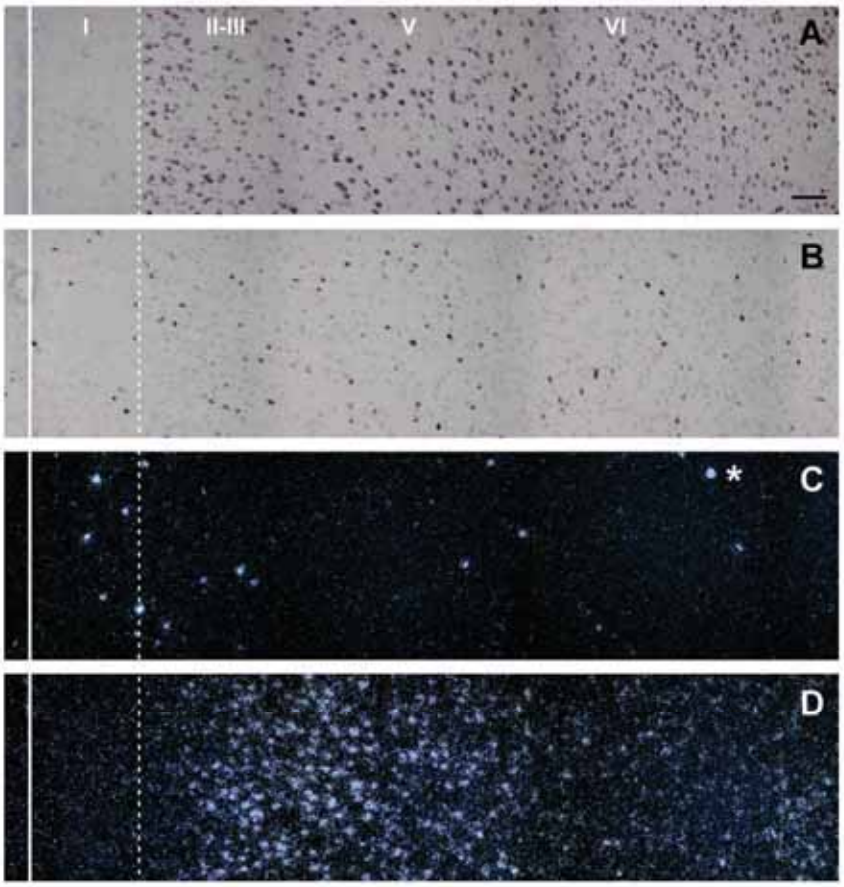

Figure 6. Composite photomicrographs showing the localization of cells expressing vGluT1 (*A*), GAD (*B*), 5-HT_3 (*C*) and 5-HT_{2A} (*D*) mRNAs through layers I–VI at the level of the prelimbic area in the rat PFC. The continuous vertical line denotes the location of the midline whereas the dotted line shows the approximate border between layer I and II. Each panel (*A*–*D*) corresponds to three consecutive microscopic fields. Pyramidal neurons (as visualized by vGluT1 mRNA) are present in layers II–VI whereas GAD mRNA-positive cells are present in all layers, including layer I. Note the different location of cells expressing 5-HT_3 (*C*) and 5-HT_{2A} receptors (*D*). 5-HT_3 receptor transcript is expressed by a limited number of cells present in layers I–III, particularly in the border between layers I and II. However, they represent 40% of GABAergic neurons in layer I. On the other hand, cells in these locations, particularly in layer I, do not express 5-HT_{2A} receptors (note that only a small proportion of the latter receptors are expressed by GABAergic neurons, Santana *et al.*, 2004). The asterisk denotes an artifact of the emulsion, seen in the dark field. Scale bar = 150 μm.

recorded intracellularly, GABA interneurons have been classified as fast-spiking and non-fast-spiking (both regular and irregular) cells (Cauli *et al.*, 1997; Férézou *et al.*, 2002; Kawaguchi and Kondo, 2002). Although extracellular recordings cannot discriminate between these cellular types, here we observed two main firing patterns of putative GABAergic interneurons, namely slow (non-fast-spiking, not firing in trains, discharge rate <3 spikes/s) and fast-spiking cells (firing in trains, discharge rate >10 spikes/s; Constantinidis and Goldman-Rakic, 2002). Indeed, due to the inherent complexity of the *in vivo* recordings of putative GABAergic neurons, a limitation of the present study is that the recorded units were not neurochemically characterized. However, it is unlikely that these were pyramidal neurons, in view of the following reasons. First, they were not antidromically activated from the DR or the mediodorsal thalamus, which make up two main targets of the axons of mPFC pyramidal neurons, where recordings were made (Thierry *et al.*, 1983; Peyron *et al.*, 1998; Groenewegen and Uylings, 2000). Secondly, more than half of the successful recordings were made close to the midline (0.2–0.5 mm lateral) to target the GAD- + 5-HT_3-receptor-labelled cells observed in the parallel *in situ* hybridization studies. In close agreement with the present observations, Zhou and Hablitz (1999) recorded 5-HT_3 receptor-mediated responses *in vitro* in layer I of cortical slices. Thirdly, the DR-induced excitations were unequivocally mediated by 5-HT_3 receptor activation since they were reversed by the selective antagonists ondansetron and tropisetron. Thus, although there may be a very small proportion of 5-HT_3 receptors in non-GABAergic neurons (Morales and Bloom, 1997; this study) it is unlikely that these were recorded.

Effect of DR Stimulation on Putative GABAergic Neurons in mPFC

Cortical microcircuits consist of principal (pyramidal) neurons and local (mainly GABAergic) interneurons that modulate pyramidal activity (Somogyi *et al.*, 1998). 5-HT can modulate the activity of these microcircuits in various ways. Direct inhibitory and excitatory actions on pyramidal neurons are mediated by 5-HT_{1A} and 5-HT_{2A} receptors respectively (Araneda and Andrade, 1991; Aghajanian and Marek, 1997, 1999; Zhou and Hablitz, 1999). Indirect actions are mediated by the activation of 5-HT receptors present on GABAergic interneurons and afferent terminals (heteroceptors; e.g. 5-HT_{1B}) (Ashby *et al.*, 1990; Tanaka and North, 1993; Zhou and Hablitz, 1999). The electrical stimulation of the DR and MnR in the anesthetized rat can excite or inhibit pyramidal neurons in the cingulate and prelimbic PFC through the activation of 5-HT_{2A} and 5-HT_{1A} receptors, respectively (Puig *et al.*, 2003; Amargós-Bosch *et al.*, 2004). In this manner, 5-HT may influence the descending excitatory input into limbic and motor structures where the prefrontal cortex projects (Groenewegen and Uylings, 2000).

However, the role of 5-HT_3 receptors in the control of cortical neurons is less well understood. These receptors have been reported to be present in axons and in the somatodendritic region of cortical neurons (Miquel *et al.*, 2002). The microiontophoretic application of 5-HT and selective 5-HT_3 agonists in the rat mPFC suppressed the firing of cells in layers II–III, an effect blocked by 5-HT_3 receptor antagonists (Ashby *et al.*, 1989, 1991, 1992). Likewise, the stimulation of ascending serotonergic fibers at high frequency (15 Hz) evoked a suppression of cortical, possibly pyramidal, cells which was also blocked by 5-HT_3 antagonists (Ashby *et al.*, 1991, 1992). Based on the inability of the microiontophoretic application of the $GABA_A$ receptor antagonist SR 95103 to block these effects, it was concluded that cortical neurons were directly inhibited through 5-HT_3 receptor activation (Ashby *et al.*, 1989, 1991, 1992). In contrast to these reports, whole cell recordings in rat sensorimotor cortex revealed that 5-HT induces a fast synaptic excitation in a subpopulation of regular or irregular slow-spiking (but not fast-spiking) VIP- and CCK-containing GABAergic interneurons in layer II (Férézou *et al.*, 2002). These effects were mimicked by the 5-HT_3 receptor agonist *m*-phenylbiguanide and blocked by tropisetron, indicating the involvement of 5-HT_3 receptors, whose presence in the recorded neurons was determined by single cell RT-PCR (Férézou *et al.*, 2002). Moreover, 5-HT and the 5-HT_3 agonist 1-(*m*-chlorophenyl)-biguanide increased a TTX-independent inward current in layer I interneurons (Zhou and Hablitz, 1999). This cortical effect is consistent with the ionic characteristics of the 5-HT_3 receptor (Maricq *et al.*, 1991) and agrees with earlier data in hippocampus showing that 5-HT can excite GABA interneurons through 5-HT_3 receptors (Ropert and Guy, 1991; Kawa, 1994; McMahon and Kauer, 1997). Thus, these observations suggest that the 5-HT_3 receptor-mediated inhibitory action of 5-HT on cortical pyramidal neurons is indirect, involving an increase of local GABA inputs.

Our *in vivo* data in mPFC accord with the above *in vitro* observations (Zhou and Hablitz, 1999; Férézou *et al.*, 2002) and indicate that 5-HT, released in the PFC by the physiological stimulation of the DR, can excite slow-spiking GABAergic neurons through the activation of 5-HT_3 receptors. However, unlike to the exogenous *in vitro* application of 5-HT (Zhou and Hablitz, 1999), the response to endogenous 5-HT does not appear to desensitize, at least during the observation period used herein (4 min). The inability of the DR stimulation to evoke a similar excitation in spontaneous fast-spiking interneurons agrees with the fact that 5-HT_3 receptors are only expressed by a subpopulation of GABAergic neurons (Morales and Bloom, 1997; Férézou *et al.*, 2002; this study). We cannot give an estimate of the proportion of cells responding to DR stimulation with 5-HT_3 receptor-mediated responses, but indeed this is very low, consistent with the low proportion of neurons expressing 5-HT_3 receptor observed in the parallel histological study. Systematic descents in the recording area enabled to record few cells that (i) were spontaneously firing, (ii) were not antidromically activated from the DR or the mediodorsal thalamus and (iii) responded to DR stimulation with an excitation that (iv) was blocked by 5-HT_3 receptor antagonists. Hence, although the total number of cells reported here may appear low (n = 11), a much larger number were recorded to obtain such data. Similarly, Férézou *et al.* (2002) reported that only 19 out of a total of 107 attempted neurons were excited *in vitro* by 5-HT through 5-HT_3 receptors in slices of sensorimotor cortex.

The latency and duration of the 5-HT receptor-mediated excitations in putative GABAergic neurons were shorter than those observed in pyramidal neurons in the same areas of the PFC after the stimulation of the DR at the same rate (the latter are 5-HT_{2A} receptor-mediated; Puig *et al.*, 2003; Amargós-Bosch *et al.*, 2004). This difference may indicate a higher conduction velocity of the 5-HT fibers targeting 5-HT_3 receptors. Indeed, two main types of serotonergic axons have been reported that differ in their morphology (Kosofsky and Molliver, 1987). On

the other hand, this difference could also be attributed to the ionic nature of the 5-HT_3 response which results in fast synaptic actions of 5-HT on these neurons (Maricq *et al.*, 1991; Férézou *et al.*, 2002). In contrast, the actions of 5-HT_{2A} receptors on neuronal excitability are mediated by metabotropic mechanisms (Aghajanian, 1995). The short latency and duration 5-HT_3 receptor-mediated activation of GABAergic inputs onto pyramidal neurons may perhaps contribute to a short-latency, 5-HT_{1A} receptor-independent inhibition observed in pyramidal neurons after the stimulation of the DR (Amargós-Bosch *et al.*, 2004).

Localization of GABAergic Neurons Expressing 5-HT_3 Receptors

Consistent with previous data in various telencephalic areas in rat (Morales and Bloom, 1997) and mouse brain (Hermann *et al.*, 2002), here we found that a very large proportion of 5-HT_3 receptor is expressed by GABAergic neurons in PFC. Few non-GABAergic cells exhibited the presence of the 5-HT_3 receptor transcript. Given the larger proportion of pyramidal versus GABAergic cells in neocortex (the latter represent a 15% of total; Beaulieu, 1993) we cannot exclude that a minority of the 5-HT_3 receptor-positive cells are pyramidal neurons.

5-HT_3 receptor-immunoreactive cells were found through all layers in frontal, temporal and parietal cortex in monkeys (Jakab and Goldman-Rakic, 2000). In contrast, these appear to be located preferentially in superficial layers in the rat, as judged from histological and functional studies (Morales and Bloom, 1997; Zhou and Hablitz, 1999; Férézou *et al.*, 2002; this study). In particular, we show an enrichment of these cells in superficial layers of the cingulate, prelimbic and infralimbic areas of the rat PFC. This localization suggests that 5-HT_3 receptors may be the target of the dense plexus of serotonergic fibers in superficial cortical layers (Blue *et al.*, 1988). Indeed, the expression of other cortical 5-HT receptors, such as 5-HT_{1A}, 5-HT_{2A}, or 5-HT_{2C} is more marked in intermediate and deep layers (Pompeiano *et al.*, 1992, 1994; Amargós-Bosch *et al.*, 2004; Santana *et al.*, 2004; see also Fig. 6). Interestingly, the distribution of cells expressing 5-HT_3 and 5-HT_{2A} receptors in PFC seems complementary. The latter were expressed in glutamatergic and GABAergic neurons in layers III–V of the PFC, with a conspicuous absence in layers I–II and a low expression in layer VI (Amargós-Bosch *et al.*, 2004; Santana *et al.*, 2004; this study). Only a small proportion of all 5-HT_{2A} receptor-expressing cells is GABAergic (Santana *et al.*, 2004), although their distribution follows the pattern of all 5-HT_{2A} receptor-containing cells. In contrast, 5-HT_3 receptor-expressing cells were found near the midline (particularly layers I–III) and – to a much lesser extent – in layer VI. 5-HT_3 receptors have been localized to calbindin- and calretinin-containing, small size GABAergic interneurons, whereas 5-HT_{2A} receptors are expressed by parvalbumin-containing large size interneurons (e.g. basket cells) (Morales and Bloom, 1997; Jakab and Goldman-Rakic, 1998, 2000). The presence of 5-HT_3 receptors in layer I GABAergic neurons, a cortical level devoid of pyramidal cell bodies (see, for instance, Fig. 6), suggests that 5-HT can modulate the inputs onto the apical dendrites of pyramidal neurons in PFC via 5-HT_3 receptors located in GABAergic interneurons. In this manner, 5-HT might modulate the cortico-cortical and thalamo-cortical inputs into superficial layers through an enhancement of synaptic GABAergic inputs (Krettek and Price, 1977; Linke and Schwegler, 2000; Mitchell and Cauler, 2001). On the other hand, 5-HT_{2A} receptors are involved in the feed-forward inhibition of pyramidal neurons through large, perisomatic parvalbumin-containing GABAergic neurons (Jakab and Goldman-Rakic, 2000). Thus, although the present study did not characterize the subtype(s) of GABAergic interneurons expressing 5-HT_3 and 5-HT_{2A} receptors, the distinct localization of cells expressing one or other receptor strongly supports an anatomical and functional segregation of both receptors in cortical microcircuits in the rat PFC, as observed in macaque cortex (Jakab and Goldman-Rakic, 2000). Moreover, 5-HT_3 receptor-mediated excitations are faster and last less than those induced by the activation of 5-HT_{2A} receptors, which indicates that 5-HT_{2A} and 5-HT_3 receptor-mediated responses are also temporally segregated.

In summary, the present study adds to previous *in vivo* data indicating that endogenous 5-HT, released by the physiological stimulation of the DR, is able to control the activity of neurons in the cingulate and prelimbic areas of the PFC through various cortical receptors, in particular the 5-HT_{1A}, 5-HT_{2A} and 5-HT_3 subtypes (Puig *et al.*, 2003; Amargós-Bosch *et al.*, 2004). The distinct temporal patterns of activation and the different cellular localizations of these receptors suggest a complex regulation of the cortical activity by 5-HT which deserves further investigation.

Notes

Work supported by grants from SAF2001-2133 and La Marató de TV3. P.C. is recipient of a Ramón y Cajal contract from the Ministry of Science and Technology. N.S. and M.V.P. are recipients of predoctoral fellowships from CICYT and IDIBAPS, respectively. We thank VITA-INVEST for the generous supply of ondansetron.

Address correspondence to Francesc Artigas, Department of Neurochemistry, Institut d'Investigacions Biomèdiques de Barcelona (CSIC), IDIBAPS, Rosselló 161, 6th floor, 08036 Barcelona, Spain. Email: fapnqi@iibb.csic.es.

References

Aghajanian GK (1995) Electrophysiology of serotonin receptor subtypes and signal transduction pathways. In: Pscyhopharmacology: the fourth generation of progress (Bloom FE, Meltzer HY, eds), pp. 451–460. New York: Raven Press.

Aghajanian GK, Marek GJ (1997) Serotonin induces excitatory postsynaptic potentials in apical dendrites of neocortical pyramidal cells. Neuropharmacology 36:589–599.

Aghajanian GK, Marek GJ (1999) Serotonin-glutamate interactions: a new target for antipsychotic drugs. Neuropsychopharmacology 21:S122–S133.

Amargós-Bosch M, Bortolozzi A, Puig MV, Serrats , Adell A, Celada P, Toth M, Mengod G, Artigas F (2004) Co-expression and *in vivo* interaction of serotonin$_{1a}$ and serotonin$_{2a}$ receptors in pyramidal neurons of prefrontal cortex. Cereb Cortex 14:281–299.

Araneda R, Andrade R (1991) 5-Hydroxytryptamine-2 and 5-hydroxytryptamine-1A receptors mediate opposing responses on membrane excitability in rat association cortex. Neuroscience 40:399–412.

Arango V, Underwood MD, Mann JJ (2002) Serotonin brain circuits involved in major depression and suicide. Prog Brain Res 136:443–453.

Ashby CR, Edwards E, Harkins K, Wang RY (1989) Characterization of 5-hydroxytryptamine$_3$ receptors in the medial prefrontal cortex: a microiontophoretic study. Eur J Pharmacol 173:193–196.

Ashby CR, Jiang LH, Kasser RJ, Wang RY (1990) Electrophysiological characterization of 5-hydroxytryptamine-2 receptors in the rat medial prefrontal cortex. J Pharmacol Exp Ther 252:171–178.

Ashby CR Jr, Minabe Y, Edwards E, Wang RY (1991) 5-HT_3-like receptors in the rat medial prefrontal cortex: an electrophysiological study. Brain Res 550:181–191.

Ashby CR, Edwards E, Wang RY (1992) Action of serotonin in the medial prefrontal cortex: mediation by serotonin3-like receptors. Synapse 10:7–15.

Beaulieu C (1993) Numerical data on neocortical neurons in adult rat, with special reference to the GABA population. Brain Res 609:284–292.

Blandina P, Goldfarb J, Craddock-Royal B, Green JP (1989) Release of endogenous dopamine by stimulation of 5-hydroxytryptamine$_3$ receptors in rat striatum. J Pharmacol Exp Ther 251:803–809.

Blue ME, Yagaloff KA, Mamounas LA, Hartig PR, Molliver ME (1988) Correspondence between 5-HT_2 receptors and serotonergic axons in rat neocortex. Brain Res 453:315–328.

Cauli B, Audinat E, Lambolez B, Angulo MC, Ropert N, Tsuzuki K, Hestrin S, Rossier J (1997) Molecular and physiological diversity of cortical nonpyramidal cells. J Neurosci 17:3894–3906.

Celada P, Puig MV, Casanovas JM, Guillazo G, Artigas F (2001) Control of dorsal raphe serotonergic neurons by the medial prefrontal cortex: involvement of serotonin-1A GABA(A) and glutamate receptors. J Neurosci 21:9917–9929.

Chen J, Paredes W, Van Praag HM, Lowinson JH, Gardner EL (1992) Presynaptic dopamine release is enhanced by 5-HT_3 receptor activation in medial prefrontal cortex of freely moving rats. Synapse 10:264–266.

Constantinidis C, Goldman-Rakic PS (2002) Correlated discharges among putative pyramidal neurons and interneurons in the primate prefrontal cortex. J Neurophysiol 88:3487–3497.

De Deurwaerdère P, Stinus L, Spampinato U (1998) Opposite change of *in vivo* dopamine release in the rat nucleus accumbens and striatum that follows electrical stimulation of dorsal raphe nucleus: role of 5-HT_3 receptors. J Neurosci 18:6528–6538.

De Quervain DJ, Henke K, Aerni A, Coluccia D, Wollmer MA, Hock C, Nitsch RM, Papassotiropoulos A (2003) A functional genetic variation of the 5-HT_{2A} receptor affects human memory. Nat Neurosci 6:1141–1142.

De Felipe J (2002) Cortical interneurons: from Cajal to 2001. Prog Brain Res 136:215–238.

Edwards E, Ashby CRJ, Wang RY (1991) The effect of typical and atypical antipsychotic drugs on the stimulation of phosphoinositide hydrolysis produced by the 5-HT_3 receptor agonist 2-methyl-serotonin. Brain Res 545:276–278.

Erlander MG, Tillakaratne NJ, Feldblum S, Patel N, Tobin AJ (1991) Two genes encode distinct glutamate decarboxylases. Neuron 7:91–100.

Esclapez M, Tillakaratne NJ, Tobin AJ, Houser CR (1993) Comparative localization of mRNAs encoding two forms of glutamic acid decarboxylase with nonradioactive *in situ* hybridization methods. J Comp Neurol 331:339–362.

Esclapez M, Tillakaratne NJ, Kaufman DL, Tobin AJ, Houser CR (1994) Comparative localization of two forms of glutamic acid decarboxylase and their mRNAs in rat brain supports the concept of functional differences between the forms. J Neurosci 14:1834–1855.

Feldblum S, Erlander MG, Tobin AJ (1993) Different distributions of GAD_{65} and GAD_{67} mRNAs suggest that the two glutamate decarboxylases play distinctive functional roles. J Neurosci Res 34:689–706.

Férézou I, Cauli B, Hill EL, Rossier J, Hamel E, Lambolez B (2002) 5-HT_3 receptors mediate serotonergic fast synaptic excitation of neocortical vasoactive intestinal peptide/cholecystokinin interneurons. J Neurosci 22:7389–7397.

Fremeau RT Jr, Troyer MD, Pahner I, Nygaard GO, Tran CH, Reimer RJ, Bellocchio EE, Fortin D, Storm-Mathisen J, Edwards RH (2001) The expression of vesicular glutamate transporters defines two classes of excitatory synapse. Neuron 31:247–260.

Freund TF (2003) Interneuron diversity series: rhythm and mood in perisomatic inhibition. Trends Neurosci 26:489–495.

Fuller JH, Schlag JD (1976) Determination of antidromic excitation by the collision test: problems of interpretation. Brain Res 112:283–298.

Fuster JM (2001) The prefrontal cortex – an update: time is of the essence. Neuron 30:319–333.

Goldman-Rakic PS (1996) Regional and cellular fractionation of working memory. Proc Natl Acad Sci USA 93:13473–13480.

Gras C, Herzog E, Bellenchi GC, Bernard V, Ravassard P, Pohl M, Gasnier B, Giros B, El Mestikawy S (2002) A third vesicular glutamate transporter expressed by cholinergic and serotoninergic neurons. J Neurosci 22:5442–5451.

Groenewegen HJ, Uylings HB (2000) The prefrontal cortex and the integration of sensory limbic and autonomic information. Prog Brain Res 126:3–28.

Hall H, Farde L, Halldin C, Lundkvist C, Sedvall G (2000) Autoradiographic localization of 5-HT(2A) receptors in the human brain using [^{3}H]M100907 and [^{11}C]M100907. Synapse 38:421–431.

Harder JA, Ridley RM (2000) The 5-HT_{1A} antagonist WAY 100 635 alleviates cognitive impairments induced by dizocilpine (MK-801) in monkeys. Neuropharmacology 39:547–552.

Hermann H, Marsicano G, Lutz B (2002) Coexpression of the cannabinoid receptor type 1 with dopamine and serotonin receptors in distinct neuronal subpopulations of the adult mouse forebrain. Neuroscience 109:451–460.

Higgins GA, Kilpatrick GJ (1999) 5-HT(3) receptor antagonists. Expert Opin Invest Drugs 8:2183–2188.

Jakab RL, Goldman-Rakic PS (1998) 5-Hydroxytryptamine(2A) serotonin receptors in the primate cerebral cortex: possible site of action of hallucinogenic and antipsychotic drugs in pyramidal cell apical dendrites. Proc Natl Acad Sci USA 95:735–740.

Jakab RL, Goldman-Rakic PS (2000) Segregation of serotonin 5-HT_{2A} and 5-HT_3 receptors in inhibitory circuits of the primate cerebral cortex. J Comp Neurol 417:337–348.

Kawa K (1994) Distribution and functional properties of 5-HT_3 receptors in the rat hippocampal dentate gyrus: a patch-clamp study. J Neurophysiol 71:1935–1947.

Kawaguchi Y, Kondo S (2002) Parvalbumin, somatostatin and cholecystokinin as chemical markers for specific GABAergic interneuron types in the rat frontal cortex. J Neurocytol 31:277–287.

Kosofsky BE, Molliver ME (1987) The serotoninergic innervation of cerebral cortex: different classes of axon terminals arise from dorsal and median raphe nuclei. Synapse 1:153–168.

Krettek JE, Price JL (1977) The cortical projections of the mediodorsal nucleus and adjacent thalamic nuclei in the rat. J Comp Neurol 171:157–191.

Kroeze WK, Roth BL (1998) The molecular biology of serotonin receptors: therapeutic implications for the interface of mood and psychosis. Biol Psychiatry 44:1128–1142.

Landry M, Holmberg K, Zhang X, Hökfelt T (2000) Effect of axotomy on expression of NPY galanin and NPY Y1 and Y2 receptors in dorsal root ganglia and the superior cervical ganglion studied with double-labeling *in situ* hybridization and immunohistochemistry. Exp Neurol 162:361–384.

Linke R, Schwegler H (2000) Convergent and complementary projections of the caudal paralaminar thalamic nuclei to rat temporal and insular cortex. Cereb Cortex 10:753–771.

McMahon LL, Kauer JA (1997) Hippocampal interneurons are excited via serotonin-gated ion channels. J Neurophysiol 78:2493–2502.

Maricq AV, Peterson AS, Brake AJ, Myers RM, Julius D (1991) Primary structure and functional expression of the 5HT_3 receptor, a serotonin-gated ion channel. Science 254:432–437.

Martinez D, Hwang DR, Mawlawi O, Slifstein M, Kent J, Simpson N, Parsey RV, Hashimoto T, Huang YY, Shinn A, VanHeertum R, Abidargham A, Caltabiano S, Malizia A, Cowley H, Mann JJ, Laruelle M (2001) Differential occupancy of somatodendritic and postsynaptic 5HT(1A) receptors by pindolol: a dose-occupancy study with [C-11]WAY 100635 and positron emission tomography in humans. Neuropsychopharmacology 24:209–229.

Mello e Souza T, Rodrigues C, Souza MM, Vinade E, Coitinho A, Choi H, Izquierdo I (2001) Involvement of the serotonergic type 1A (5-

HT1A) receptor in the agranular insular cortex in the consolidation of memory for inhibitory avoidance in rats. Behav Pharmacol 12:349–353.

Meltzer HY (1999) The role of serotonin in antipsychotic drug action. Neuropsychopharmacology 21:S106–S115.

Miller EK, Cohen JD (2001) An integrative theory of prefrontal cortex function. Annu Rev Neurosci 24:167–202.

Miquel MC, Emerit MB, Nosjean A, Simon A, Rumajogee P, Brisorgueil MJ, Doucet E, Hamon M, Verge D (2002) Differential subcellular localization of the 5-HT_3-As receptor subunit in the rat central nervous system. Eur J Neurosci 15:449–457.

Misane I, Ögren SO (2003) Selective 5-HT_{1A} antagonists WAY 100635 and NAD-299 attenuate the impairment of passive avoidance caused by scopolamine in the rat. Neuropsychopharmacology 28:253–264.

Mitchell BD, Cauler LJ (2001) Corticocortical and thalamocortical projections to layer I of the frontal neocortex in rats.Brain Res. 921:68–77.

Morales M, Bloom FE (1997) The 5-HT_3 receptor is present in different subpopulations of GABAergic neurons in the rat telencephalon. J Neurosci 17:3157–3167.

Morales M, Battenberg E, Delecea L, Bloom FE (1996) The type 3 serotonin receptor is expressed in a subpopulation of GABAergic neurons in the rat neocortex and hippocampus. Brain Res 731:199–202.

O'Donnell P (2003) Dopamine gating of forebrain neural ensembles. Eur J Neurosci 17:429–435.

Oliveira AL, Hydling F, Olsson E, Shi T, Edwards RH, Fujiyama F, Kaneko T, Hokfelt T, Cullheim S, Meister B (2003) Cellular localization of three vesicular glutamate transporter mRNAs and proteins in rat spinal cord and dorsal root ganglia. Synapse 50:117–129.

Paxinos G, Watson C (1998) The rat brain in stereotaxic coordinates, 4th edn. Sydney: Academic Press.

Peyron C, Petit JM, Rampon C, Jouvet M, Luppi PH (1998) Forebrain afferents to the rat dorsal raphe nucleus demonstrated by retrograde and anterograde tracing methods. Neuroscience 82:443–468.

Pompeiano M, Palacios JM, Mengod G (1992) Distribution and cellular localization of mRNA coding for 5-HT_{1A} receptor in the rat brain: correlation with receptor binding. J Neurosci 12:440–453.

Pompeiano M, Palacios JM, Mengod G (1994) Distribution of the serotonin 5-HT_2 receptor family mRNAs: comparison between 5-HT_{2A} and 5-HT_{2C} receptors. Mol Brain Res 23:163–178.

Pritchett DB, Bach AW, Wozny M, Taleb O, Dal Toso R, Shih JC, Seeburg PH (1988) Structure and functional expression of cloned rat serotonin 5HT_2 receptor. EMBO J 7:4135–4140.

Puig MV, Celada P, Díaz-Mataix L, Artigas F (2003) *In vivo* modulation of the activity of pyramidal neurons in the rat medial prefrontal cortex by 5-HT_{2A} receptors. Relationship to thalamocortical afferents. Cereb Cortex 13:1870–1882.

Puig MV, Artigas F, Celada P (2004) Modulation of the activity of pyramidal neurons in rat prefrontal cortex by raphe stimulation *in vivo*: involvement of serotonin and GABA. Cereb Cortex (in press).

Ropert N, Guy N (1991) Serotonin facilitates GABAergic transmission in the CA1 region of rat hippocampus *in vitro*. J Physiol 441:121–136.

Santana N, Bortolozzi A, Serrats J, Mengod G, Artigas F (2004) Expression of serotonin$_{1A}$ and serotonin$_{2A}$ receptors in pyramidal and GABAergic neurons of the rat prefrontal cortex. Cereb Cortex (in press).

Serrats J, Mengod G, Cortés R (2003) Cellular localization of 5-HT_{1A} and 5-HT_{1B} receptor mRNAs in the raphe nuclei: A double *in situ* hybridization study throughout the raphe nuclei. Eur Neuropsychopharmacol 13(Suppl. 4):S104.

Sirota P, Mosheva T, Shabtay H, Giladi N, Korczyn AD (2000) Use of the selective serotonin 3 receptor antagonist ondansetron in the treatment of neuroleptic-induced tardive dyskinesia. Am J Psychiatry 157:287–289.

Somogyi P, Tanás G, Lujan R, Buhl EH (1998) Salient features of the synaptic organization in the cerebral cortex. Brain Res Rev 26:113–135.

Staubli U, Xu FB (1995) Effects of 5-HT_3 receptor antagonism on hippocampal theta rhythm, memory, and LTP induction in the freely moving rat. J Neurosci 15:2445–2452.

Swanson LW (1998) Brain maps: structure of the rat brain. Amsterdam: Elsevier.

Takamori S, Rhee JS, Rosenmund C, Jahn R (2000) Identification of a vesicular glutamate transporter that defines a glutamatergic phenotype in neurons. Nature 407:189–193.

Takamori S, Rhee JS, Rosenmund C, Jahn R (2001) Identification of differentiation – associated brain-specific phosphate transporter as a second vesicular glutamate transporter (VGLUT2). J Neurosci 21:193T.

Talvik-Lotfi M, Nyberg S, Nordstrom AL, Ito H, Halldin C, Brunner F, Farde L (2000) High 5HT_{2A} receptor occupancy in M100907-treated schizophrenic patients. Psychopharmacology 148:400–443.

Tanaka E, North RA (1993) Actions of 5 hydroxytryptamine on neurons of the rat cingulate cortex. J Neurophysiol 69:1749–1757.

Thierry AM, Deniau JM, Chevalier G, Ferron A, Glowinski J (1983) An electrophysiological analysis of some afferent and efferent pathways of the rat prefrontal cortex. Prog Brain Res 58:257–261.

Tomiyama M, Palacios JM, Cortés R, Vilaró MT, Mengod G (1997) Distribution of AMPA receptor subunit mRNAs in the human basal ganglia: an *in situ* hybridization study. Brain Res Mol Brain Res 46:281–289.

Wang M, Vijayraraghavan S, Goldman-Rakic PS (2003) Selective D2 receptor actions on working memory circuitry. Program No. 835.9. 2003 Absract/Viewer Itinerary Planner. Washington, DC: Society for Neuroscience.

Watling KJ, Beer MS, Stanton JA (1989) Effects of clozapine and other neuroleptics on binding of [3H]-Q ICS 205–930 to central 5-HT_3 recognition sites. Br J Pharmacol 98(Suppl.):813P.

Williams GV, Goldman-Rakic PS (1995) Modulation of memory fields by dopamine D1 receptors in prefrontal cortex. Nature 376:572–575.

Williams GV, Rao SG, Goldman-Rakic PS (2002) The physiological role of 5-HT_{2A} receptors in working memory. J Neurosci 22:2843–2854.

Zhou FM, Hablitz JJ (1999) Activation of serotonin receptors modulates synaptic transmission in rat cerebral cortex. J Neurophysiol 82:2989–2999.

Ziegler DR, Cullinan WE, Herman JP (2002) Distribution of vesicular glutamate transporter mRNA in rat hypothalamus. J Comp Neurol 448:217–229.

Trabajo 3

Antipsychotic drugs reverse the disruption in prefrontal cortex function produced by NMDA receptor blockade with phencyclidine

Kargieman L, Santana N, Mengod G, Celada P * and Artigas F*

*Authors with equal contribution to the study

Proceedings of the National Academy of Sciences, aceptado para publicación

La administración sistémica de fenciclidina (PCP), utilizada como modelo farmacológico de esquizofrenia, aumentó marcadamente la expresión de *c-fos* en una gran proporción de neuronas piramidales (50%) de CPF. Este aumento se dio tanto en el nivel de expresión celular como en el número de células que expresaron este marcador de actividad neuronal. Las interneuronas GABAérgicas de corteza prefrontal sin embargo, no experimentaron un aumento de la expresión de *c-fos* tras la administración de PCP. Por otra parte, la PCP aumentó la frecuencia de descarga del 45% de las neuronas piramidales registradas en CPF y la redujo en el 33% de éstas. Además, la administración sistémica de PCP redujo marcadamente la sincronía cortical en el rango de frecuencia delta (0.3-4 Hz), resultando en una descarga aleatoria de las neuronas piramidales. Ambos efectos (aumento de la expresión de *c-fos* y aumento de la excitablilidad neuronal) fueron revertidos por fármacos antipsicóticos.

La autora de la presente tesis contribuyó a este trabajo con los experimentos de doble hibridación *in situ*.

BIOLOGICAL SCIENCES

Pharmacology

Antipsychotic drugs reverse the disruption in prefrontal cortex function produced by NMDA receptor blockade with phencyclidine

Lucila Kargieman, Noemí Santana, Guadalupe Mengod, Pau Celada* and Francesc Artigas*

Department of Neurochemistry and Neuropharmacology
Institut d' Investigacions Biomèdiques de Barcelona (CSIC), IDIBAPS
08036 Barcelona, Spain

Corresponding authors:
Francesc Artigas, PhD; Pau Celada, PhD.
Dept. of Neurochemistry and Neuropharmacology,
Institut d' Investigacions Biomèdiques de Barcelona (CSIC), IDIBAPS,
Rosselló, 161, 6th floor,
08036 Barcelona, Spain.

Phone: +3493-363 8315;
Fax: +3493-363 8301; e-mail:
E-mail: fapnqi@iibb.csic.es

*Authors with equal contribution to the study

Abbreviations: CLZ, clozapine; CM, centromedial nucleus; GAD, glutamate decarboxylase; HAL, haloperidol; LFP, local field potential; MD, mediodorsal nucleus; PCP, phencyclidine; mPFC medial prefrontal cortex: vGluT1, vesicular glutamate transporter 1.

Abstract.

NMDA receptor (NMDA-R) antagonists are extensively used as schizophrenia models due to their ability to evoke positive and negative symptoms as well as cognitive deficits similar to those of the illness. Cognitive deficits in schizophrenia are associated with prefrontal cortex (PFC) abnormalities. These deficits are of particular interest since an early improvement in cognitive performance predicts a better long-term clinical outcome. Here we examined the effect of the non-competitive NMDA-R antagonist phencyclidine (PCP) on PFC function to understand the cellular and network elements involved in its schizomimeitc actions. PCP induces a marked disruption of the activity of the PFC in the rat, increasing and decreasing the activity of 45% and 33% of the pyramidal neurons recorded, respectively (22% of the neurons were unaffected). Concurrently, PCP markedly reduced cortical synchrony in the delta frequency range (0.3-4 Hz) as assessed by recording local field potentials. The subsequent administration of the antipsychotic drugs haloperidol and clozapine reversed PCP effects on pyramidal cell firing and cortical synchronization. PCP increased *c-fos* expression in PFC pyramidal neurons, an effect prevented by the administration of clozapine. PCP also enhanced *c-fos* expression in the centromedial and mediodorsal (but not reticular) nuclei of the thalamus, suggesting the participation of enhanced thalamocortical excitatory inputs. These results shed new light on the involvement of PFC in the schizomimetic action of NMDA-R antagonists and show that antipsychotic drugs may partly exert their therapeutic effect by normalizing a disrupted PFC activity, an effect that may add to subcortical dopamine receptor blockade

Introduction

Schizophrenia is associated with alterations in several brain areas, including the thalamus, the hippocampus, the amygdala and the prefrontal cortex (PFC), which are thought to underlie the deficits in working memory and executive functions exhibited by schizophrenic patients.[1-3] Autopsy and neuroimaging studies have revealed the existence of a reduced PFC volume, reduced layer thickness, tight packing of pyramidal neurons and reduced neuropil in the brains of schizophrenic patients.[1,2,4,5] Moreover, alterations in key neurotransmitters such as glutamate, GABA and dopamine have been reported in PFC.[3,5,6]

Non-competitive *N*-methyl-D-aspartate (NMDA) receptor (NMDA-R) antagonists such as the dissociative anesthetics ketamine and phencyclidine (PCP), have been extensively used as pharmacological models of schizophrenia due to their ability to evoke positive and negative symptoms of schizophrenia as well as the characteristic cognitive deficits of the illness in humans.[3,7] Neuroimaging studies suggest that these effects are associated with an increased PFC activity.[8] On the other hand, NMDA-R antagonists evoke a behavioral syndrome in experimental animals characterized by hyperlocomotion, stereotypies and disruption in pre-pulse inhibition of the startle response which is totally or partly antagonized by antipsychotic drugs.[9,10] However, the cellular elements and brain networks involved in these actions are still poorly known. Of great interest is the knowledge of the neurobiological basis of the cognitive deficits evoked by NMDA-R antagonists, since these are central to the pathology of schizophrenia and the improvement in cognitive performance may predict better therapeutic outcome.[11]

The aim of the present study was to examine the effects of PCP on PFC function and the possible reversal of these effects by antipsychotic drugs, using *in vivo* measures of cellular (single unit

extracellular recordings) and population activity (local field potentials, LFP). Additionally, we examined the effect of PCP on the expression of *c-fos*, a marker of neuronal activity, in PFC and afferent areas.

Materials and Methods

Animals and treatments. Male albino Wistar rats weighing 250–320 g were used (Iffa Credo, Lyon, France). Animal care followed the EU regulations (O.J. of the European Communities L358/1, December 18, 1986) and was approved by the Institutional Animal Care and Use Committee. Stereotaxic coordinates (in millimeters) were taken from bregma and duramater.[34] PCP and CLZ were from RBI (Natick, MA) and HAL (intramuscular preparation) was from Laboratorios Esteve (Barcelona, Spain).

In *c-fos* experiments, 4 groups of rats were administered i.p. with saline + saline, saline + PCP (10 mg/kg), CLZ (5 mg/kg) + saline and CLZ (5 mg/kg) + PCP (10 mg/kg), respectively. Time between injections was 30 min and rats were killed by anesthetic overdose and decapitated 1 h after the second injection. The brains rapidly removed, frozen on dry ice and stored at -20ºC.

Electrophysiology: single unit and LFP recordings. Rats were anesthetized (chloral hydrate, 400 mg/kg, i.p. followed by 50–70 mg/kg/h using a perfusion pump) and positioned in a David Kopf stereotaxic frame. Body temperature was maintained at 37°C with a heating pad. Pyramidal neurons were recorded extracellularly with glass micropipettes as described.[18,35] Briefly, single-unit extracellular recordings were amplified with a Neurodata IR283 (Cygnus Technology, Delaware Water Gap, PA), postamplified and filtered with a Cibertec (Madrid, Spain) amplifier and computed on-line using a DAT 1401plus interface system Spike2 software (Cambridge Electronic Design, Cambridge, UK). Descents in the mPFC were carried out at AP+3.2 to +3.4, L-0.5 to -1.0, DV -1.9 to -4.8 below brain surface. All recorded units were identified as pyramidal neurons by antidromic activation from DR or VTA and collision extinction with spontaneously occurring spikes as described.[18] After stable baseline activity for 5 min, PCP was injected, followed by CLZ or HAL in reversal experiments. Only one neuron per rat was recorded. In some cases, recording electrodes were filled with Pontamine sky blue to verify the recording site. Brain sections were stained with neutral red, according to standard procedures.

In situ hybridization histochemistry. The oligonucleotide probes used were: *c-fos* complementary to bases 131-178 (GenBank acc. no NM_022197); vesicular glutamate transporter vGluT1 (a glutamatergic cell marker) complementary to bases 127-172 and 1756-1800 (GenBank acc. no U07609); two oligonucleotides for each isoform glutamic acid decarboxylase (GAD65 and GAD67 to label GABAergic cells) complementary to bases 159-213 and 514-558 (GenBank acc. no NM_012563) and bp 191-235 and 1600-1653 (GenBank acc. no NM_017007). Labeling of the probes, tissue sectioning and *in situ* hybridization procedures were carried out as previously described.[35]

Data analysis. Changes in the firing rate or the proportion of burst firing in pyramidal neurons were assessed using ANOVA or paired Student's t test, as appropriate. Values were quantified during the last 2 min of the 5-min baseline recording and during 2 min after PCP or antipsychotic administration (omitting the first minute after injection). Drug response was defined as a ±30% change in firing rate from baseline. Bust analysis was carried out (Spike 2 software) using the method of Laviolette et al.[36] Briefly, a burst episode was defined as the occurrence of two or more spikes with an interspike interval of <45 ms.

Power spectra were constructed using Fast Fourier Transformations (FFT) of 1-min signal intervals (band-pass filter of 0.1-100 Hz) corresponding to baseline, PCP and PCP + antipsychotics with a resolution of 0.29 Hz (FFT size of 8192). Data are given as AUC of the power spectrum between 0.3-4 Hz. The temporal

coincidence of discharged spikes with the active phase (up) of delta oscillations recorded in PFC was examined (1-min periods) with a custom made script for the Spike 2 software. Briefly, the mean LFP voltage value was calculated for each 1-min period and the number of spikes occurring below and above this mean value were computed.

Photomicrographs were obtained with a Nikon Eclipse E1000 microscope. Cell counting was performed manually at the microscope. Only cellular profiles showing great abundance of both transcripts were considered to co-express both mRNAs. A semiquantitative measure of the optical densities was conducted for *in situ* hybridization studies with the AIS^R computerized image analysis system (Imaging Research Inc, St Catharines, Ontario, Canada). For each rat, individual values of optical densities and cell counts in prelimbic area of PFC were calculated as the mean of 2 adjacent sections of 3 rats per treatment group. The number of silver grains (representative of the level of expression of *c-fos*) in each *c-fos*-positive cell was counted manually in the same sections at a higher magnification in adjacent microscopic fields within the prelimbic area. Statistical analysis was performed using a statistical software package (GraphPad Prism 4, GraphPad Software Inc, San Diego, CA, USA). $p<0.05$ was considered statistically significant.

Results

Effects of PCP on the activity of mPFC pyramidal neurons

The effect of PCP was examined in 80 rats (one neuron per rat). The duration of the action potential was 0.97±0.05 ms (up phase; n = 80). All recorded units were pyramidal neurons in layers V-VI (mainly in prelimbic PFC), as assessed by antidromic activation from midbrain (46 from dorsal raphe, 34 from ventral tegmental area; see methods). Baseline firing rate was 2.2 ± 0.3 spikes/s (n = 80). Saline injections did not alter the firing rate of pyramidal neurons. PCP administration (0.25 mg/kg i.v.) evoked three types of responses. A 45 % of the neurons had their firing rate enhanced (to 286 % of baseline), another 33 % were inhibited (to 43 % of baseline) and the rest (22%) were unaffected by PCP (Fig. 1). A detailed account of the effects of PCP on firing rate and burst firing is given in Supplemental material 1. Figure 1 shows representative examples of neurons excited and inhibited by PCP as well as mean effects on firing rate.

The effect of PCP administration (0.25 mg/kg i.v.) on local field potentials (LFP) was examined in 20 rats. In some of them, single units and LFPs were simultaneously recorded and the signal split using the appropriate filters. PCP markedly reduced the cortical synchrony in the range 0.3-4 Hz (delta frequency). Saline injections did not alter LFPs. Overall, PCP reduced the power spectrum from 0.26±0.04 to 0.10±0.02 $\mu V^2/Hz$ ($p<0.001$, Student's *t*-test; n = 20). The reduction in the LFP amplitude was observed in all cases, irrespectively of whether the recorded unit was excited or inhibited by PCP. Fig. 2 shows examples of the effect of PCP on LFPs.

PCP induced a temporal disorganization of the discharge of pyramidal neurons. In baseline conditions, pyramidal discharge occurred only during the active phase of the LFP (corresponding to depolarized or "up" states recorded intracellularly[12]) (Fig. 2). The percentage of spikes discharged during active ("up") phases in baseline conditions was 90±3 %. PCP reduced this value to 59±11 % ($p<0.02$, paired Student's *t*- test; n = 9) (note that maximal effect size is to 50%, i.e. random discharge).

Antipsychotic drug reversal of PCP effects

Clozapine (CLZ, 1 mg/kg i.v.) or haloperidol (HAL, 0.1 mg/kg i.v.) had no significant effect on the spontaneous activity of mPFC pyramidal neurons, from 1.0±0.3 to 0.7±0.2 spikes/s (CLZ; n = 9) and from 4.2±1.8 to 3.6±1.7 spikes/s (HAL; n = 5). However, CLZ and HAL reversed the PCP-induced increase in pyramidal cell firing (Figure 3). Reversal was attempted in 16 neurons excited by 0.25 mg/kg i.v. PCP (9 with CLZ, 7 with HAL). CLZ (1 mg/kg, except 2 units at 2 mg/kg) reversed PCP effect ($F_{2,16}$ = 13.09 ; $p<0.001$). Likewise, HAL (0.1 mg/kg except

in 2 units at 0.2 mg/kg) reversed PCP effect ($F_{2,12}$ = 45.33, p<0.0001) (Fig. 3C). Similarly, both antipsychotic drugs significantly reversed the increase in burst activity induced by PCP (baseline = 85±28, PCP = 341±138, PCP+CLZ = 113±30, $F_{2,14}$ = 5.55, p < 0.02; baseline= 50±18, PCP = 338±112, PCP + HAL = 77±21, $F_{2,12}$ = 6.03, p < 0.02; data in spikes fired in bursts/2 min). PCP-induced inhibitions were not reversed by antipsychotics (n = 5 with CLZ, n = 3 with HAL).

CLZ and HAL also significantly reversed the loss in cortical synchrony in the 0.3-4 Hz range induced by PCP. A total of 17 rats were used in these experiments. The examples in fig. 3 show concurrent effects on the firing rate of recorded unit and on LFP. One way ANOVA revealed a significant effect of treatment ($F_{2,20}$ = 12.97, p<0.0002 for PCP + CLZ , n = 11 and $F_{2,10}$ = 25.02, p<0.0001 for PCP + HAL, n = 6) (see also Supplemental material 2)

Induction of c-fos in pyramidal neurons by PCP

PCP (10 mg/kg i.p.) administration increased the expression of *c-fos* in various fields of the PFC, but mainly its medial part (layers III-VI of the cingulate, prelimbic and infralimbic cortices) containing the area where extracellular recordings were made (Fig. 4). PCP also increased *c-fos* expression in the piriform cortex and in a narrow band of cells in the boundary between layers III and V, extending over dorsal a lateral aspects of the PFC (Fig. 4).

CLZ (5 mg/kg i.p., 30 min before PCP) did not affect *c-fos* expression but prevented the increase induced by PCP, as assessed by measuring optical density in films exposed to the hybridized sections ($F_{3,11}$ = 7.10, p<0.0001, one-way ANOVA; prelimbic area) (Fig. 4E). The same pattern of change was obtained in the infralimbic area and the piriform cortex (data not shown).

Double *in situ* hybridization experiments revealed that the enhanced *c-fos* signal seen in films corresponds to an increase in the number of pyramidal (vGluT1-positive) neurons expressing *c-fos* (Fig. 4B, 4C, 4F) and also to a parallel increase in cellular expression (Fig. 4C, 4G). PCP increased 2.8-fold the proportion of *c-fos* positive pyramidal neurons (Fig. 4F) and 2.4-fold the individual *c-fos* expression, as measured by counting the number of silver grains in positive cells (Fig. 4G, compare also panels B1/C1 and B2/C2 in Fig. 4). CLZ pre-treatment prevented the increase in the number of *c-fos*-positive, vGluT1-positive cells ($F_{3,11}$ = 37.52, p<0.0001; see group differences in Fig. 4F) and the increase in individual cellular expression in the same neurons ($F_{3,214}$ = 19.32, p < 0.00001; see group differences in Fig. 4G; silver grains were counted in a total of 218 vGluT1-positive cells).

CLZ alone did not modify *c-fos* expression in GABAergic interneurons but markedly enhanced it in rats treated also with PCP (Fig. 4D-4F). Given the occurrence of different subpopulations of local GABAergic neurons in different cortical layers and their differential involvement in schizophrenia[5], we analyzed separately drug effects in superficial (I, II/III) and deep layers (V, VI). There was no effect of treatment in superficial layers, yet one-way ANOVA revealed a significant effect of treatment on *c-fos* expression in deep layers ($F_{3,11}$ = 9.4, p<0.01) which was due to the increase in the number of *c-fos*-positive GABA cells in the CLZ + PCP group (Fig. 4F). A similar change was noted in the individual *c-fos* expression in GABAergic neurons, as judged by the number of silver grains per cell ($F_{3,79}$ = 8.81, p < 0.00001; Fig. 4G; silver grains were counted in a total of 83 GAD-positive cells).

Expression of c-fos in afferent areas to PFC

To identify afferent areas to PFC potentially involved in the increased PFC activity induced by PCP (see discussion below) we examined the effect of PCP on *c-fos* expression in the ventral hippocampus and the thalamus (mediodorsal, centromedial and reticular nuclei; MD, CM and Rt, respectively). PCP induced a very small increase in the number of *c-fos* positive cells in the CA1/subiculum whereas it moderately increased *c-fos* positive cells in the adjacent entorhinal cortex. Double *in situ* hybridization (vGluT1 and *c-fos* mRNAs) revealed that *c-fos*

expression took place exclusively in pyramidal cells (Supplemental material 3).

Unlike in hippocampus, PCP induced a dramatic increase in the number of *c-fos*-positive cells in the CM and MD nuclei as well as in adjacent midline and intralaminar nuclei. Optical density measures in films exposed to these sections indicated a significant effect of PCP on *c-fos* expression (from 0,133±0,003 in SAL + SAL rats to 0,223±0,019 in SAL + PCP rats n=3 in both groups; $p<0.01$). Double *in situ* hybridization revealed that *c-fos* was expressed by vGlut1-positive thalamic relay neurons in the CM and MD nuclei. However, PCP did not enhance *c-fos* expression in GABA neurons of the Rt nucleus (Supplemental material 4).

Figure legends

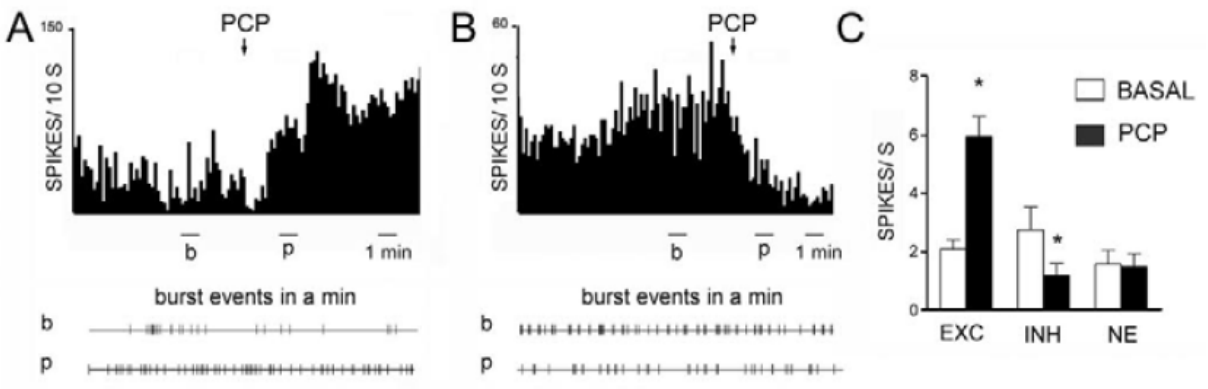

Figure 1. Panels A and B show two representative examples of pyramidal neurons whose discharge was increased and decreased, respectively, by PCP administration (0.25 mg/kg i.v.; vertical arrows). The two traces below integrated firing rate histograms in each panel show the burst episodes in 1-min intervals during basal conditions (b) and after PCP administration (p) (shown in the abcissa of integrated firing rate histograms). In these horizontal traces, each vertical line corresponds to one burst episode. C) Bar histogram showing the effect of PCP on the firing rate of pyramidal neurons according to the type of response. EXC= neurons excited by PCP (n = 36); INH = neurons inhibited by PCP (n = 26), NE = neurons unaffected by PCP (n = 18). *p<0.05 vs. baseline.

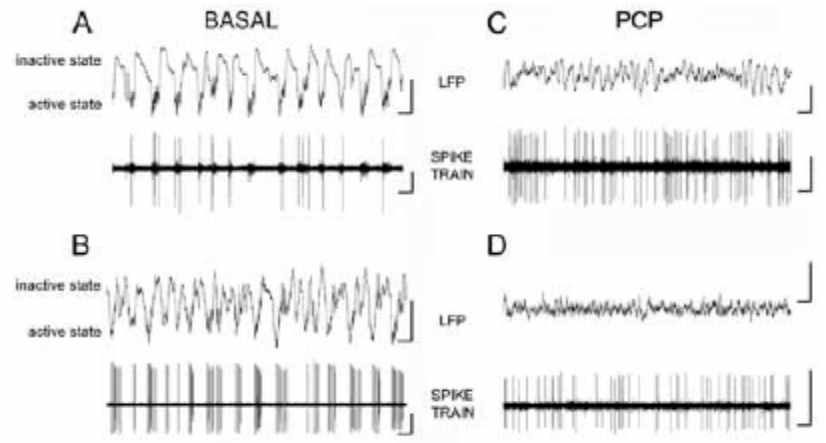

Figure 2. A, B) Synchronization of the discharge of pyramidal neurons with the active phase of 0.3-4 Hz oscillations in mPFC in basal conditions. Note the temporal coincidence of spikes with active phases of the recorded LFPs (downward infections in the figure). C, D) This temporal association was lost after PCP administration. Time bars: abscissa 1 s; ordinate 1 mV.

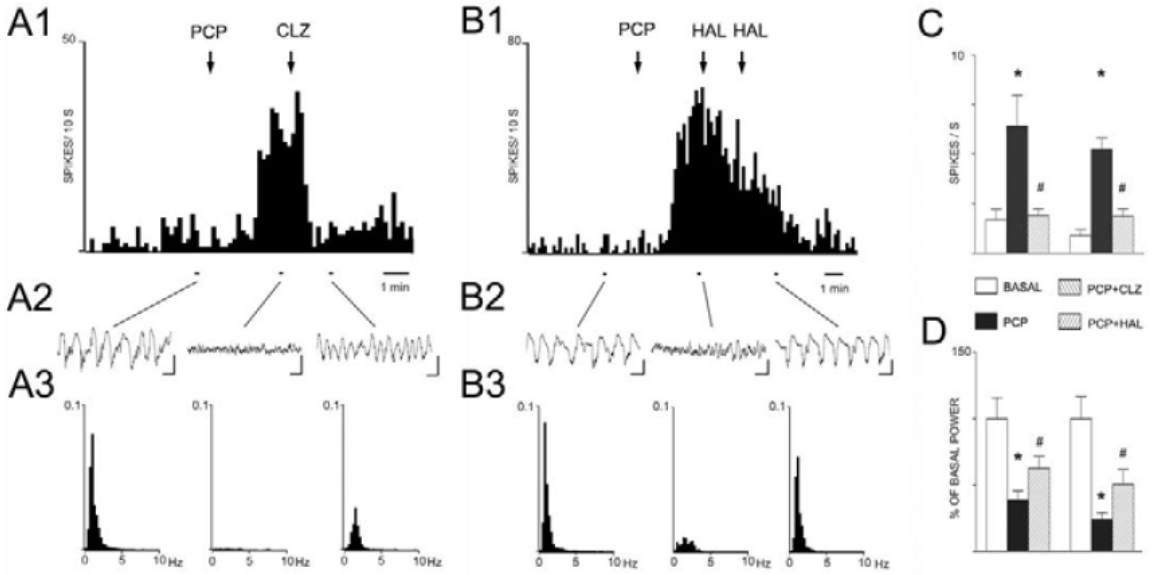

Figure 3. A1 and B1. Examples of two pyramidal neurons in mPFC showing an increase in the discharge rate after PCP administration (0.25 mg/kg i.v.; first arrow) which was reversed by the subsequent administration of clozapine (CLZ, 1 mg/kg i.v.) (A1) or haloperidol (HAL, 0.1 + 0.1 mg/kg i.v.) (B1). A2 and B2 show the corresponding LFP recordings (10 s each) obtained in basal conditions and after PCP and PCP + antipsychotic treatments (10-s periods are shown in the abscissa of panels A1 and B1). Note the marked suppression of oscillations induced by PCP administration. A3 and B3 show the power spectra of the above recordings (1 min each, around the 10-s above 10-s periods). C and D are bar histograms showing the effects of PCP and reversal by CLZ and HAL on cell firing (panel C) and local field potentials (panel D). *$p<0.05$ vs. baseline, $^{\#}p<0.05$ vs. PCP alone.

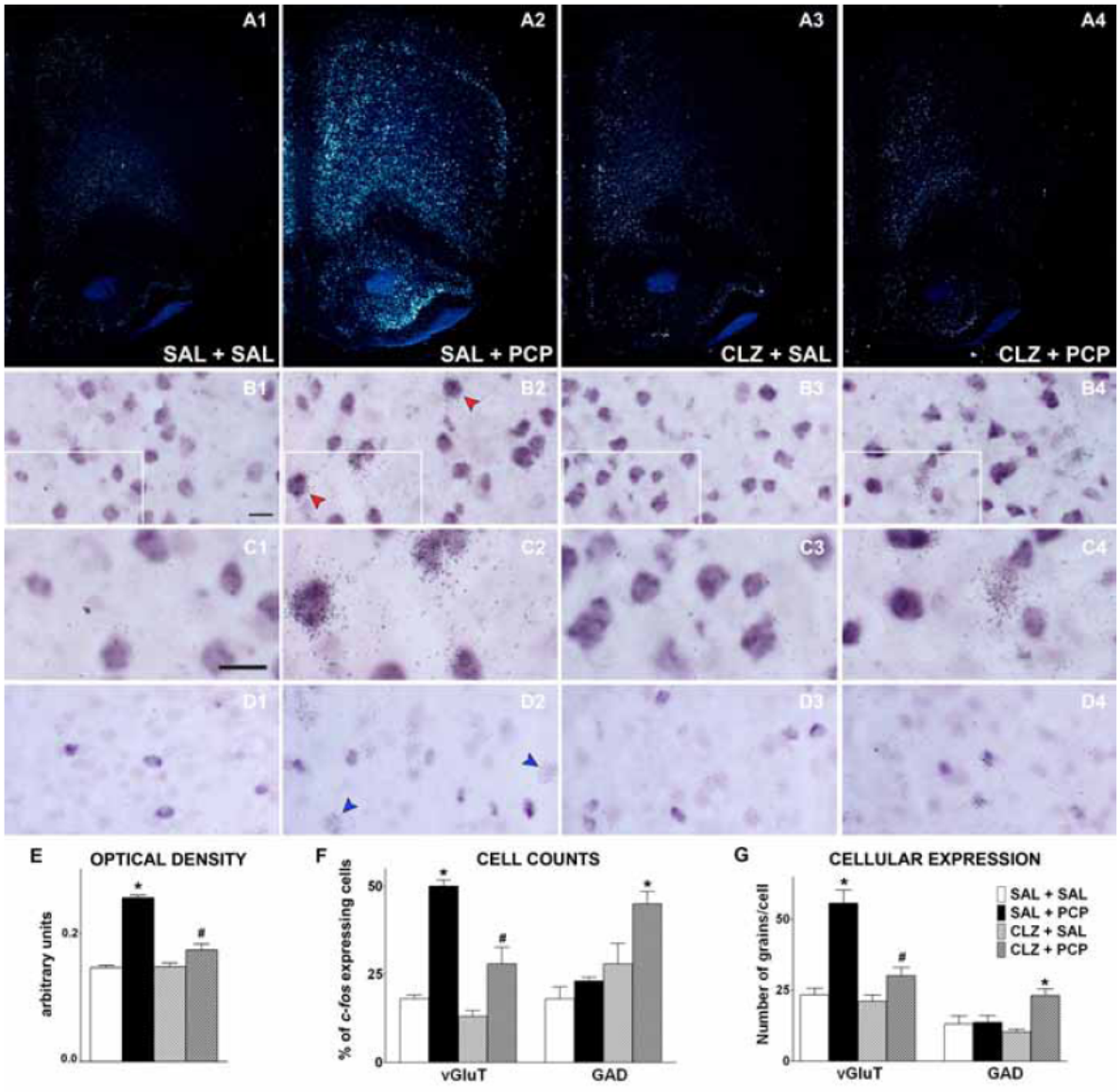

Figure 4. A) Macroscopic dark-field images from emulsion-dipped coronal sections at the level of PFC (AP ~+3.2 mm) from control and treated rats showing the localization of cells expressing *c-fos* mRNA. Note the PCP-induced expression of *c-fos* in various areas of the PFC, notably in the prelimbic area, where most of the extracellular recordings were made. CLZ antagonized the increase in *c-fos* expression induced by PCP. B) High magnification photomicrographs showing the detection in mPFC (prelimbic area) of *c-fos* mRNA using ^{33}P-labeled oligonucleotides (silver grains) in pyramidal cells, visualized by hybridization with Dig-labeled oligonucleotides complementary to vGluT1 mRNA (dark precipitates). Note the increase in the number of *c-fos* positive cells and the density of silver grains per cell induced by PCP as well as the CLZ-induced antagonism of this effect. Red arrows mark some double-labeled cells (B1: SAL + SAL; B2: SAL + PCP; B3: CLZ + SAL; B4: CLZ + PCP). C) Enlargement of the areas marked in B. D) High magnification photomicrographs showing the expression of *c-fos* mRNA (silver grains) in GABAergic cells of the prelimbic PFC, visualized by GAD mRNA (dark precipitate). Note the increase in the number of *c-fos* positive cells not expressing GAD mRNA in the SAL + PCP group (C2) (blue arrows) and the increase in GAD mRNA positive cells in the CLZ + PCP group (C4). E) Bar graph showing drug-

induced changes in *c-fos* expression in the prelimbic mPFC. Bars show mean± SEM of 3 rats/group and correspond to the optical density measured in films exposed to coronal sections of PFC (see Methods). F) Bar graphs showing drug effects on the percentage of pyramidal (vGlut1-positive; left panel) and GABAergic neurons (GAD-positive; right panel) expressing *c-fos* mRNA after each treatment. *p<0.01 vs. SAL + SAL; #p<0.01 vs. SAL + PCP. G) Bar graph showing drug effects on the individual cell expression of *c-fos* (number of silver grains/cell) in pyramidal (vGluT1-positive; left panel) and GABAergic neurons (GAD-positive, right panel. *p<0.01 vs. SAL + SAL; #p<0.01 vs. SAL + PCP. Bars size = 20 µm.

Discussion

The present findings indicate that the psychotomimetic actions of PCP are associated with a profound disruption of the PFC function. PCP affected 78% of the recorded pyramidal neurons (45% excited, 33% inhibited), and markedly reduced the cortical synchrony in the delta frequency range (0.3-4 Hz). Since the recorded units project to midbrain, it is unknown whether PCP may equally affect pyramidal neurons projecting to other areas (e.g., nucleus accumbens). These effects were reversed by the subsequent administration of a classical (HAL) and atypical (CLZ) antipsychotics, indicating a cellular convergence of the effects of both drugs in PFC, irrespectively of their different pharmacological properties. Further, PCP markedly increased the expression of *c-fos* in a substantial proportion of pyramidal neurons (50%) but not in GABA interneurons, an effect also prevented by CLZ administration. Two other studies examined the effect of PCP[13] and MK-801[14] on the discharge rate of putative pyramidal PFC neurons *in vivo*. However, to our knowledge, this is the first study demonstrating that a) PCP deeply affects cortical synchrony, and b) cellular and population effects of PCP in PFC are reversed by antipsychotic drugs. Further, *c-fos* data strongly support the involvement of thalamocortical inputs as mediators of PCP effects in PFC.

Delta waves reflect synchronized activity changes of cortical neuronal networks and are an emergent property of thalamocortical circuits dependent on the presence and interplay of specific currents (I_h and I_T) in thalamocortical neurons.[12] Here we show that PCP evokes a profound loss of the efficiency of cortical information processing, dramatically changing the activity patterns of PFC pyramidal neurons and suppressing delta rhythm. The loss of synchrony induced by PCP and the resulting random discharge of pyramidal neurons is likely to have profound effects on PFC-dependent functions. It may also affect subcortical regions as a result of the top-down processing of information in cortico-limbic circuits. Interestingly, PCP reduced the frequency and duration of depolarized ("up") sates of nucleus accumbens neurons recorded intracellualrly, which depends on hippocampal input, and affected their response to PFC stimulation.[15]

Overall, these observations indicate that PCP disrupts the activity of cortico--limbic networks, compromising the functional connectivity between brain areas altered in schizophrenia.[1,2,5] Yet it is unknown to what extent PCP-evoked changes in the PFC of anesthetized rats are related to the alterations in oscillations seen in the PFC of schizophrenic patients and the associated cognitive deficits.[16,17] Despite this limitation, it is interesting to note that two other agents modeling schizophrenia in rodents induce changes similar to those of PCP. Thus, the hallucinogen DOI (5-HT_{2A} receptor agonist) alters the activity pattern of PFC pyramidal neurons similarly to PCP[18] and suppresses cortical delta rhythm (Celada et al., unpublished observations). These common effects suggest a link between the altered PFC activity and the hallucinations induced by both agents. Also, the mitotoxic agent methylazoxymethanol, used as a neurodevelopmental model of schizophrenia, evoked a similar reduction of cortical synchrony in the delta range.[19]

The reduction in cell firing evoked by PCP in some neurons is consistent with the excitatory role of cortical NMDA-R on pyramidal neurons and their

blockade by PCP.[13,20] On the other hand, the increase in firing rate and *c-fos* expression in most PCP-sensitive neurons agrees with the increased PFC glutamate output induced by non-competitive NMDA-R blockade.[21,22] Excitatory PCP effects on pyramidal neurons may be caused by disinhibition of PFC GABA interneurons, as suggested for MK-801.[14] They may be also caused by NMDA-R blockade of GABAergic neurons outside the PFC, and further disinhibition of excitatory neurons that project to PFC.[3,23,24] The hippocampus has been claimed to mediate this effect via the CA1-PFC pathway.[24] However, the present results do not support this view since PCP had a very minor effect on the number of glutamatergic cells expressing *c-fos* in CA1/subiculum. In contrast, PCP markedly increased the number of *c-fos*-positive cells in the CM and MD thalamic nuclei (vGluT1-positive), which densely project to PFC, but not in GABAergic cells of the reticular nucleus (Rt) which provides inhibitory feed-back to relay neurons in the rest of thalamic nuclei, including CM and MD.

Thus, PCP markedly affects reciprocal excitatory thalamocortical circuits. PCP may disinhibit corticothalamic PFC neurons by acting on PFC GABA interneurons. Likewise, it may increase thalamocortical excitatory inputs by blocking NMDA-R in Rt and/or afferent inhibitory areas to the thalamus (e.g., ventral pallidum). Both possibilities require further testing, yet the latter hypothesis is consistent with previous observations indicating that the removal of inhibitory $GABA_A$ tone in MD/CM nuclei increases *c-fos* expression and pyramidal discharge rate in PFC[18,25] as observed here with PCP. The involvement of thalamocortical inputs is also suggested by the increased *c-fos* expression produced by PCP in deep layer III/superficial layer V of PFC and layer IV of parietal cortex (Santana et al., unpublished observations), which are target of inputs from MD onto PFC pyramidal neurons in the rat.[26] Additionally, given the increase in vGluT1-positive cells expressing *c-fos* in the entorhinal cortex and its direct connectivity with PFC[27], this pathway cannot be excluded.

Another relevant observation is that CLZ and HAL normalized the PCP-induced disruption of cortical function at cellular and population levels. Both drugs are equally effective to reverse the effect of NMDA-R blockade in some experimental models (e.g.. increase in glutamate output[21,22]) yet differences have been noted in behavioral models.[3,10] CLZ and HAL possibly reverse PCP effects by antagonizing, at the doses used, 5-HT_{2A} and dopamine D2 receptors, respectively. These actions prevented neurochemical and behavioral effects of NMDA-R antagonists.[3,,28,29] yet discrepant results have also been reported.[30] The cellular basis for these effects is still poorly understood. 5-HT_{2A} receptor blockade may attenuate glutamatergic transmission in mPFC.[31] On the other hand ventral tegmental area stimulation excited fast spiking interneurons and concurrently inhibited PFC pyramidal neurons.[32] Thus, HAL may attenuate PCP-induced pyramidal excitation via activation of dopamine D1 receptors secondary to an autoreceptor-mediated increase of PFC dopamine release.

Finally, the CLZ-induced prevention of PCP effects on *c-fos* expression in pyramidal PFC neurons agrees with the above electrophysiological observations, despite the different administration routes used. Interestingly, CLZ alone did not alter *c-fos* expression in GABAergic neurons yet increased it in animals treated with PCP, suggesting an state-dependent action. This effect occurred in deeper cortical layers, perhaps in large parvalbumin-positive GABAergic interneurons, which are densely expressed in layer V[33] and have been implicated in the pathophysiology of schizophrenia.[5] The increased activity of GABAergic cells induced by CLZ + PCP may be related to the normalized pyramidal discharge through enhanced local inhibitory inputs.

Acknowledgements

Work supported by grant SAF 2004-05525. Support from the Generalitat de Catalunya (2005SGR00758) and the Spanish Ministry of Health, Instituto de Salud Carlos III, RETICS

RD06/0011(REM-TAP Network) is also acknowledged. LK and NS are recipient of predoctoral fellowships from the Ministry of Science and Education. We thank Judith Ballart for skilful technical assistance. Thanks are also given to Ranulfo Romo and Kyei Y. Tseng for critical reading and helpful suggestions on the manuscript

References

1. Harrison, P. J. (1999) *Brain* **122**, 593-624.
2. Lewis, D. A. & Lieberman, J. A. (2000) *Neuron* **28**, 325-334.
3. Krystal, J. H., D'Souza, D. C., Mathalon, D., Perry, E., Belger, A. & Hoffman, R. (2003) *Psychopharmacology (Berl)* **169**, 215-233.
4. Selemon, L. D. & Goldman-Rakic, P. S. (1999) *Biol. Psychiatry* **45**, 17-25.
5. Lewis, D. A., Hashimoto, T. & Volk, D. W. (2005) *Nat. Rev. Neurosci.* **6**, 312-324.
6. Weinberger, D. R., Egan, M. F., Bertolino, A., Callicott, J. H., Mattay, V. S., Lipska, B. K., Berman, K. F. & Goldberg, T. E. (2001) *Biol. Psychiatry* **50**, 825-844.
7. Javitt, D. C. & Zukin, S. R. (1991) *Am. J. Psychiatry* **148**, 1301-1308.
8. Breier, A., Malhotra, A. K., Pinals, D. A., Weisenfeld, N. I. & Pickar, D. (1997) *Am. J. Psychiatry* **154**, 805-811.
9. Carlsson, M. & Carlsson, A. (1989) *J. Neural Transm.* **75**, 221-226.
10. Geyer, M. A., Krebs-Thomson, K., Braff, D. L. & Swerdlow, N. R. (2001) *Psychopharmacology (Berl)* **156**, 117-154.
11. Elvevag, B. & Goldberg, T. E. (2000) *Crit Rev. Neurobiol.* **14**, 1-21.
12. Steriade, M., McCormick, D. A. & Sejnowski, T. J. (1993) *Science* **262**, 679-685.
13. Suzuki, Y., Jodo, E., Takeuchi, S., Niwa, S. & Kayama, Y. (2002) *Neuroscience* **114**, 769-779.
14. Jackson, M.E., Honayoun, H. & Moghaddam, B. (2004) *Proc. Natl. Acad. Sci. USA* **101**, 8467-8472
15. O'Donnel, P. & Grace, A.A. (1998) *Neuroscience* **87**, 823-830.
16. Winterer, G. & Weinberger, D.R. (2004) *Trends Neurosci.* **27**, 683-690.
17. Uhlhaas, P.J. & Singer, W. (2006) *Neuron* **52**, 155-168.
18. Puig, M. V., Celada, P., Diaz-Mataix, L. & Artigas, F. (2003) *Cereb. Cortex* **13**, 870-882.
19. Goto, Y. & Grace, A. A. (2006) *Biol. Psychiatry* **60**, 1259-1267.
20. Shi, W. X. & Zhang, X. X. (2003) *J. Pharmacol. Exp. Ther.* **305**, 680-687.
21. Adams, B. & Moghaddam, B. (1998) *J. Neurosci.* **18**, 5545-5554.
22. Lopez-Gil, X., Babot, Z., Amargos-Bosch, M., Sunol, C., Artigas, F. & Adell, A. (2007) *Neuropsychopharmacology*. (in press)
23. Tsai, G. & Coyle, J. T. (2002) *Annu. Rev. Pharmacol. Toxicol.* **42**, 165-179.
24. Jodo, E., Suzuki, Y., Katayama, T., Hoshino, K. Y., Takeuchi, S., Niwa, S. & Kayama, Y. (2005) *Cereb. Cortex* **15**, 663-669.
25. Bubser, M., de Brabander, J. M., Timmerman, W., Feenstra, M. G., Erdtsieck-Ernste, E. B., Rinkens, A., van Uum, J. F. & Westerink, B. H. (1998) *Synapse* **30**, 156-165.
26. Kuroda, M., Yokofujita, J., & Murakami, K. (1998) *Prog Neurobiol.***54**, 417-458
27. Insausti, R., Herrero, M. T. & Witter, M. P. (1997) *Hippocampus* **7**, 146-183.
28. Martin, P., Waters, N., Waters, S., Carlsson, A. &, Carlsson, M. (1997) *Eur.J Pharmacol.* **335**, 107-116.
29. Ceglia, I., Carli, M., Baviera, M., Renoldi, G., Calcagno, E. & Invernizzi, R. W. (2004) *J Neurochem* **91**, 189-199.
30. Adams, B.W. & Moghaddam, B. (2001) *Biol Psychiatry* **50**, 750-757.
31. Aghajanian, G.K. & Marek, G.J. (1999) *Brain Res.* **825**, 161-171
32. Tseng, K.Y., Mallet, N., Toreson, K.L., Le Moine, C., Gonon, F. & O'Donnell P (2006) *Synapse***59**, 412-417
33. Grobin, A.C., Lieberman, J.A., Morrow, L. (2003) *J Neurosci.* **23**, 1832-1839.
34. Paxinos, G. & Watson, C. (1998) The Rat Brain in Stereotaxic Coordinates. Sydney: Academic Press.
35. Amargós-Bosch, M., Bortolozzi, A., Puig, M. V., Serrats, J., Adell, A., Celada, P., Toth, M., Mengod, G. & Artigas, F. (2004) *Cereb. Cortex* **14**, 281-299.
36. Laviolette, S. R., Lipski, W. J. & Grace, A. A. (2005) *J. Neurosci.* **25**, 6066-6075.

Trabajo 4:

Cellular convergence of serotonergic and noradrenergic signals in rat prefrontal cortex through 5-HT_{2A} / α_1-adrenergic receptor heterodimers.

Noemí Santana, Juan F. López-Giménez, Graeme Milligan, Guadalupe Mengod, Francesc Artigas.

En preparación

En este trabajo examinamos la expresión celular de los receptores α1-adrenérgicos en neuronas piramidales y GABAérgicas en corteza prefrontal (CPF) y su colocalización con los receptores serotoninérgicos 5-HT_{2A}. Los adrenoceptores α1 se expresaron en una alta proporción de neuronas piramidales (62-85%) y GABAérgicas (52-79%) en CPF medial y coexpresaron con el 80% de las células positivas para el 5-HT2A. Además, mediante las técnicas de co-inmunoprecipitación y FRET, se demostró la interacción heterodimérica entre el receptor serotoninérgico 5-HT_{2A} con cada uno de los subtipos del receptor α1-adrenérgico.

Cellular convergence of serotonergic and noradrenergic signals in rat prefrontal cortex through 5-HT_{2A} / α_1-adrenergic receptor heterodimers

Abbreviated title: 5-HT_{2A} and α_1-adrenergic receptors in prefrontal cortex

Noemí Santana[1], Juan F. López-Giménez[2], Graeme Milligan[2], Guadalupe Mengod[1], Francesc Artigas[1]

[1]Departamento de Neuroquímica y Neurofarmacología, Institut d'Investigacions Biomèdiques de Barcelona, CSIC, IDIBAPS;
[2]Division of Biochemistry and Molecular Biology, Institute of Biomedical and Life Sciences, University of Glasgow, Glasgow, UK

Corresponding author:
Francesc Artigas, PhD;
Dept. of Neurochemistry and Neuropharmacology,
IIBB-CSIC (IDIBAPS),
Rosselló, 161, 6th floor, 08036 Barcelona, Spain.

Phone: +3493-363 8315;
Fax: +3493-363 8301;
e-mail: fapnqi@iibb.csic.es

Abstract

The prefrontal cortex (PFC) is intimately involved in cognitive processes which are altered in schizophrenia. Brainstem ascending serotonergic and noradrenergic pathways innervate the PFC and control neuronal activity through the activation of α_1-adrenoceptors and 5-HT_{2A} receptors. Both receptors are coupled to the α subunit of $G_{q/11}$ protein and their activation raises intracellular Ca^{2+} through phospholipase C stimulation. Functional interactions between both receptors have been reported. Also, in addition to dopamine receptors, antipsychotic drugs interact with α_1-adrenoceptors and/or 5-HT_{2A} receptors. The latter receptors appear to mediate the clinical efficacy of atypical antipsychotics.

Using double *in situ* hybridization we examined the cellular expression of α_1-adrenoceptors in pyramidal (vGluT1-positive) and GABAergic ($GAD_{65/67}$-positive) neurons in rat PFC and their co-localization with 5-HT_{2A} receptors. α_1-adrenoceptors were expressed by a very high proportion of pyramidal (62-85%) and GABAergic (52-79%) neurons in the medial PFC and other PFC areas. The individual expression of α_{1A}, α_{1B} and α_{1D}-adrenoceptors was highly segregated in different layers and areas. The high (~80%) co-expression with 5-HT_{2A} receptors in many mPFC areas, together with the common intracellular signalling pathways, suggested a receptor-receptor interaction. Co-immunoprecipitation of the 5-HT_{2A} receptor with any of the three α_1-adrenoceptor subtypes, expressed in HEK293T cells indicated the formation of stable heterodimers. This was further confirmed using FRET (*fluorescence resonance energy transfer*). The very high cellular co-expression of both receptors in PFC and formation of heterodimers suggest that serotonin and noradrenaline can exert a simultaneous converging control of PFC neurons and reciprocal signal modulation through off-target allosteric modulation of heterodimeric receptors.

Key words: 5-HT_{2A} receptors · α_1-adrenergic receptors · antipsychotics · GABA interneurons · prefrontal cortex · pyramidal neurons

Introduction

The prefrontal cortex (PFC) is critically involved in many higher brain functions, including cognition, attention and behavioural planning (Fuster, 1997;Miller and Cohen, 2001). Anatomical, cellular and neurochemical alterations of the PFC have been reported in schizophrenia (Harrison, 1999;Lewis and Lieberman, 2000;Lewis et al., 2005;Selemon and Goldman-Rakic, 1999;Weinberger et al., 2001), including a presumed dopaminergic hypoactivity (Abi-Dargham et al., 2002;Akil et al., 2000).

The brainstem catecholaminergic and serotonergic systems innervate the PFC and modulate the activity of memory networks and animal behaviour (Carli et al., 2006;Dalley et al., 2004;Ramos and Arnsten, 2007;Robbins, 2000;Roberts et al., 1994;Vijayraghavan et al., 2007;Winstanley et al., 2003). Hence, dopamine finely tunes the activity of PFC neurons during spatial working memory tasks through the activation of D_1 receptors in a bell-shaped manner (Vijayraghavan et al., 2007;Williams and Goldman-Rakic, 1995). Similarly, moderately elevated levels of noradrenaline acting on α_{2A}-adrenoceptors improve cognitive performance whereas high noradrenaline release (e.g., as evoked by stress) impairs cognitive performance by activating α_{1B}-adrenoceptors (Ramos and Arnsten, 2007). On the other hand, selective blockade of 5-HT_{2A} receptors partly antagonizes the neuronal activation during a spatial working memory task (Williams et al., 2002). Further, serotonin (5-HT) depletion in monkey orbitofrontal cortex impaired reversal learning (Clarke et al., 2004) whereas the local blockade of 5-HT_{2A} receptors in PFC improves visuospatial attention and decreases impulsivity in rats (Winstanley et al., 2003).

Antipsychotic drugs used to treat schizophrenia block dopamine D_2 receptors to a different extent

(e.g., atypical drugs show a preferential 5-HT_{2A}/ D_2 action) yet both classical and atypical drugs show high affinity for α_1-adrenoceptors (Arnt and Skarsfeldt, 1998;Bymaster et al., 1996;Meltzer, 1999). Several observations suggest the existence of functional interactions between 5-HT_{2A} and α_1-adrenoceptors which may be involved in the therapeutic activity of antipsychotic drugs. Hence, head shakes induced by DOI, a 5-$HT_{2A/2C}$ receptor agonist, were abolished by 5-HT_{2A} receptor blockade, as expected, but also by haloperidol and the α_1-adrenoceptor antagonist prazosin (Dursun and Handley, 1996;Schreiber et al., 1995). These observations were paralleled by microdialysis studies showing that the increased 5-HT output induced by the local activation of 5-HT_{2A} receptors and α_1-adrenoceptors in PFC could be indistinctly attenuated by antagonists of either receptor and by classical and atypical antipsychotic drugs (Amargos-Bosch et al., 2003;Bortolozzi et al., 2003). Likewise, a functional interaction between both receptors mediates neurochemical and behavioral responses induced by opiates and psychostimulants (Auclair et al., 2004).

5-HT_{2A} and α_1-adrenoceptors are coupled to the α subunit of Gq/11 protein and their activation raises intracellular Ca^{2+} through phospholipase C (Bartrup and Newberry, 1994;Berg et al., 1998;Claro et al., 1993;Michel et al., 1993;Molinoff, 1984). Moreover, 5-HT and noradrenaline activate pyramidal neurons in PFC through 5-HT_{2A} and α_1-adrenoceptor stimulation, respectively (Araneda and Andrade, 1991;Marek and Aghajanian, 1999). Based on the common signalling pathways and existing functional interactions between both receptors, we examined the cellular localization of α_1-adrenoceptors and 5-HT_{2A} receptors in rat PFC and their putative interaction through heterodimers using *in vitro* cell systems.

Materials and Methods

Tissue preparation

Male albino Wistar rats weighing 250–300 g were used (Iffa Credo, Lyon, France). Animals were kept in a controlled environment (12 h light-dark cycle and 22 ± 2°C room temperature) with food and water provided *ad libitum*. Animal care followed the European Union regulations (O.J. of E.C. L358/1 18/12/1986) and was approved by the local Institutional Animal Care and Use Committee. Rats were killed by decapitation and the brains rapidly removed, frozen on dry ice and stored at –20°C. Tissue sections, 14 µm thick, were cut using a microtome-cryostat (HM500 OM; Microm, Walldorf, Germany), thaw-mounted onto APTS (3-aminopropyltriethoxysilane; Sigma,St Louis, MO) coated slides and kept at –20°C until use.

Hybridization probes.

The oligodeoxyribonucleotide probes used were complementary to the following bases: 2-46 and 1395-1439 of the rat α_{1A}-adrenergic receptor mRNA (GenBank Accession No. NM_017191.1); 365-409 and 2216-2260 of the rat α_{1B}-adrenergic receptor mRNA (GenBank Accession No. X51585); 1167-1212 of the rat α_{1D}-adrenergic receptor mRNA (GenBank Accession No.NM_024483.1); 514–558 of the isoform of the enzime glutamate descarboxilase (GAD_{65}) mRNA (GenBank Accession No. NM_012563); 1600–1653 of the GAD_{67} mRNA (GenBank Accession. N.o NM_017007); 127–172 and 1756–1800 of the vGluT1 mRNA (vesicular glutamate transporter) (GenBank Accession No. U07609); 128-170, 180-224, 836-880, 939-987, 1301-1345 and 1380-1427 of the rat 5-HT_{2A} serotonin receptor mRNA (GenBank Accession No. NM_017254).

All probes were synthesized and HPLC purified by Isogen Bioscience BV (Maarsden, The Netherlands). Each receptor oligonucleotide was individually labeled (2 pmol) at the 3'-end either with [^{33}P]-dATP (>2500 Ci/mmol; DuPont-NEN, Boston, MA) using terminal deoxynucleotidyltransferase (TdT, Calbiochem, La Jolla, CA, USA). GAD and vGluT oligonucleotides (100 pmol) were non-radioactively labeled with TdT (Roche Diagnostics GmbH, Mannheim, Germany) and Dig-11-dUTP (Boehringer Mannheim). Oligonucleotides were purified by centrifugation using ProbeQuant™ G-50 Micro Columns (GE Healthcare UK Limited, Buckinghamshire, UK).

In situ hybridization histochemistry procedure

The protocols for single- and double-label *in situ* hybridization were based on previously described procedures (Landry et al., 2000;Tomiyama et al., 1997). Frozen tissue sections were first brought to room temperature, fixed for 20 min at 4°C in 4% paraformaldehyde in phosphate buffered saline (1× PBS: 8 mM Na_2HPO_4, 1.4 mM KH_2PO_4, 136 mM NaCl, 2.6 mM KCl), washed for 5 min in 3× PBS at

room temperature, twice for 5 min each in 1× PBS and incubated for 2 min at 21°C in a solution of predigested pronase (Calbiochem, San Diego, CA) at a final concentration of 24 U/ml in 50 mM Tris–HCl pH 7.5, 5 mM EDTA. The enzymatic activity was stopped by immersion for 30 s in 2 mg/ml glycine in 1× PBS. Tissues were finally rinsed in 1× PBS and dehydrated through a graded series of ethanol. For hybridization, the radioactively-labeled and the non-radioactively labeled probes were diluted in a solution containing 50% formamide, 4× SSC (1× SSC: 150 mM NaCl, 15 mM sodium citrate), 1× Denhardt's solution (0.02% Ficoll, 0.02% polyvinylpyrrolidone, 0.02% bovine serum albumin), 10% dextran sulfate, 1% sarkosyl, 20 mM phosphate buffer pH 7.0, 250 µg/ml yeast tRNA and 500 µg/ml salmon sperm DNA. The final concentrations of radioactive and Dig-labeled probes in the hybridization buffer were in the same range (~1.5 nM). Tissue sections were covered with hybridization solution containing the labeled probe(s), overlaid with Nescofilm coverslips (Bando Chemical Ind., Kobe, Japan) and incubated overnight at 42°C in humid boxes. Sections were then washed four times (45 min each) in a buffer containing 0.6 M NaCl and 10 mM Tris–HCl (pH 7.5) at 60°C.

Development of radioactive and non-radioactive hybridization signal

Hybridized sections were treated as described by Landry *et al.* (2000). Briefly, after washing, the slides were immersed for 30 min in a buffer containing 0.1 M Tris–HCl pH 7.5, 1 M NaCl, 2 mM $MgCl_2$ and 0.5% bovine serum albumin (Sigma) and incubated overnight at 4°C in the same solution with alkaline-phosphate-conjugated anti-digoxigenin-F(ab) fragments (1:5000; Boehringer Mannheim). Afterwards, they were washed three times (10 min each) in the same buffer (without antibody) and twice in an alkaline buffer containing 0.1 M Tris–HCl pH 9.5, 0.1 M NaCl and 5 mM $MgCl_2$. Alkaline phosphatase activity was developed by incubating the sections with 3.3 mg nitroblue tetrazolium and 3.3 mg bromochloroindolyl phosphate (Gibco BRL, Gaithersburg, MD) diluted in 10 ml of alkaline buffer. The enzymatic reaction was blocked by extensive rinsing in the alkaline buffer containing 1 mM EDTA. The sections were then briefly dipped in 70 and 100% ethanol, air-dried and dipped into Ilford K5 nuclear emulsion (Ilford, Mobberly, Cheshire, UK) diluted 1:1 with distilled water. They were exposed in the dark at 4°C for 5 weeks and finally developed in Kodak D19 (Kodak, Rochester, NY) for 5 min and fixed in Ilford Hypam fixer (Ilford).

Construction of epitope-tagged receptors and fusion proteins

Generation and subcloning of the different receptor constructs were essentially as described before (Carrillo et al., 2004). Briefly, epitope tags were added at the amino terminus of the different receptors (5-HT_{2A} serotonin receptor and α_{1B}-adrenoceptor) by PCR techniques using forward primers containing the sequence of the tag to be inserted. The amino acid sequence for the different epitope tags are as follows: EQKLISEEDL for c-myc and YTDLEMNRLGK for VSV. Fusion proteins including receptor (5-HT_{2A} serotonin receptor and α_{1A}, α_{1B} and α_{1D}-adrenoceptors) and fluorescent protein (yellow fluorescent protein (YFP) and cyan fluorescent protein (CFP)) were constructed amplifying the sequence corresponding to the receptor by PCR and removing the stop codon. This PCR product was ligated to the fluorescent protein sequence amplified by PCR containing the same endonuclease restriction site. The end product of this ligation corresponds to a single open reading frame encoding for the receptor-fluorescent fusion protein. All the constructs were subcloned into pCDNA3 plasmid (Invitrogen).

Cell cultures

All materials for tissue culture were from Invitrogen (Paisley, UK). HEK293T cells were maintained in Dulbecco's modified Eagle's medium (DMEM, Sigma) supplemented with 0.292 g/l L-glutamine and 10% (v/v) newborn calf serum and incubated at 37°C with 5% CO_2. Cells were grown to approximately 60 to 80% confluence before transient transfection using Lipofectamine Transfection Reagent (Invitrogen) for the co-immunoprecipitation experiments and Effectene® transfection reagent (Qiagen, Germany) for FRET experiments, both according to the manufacturer's instructions.

Co-immunoprecipitation (Co-IP) Studies

Cells were harvested 24 h following transfection and resuspended in RIPA buffer (50 mM HEPES, 150 mM NaCl, 0.5% sodium deoxycholate, 0.1% SDS, 1% Triton X-100, 10 mM NaF, 5 mM EDTA, 0.1 mM

$NaPO_4$, 5% ethylene glycol). Cells were placed on a rotating wheel for 1 h at 4 °C. Samples were then centrifuged for 1h at 100,000 x *g* at 4 °C, and the supernatant was transferred to a fresh tube containing 50 µl of protein G beads (Sigma) to pre-clear the samples. Following incubation on a rotating wheel for 1 h at 4 °C, the samples were re-centrifuged at 20,800 x *g* at 4 °C for 1 min, and the protein concentration of the supernatant was determined. Samples containing equal protein amounts were incubated overnight with 40 µl of protein G beads, 30 U/ml endoglycosidase F (Sigma) and the corresponding immunoprecipitating antibody (2 µl of anti-GPF(sheep) for the c-myc-5-HT_{2A} /α_{1A}-YFP and c-myc-5-HT_{2A} /α_{1D}-YFP Co-IPs and 1 µl of anti-VSV monoclonal antibody (Roche Diagnostics) for the c-myc-5-HT_{2A}/ VSV-α_{1B} Co-IP) at 4 °C on a rotating wheel, and fractions were reserved to monitor protein expression in the cell lysates. Samples were centrifuged at 20,800 x *g* for 1 min at 4 °C, and the protein G beads were washed three times with RIPA buffer. Following addition of 1x Laemmli reducing buffer and heating to 65 °C for 10 min, both immunoprecipitated samples and cell lysate controls were resolved by SDS-PAGE using pre-cast 4-12% acrylamide Novex Bistris gels (Invitrogen BV). Proteins were transferred onto PVDF membranes. These membranes were incubated in 5% (w/v) low fat milk, 0.1% Tween 20/ Tris-buffered saline (TBS) (v/v) solution at room temperature on a rotating shaker for 2 h and then incubated at 4 °C overnight with primary antibody (Policlonal Anti-c-Myc(rabbit) (Cell signalling), for the myc-5-HT_{2A}/α_{1A}-YFP and myc-5-HT_{2A}/α_{1D}-YFP Co-IPs and Monoclonal Anti-c-Myc Biotin Conjugate (Sigma) for the myc-5-HT_{2A}/VSV-α_{1B} Co-IP). The two lysate membranes were incubated with the same antibodies or anti-GFP(sheep) (for the myc-5-HT_{2A}/α_{1A}-YFP and myc-5-HT_{2A}/α1d-YFP Co-IPs), and anti-VSV monoclonal antibody (Roche Diagnostics) (for the myc-5-HT_{2A}/VSV-α_{1B} Co-IP). All antibodies were diluted in 5% (w/v) low fat milk, 0.1% Tween 20/TBS (v/v) solution. The membrane was washed three times in 0.1% Tween 20/TBS before addition of secondary antibody (horseradish peroxidase (HRP)-linked anti-rabbit IgG (Amersham Biosciences) and HRP-linked anti-goat IgG (Pierce) for the myc-5-HT_{2A}/α_{1A}-YFP and myc-5-HT_{2A}/α_{1D}-YFP Co-IPs; HRP-linked streptavidin (Pierce) and HRP-linked anti-mouse IgG (Amersham) for the myc-5-HT_{2A}/VSV-α_{1B} Co-IP). Following further washes, the membrane was subsequently developed using ECL solution (Pierce Chemical, Cramlington, Northumberland, UK).

Fluorescent Microscopy and FRET Imaging in Living Cells.

An Eclipse TE2000-E (Nikon, Melville, NY) fluorescence inverted microscope was used for living cell microscopy and FRET imaging. HEK293T cells were grown on polylysine-treated glass coverslips and transiently transfected with the different CFP/eYFP fusion proteins. These coverslips were mounted into a microscope chamber containing physiological saline solution (130 nM NaCl, 5 mM KCl, 1 mM $CaCl_2$, 1 mM $MgCl_2$, 20 mM HEPES, and 10 mM D-glucose, pH 7.4). Images were sequentially obtained in the following order: eYFP, CFP, and FRET filter channels by means of an Optoscan monochromator (Cairn Research, Faversham, Kent, UK) and a dichroic mirror 86002v2bs (Chroma Technology Corporation, Rockingham, VT). The filter sets were the following: eYFP (excitation, 500/5 nm; emission, 535/30 nm); CFP (excitation, 430/12 nm; emission, 470/30 nm); and FRET (excitation, 430/12 nm; emission, 535/30 nm). Illumination time and binning modes were 250 ms and 2 x 2, respectively. MetaMorph imaging software (Universal Imaging Corporation, West Chester, PA) was used to quantify FRET images

Determination of Bleed-Through Coefficients. Bleed-through coefficients were defined as the ratio between the amount of fluorescence detected in the FRET filter set and the fluorescence detected for each single fluorescent protein at its own filter set (CFP and eYFP). To obtain these coefficients, cells were transfected with each of the fluorescent proteins individually, and the fluorescence measurements resulted in the following parameters: $F_{CFP\text{-}YFP}$/CFP = 0.68, $F_{CFP\text{-}YFP}$/YFP = 0.16.

*FRET Signal Correction and Normalization***.** Because the fluorescence detected in the FRET channel (raw FRET) comprises not only the actual FRET but also the bleed-through from the fluorescent proteins expressed, this signal was corrected using the bleed-through coefficients determined previously. In addition, this corrected FRET was also normalized to generate a final value independent of protein expression levels. For this purpose, the equation $FRET^N$ = raw FRET/$\Sigma(FP^*B_x)$

was used, where *FP* is the intensity of each fluorescent protein involved in the final FRET, and B_x is its corresponding bleed-through coefficient (i.e., fluorescence intensity in the background-corrected FRET channel image divided by the total spillover from the relevant FRET partners). Thus, in the absence of energy transfer, $FRET^N$ has a predicted value of 1, whereas values greater than 1 would reflect the occurrence of FRET.

Analysis of the Results

Tissue sections were examined in bright- and dark-field in a Wild 420 macroscope (Leica, Heerbrugg, Germany) and in a Nikon Eclipse E1000 microscope (Nikon, Tokyo, Japan) equipped with bright- and dark-field condensers for transmitted light and with epi-illumination. Micrography was performed using a digital camera (DXM1200 3.0; Nikon) and analySIS Software (Soft Imaging System GmbH, Germany). Bright-field images were captured with transmitted light. Dark-field images were captured with Darklite illuminator (Micro Video Instruments, Avon, MA). The figures were prepared for publication using Adobe Photoshop software (Adobe Software, Mountain View, CA). The cellular counting was made in an Olympus AX70 Stereo Microscope using CAST software for stereological analysis. Dig-labelled cells were considered positive when a dark precipitate was clearly distinguished from background. Only cellular profiles showing great abundance of the corresponding receptor mRNA and the cell type identifier (either GAD or vGluT1 mRNAs) were considered to be double-labelled. Cells with a dense Dig labelling and occasional silver grains (or vice versa) were not considered to co-express both transcripts. Co-expression of 5-HT_{2A} receptor mRNA and α_1-adrenoceptor mRNA (α_{1A}-, α_{1D}- and α_{1D}-adrenoceptors) was estimated by counting the number of α_1-adrenoceptor-positive cells (^{33}P-oligonucleotides) which also expressed 5-HT_{2A} receptor mRNA (Dig- positive cells). The relative proportion was estimated by considering 100% the 5-HT_{2A} receptor-positive cells. Analysis of variance (ANOVA) and *post hoc* Tukey's test were performed using GraphPad Prism software (GraphPad Software, San Diego, CA). $P < 0.05$ was considered statistically significant.

Results

Expression of α_1-adrenoceptors in the rat PFC

The various subtypes of α_1-adrenoceptors were abundantly expressed in rat PFC, in particular α_{1A}- and α_{1D}-adrenoceptors. Figure 1 shows the distribution of each individual α_1-adrenoceptor transcript. Several features can be recognized, as follows. First, virtually all subdivisions of the PFC contained cells expressing one or other α_1-adrenoceptor. Second, most abundant transcripts were those corresponding to α_{1A}- and α_{1D}-adrenoceptors, whereas the expression of α_{1B}-adrenoceptor was more moderate, particularly in the medial PFC. Third, with few exceptions, the various α_1-adrenoceptor transcripts showed an almost non-overlapping regional distribution within the PFC. This was particularly remarkable for to α_{1A}- and α_{1D}-adrenoceptors. The former transcript was densely expressed in deep layers (VIa, VIb) of the medial, dorsal and lateral (agranular insular) PFC and the claustrum as well as in ventral areas, such as orbital and piriform cortices, the endopiriform nucleus and the tenia tecta. In contrast, the α_{1D}-adrenoceptor transcript was particularly abundant in intermediate layers (layer III-outer layer V) in medial and dorsolateral aspects of the PFC and had a much more restricted expression in ventral aspects. In addition to his differential regional distribution (see panels A and C in fig. 1), there was a common expression of both receptors in superficial layers in medial and dorsolateral aspects of the PFC.

The density and of the α_{1B}- adrenoceptor transcript was lower than that of α_{1A}- and α_{1D}-adrenoceptors. Also, its regional distribution was more restricted, being localized to the cingulate and prelimbic areas, with a minimal expression in the infralimbic area. However, it was moderately expressed in layers III-V of the dorsal and lateral PFC. The orbital and piriform cortices showed an even more moderate expression of the α_{1B}-adrenoceptor transcript.

Expression of α_1-adrenoceptors in pyramidal and GABAergic neurons of the rat PFC

In double *in situ* hybridization experiments, we observed the presence of all three types of α_1-adrenoceptors in pyramidal (vGluT1-positive) and GABAergic ($GAD_{65/67}$-positive) neurons. Figures 2-4 show representative examples of the presence of α_{1A}-, α_{1B}- and α_{1D}-adrenoceptor transcripts in pyramidal and GABAergic neurons in various layers of the mPFC. Table 1 shows the proportion of

pyramidal and GABAergic neurons in the cingulate, prelimbic and infralimbic areas of the mPFC expressing α_1-adrenoceptors. Although we did not perform a quantitative estimation of the proportion of pyramidal and GABAergic neurons expressing each individual subtype, the transcripts for α_{1A}- and α_{1D}-adrenoceptors seem to account for most of the expression, as judged from the large number of pyramidal and GABAergic cells expressing these two adrenoceptor types. Hence, figures 2 and 4 show an abundance of vGlutT1- and GAD-positive cells expressing, respectively, α_{1A}- and α_{1D}-adrenoceptors. In contrast, the proportion of cells expressing α_{1B}-adrenoceptors was low, as shown in fig. 3.

The proportion of pyramidal neurons expressing α_1-adrenoceptors in the different cortical layers and areas of the mPFC was very high (from 52 to 85%), being maximal in layers II-III and V of the cingulate and prelimbic areas (71-85 %). The proportion of pyramidal neurons expressing α_1-adrenoceptors was more moderate in layer VI and in the infralimbic area.

Likewise, we found a very high proportion of GABAergic neurons that also expressed α_1-adrenoceptors (from 52 to 79%). GABAergic cells expressing each of the three α_1-adrenoceptor subtypes were found in different cortical layers, including layer I. Figures 2-4 show also representative examples of GABAergic cells expressing α_{1A}-, α_{1B}- and α_{1D}-adrenoceptors in the mPFC. Interestingly, and despite the individual cellular expression of the α_{1B}-adrenoceptor subtype was low, some cells exhibited a remarkable high level of expression, such as those shown in panels C1 to C3 in figure 3. Some of these cells were GABAergic, such as that shown in panel C1 (layer I) whereas others were glutamatergic (panel C3). Interestingly, no such high levels of expression were seen for the other two adrenoceptor types.

Co-expression of α_1-adrenoceptors and 5-HT$_{2A}$ receptors in rat PFC

The regional distribution of α_1-adrenoceptor and 5-HT$_{2A}$ receptor mRNAs was very similar in PFC. Panels A and B in figure 5 are dark-field photomicrographs showing the localization of both transcripts. It should be noted that the panel B corresponds to the combined expression of all three α_1-adrenoceptor types. This was obtained by exposing PFC sections to a combination of the oligonucleotides selective for α_{1A}-, α_{1B}- and α_{1D}-adrenoceptor mRNAs, as described in methods.

With the exception of layer VIb, and the more ventral part of the infralimbic cortex, where 5-HT$_{2A}$ receptor mRNA exhibits a low expression, virtually all other areas in PFC showed an abundant expression of both receptors. These areas included the cingulate and prelimbic areas of the mPFC, motor, agranular insular, orbital and piriform cortices and tenia tecta. The reader is referred to fig. 1 for the detailed comparison of the expression of 5-HT$_{2A}$ receptors with each one of the three α_1-adrenoceptors.

Double *in situ* hybridization experiments were conducted to examine the possible cellular co-localization of 5-HT$_{2A}$ receptors with α_{1A}-, α_{1B}- and α_{1D}-adrenoceptors as well as with the three subtypes together, using the oligonucleotide combination. 5-HT$_{2A}$ receptor probes were non-radioactively labelled with digoxigenin whereas α_1-adrenoceptor mRNAs were detected with radioactive probes. Figure 6 shows the extensive cellular co-expression of 5-HT$_{2A}$ receptors with α_1,adrenoceptors, especially with α_{1A}-, and α_{1D}-adrenoceptor subtypes, in various fields of the mPFC as well as in other PFC areas such as piriform cortex, tenia tecta or agranular insular cortex. We performed a detailed estimation of the percentage of cellular co-expression of 5-HT$_{2A}$ receptors with α_1-adrenoceptors in layers II-III of the mPFC (cingulate, prelimbic and infralimbic areas). Given the limited expression and restricted localization of α_{1B}-adrenoceptors, we did not carry out the cellular counting of this receptor subtype. Taking 100% as all cells expressing 5-HT$_{2A}$ receptors, the percentage of cells expressing also α_1-adrenoceptors varied between 44% in the infralimbic area to 75 and 80% in the prelimbic and cingulate areas, respectively. The co-expression in the infralimbic area must be considered as a lower limit, given the low abundance of 5-HT$_{2A}$ receptors compared to other areas rich in both receptor mRNAs. Given the preferential expression of α_{1D}-adrenoceptors in superficial layers, where cell counts were performed, this type was the one contributing most to the co-expression with 5-HT$_{2A}$ receptors (Fig. 7). However, it is likely that similar counts performed in areas showing abundant expression of 5-HT$_{2A}$ and α_{1A}-adrenoceptors, such as the motor area or the agranular insular cortex

would also give very high levels of co-expression, as shown in fig. 6.

5-HT$_{2A}$-α_1-adrenoceptor heterodimerization: Co-immunoprecipitation and FRET (Fluorescence Resonance Energy Transfer) studies

The formation of heterodimers between 5-HT$_{2A}$ receptors and each one of the three α_1-adrenoceptor subtypes was assessed by co-immunoprecipitation and FRET techniques in HEK293T cells transiently expressing 5-HT$_{2A}$ receptors and α_1-adrenoceptors.

In co-immunoprecipitation studies, 5-HT$_{2A}$ receptors were tagged with c-Myc epitope, whereas α_{1A}- and α_{1D}-adrenoceptors were tagged with YFP protein and α_{1B}-adrenoceptors with VSV epitope tag, as indicated in experimental procedures. Fusion proteins were transiently expressed in HEK293T cells, which were lysated and immunoprecipitated (see Methods). Figures 8-10 show the presence of stable heterodimers between 5-HT$_{2A}$ receptors and each one of the α_1-adrenoceptor types. Lane 1 and 2 in each figure correspond to cells transfected with c-Myc-5-HT$_{2A}$ and VSV-α_{1B} or $\alpha_{1A/1D}$-YFP, respectively whereas lane 3 corresponds to cells transfected with both receptor constructs. Lane 4 correspond to a mixture of cells individually transfected with c-Myc-5-HT$_{2A}$ receptor and VSV-$\alpha_{1A/1B/1D}$ adrenoceptor subtype, mixed prior to immunoprecipitation and lane 5 corresponds to non-transfected HEK293T cells. The presence of the 5-HT$_{2A}$ receptor, at molecular weight of approximately 50 kDa is clearly visible in each of the three co-immunoprecipitation experiments.

Figure 11 shows confocal microscopy images of the individual fluorescent signals corresponding to 5-HT$_{2A}$-CFP (donor) and $\alpha_{1A/1B/1D}$-YFP (acceptor) in HEK293T cells as well as the FRET signal corresponding to each one of the α_1-YFP and 5-HT$_{2A}$-CFP pairs. FRET efficiency for all three α_1-YFP / 5-HT$_{2A}$-CFP pairs was in the range 30-35% (Fig. 11). Control cells transfected with only CFP and YFP proteins showed no detectable FRET signal (efficiency <5%)

Figure legends

Table 1. Expression of α_1-adrenoceptors in pyramidal (vGluT1-positive) and GABAergic ($GAD_{65/67}$-positive) neurons of the rat mPFC

		Layers I-III	Layer V	Layer VI
vGluT1-positive	ACAd	85 ± 4 *	71 ± 9	65 ± 8
	PL	80 ± 3 *	79 ± 8 *	59 ± 2
	IL	62 ± 8	63 ± 8	
GAD-positive	ACAd	79 ± 10	73 ± 14	62 ± 1
	PL	79 ± 5 *	72 ± 5	57 ± 8
	IL	74 ± 3	52 ± 6 **	

Data (mean ± SEM) are percentages of pyramidal or GABAergic neurons expressing α_1-adrenoceptors in the various cortical layers of the dorsal anterior cingulate (ACAd),prelimbic (PL) and infralimbic (IL) areas of the rat mPFC. *P<0.05 vs layer VI, **P<0.05 vs layers I-III, Tukey t test post-ANOVA.

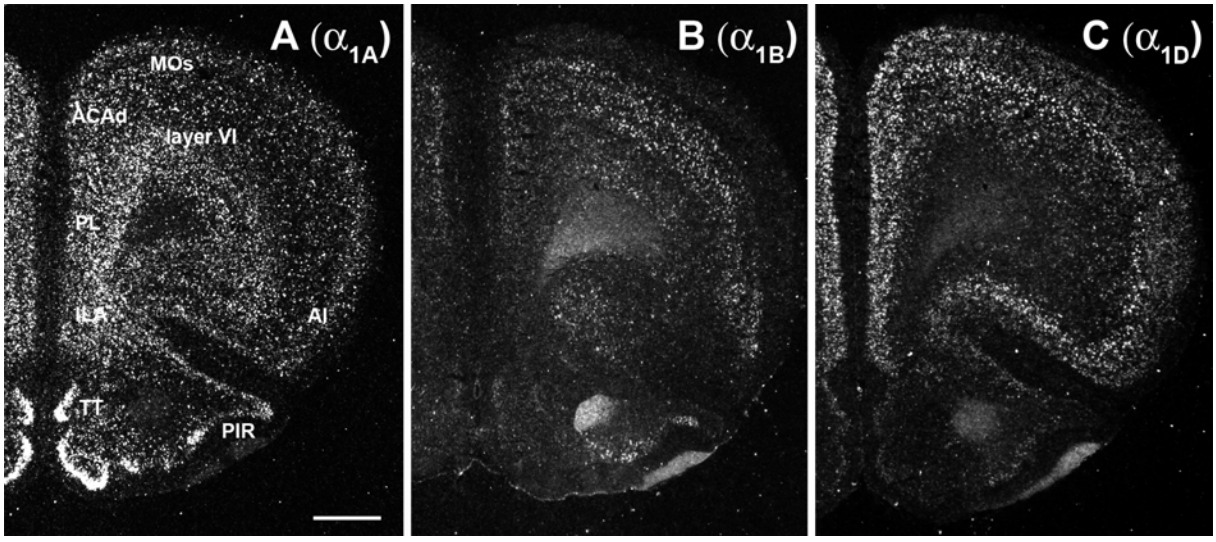

Figure 1. Low magnification dark-field photomicrographs showing the localization of (A) α_{1A}-adrenoceptor, (B) α_{1B}-adrenoceptor, and (C) α_{1D}-adrenoceptor mRNAs in the rat prefrontal cortex using *in situ* hybridization histochemistry. The sections correspond approximately to AP +3.7 mm (Paxinos and Watson, 2005). Each receptor transcript was detected with ^{33}P-labeled oligonucleotides. A) α_{1A}-adrenoceptor mRNA was localized to a large number of cells in superficial, middle and, particularly, deep layers of the various areas of the medial prefrontal cortex, such as the anterior cingulate (ACAd), prelimbic (PL) and infralimbic (IL) areas. It was also present in dorsal and lateral aspects of the prefrontal cortex, such as the motor area (MO) and the agranular insular (AI) cortex as well as in ventral prefrontal areas (piriform cortex, PIR, and tenia tecta, TT). B) The localization of α_{1B}-adrenoceptor RNA was mainly restricted to intermediate layers (III-upper layer V) in dorsolateral aspects of the prefrontal cortex and in ventral orbital cortex. A moderate number of cells, in the

cingulate and prelimbic areas of the mPFC as well as in more lateral aspect of the piriform cortex, also expressed α_{1B}-adrenoceptor RNA. C) α_{1D}-adrenoceptor RNA was also very abundant yet with a different, and almost complementary, distribution than that of α_{1A}-adrenoceptor RNA. It was expressed by a large number of cells in superficial layer V and, to a lower extent, by cells in layers II-III. The various areas of mPFC, including the infralimbic area, contained a large number of cells expressing α_{1D}-adrenoceptor RNA in intermediate layers. However, unlike α_{1A}-adrenoceptor mRNA, it was expressed by a reduced number cells in layer VI and in ventral aspects of the PFC. ACAd, dorsal anterior cingulate; PL, prelimbic area; ILA infralimbic area, TT, tenia tecta, PIR, piriform cortex; AI, agranular insular cortex; MOs, secondary motor area (nomenclature from Swanson 98).Bar

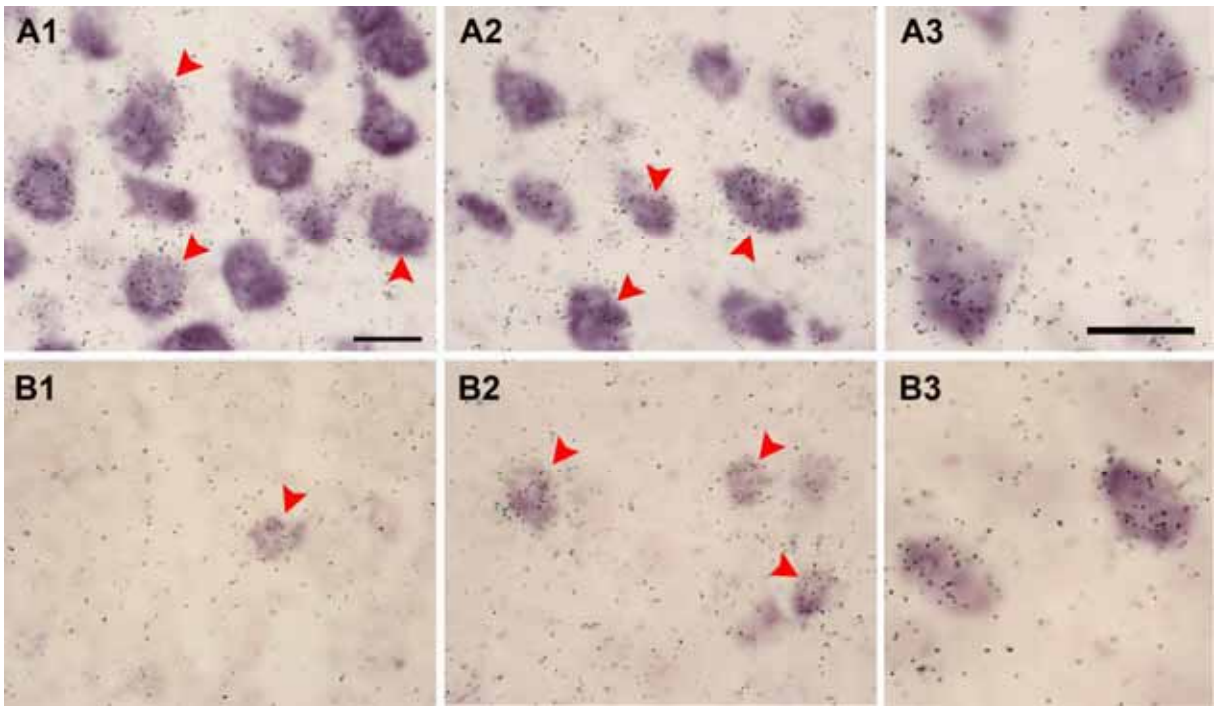

size: 1 mm

Figure 2. *Upper row* (A1-A3). High magnification photomicrographs showing the presence of α_{1A}-adrenoceptor mRNA (^{33}P-labeled oligonucleotides, seen as silver grains) in layer V pyramidal cells of the prelimbic area. Pyramidal neurons were identified by the presence of vGluT1 mRNA (Dig-labeled oligonucleotides). Red arrowheads mark cells positive for both transcripts. For the sake of simplicity, only few cells of each type are marked. A majority of glutamatergic cells expressed the α_{1A} receptor mRNA, as denoted by the double labeling. *Lower row* (B1-B3). The α_{1A} receptor mRNA was also found in GABAergic cells throughout the prefrontal cortex. B1 and B2 show the presence of α_{1A} receptor mRNA in some GABAergic cells of layer I and deep layers, respectively, of the prelimbic area in the mPFC. B3 shows double labeled cells in the prelimbic area at higher magnification. Bar size: 20 µm.

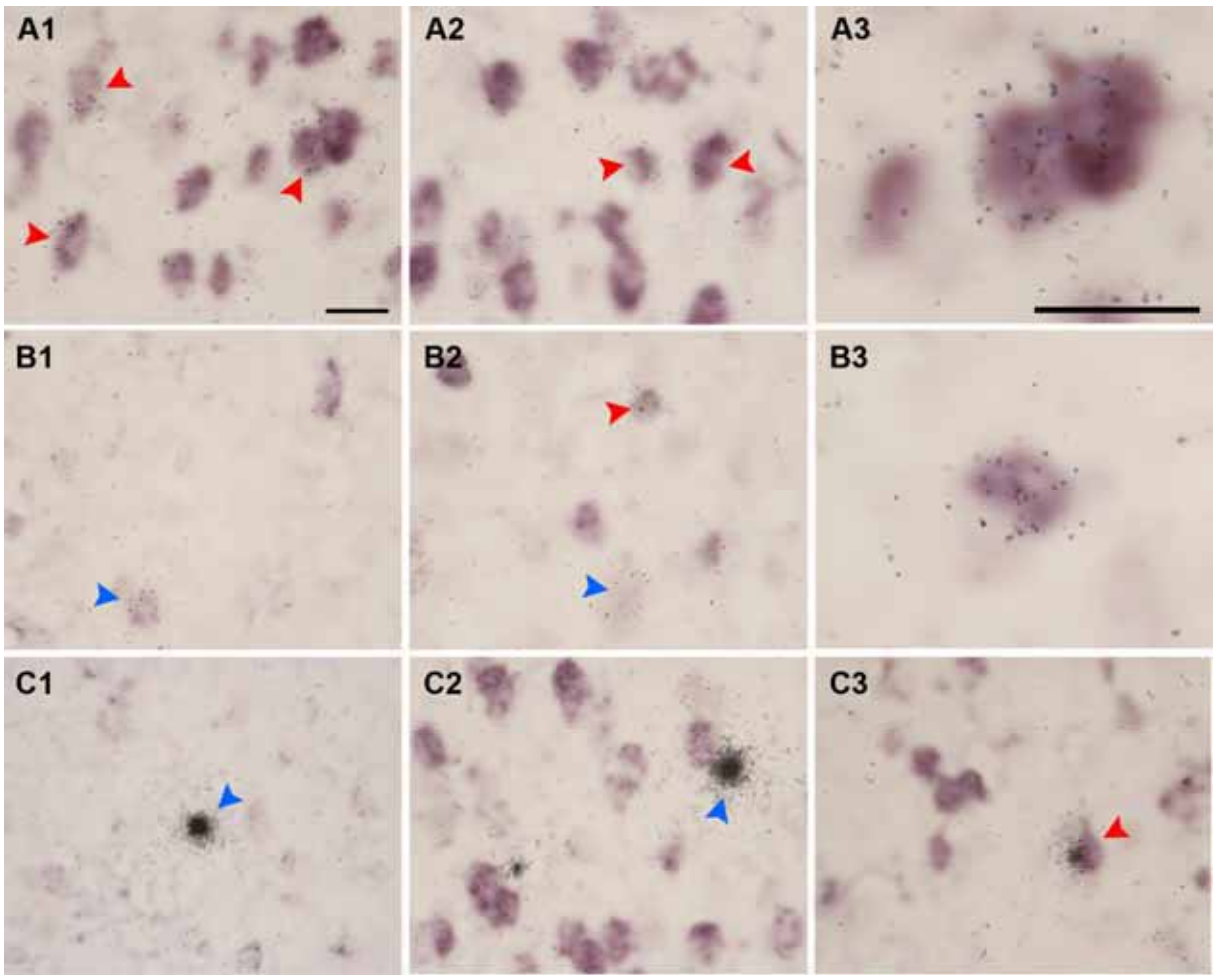

Figure 3. *Upper row* (A1-A3). High magnification photomicrographs showing the presence of α_{1B}-adrenoceptor mRNA (silver grains) in pyramidal cells, identified by the presence of vGluT1 mRNA (dark precipitates). A1 corresponds to layer II-III of anterior dorsal anterior cingulate (ACAd). A2 shows double labeled cells in intermediate layers (III-V) of prelimbic cortex. A3 shows a higher magnification of individual cells expressing both transcripts in the same area. *Middle row* (B1-B3). The α_{1B} receptor mRNA was also found in GABAergic cells. B1 and B2 show the presence of α_{1B} receptor mRNA in some GABAergic cells of superficial layers. B1 and B2 show double-labeled cells in layers I and II-III, respectively, of the prelimbic cortex. B3 shows a double labeled cell in layer II-III of prelimbic cortex at a higher magnification. *Lower row* (C1-C3). Cells expressing high amounts of α_{1B}-adrenoceptor were found in superficial layers of prelimbic cortex. C1: layer I. C2 and C3: layer II. Red arrowheads mark some cells positive for the cellular phenotype examined and for α_{1B}-adrenoceptor mRNA. Blue arrowheads mark cells only positive for α_{1B}-adrenoceptor mRNA. Bar size: 20 µm.

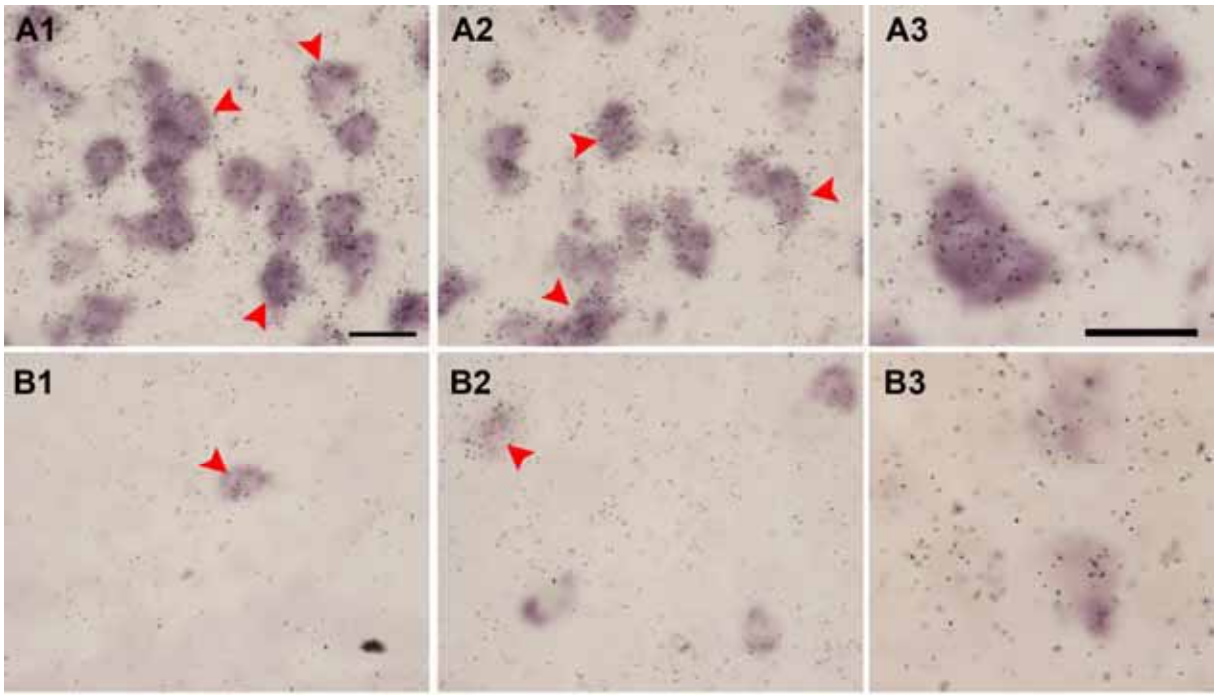

Figure 4. *Upper row* (A1-A3). High magnification photomicrographs showing the presence of α_{1D} receptor mRNA (^{33}P-labeled oligonucleotides) in pyramidal cells, identified by the presence of vGluT1 mRNA (Dig-labeled oligonucleotides).of layers II-III of prelimbic cortex. Red arrowheads mark cells positive for both transcripts. For the sake of simplicity, only few cells of each type are marked. Note that the majority of glutamatergic cells expressed the α_{1D}-adrenoceptor mRNA. *Lower row* (B1-B3). The α_{1D} receptor mRNA was also found in GABAergic cells. B1 shows the presence of α_{1D}-adrenoceptor transcript in a GABAergic cell of prelimbic layer I. B2 was taken in layers II-III of PL. B3 shows a higher magnification of a double-labeled cell in layer V of prelimbic cortex. Bar size: 20 µm.

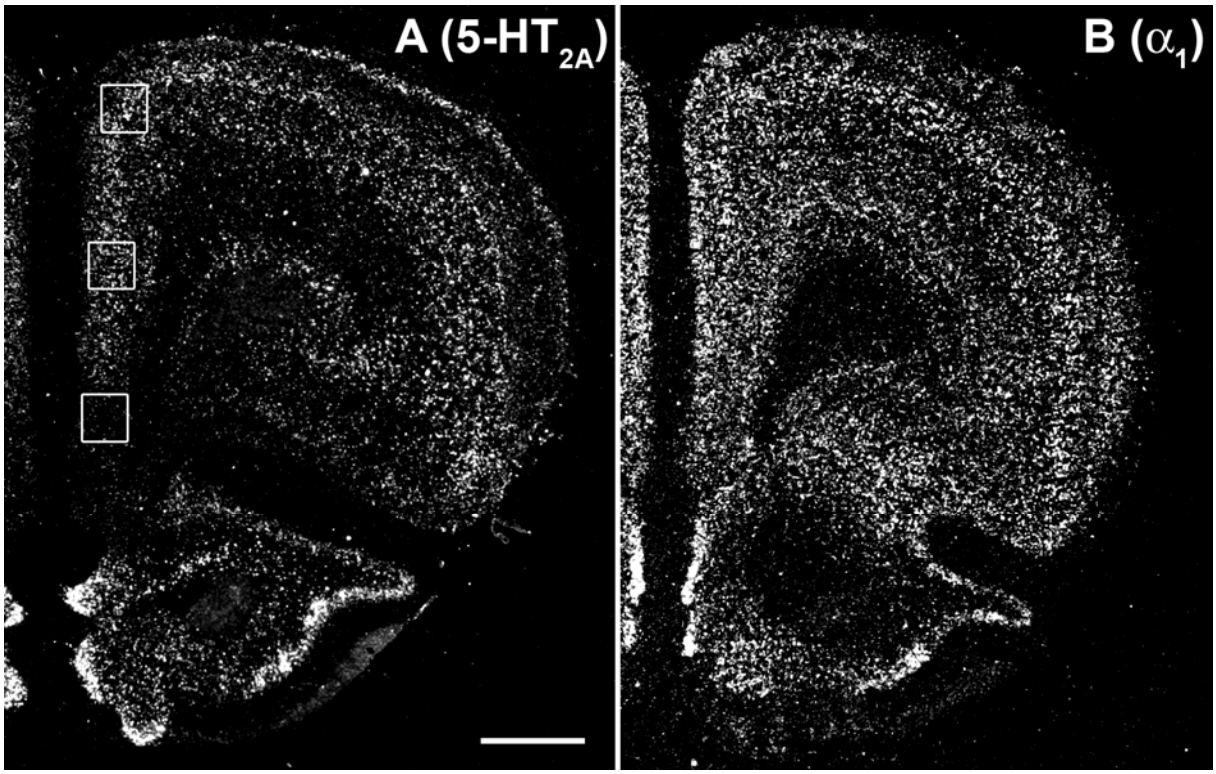

Figure 5. Low magnification dark-field photomicrographs showing the localization of (A) 5-HT_{2A} receptor mRNA, and (B) α_1-adrenoceptor mRNA in rat prefrontal cortex. using *in situ* hybridization histochemistry. The sections correspond approximately to AP +3.7 mm (Paxinos and Watson, 2005). Each receptor transcript was labeled with ^{33}P-labeled oligonucleotides. A) As previously described (Amargos-Bosch et al., 2004;Santana et al., 2004), cells expressing 5-HT_{2A} receptors are located in most dorsal and ventral PFC regions, yet a low density of expressing cells was found in the infralimbic area and layer VIa of the mPFC. Note the presence of cells containing the 5-HT_{2A} receptor transcript in various cortical layers. This was particularly evident in the dorsal and lateral aspects of PFC. B) Cells expressing one or other type of α_1-adrenoceptors were still more abundant than those expressing 5-HT_{2A} receptors. Virtually all areas of the PFC showed the presence of $\alpha_{1A/1B/1D}$-adrenoceptor mRNAs, Open squares mark the approximate location of areas where co-expression of both receptors was examined (Fig. 7). Bar size: 1mm.

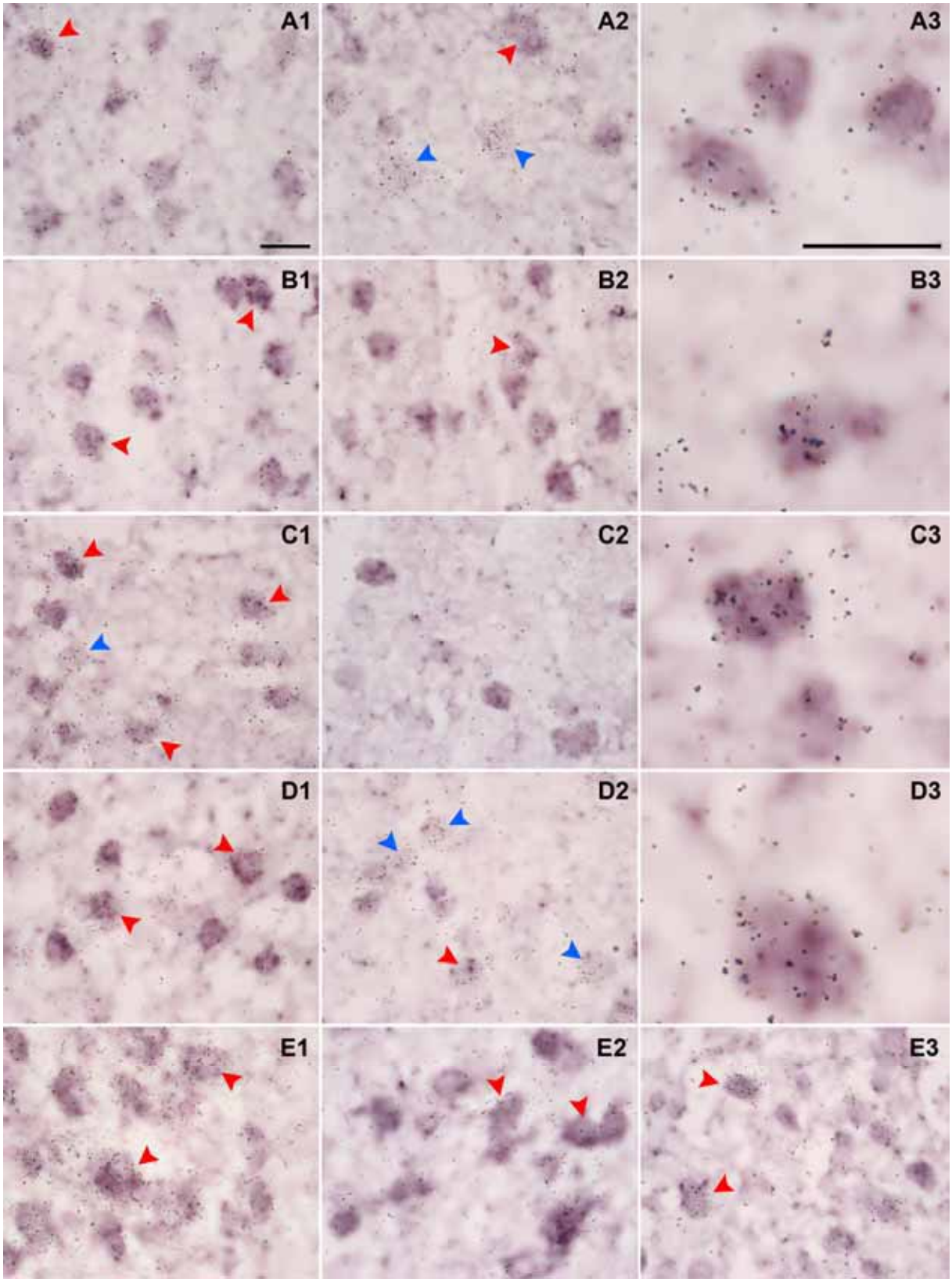

Figure 6. Co-localization of 5-HT_{2A} mRNA (dark precipitates) with the different types of α_1-adrenoceptor mRNAs (silver grains) in various areas of the rat prefrontal cortex. A1-A3) Co-localization with α_{1A}-adrenoceptors in the prelimbic cortex; A1 and A3 show, at different magnification, cells expressing both receptor mRNAs in layers II-III whereas A2 shows some cells in layer VI. Note the presence of cells positive for α_{1A}-adrenoceptors and negative

for 5-HT_{2A} receptors (blue arrowheads), as expected from the scarcity of cells expressing 5-HT_{2A} receptors and abundance of α_{1A}-adrenoceptors in deep layers. B1-B3) Co-localization of 5-HT_{2A} receptors with α_{1B}-adrenoceptors in layers II-III of the anterior cingulate (B1 and B3) and prelimbic (B2) cortices. As expected from the negative dorso-ventral gradient of expression of α_{1B}-adrenoceptors in the mPFC, there was a greater co-expression in cingulate cortex. C1-C3) Co-localization of 5-HT_{2A} receptors with α_{1D}-adrenoceptors in layers II-III of the anterior cingulate (C1 and C3) and layer VIb of the prelimbic cortex (C2). Note the absence of the α_{1D}-adrenoceptors transcript in deep layers, and consequently, the low level of co-expression with 5-HT_{2A} receptors. D1-D3) Co-localization of 5-HT_{2A} receptor mRNA with $\alpha_{1A/1B/1D}$-adrenoceptor mRNAs (multiple probes). D1 and D3 correspond to layers II-III and D2 corresponds to layer VI, all in prelimbic cortex. As for the individual α_1-adrenoceptor mRNAs, note the low co-expression in layer VI due to the small number of 5-HT_{2A}-positve cells in this area. Several cells positive for one or other α_1-adrenoceptor mRNAs (likely the α_{1A} subtype) and negative for 5-HT_{2A} receptor mRNA are marked with blue arrowheads. Panels E1-E3 show the high co-expression of both receptors in areas other than the mPFC. E1 shows the co-localization of the 5-HT_{2A} receptor mRNA with α_{1A}-adrenoceptor mRNA in tenia tecta. E2 and E3 show, respectively, the co-localization of 5-HT_{2A} receptor mRNA with α_1-adrenoceptor mRNAs (multiple probes) in the piriform cortex (PIR) and the ventral part of the agranular insular cortex (AI). Bar size: 20 µm.

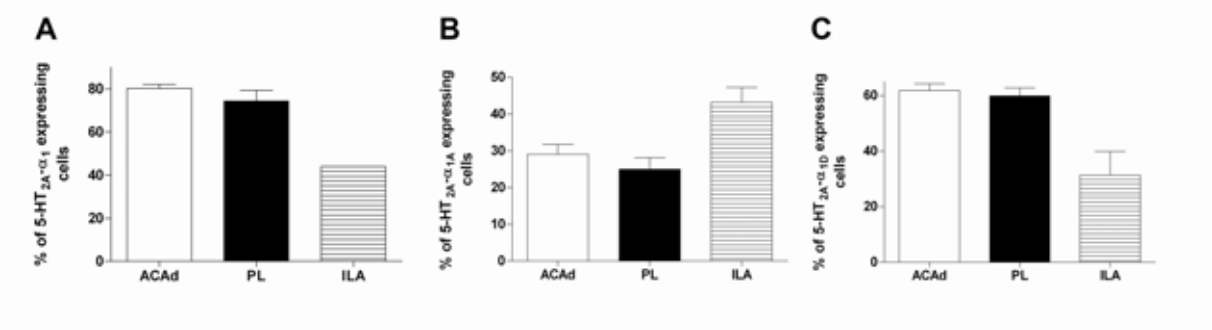

Figure 7. Bar graphs showing the proportion of 5-HT_{2A} receptor-positive cells which also express the transcripts for all α_1-adrenoceptors (A) and for the α_{1A} (B) and α_{1D} (C) types in layers II-III of the various areas of the mPFC (ACAd, dorsal anterior cingulate; PL, prelimbic; IL, infralimbic). Data are means ± SEM of three rats (duplicate sections per rat). The absolute number of 5-HT_{2A} receptor-positive cells in these sections were 41 ± 1 (ACAd), 41 ± 2 (PL), and 12 ± 2 (IL) cells per microscopic field.

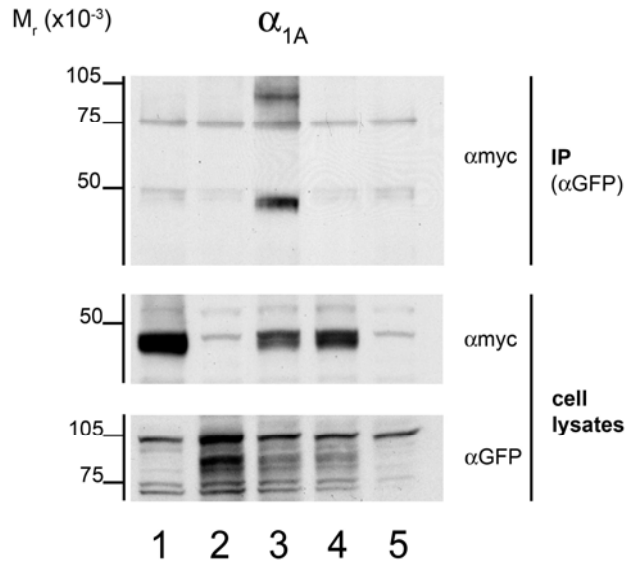

Figure 8. Heterodimeric/oligomeric interaction between co-expressed forms of 5-HT$_{2A}$ serotonin receptor and α_{1A}-adrenoceptors revealed by co-immunoprecipitation. HEK293T cells were transfected to transiently express c-Myc-5-HT$_{2A}$ receptors (lane 1) or/and α_{1A}-adrenoceptors-YFP (lanes 2 and 3, respectively). A mix control (lane 4) was included, corresponding to cells individually expressing both constructs and mixed prior to immunoprecipitation. Untransfected HEK293T cells were used as a negative control (lane 5). *Upper panel,* cell lysates were immunoprecipitated (IP) with anti-GFP antibody, and samples were resolved by SDS-PAGE and then immunoblotted with anti-c-Myc antibody. *Lower panels,* Western blot analysis of cell lysates using anti-c-Myc and anti-GFP antibodies was also performed to confirm the anticipated pattern of protein expression.

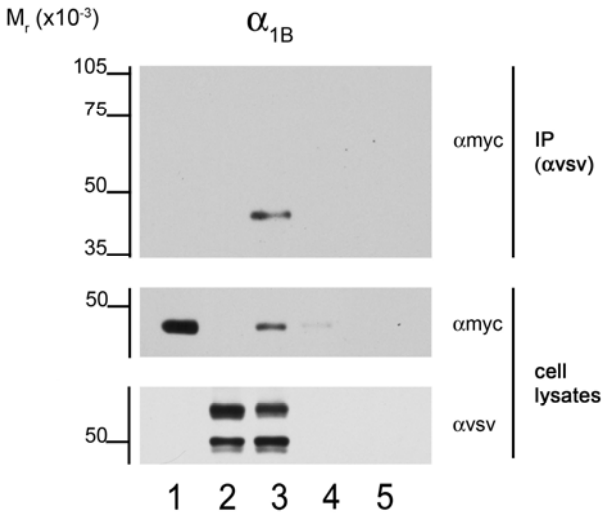

Figure 9. Heterodimeric/oligomeric interaction between co-expressed forms of 5-HT$_{2A}$ serotonin receptor and α_{1B}-adrenoceptors revealed by co-immunoprecipitation. HEK293T cells were transfected to transiently express c-Myc-5-HT$_{2A}$ receptors (lane 1) or/and VSV-α_{1B}-adrenoceptors (lanes 2 and 3, respectively). A mix control (lane 4) was included corresponding to cells individually expressing both constructs and mixed prior to immunoprecipitation. Untransfected HEK293T cells were used as a negative control (lane 5). *Upper panel,* cell lysates were immunoprecipitated (IP) with anti-VSV antibody, and samples were resolved by SDS-PAGE and then immunoblotted with anti-c-Myc antibody. *Lower panels,* Western blot analysis of cell lysates using anti-c-Myc and anti-VSV antibodies was also performed to confirm the anticipated pattern of protein expression.

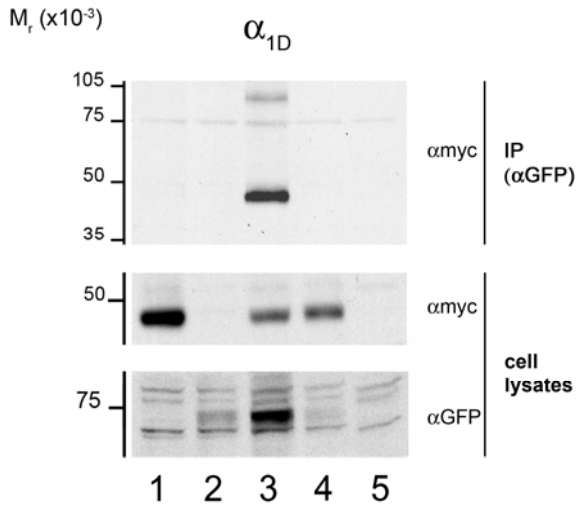

Figure 10. Heterodimeric/oligomeric interaction between co-expressed forms of 5-HT$_{2A}$ receptors and α_{1D}-adrenoceptors revealed by co-immunoprecipitation**.** HEK293T cells were transfected to transiently express c-myc-5-HT$_{2A}$ receptors (lane 1) or/and α_{1D}-adrenoceptors-YFP (lanes 2 and 3, respectively). A mix control (lane 4) was included corresponding to cells individually expressing the constructs and mixed prior to immunoprecipitation. Untransfected HEK293T cells were used as a negative control (lane 5). *Upper panel,* cell lysates were immunoprecipitated (IP) with anti-GFP antibody, and samples were resolved by SDS-PAGE and then immunoblotted with anti-c-Myc antibody. *Lower panels,* Western blot analysis of cell lysates using anti-c-Myc and anti-GFP antibodies was also performed to confirm the anticipated pattern of protein expression.

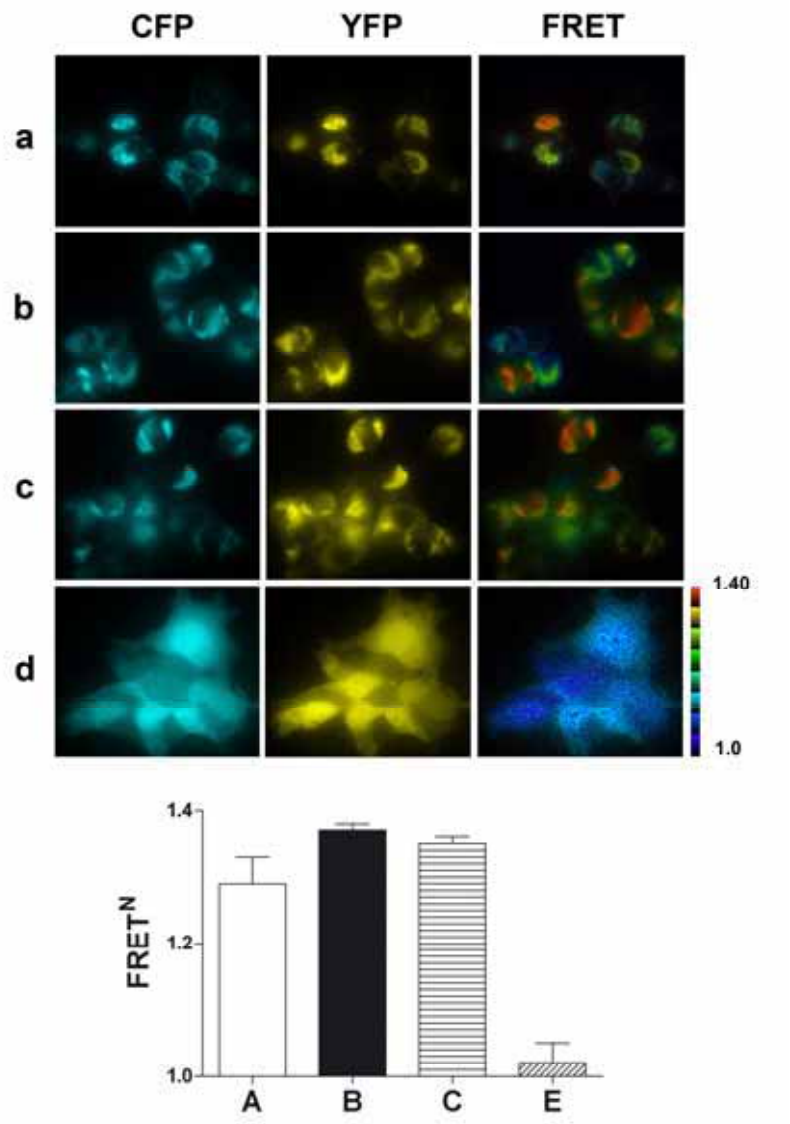

Figure 11. FRET imaging of 5-HT_{2A} and α_1 heteromeric interactions in single cells. 5-HT_{2A} and α_{1A}- (a), α_{1B}- (b) or α_{1D}-adrenoceptors (c) were co-expressed in HEK293T cells. *Left-hand panels*, CFP; *center panels*, YFP; *right-hand panels*, corrected FRET. a) c-Myc-5-HT_{2A}-YFP + α_{1A}-CFP. b) c-Myc-5-HT_{2A}-YFP + α_{1B}-CFP. c) c-Myc-5-HT_{2A}-YFP + α_{1D}-CFP. e) CFP + YFP. The bar graph shows the intensity of FRET signals for the different receptor pairs, calculated as described in Methods. Data are means ± SEM, n=30 cells.

Discussion

The present study shows that the three α_1-adrenoceptor subtypes are expressed in rat PFC in a very high proportion of pyramidal projection neurons and local GABAergic interneurons. They show a complementary and almost non-overlapping distribution in the different PFC subdivisions, which suggests specific roles for each one in the various functions subserved by the PFC. Each α_1-adrenoceptor type was co-expressed with 5-HT_{2A} receptors in all subdivisions of the PFC examined, which indicates a convergence of noradrenergic and serotonergic signals in the same PFC neurons through these excitatory receptors. Finally, co-immunoprecipitation and FRET studies give support to the concept that co-expressed α_1-adrenoceptors and 5-HT_{2A} receptors may actually from heterodimers.

To our knowledge, this is the first study examining the regional and cellular localization of α_1-adrenoceptors in rat PFC. The three α_1-adrenoceptor types occur in various cortical areas (Day et al., 1997;Pieribone et al., 1994) and when examined, their distribution in PFC coincides essentially with our observations (Pieribone et al., 1994). The present study has enabled to quantify the proportion of pyramidal (vGluT1-positive) and GABAergic ($GAD_{65/67}$-positive) neurons expressing each α_1-adrenoceptor type. Interestingly, the proportion of neurons of each type expressing one or other type of α_1-adrenoceptors was surprisingly high, reaching 85% in ACAd and values around 80% in other PFC subdivisions. These values are greater than those found for 5-HT_{1A} and 5-HT_{2A} receptors (up to 66% for 5-HT_{2A} receptor mRNA in ACAd), 5-HT_4 receptors or dopamine D_1 and D_2 receptors (Santana et al., 2004); Vilaró et al, unpublished observations; Santana et al., unpublished observations).

The difference between the proportion of PFC GABAergic interneurons expressing α_1-adrenoceptors or other types of monoaminergic receptors was even more striking. Hence, a maximal proportion of 32-34% of neurons in ACAd and PL were found to express the 5-HT_{2A} receptor mRNA (Santana et al., 2004). Also, the 5-HT_3 receptor, which is almost exclusively expressed by GABAergic interneurons in PFC and hippocampus (Morales et al., 1996;Puig et al., 2004) was found to be present in 40, 18, 6 and 8% of GABAergic neurons in layers I, II–III, V and VI, respectively (Puig et al., 2004). Likewise, dopamine D_1 and D_2 receptor mRNAs are present in 5-38% of GABAergic neurons in various PFC subdivisions (Santana et al. in preparation). Overall, the presence of α_1-adrenoceptors in such a large proportion of projection neurons and local interneurons in PFC indicates that noradrenaline can modulate the activity of the vast majority of PFC neurons via excitatory actions.

Indeed, noradrenaline depolarized and exerted a potent stimulatory action of the firing of layer V pyramidal neurons in mPFC *in vitro* which was blocked by prazosin (Araneda and Andrade, 1991). Moreover, this agent (but not yohimbine, an α_2-adrenoceptor antagonist) also blocked the noradrenaline-induced increase in excitatory postsynaptic currents recorded in layer V neurons of rat mPFC slices (Marek and Aghajanian, 1999). Interestingly, both effects (increased pyramidal excitability and firing) were also evoked by 5-HT acting on 5-HT_{2A} receptors (Araneda and Andrade, 1991;Marek and Aghajanian, 1999).

It has been generally assumed that the noradrenaline-evoked increase in pyramidal neuron excitation involves postsynaptic α_1-adrenoceptors. However, there have been controversial views on the localization of 5-HT_{2A} receptors mediating the increase in EPSCs. This is a measure of synaptic efficacy that depends on the release of glutamate. 5-HT_{2A} receptors mediating the 5-HT evoked increase in EPSCs were initially assumed to be localized on thalamocortical terminals reaching the mPFC (Aghajanian and Marek, 1997). According to these views, the action of hallucinogens acting on 5-HT_{2A} receptors such as lysergic acid diethylamide or DOI would result from an increase in thalamocortical inputs onto the PFC (Aghajanian and Marek, 1999). However, the 5-$HT_{2A/2C}$ receptor agonist DOI enhanced pyramidal cell firing in rat mPFC by a 5-HT_{2A} receptor-dependent mechanism in control rats and in rats with extensive thalamic lesions (Puig et al., 2003), including the mediodorsal and centromedial nuclei that project to the PFC (Berendse and Groenewegen, 1991;Kuroda et al., 1998). Histological studies show a large abundance of intrinsic 5-HT_{2A} receptors in pyramidal and GABAergic neurons of the rat PFC (Amargos-Bosch et al., 2004;Santana et al., 2004). Electron microscopy studies revealed that the majority of 5-HT_{2A} receptor immunoreactivity in mPFC was

located in dendrites and spines of pyramidal neurons and only a minority was present in non-glutamatergic axons (Miner et al., 2003). Finally, a recent study in mouse PFC suggests that 5-HT may induce EPSCs via activation of postsynaptic 5-HT_{2A} receptors in a subpopulation of pyramidal neurons via recurrent local excitatory networks (Beique et al., 2007). Overall, these observations are discordant with the presynaptic localization of 5-HT_{2A} receptors inducing EPSCs in pyramidal neurons and indicate that the vast majority of excitatory 5-HT_{2A} receptors are located on pyramidal neurons of PFC.

The remarkably high co-expression of 5-HT_{2A} receptor mRNA with that of α_1-adrenoceptors suggests a convergence of excitatory signals evoked by 5-HT and noradrenaline on PFC neurons. Given the relatively lower proportion of GABA cells expressing 5-HT_{2A} receptors, compared to the greater population expressing α_1-adrenoceptors, it is likely that most of the co-expression takes place in pyramidal neurons. This observation, together with the common signalling pathways of both receptors (Bartrup and Newberry, 1994;Berg et al., 1998;Claro et al., 1993;Michel et al., 1993;Molinoff, 1984) suggests a close association between them in the living rat brain.

G-protein-coupled receptors (GPCRs), to which monoamine receptors belong, can exist as dimers or higher-order oligomers and establish functionally relevant interactions. After initial suggestions based on an unexplained cooperativity in ligand binding studies (Agnati et al., 1982) molecular and functional studies on $GABA_B$ receptors revealed that these can only function as dimers of $GABA_B$ r1 and $GABA_B$ r2 units (Jones et al., 1998;Kaupmann et al., 1998;White et al., 1998). Recent studies indicate that α_1-adrenoceptors can also homo- and heterodimerize. The three members of the family are able to form homodimers and can also heterodimerize with some selectivity. Hence, the α_{1D}–adrenergic receptor is not normally expressed on the cell surface of most cells unless it dimerizes with α_{1B}-adrenoceptors or ß$_2$-adrenergic receptors, which indicates an important role of heterodimerization in the intracellular receptor trafficking (Hague et al., 2006;Uberti et al., 2005). Likewise, certain 5-HT receptors such as the 5-HT_{1B} and 5-HT_{1D} receptors form homodimers when expressed alone and heterodimers when co-expressed (Xie et al., 1999). Likewise, dimerization appears essential for 5-HT_{2C} receptor function (Herrick-Davis et al., 2005).

The present observations, using co-immunoprecipitation and FRET in HEK293T cells, indicate that 5-HT_{2A} and each α_1-adrenoceptor type can form stable heterodimers. It is unclear whether GPCRs dimerization occurs *in vivo*, yet a number of functional observations give support to this hypothesis for certain receptor pairs, such as the $GABA_B$ homodimers or the adenosine/dopamine receptors. In the case of 5-HT_{2A} and α_1-adrenoceptors, this possibility if supported by a number of observations. First, as shown in the present study, both receptors are co-expressed in a large proportion of PFC (mainly pyramidal) neurons, a first requisite for their intracellular interaction. Secondly, the cellular localization α_1-adrenoceptors in the cerebral cortex overlaps with that of 5-HT_{2A} receptors as examined by immunohistochemistry. Both have been found to be localized in cell bodies and apical dendrites of pyramidal neurons (Acosta-Martinez et al., 1999;Cornea-Hebert et al., 1999;Jakab and Goldman-Rakic, 1998;Jakab and Goldman-Rakic, 2000;Martin-Ruiz et al., 2001). Third, several functional interactions have been reported between 5-HT_{2A} and α_1-adrenoceptors in the rat. Hence, behavioural and neurochemical studies reported the ability of the α_1-adrenoceptor antagonist prazosin to antagonize the effect of the 5-HT_{2A} receptor agonist DOI (Bortolozzi et al., 2003;Dursun and Handley, 1996;Schreiber et al., 1995). Moreover, the selective 5-HT_{2A} receptor antagonist M100907 reversed the increase in mPFC 5-HT release induced by local application of cirazoline, an α_1-adrenoceptor agonist (Amargos-Bosch et al., 2003) and both antagonists (M100907 and prazosin) were equally effective in reversing the increase in mPFC 5-HT release induced by the activation of AMPA receptors in mPFC (Amargos-Bosch et al., 2007). Finally, a functional interaction between both receptors mediates neurochemical and behavioral responses induced by opiates and psychostimulants, as assessed in genetically modified mice (Auclair et al., 2004).

The present observations may provide a molecular and cellular basis for the above interactions, yet the exact way through which they occur is still unknown. One possible mechanism is the off-target allosteric interaction (Millligan et al, personal communication). Hence, ligands of one receptor of the heterodimeric complex may alter the

binding properties of the other member of the pair. This would explain the apparent functional antagonism of prazosin on the actions of 5-HT_{2A} receptor agonists (and viceversa).

The presence of α_1-adrenoceptors and 5-HT_{2A} receptors in the same PFC neurons and possible formation of heterodimers may have important functional and therapeutic implications. On the one hand, the activity of cortical areas may be concurrently regulated by the ascending 5-HT and NA systems. Since both neuronal groups are REM-off (Aston-Jones et al., 1991;Jacobs and Azmitia, 1992) the combined activity of 5-HT and NA at excitatory α_1-adrenoceptors and 5-HT_{2A} receptors may have a synergic effect on the activity of cortical neurons during wakefulness. Also, both receptors have been involved in working memory through the modulation of neuronal activity in dorsolateral PFC (Ramos and Arnsten, 2007;Williams et al., 2002). On the other hand, antidepressants such as the dual (5-HT and NA) reuptake inhibitors (Artigas, 1995) are known to be more efficacious than selective 5-HT reuptake inhibitors, an action which may occur through summation of effects on the same cellular elements. Finally, conventional and atypical antipsychotics share the ability to antagonize α_1-adrenoceptors whereas only the latter drugs antagonize 5-HT_{2A} receptors (Arnt and Skarsfeldt, 1998;Bymaster et al., 1996). The therapeutic potential of α_1-adrenoceptor blockade in schizophrenia has often been neglected due to its cardiovascular effects despite the fact that prazosin enhanced the antipsychotic actions of dopamine D_2 receptor blockade. The present observations support that α_1-adrenoceptor and 5-HT_{2A} receptor blockade may add to each other.

In summary, the present study shows that the ascending 5-HT and NA systems share common actions in the PFC through the concurrent expression of α_1-adrenoceptors and 5-HT_{2A} receptors in the vast majority of PFC neurons and the possible formation of heterodimers.

Acknowledgements

Work supported by grant SAF 2004-05525 and Support from the Generalitat de Catalunya (2005SGR00758) and the Spanish Ministry of Health, Instituto de Salud Carlos III, RETICS RD06/0011(REM-TAP Network) is also acknowledged. NS is recipient of a predoctoral fellowship from the Ministry of Science and Education. We thank Judith Ballart for skilful technical assistance

References

Abi-Dargham A, Mawlawi O, Lombardo I, Gil R, Martinez D, Huang Y, Hwang DR, Keilp J, Kochan L, Van Heertum R, Gorman JM, Laruelle M (2002) Prefrontal dopamine D1 receptors and working memory in schizophrenia. J Neurosci 22: 3708-3719.

Acosta-Martinez M, Fiber JM, Brown RD, Etgen AM (1999) Localization of alpha(1B)-adrenergic receptor in female rat brain regions involved in stress and neuroendocrine function. Neurochemistry International 35: 383-391.

Aghajanian GK, Marek GJ (1997) Serotonin induces excitatory postsynaptic potentials in apical dendrites of neocortical pyramidal cells. Neuropharmacology 36: 589-599.

Aghajanian GK, Marek GJ (1999) Serotonin, via 5-HT2A receptors, increases EPSCs in layer V pyramidal cells of prefrontal cortex by an asynchronous mode of glutamate release. Brain Res 825: 161-171.

Agnati LF, Fuxe K, Zoli M, Rondanini C, Ogren SO (1982) New Vistas on Synaptic Plasticity - the Receptor Mosaic Hypothesis of the Engram. Medical Biology 60: 183-190.

Akil M, Edgar CL, Pierri JN, Casali S, Lewis DA (2000) Decreased density of tyrosine hydroxylase-immunoreactive axons in the entorhinal cortex of schizophrenic subjects. Biol Psychiatry 47: 361-370.

Amargos-Bosch M, Adell A, Artigas F (2007) Antipsychotic drugs reverse the AMPA receptor-stimulated release of 5-HT in the medial prefrontal cortex. J Neurochem 102: 550-561.

Amargos-Bosch M, Adell A, Bortolozzi A, Artigas F (2003) Stimulation of alpha(1)adrenoceptors in the rat medial prefrontal cortex increases the local in vivo 5-hydroxytryptamine release: reversal by antipsychotic drugs. Journal of Neurochemistry 87: 831-842.

Amargos-Bosch M, Bortolozzi A, Puig MV, Serrats J, Adell A, Celada P, Toth M, Mengod G, Artigas F (2004) Co-expression and in vivo interaction of serotonin(1A) and serotonin(2A) receptors in pyramidal neurons of prefrontal cortex. Cerebral Cortex 14: 281-299.

Araneda R, Andrade R (1991) 5-Hydroxytryptamine2 and 5-Hydroxytryptamine1A Receptors Mediate Opposing Responses on Membrane Excitability in Rat-Association Cortex. Neuroscience 40: 399-412.

Arnt J, Skarsfeldt T (1998) Do novel antipsychotics have similar pharmacological characteristics? A review of the evidence. Neuropsychopharmacology 18: 63-101.

Artigas F (1995) Selective Serotonin Noradrenaline Reuptake Inhibitors (Snris) - Pharmacology and Therapeutic Potential in the Treatment of Depressive-Disorders. Cns Drugs 4: 79-89.

Aston-Jones G, Chiang C, Alexinsky T (1991) Discharge of noradrenergic locus coeruleus neurons in behaving

rats and monkeys suggests a role in vigilance. Prog Brain Res 88: 501-520.

Auclair A, Blanc G, Glowinski J, Tassin JP (2004) Role of serotonin(2A) receptors in the D-amphetamine-induced release of dopamine: comparison with previous data on alpha 1b-adrenergic receptors. Journal of Neurochemistry 91: 318-326.

Bartrup JT, Newberry NR (1994) 5-HT2A receptor-mediated outward current in C6 glioma cells is mimicked by intracellular IP3 release. Neuroreport 5: 1245-1248.

Beique JC, Imad M, Mladenovic L, Gingrich JA, Andrade R (2007) Mechanism of the 5-hydroxytryptamine 2A receptor-mediated facilitation of synaptic activity in prefrontal cortex. Proc Natl Acad Sci U S A 104: 9870-9875.

Berendse HW, Groenewegen HJ (1991) Restricted cortical termination fields of the midline and intralaminar thalamic nuclei in the rat. Neuroscience 42: 73-102.

Berg KA, Maayani S, Goldfarb J, Scaramellini C, Leff P, Clarke WP (1998) Effector pathway-dependent relative efficacy at serotonin type 2A and 2C receptors: Evidence for agonist-directed trafficking of receptor stimulus. Molecular Pharmacology 54: 94-104.

Bortolozzi A, Amargos-Bosch M, Adell A, Diaz-Mataix L, Serrats J, Pons S, Artigas F (2003) In vivo modulation of 5-hydroxytryptamine release in mouse prefrontal cortex by local 5-HT2A receptors: effect of antipsychotic drugs. European Journal of Neuroscience 18: 1235-1246.

Bymaster FP, HemrickLuecke SK, Perry KW, Fuller RW (1996) Neurochemical evidence for antagonism by olanzapine of dopamine, serotonin, alpha(1)-adrenergic and muscarinic receptors in vivo in rats. Psychopharmacology 124: 87-94.

Carli M, Baviera M, Invernizzi RW, Balducci C (2006) Dissociable contribution of 5-HT1A and 5-HT2A receptors in the medial prefrontal cortex to different aspects of executive control such as impulsivity and compulsive perseveration in rats. Neuropsychopharmacology 31: 757-767.

Carrillo JJ, Lopez-Gimenez JF, Milligan G (2004) Multiple interactions between transmembrane helices generate the oligomeric alpha1b-adrenoceptor. Mol Pharmacol 66: 1123-1137.

Clarke HF, Dalley JW, Crofts HS, Robbins TW, Roberts AC (2004) Cognitive inflexibility after prefrontal serotonin depletion. Science 304: 878-880.

Claro E, Fain JN, Picatoste F (1993) Noradrenaline Stimulation Unbalances the Phosphoinositide Cycle in Rat Cerebral Cortical Slices. Journal of Neurochemistry 60: 2078-2086.

Cornea-Hebert V, Riad M, Wu C, Singh SK, Descarries L (1999) Cellular and subcellular distribution of the serotonin 5-HT2A receptor in the central nervous system of adult rat. Journal of Comparative Neurology 409: 187-209.

Dalley JW, Theobald DE, Bouger P, Chudasama Y, Cardinal RN, Robbins TW (2004) Cortical cholinergic function and deficits in visual attentional performance in rats following 192 IgG-saporin-induced lesions of the medial prefrontal cortex. Cerebral Cortex 14: 922-932.

Day HE, Campeau S, Watson SJ, Jr., Akil H (1997) Distribution of alpha 1a-, alpha 1b- and alpha 1d-adrenergic receptor mRNA in the rat brain and spinal cord. J Chem Neuroanat 13: 115-139.

Dursun SM, Handley SL (1996) Similarities in the pharmacology of spontaneous and DOI-induced head-shakes suggest 5HT2A receptors are active under physiological conditions. Psychopharmacology (Berl) 128: 198-205.

Fuster JM (1997) The Prefrontal Cortex. Anatomy, Physiology, and Neuropsychology of the Frontal Lobe. Philadelphia-New York: Lipincott-Raven.

Hague C, Lee SE, Chen ZJ, Prinster SC, Hall RA, Minneman KP (2006) Heterodimers of alpha1B and alpha1D-adrenergic receptors form a single functional entity. Faseb Journal 20: A253-A254.

Harrison PJ (1999) Neurochemical alterations in schizophrenia affecting the putative receptor targets of atypical antipsychotics - Focus on dopamine (D-1, D-3, D-4) and 5-HT2a receptors. British Journal of Psychiatry 174: 12-22.

Herrick-Davis K, Grinde E, Harrigan TJ, Mazurkiewicz JE (2005) Inhibition of serotonin 5-hydroxytryptamine2C receptor function through heterodimerization - Receptor dimers bind two molecules of ligand and one G-protein. Journal of Biological Chemistry 280: 40144-40151.

Jacobs BL, Azmitia EC (1992) Structure and function of the brain serotonin system. Physiol Rev 72: 165-229.

Jakab RL, Goldman-Rakic PS (1998) 5-Hydroxytryptamine2A serotonin receptors in the primate cerebral cortex: possible site of action of hallucinogenic and antipsychotic drugs in pyramidal cell apical dendrites. Proc Natl Acad Sci U S A 95: 735-740.

Jakab RL, Goldman-Rakic PS (2000) Segregation of serotonin 5-HT2A and 5-HT3 receptors in inhibitory circuits of the primate cerebral cortex. J Comp Neurol 417: 337-348.

Jones KA, Borowsky B, Tamm JA, Craig DA, Durkin MM, Dai M, Yao WJ, Johnson M, Gunwaldsen C, Huang LY, Tang C, Shen Q, Salon JA, Morse K, Laz T, Smith KE, Nagarathnam D, Noble SA, Branchek TA, Gerald C (1998) GABA(B) receptors function as a heteromeric assembly of the subunits GABA(B)R1 and GABA(B)R2. Nature 396: 674-679.

Kaupmann K, Malitschek B, Schuler V, Heid J, Froestl W, Beck P, Mosbacher J, Bischoff S, Kulik A, Shigemoto R, Karschin A, Bettler B (1998) GABA(B)-receptor subtypes assemble into functional heteromeric complexes. Nature 396: 683-687.

Kuroda M, Yokofujita J, Murakami K (1998) An ultrastructural study of the neural circuit between the

prefrontal cortex and the mediodorsal nucleus of the thalamus. Prog Neurobiol 54: 417-458.

Landry M, Holmberg K, Zhang X, Hokfelt T (2000) Effect of axotomy on expression of NPY, galanin, and NPY Y1 and Y2 receptors in dorsal root ganglia and the superior cervical ganglion studied with double-labeling in situ hybridization and immunohistochemistry. Exp Neurol 162: 361-384.

Lewis DA, Lieberman JA (2000) Catching up on schizophrenia: natural history and neurobiology. Neuron 28: 325-334.

Lewis SJ, Zammit S, Gunnell D, Smith GD (2005) A meta-analysis of the MTHFR C677T polymorphism and schizophrenia risk. Am J Med Genet B Neuropsychiatr Genet 135: 2-4.

Marek GJ, Aghajanian GK (1999) 5-HT2A receptor or alpha1-adrenoceptor activation induces excitatory postsynaptic currents in layer V pyramidal cells of the medial prefrontal cortex. Eur J Pharmacol 367: 197-206.

Martin-Ruiz R, Puig MV, Celada P, Shapiro DA, Roth BL, Mengod G, Artigas F (2001) Control of serotonergic function in medial prefrontal cortex by serotonin-2A receptors through a glutamate-dependent mechanism. Journal of Neuroscience 21: 9856-9866.

Meltzer HY (1999) Treatment of schizophrenia and spectrum disorders: pharmacotherapy, psychosocial treatments, and neurotransmitter interactions. Biol Psychiatry 46: 1321-1327.

Michel MC, Erdbrugger W, Bischoff A, Brodde OE (1993) Differential Phospholipase-A(2) and Phospholipase-C Coupling for Rat Renal Angiotensin-Ii, Neuropeptide-y and Alpha(1)-Adrenergic Receptors. Faseb Journal 7: A467.

Miller EK, Cohen JD (2001) An integrative theory of prefrontal cortex function. Annu Rev Neurosci 24: 167-202.

Miner LAH, Backstrom JR, Sanders-Bush E, Sesack SR (2003) Ultrastructural localization of serotonin(2A) receptors in the middle layers of the rat prelimbic prefrontal cortex. Neuroscience 116: 107-117.

Molinoff PB (1984) Alpha- and beta-adrenergic receptor subtypes properties, distribution and regulation. Drugs 28 Suppl 2: 1-15.

Morales M, Battenberg E, deLecea L, Bloom FE (1996) The type 3 serotonin receptor is expressed in a subpopulation of GABAergic neurons in the rat neocortex and hippocampus. Brain Research 731: 199-202.

Paxinos G, Watson C (2005) The Rat Brain in stereotaxic coordinates. San Diego: Elsevier Academic Press.

Pieribone VA, Nicholas AP, Dagerlind A, Hokfelt T (1994) Distribution of alpha 1 adrenoceptors in rat brain revealed by in situ hybridization experiments utilizing subtype-specific probes. J Neurosci 14: 4252-4268.

Puig MV, Celada P, Diaz-Mataix L, Artigas F (2003) In vivo modulation of the activity of pyramidal neurons in the rat medial prefrontal cortex by 5-HT2A receptors: Relationship to thalamocortical afferents. Cerebral Cortex 13: 870-882.

Puig MV, Santana N, Celada P, Mengod G, Artigas F (2004) In vivo excitation of GABA interneurons in the medial prefrontal cortex through 5-HT3 receptors. Cerebral Cortex 14: 1365-1375.

Ramos BP, Arnsten AF (2007) Adrenergic pharmacology and cognition: focus on the prefrontal cortex. Pharmacol Ther 113: 523-536.

Robbins TW (2000) From arousal to cognition: the integrative position of the prefrontal cortex. Prog Brain Res 126: 469-483.

Roberts AC, De Salvia MA, Wilkinson LS, Collins P, Muir JL, Everitt BJ, Robbins TW (1994) 6-Hydroxydopamine lesions of the prefrontal cortex in monkeys enhance performance on an analog of the Wisconsin Card Sort Test: possible interactions with subcortical dopamine. J Neurosci 14: 2531-2544.

Santana N, Bortolozzi A, Serrats J, Mengod G, Artigas F (2004) Expression of serotonin1A and serotonin2A receptors in pyramidal and GABAergic neurons of the rat prefrontal cortex. Cereb Cortex 14: 1100-1109.

Schreiber R, Brocco M, Audinot V, Gobert A, Veiga S, Millan MJ (1995) (1-(2,5-Dimethoxy-4 Iodophenyl)-2-Aminopropane)-Induced Head-Twitches in the Rat Are Mediated by 5-Hydroxytryptamine (5-Ht)(2A) Receptors - Modulation by Novel 5-Ht2A/2C Antagonists, D-1 Antagonists and 5-Ht1A Agonists. Journal of Pharmacology and Experimental Therapeutics 273: 101-112.

Selemon LD, Goldman-Rakic PS (1999) The reduced neuropil hypothesis: a circuit based model of schizophrenia. Biol Psychiatry 45: 17-25.

Tomiyama M, Palacios JM, Cortes R, Vilaro MT, Mengod G (1997) Distribution of AMPA receptor subunit mRNAs in the human basal ganglia: an in situ hybridization study. Mol Brain Res 46: 281-289.

Uberti MA, Hague C, Oller H, Minneman KP, Hall RA (2005) Heterodimerization with beta2-adrenergic receptors promotes surface expression and functional activity of alpha1D-adrenergic receptors. J Pharmacol Exp Ther 313: 16-23.

Vijayraghavan S, Wang M, Birnbaum SG, Williams GV, Arnsten AF (2007) Inverted-U dopamine D1 receptor actions on prefrontal neurons engaged in working memory. Nat Neurosci 10: 376-384.

Weinberger DR, Egan MF, Bertolino A, Callicott JH, Mattay VS, Lipska BK, Berman KF, Goldberg TE (2001) Prefrontal neurons and the genetics of schizophrenia. Biol Psychiatry 50: 825-844.

White JH, Wise A, Main MJ, Green A, Fraser NJ, Disney GH, Barnes AA, Emson P, Foord SM, Marshall FH (1998) Heterodimerization is required for the formation of a functional GABA(B) receptor. Nature 396: 679-682.

Williams GV, Goldman-Rakic PS (1995) Modulation of memory fields by dopamine D1 receptors in prefrontal cortex. Nature 376: 572-575.

Williams GV, Rao SG, Goldman-Rakic PS (2002) The physiological role of 5-HT2A receptors in working memory. J Neurosci 22: 2843-2854.

Winstanley CA, Chudasama Y, Dalley JW, Theobald DE, Glennon JC, Robbins TW (2003) Intra-prefrontal 8-OH-DPAT and M100907 improve visuospatial attention and decrease impulsivity on the five-choice serial reaction time task in rats. Psychopharmacology (Berl) 167: 304-314.

Xie Z, Lee SP, O'Dowd BF, George SR (1999) Serotonin 5-HT1B and 5-HT1D receptors form homodimers when expressed alone and heterodimers when co-expressed. FEBS Lett 456: 63-67.

Trabajo 5:

Quantitative Analysis of the Expression of Dopamine D_1 and D_2 Receptors in Pyramidal and GABAergic Neurons of the Rat Prefrontal Cortex

Noemí Santana, Guadalupe Mengod and Francesc Artigas.

En preparación

En este trabajo se examinó la expresión de los ARNm de los receptores dopaminérgicos D_1 y D_2 en neuronas piramidales (positivas para vGluT1) y GABAérgicas (positivas para GAD) en la corteza prefrontal (CPF) de rata. Los ARNm de ambos receptores se expresaron predominantemente en capas V-VI de la CPF medial, las áreas cingulada y motora así como en áreas ventrales de la CPF. Las neuronas que expresaron el receptor D_1 fueron más abundantes que las que expresaron el receptor D_2. Algunas neuronas piramidales y GABAérgicas expresaron densidades muy altas del ARNm del receptor D_1. Los receptores D_1 se expresaron por una mayor proporción de células GABAérgicas que piramidales mientras que lo contrario ocurrió en el caso de los receptores D_2.

Quantitative Analysis of the Expression of Dopamine D_1 and D_2 Receptors in Pyramidal and GABAergic Neurons of the Rat Prefrontal Cortex

***Abbreviated title**:* Dopamine receptors in prefrontal cortex

Noemí Santana, Guadalupe Mengod and Francesc Artigas

Department of Neurochemistry and Neuropharmacology

Institut d' Investigacions Biomèdiques de Barcelona (CSIC), IDIBAPS

08036 Barcelona, Spain

Corresponding author:
Francesc Artigas, PhD;
Dept. of Neurochemistry and Neuropharmacology,
Institut d' Investigacions Biomèdiques de Barcelona (CSIC), IDIBAPS
Rosselló, 161, 6th floor, 08036 Barcelona, Spain.

Phone: +3493-363 8315;
Fax: +3493-363 8301;
e-mail: fapnqi@iibb.csic.es

Abstract

Mesocortical dopamine (DA) plays a key role in cognition and executive functions through the activation of postsynaptic receptors. In particular, fine tuning of DA D_1 receptors is critical for working memory. Derangements of the dopaminergic neurotransmission are suspected in the prefrontal cortex (PFC) of schizophrenic patients. Moreover, antipsychotic drugs interact with DA receptors. The cellular basis of the actions of DA on PFC activity is not clearly understood despite extensive but often contradictory results. This is partly due to the multiple signaling systems targeted by DA but also to a poor knowledge of the cellular and regional localization of DA receptors within the PFC. Using double *in situ* hybridization, we examined the expression of D_1 and D_2 receptor mRNAs in pyramidal (vGluT1-positive) and GABAergic neurons ($GAD_{65/67}$-positive) in rat PFC. Consistent with the denser dopaminergic innervation of deep layers, both receptor mRNAs were predominantly expressed in layers V-VI of the medial PFC (mPFC), the cingulate and motor areas as well as (mostly D_1 receptors) in ventral PFC areas. Neurons expressing D_1 receptors were more abundant than those expressing D_2 receptors. Some pyramidal and GABAergic neurons expressed very high densities of D_1 (but not D_2) receptor mRNA. D_1 receptors were expressed by a greater proportion of GABAergic than pyramidal cells whereas the opposite holds true for D_2 receptors. These results she new light onto the existing discrepancies in the cellular actions of DA in PFC and indicate that DA actions on projection pyramidal neurons are layer-specific and depend on precise local interactions.

Key words: Dopamine D_1 receptors · Dopamine D_2 receptors · antipsychotics · GABA interneurons · prefrontal cortex · pyramidal neurons

Introduction

Brain dopamine (DA) systems are involved in a wide variety of functions including motivation, attention, reward, cognition and movement (Graybiel et al., 1994;Williams and Goldman-Rakic, 1995;Schultz, 1998;Koob and Le Moal, 2001;Dalley et al., 2004;Grace et al., 2007;Iversen and Iversen, 2007). Derangements of the DA pathways arising n the ventral tegmental area (VTA) have been suspected in various psychiatric conditions including schizoprhenia, depression, drug addiction or attention deficit hyperactivity disorder (Grace, 1991;Willner et al., 1992;Everitt and Robbins, 2000;Koob and Le Moal, 2001;Castellanos and Tannock, 2002). In particular, the mesocortical DA system plays a major role in cognitive processes by modulating the memory fields of pyramidal neurons in the dorsolateral prefrontal cortex (PFC) of primates. Hence, partial blockade of D_1 receptors in monkey PFC magnified the enhanced neuronal activity during the delay period in a working memory task (Williams and Goldman-Rakic, 1995). Yet, full D_1 receptor blockade canceled this effect suggesting a bell-shaped relationship between DA D_1 receptor occupancy and cognitive performance (Goldman-Rakic et al., 2000;Vijayraghavan et al., 2007). On the other hand, blockade of DA $D_{2/3}$ receptors attenuated the activity of cortical neurons during the delay period in a working memory task (Williams and Goldman-Rakic, 1995). Moreover, the cognitive deficits induced by chronic $D_{2/3}$ receptor blockade by antipsychotics are reversed by D_1 agonist administration (Castner et al., 2000). The cellular basis for the DA actions in PFC have been extensively investigated and a plethora of studies have examined the effect of DA or selective D_1 and D_2 receptor agonists in the PFC of rodents and non-human primates (Thierry et al., 1990;Grace, 1991;O'Donnell, 2003). The vast majority of studies have assessed the effects of DA receptor stimulation on projection (pyramidal) neurons while a few have also assessed the effects on GABAergic interneurons. However, despite extensive research effort, there is not a unified view of DA actions in PFC and many of these studies

have arrived at non-convergent and often contradictory conclusions.

This situation likely results from methodological reasons (e.g., *in vitro* vs. *in vivo* approaches) and from the multiplicity of short-term (ms) and long-term (min, hr) signaling mechanisms coupled to D_1 and D_2 receptor families (Svenningsson et al., 2004;Beaulieu et al., 2007;Bolan et al., 2007) .The presence of DA receptors in pyramidal and GABAergic neurons adds a further element of complexity. Hence, the net *in vivo* effect of DA or a dopaminergic agonist on a given pyramidal neuron will depend on the relative abundance of each DA receptor in the examined neuron, the GABAergic neuron(s) in the vicinity and their interaction though feedback and feed-forward mechanisms.

In order to provide a more detailed insight on the cellular basis of DA actions in PFC, we performed a quantitative estimation of the proportion of pyramidal and GABAergic neurons expressing DA D_1 and D_2 receptors in the various areas of the rat PFC paying also a special attention to their layer distribution and relative localization.

Materials and Methods

Tissue preparation

Male albino Wistar rats were from Iffa Credo, Lyon, France. Three groups of rats weighing 35-45g, 130-140g or 250-300g, corresponding to animals with 2, 5 and 10 weeks of postnatal age were used. Animals were kept in a controlled environment (12 h light-dark cycle and 22 ± 2°C room temperature) with food and water provided *ad libitum*. Animal care followed the European Union regulations (O.J. of E.C. L358/1 18/12/1986) and was approved by the local Institutional Animal Care and Use Committee. The rats were killed by decapitation and the brains rapidly removed, frozen on dry ice and stored at –20°C. Tissue sections, 14 µm thick, were cut using a microtome-cryostat (HM500 OM; Microm, Walldorf, Germany), thaw-mounted onto APTS (3-aminopropyltriethoxysilane; Sigma,St Louis, MO) coated slides and kept at –20°C until use.

Hybridization probes

The oligodeoxyribonucleotide probes used were complementary to the following bases: 752-796, 1805-1852 and 797-841 of the rat D_1 receptor mRNA (GenBank Accession No. NM_012546.1); 347-388, 1211-1258 and 1211-1258 of the D_2 receptor mRNA (GenBank Accession No. NM_012547.1). 514–558 of the isoform of the enzime glutamate descarboxilase (GAD65) mRNA (GenBank Accession No. NM_012563); 191–235 of the GAD67 mRNA (GenBank Accession. N.o NM_017007); 127–172 and 1756–1800 of the vGluT1 mRNA (vesicular glutamate transporter) (GenBank Accession No. U07609).The probes for D_1 and D_2 receptors were synthesized on a 380 Applied Biosystem DNA synthesizer (Foster City Biosystem, Foster City, CA, USA) and purified on a 20% polyacrylamide / 8 *M* urea preparative sequencing gel. The rest of the probes were synthesized and HPLC purified by Isogen Bioscience BV (Maarsden, The Netherlands). Each D_1 and D_2 receptor oligonucleotide was individually labeled (2 pmol) at the 3'-end either with [33P]-dATP (>2500 Ci/mmol; DuPont-NEN, Boston, MA) using terminal deoxynucleotidyltransferase (TdT, Calbiochem, La Jolla, CA, USA). GAD and vGluT oligonucleotides (100 pmol) were non-radioactively labeled with TdT (Roche Diagnostics GmbH, Mannheim, Germany) and Dig-11-dUTP (Boehringer Mannheim). Oligonucleotides were purified by centrifugation using QIAquick Nucleotide Removal Kit (QIAGEN GmbH, Hilden, Germany).

In situ hybridization histochemistry procedure

The protocols for single- and double-label *in situ* hybridization were based on previously described procedures (Tomiyama et al., 1997;Landry et al., 2000), as recently used for the assessment of 5-HT receptors in PFC (Santana et al., 2004). Frozen tissue sections were first brought to room temperature, fixed for 20 min at 4°C in 4% paraformaldehyde in phosphate buffered saline (1× PBS: 8 mM Na_2HPO_4, 1.4 mM KH_2PO_4, 136 mM NaCl, 2.6 mM KCl), washed for 5 min in 3× PBS at room temperature, twice for 5 min each in 1× PBS and incubated for 2 min at 21°C in a solution of predigested pronase (Calbiochem, San Diego, CA) at a final concentration of 24 U/ml in 50 mM Tris–HCl pH 7.5, 5 mM EDTA. The enzymatic activity was stopped by immersion for 30 s in 2 mg/ml glycine in 1× PBS. Tissues were finally rinsed in 1× PBS and dehydrated through a graded series of ethanol. For hybridization, the radioactively-labeled and the non-radioactively labeled probes were diluted in a solution containing 50% formamide, 4× SSC (1× SSC: 150 mM NaCl, 15 mM sodium citrate), 1× Denhardt's solution (0.02% Ficoll, 0.02% polyvinylpyrrolidone, 0.02% bovine serum albumin), 10% dextran sulfate, 1% sarkosyl, 20 mM phosphate

buffer pH 7.0, 250 µg/ml yeast tRNA and 500 µg/ml salmon sperm DNA. The final concentrations of radioactive and Dig-labeled probes in the hybridization buffer were in the same range (~1.5 nM). Tissue sections were covered with hybridization solution containing the labeled probe(s), overlaid with Nescofilm coverslips (Bando Chemical Ind., Kobe, Japan) and incubated overnight at 42°C in humid boxes. Sections were then washed four times (45 min each) in a buffer containing 0.6 M NaCl and 10 mM Tris–HCl (pH 7.5) at 60°C.

Development of radioactive and non-radioactive hybridization signal

Hybridized sections were treated as described by (Landry et al., 2000). Briefly, after washing, the slides were immersed for 30 min in a buffer containing 0.1 M Tris–HCl pH 7.5, 1 M NaCl, 2 mM $MgCl_2$ and 0.5% bovine serum albumin (Sigma) and incubated overnight at 4°C in the same solution with alkaline-phosphate-conjugated anti-digoxigenin-F(ab) fragments (1:5000; Boehringer Mannheim). Afterwards, they were washed three times (10 min each) in the same buffer (without antibody) and twice in an alkaline buffer containing 0.1 M Tris–HCl pH 9.5, 0.1 M NaCl and 5 mM $MgCl_2$. Alkaline phosphatase activity was developed by incubating the sections with 3.3 mg nitroblue tetrazolium and 3.3 mg bromochloroindolyl phosphate (Gibco BRL, Gaithersburg, MD) diluted in 10 ml of alkaline buffer. The enzymatic reaction was blocked by extensive rinsing in the alkaline buffer containing 1 mM EDTA. The sections were then briefly dipped in 70 and 100% ethanol, air-dried and dipped into Ilford K5 nuclear emulsion (Ilford, Mobberly, Cheshire, UK) diluted 1:1 with distilled water. They were exposed in the dark at 4°C for 5 weeks and finally developed in Kodak D19 (Kodak, Rochester, NY) for 5 min and fixed in Ilford Hypam fixer (Ilford).

Specificity of the probes

The specificity of the hybridization signals has been previously established and published (Pompeiano et al., 1992;Serrats et al., 2003). These controls included the following procedures. (i) The thermal stability of the hybrids obtained was checked for every probe. (ii) For a given oligonucleotide probe, the hybridization signal was completely blocked by competition of the labeled probe in the presence of 50-fold excess of the same unlabeled oligonucleotide. (iii) Since we synthesized more than one probe for each mRNA analyzed, the hybridization signal obtained with each oligonucleotide for the same mRNA was identical at both regional and cellular levels when used independently. (iv) To assure the specificity of the non-radioactive hybridization signal, we compared the results obtained with the same probe radioactively labeled.

Analysis of the results

Tissue sections were examined in bright- and dark-field in a Wild 420 macroscope (Leica, Heerbrugg, Germany) and in a Nikon Eclipse E1000 microscope (Nikon, Tokyo, Japan) equipped with bright- and dark-field condensers for transmitted light and with epi-illumination. Micrography was performed using a digital camera (DXM1200 3.0; Nikon) and analySIS Software (Soft Imaging System GmbH, Germany). Bright-field images were captured with transmitted light. Dark-field images were captured with Darklite illuminator (Micro Video Instruments, Avon, MA). The figures were prepared for publication using Adobe Photoshop software (Adobe Software, Mountain View, CA). The cellular counting was made in an Olympus AX70 Stereo Microscope using CAST software for stereological analysis. Dig-labeled cells were considered positive when a dark precipitate was clearly distinguished from background. Only cellular profiles showing great abundance of the corresponding dopamine receptor mRNA and the cell type identifier (either GAD or vGluT1 mRNAs) were considered to be double-labeled. Cells with a dense Dig labeling and occasional silver grains (or vice versa) were not considered to co-express both transcripts. Data have been analyzed using one or two-way analysis of variance (ANOVA) followed by *post hoc* Tukey's test. $P < 0.05$ was considered statistically significant.

Results

Distribution of $D_1$and D_2 receptor mRNAs in rat PFC

Figure 1 shows the localization of DA D_1 and D_2 receptor mRNAs at different AP levels of the PFC, corresponding approximately to bregma +4.20, +3.24 and +3.00 mm (Paxinos and Watson, 2005). In agreement with the denser dopaminergic innervation of deep layers in rat PFC, both receptor transcripts were more densely expressed in layers V-VI than in superficial or intermediate layers in the mPFC. They are relatively abundant in the cingulate, prelimbic

and infralimbic cortices, yet with little overlap (layer V) ad some remarkable differences (see below for a detailed stud). Both receptors, specially the D_2 receptor mRNA, were also expressed by cells in the agranular insular cortex, the claustrum and the endopiriform nucleus.

Overall, the expression of DA D_1 and D_2 receptors in PFC was much lower than in striatal areas. For comparison, note the high expression of both transcripts in the more rostral part of *nucleus accumbens* and olfactory tubercle in Fig. 1, (panels 1C and 1F; see also Fig. 2).

Expression of DA D_1 receptors in pyramidal (vGluT1-positive) and GABAergic (GAD-positive) neurons of the rat PFC

In a previous publication examining the cellular localization of 5-HT_{1A} and 5-HT_{2A} receptors in PFC we reported on the distribution of pyramidal (vGluT1-positive) and GABAergic neurons (GAD-positive) in rat PFC using the same methodology and rats of the same age and weight than in the present study (Santana et al., 2004). High densities of pyramidal cells, as labeled by vGluT1 mRNA, were found at various cortical levels. Dense clusters of these cells were observed in the tenia tecta (not shown) and piriform cortex which also showed a greater density of label compared with that in other cortical areas, such as the prelimbic area or the anterior cingulate. In contrast, vGluT1-expressing cells were absent in layer I whereas GAD-expressing cells were scattered throughout the PFC, including layer I, near the midline. The proportion of vGluT1 and GAD-positive cells by reference to Nissl-stained adjacent sections was found to be 75 ± 5% of all Nissl-stained cells whereas the corresponding value for GAD-positive cells was 16 ± 1% (prelimbic area, data from 3 rats; each individual value is the average of 3 adjacent sections except for the Nissl-stained section, which were duplicate sections). The calculated ratio between vGluT1- and GAD-expressing cells was 4.6. This figure is relevant for the calculation of the absolute number of pyramidal and GABAergic interneurons expressing D_1 or D_2 receptors, whose relative proportions are shown below.

D_1 receptor mRNA was found in a significant proportion of pyramidal and GABAergic cells in various subdivisions of the PFC. Figure 2 shows examples of pyramidal (vGluT1-positive) and GABAergic (GAD-positive) neurons expressing the transcript for D_1 (panes A1 and B1, respectively) and D_2 receptors (A2 and B2, respectively). Panels A3 and B3 show the presence of abundant GABAergic cells expressing D_1 receptors (A3) and D_2 receptors (B3) in the more rostral part of the *nuceus accumbens*, approximately at bregma +2.70 mm. Contrary to pyramidal and GABAergic cells in PFC, which expressed these DA receptors in a limited proportion, the vas majority of GABAergic cells in the *nuceus accumbens* expressed a high density of D_1 and D_2 receptor mRNAs.

Table 1 shows the percentage of pyramidal and GABAergic neurons in the various layers of the mPFC (prelimbic area) expressing D_1 and D_2 receptor mRNAs. Two-way ANOVA analysis of the data in pyramidal neurons revealed a significant effect of the receptor type ($F_{1,4} = 24.5$, $p < 0..0$), layer ($F_{2,8} = 45.0$, $p < 0.0001$) and receptor x layer interaction ($F_{2,8} = 48.6$, $p < 0.0005$). The proportion of pyramidal neurons expressing D_1 receptors was similar in layers II-III and V (19-21 %) and was significantly higher in layer VI (38 %). Pyramidal cells expressing D_2 receptors were more abundant in layer V (25 %) than in layers II-III (5 %) or VI (13 %).

A similar analysis for he data in GABAergic cells revealed a significantly greater abundance of D_1- than D_2-positive neurons ($F_{1,4} = 159.6$, $p < 0.0005$) and significant differences between layers ($F_{2,8} = 13.3$, $p < 0.003$) with a non-significant receptor x layer interaction. Contrary o the remarkable layer differences in the expression of DA D_1 and D_2 receptors in pyramidal neurons, their distribution in GABAergic neurons was quite homogenous, with the sole exception of D_2-posiive GABAergic cells in layer VI (17 % vs. 5 and 8 % in layers II-III and V, respectively).

A close examination of tissue sections revealed a particular association between GABAergic cells not expressing D_2 receptors with pyramidal neurons expressing D_2 receptors. These cells were adjacent to each other and were found in layer V of the mPFC. Several examples are given in lower panels of Fig. 2 (C1 to C6). Associations of a pyramidal and a GABAergic neuron expressing the same receptor mRNA were found very infrequently.

Differential cellular and regional expression of D_1 and D_2 receptor mRNAs

Despite the overall greater density of D_1 and D_2 receptor mRNAs in deep layers (V, Via, VIb) of the mPFC, there was little overlap (mostly in layer V) and there were some remarkable differences in the

regional and cellular expression of both receptors. On the one hand, the level of expression of the corresponding mRNAs varied largely among individual pyramidal and GABAergic cells, as judged from the density of silver grains, proportional to the mRNA present in the labelled cells (Jonker et al., 1997). This cell-to-cell variation was particularly remarkable for the D_1 receptor transcript; the D_2 receptor mRNA appeared to be more homogeneously expressed and with a cellular density greater than the average of D_1 receptors. Figure 3 shows some examples of pyramidal and GABAergic cells expressing high levels of D_1 or D_2 receptor mRNAs. Pyramidal and GABAergic cells expressing very high densities of D_1 mRNA were found randomly scattered in layer VI with no particular distribution pattern. In contrast, there were clusters of pyramidal cells with a high expression of the D_2 receptor mRNA, as shown in Fig. 3. These "hot spots" were found in layer V of the mPFC.

In addition to the individual differences in the cellular expression of D_1 and D_2 receptors, there was an important differences in their regional distribution. Hence, DA D_2 receptor mRNA had a more restricted distribution in mPFC than D_1 receptor mRNA. Fig. 4 shows a detailed comparison of the expression of D_1 and D_2 receptor mRNAs in mPFC. Cells expressing DA D_2 receptor mRNA were primarily concentrated in layer V whereas DA D_1 receptor mRNA showed a more widespread distribution, with a larger number of positive cells in layer VI (particularly VIb; see figure 1A-C and Fig. 4) and a thin layer of positive cells in layer II. These superficial D_1-positive neurons were restricted to the infralimbic, prelimbic and -to a lesser extent- cingulate subdivisions of the PFC; dorsal and lateral aspects were devoid of these cells.

In these two locations (layer II and VI), D_1 receptor mRNA was present in pyramidal and GABAergic neurons. Panels B1 and B2 in fig. 4 show pyramidal cells expressing D_1 receptor mRNA in layer II whereas panel C1 shows a GABAergic cell also positive for D_1 receptors in the same location. The absence of D_2 receptor mRNA in this cortical layer is shown in panel A2 (dark-field) whereas panels B3 and C3 show the presence of pyramidal (B3) and GABAergic (C3) neurons not expressing D_2 receptor mRNA (the presence of D_1 receptor mRNA in layer VI and of D_2 receptor mRNA in layer V is shown in Fig. 2).

Regional differences in the expression of D_1 and D_2 receptor mRNAs were also found in the ventral PFC. D_1 receptor mRNA was much more abundant than D_2 receptor mRNA in the tenia tecta (dorsal and ventral) and the piriform cortex (Fig. 1). These differences are shown in more detail in Figs. 5 and 6, respectively. In both locations, there was a substantial proportion of pyramidal cells expressing D_1 (but not D_2) receptor mRNA, as shown in panels B1 and B2, respectively, of the corresponding figures. GABAergic cells also expressed D_1 receptors (not shown).

Figure Legends

Table 1. Proportion of pyramidal and GABAergic neurons expressing D_1 or D_2 receptor mRNA

	Layer II-III	Layer V	Layer VI
Pyramidal neurons (vGluT1-positive)			
D_1-positive	19 ± 3[a]	21 ± 2[a]	38 ± 3*[#]
D_2-positive	5 ± 1[#a]	25 ± 2*[a]	13 ± 1*[#]
GABAergic neurons ($GAD_{65/67}$-positive)			
D_1-positive	28± 1	30 ± 2	38 ± 4
D_2-positive	5 ± 2	8 ± 2	17 ± 2*

Data are percentage of neurons of each type /pyramidal or GABAergic) expressing D_1 or D_2 receptors in superficial, intermediate or deep layers of the prelimbic area in the mPFC. *$p < 0.05$ vs. layer II-III; [#]$p < 0.05$ vs. layer V; [a]$p < 0.05$ vs. layer VI, Tukey test post-ANOVA.

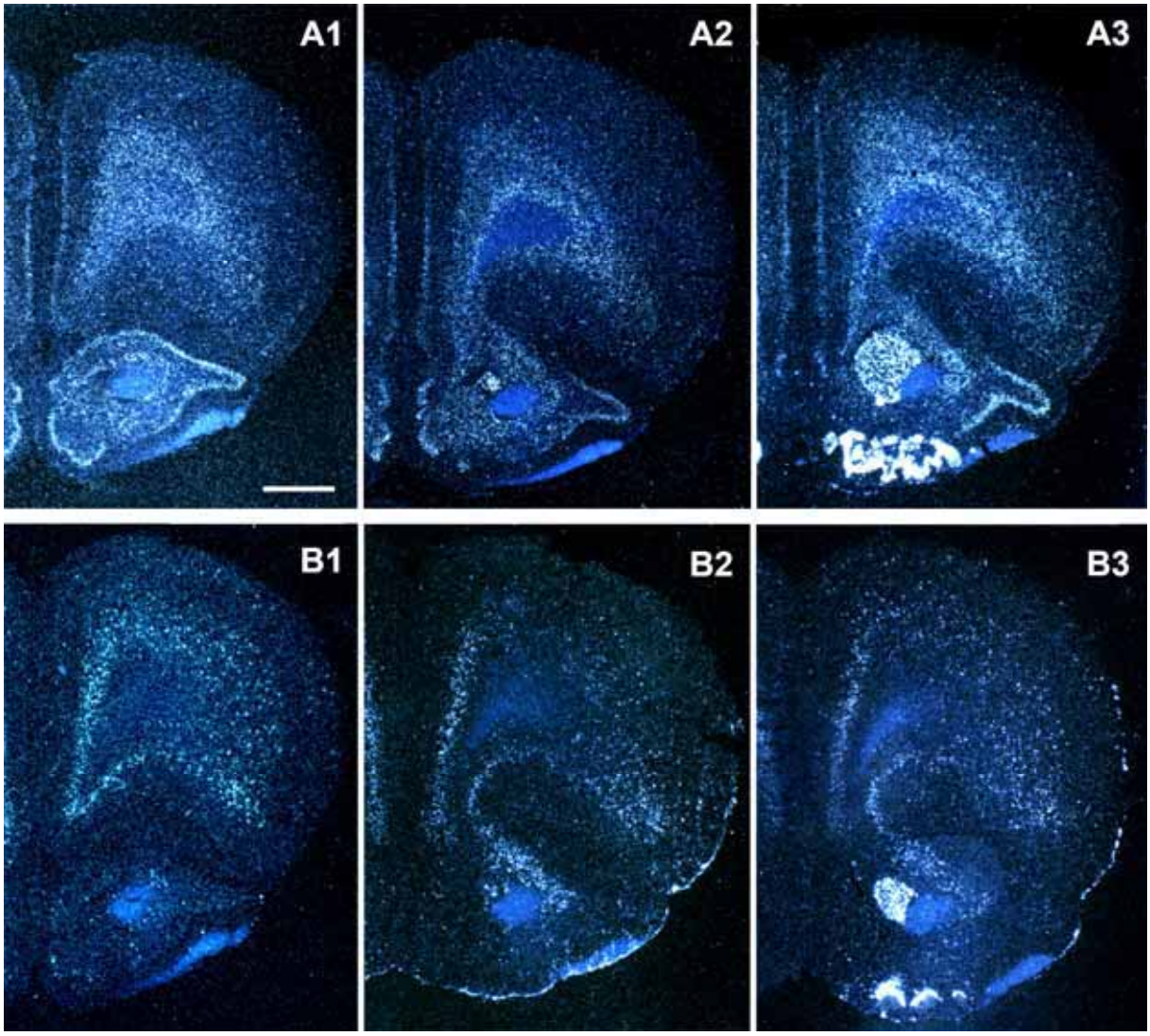

Figure 1. Dark-field photomicrographs showing the localization of DA D_1 (A1-A3) and D_2 receptor mPNAs (B1-B3) at three different AP levels of the rat PFC (approximately +4.20, 3.24 and 3.00 mm from bregma; rostro-caudal from left to right; (Paxinos and Watson, 2005). Both receptor transcripts were labeled with ^{33}P-labeled oligonucleotides. Note the preferential expression of both receptor transcripts in deep layers (D_1 layers V-VI, D_2 in layer V) of the mPFC and in the agranular insular cortex, claustrum and endopiriform nucleus. However, there was a prominent expression of D_1 (but not D_2) receptors in ventral PFC areas such aas the tenia tecta and piriform cortex. Bar size: 1 mm

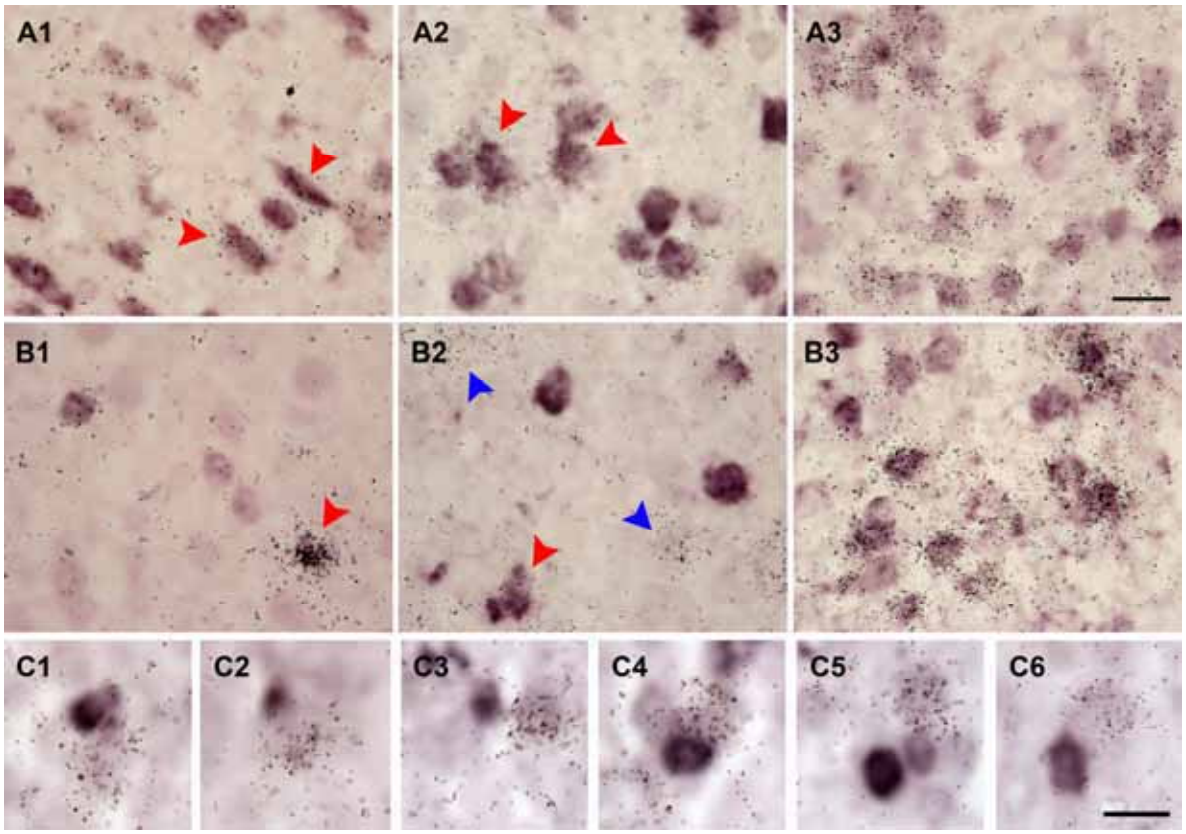

Figure 2. A1, B1. High magnification photomicrographs showing the presence of DA D_1 receptor mRNA (^{33}P-labeled oligonucleotides) in pyramidal (A1) and GABAergic cells (B1) of the mPFC (prelimbic area, layer VI), respectively identified by the presence of vGluT1 mRNA (A1) and $GAD_{65/67}$ mRNA (Dig-labeled olligonucleotides). Red arrowheads mark some double-labeled neurons. Note the presence in B1 of two GABAergic neurons with a marked difference in the expression of D_1 receptor mRNA as shown by the density of silver grains. A2, B2. High magnification photomicrographs showing the presence of DA D_2 receptor mRNA (^{33}P-labeled oligonucleotides) in pyramidal (A2) and GABAergic cells (B2) of the mPFC (prelimbic area, layer V), respectively identified by the presence of vGluT1 mRNA (A1) and $GAD_{65/67}$ mRNA (Dig-labeled olligonucleotides). Red arrowheads marke the presence of some double-labeled neurons. Note the presence of non-GABAergic, D_2 receptor-positive cells in B2 (blue arrowheads) For comparison with the proportion of cells in PFC expressing D_1 and D_2 receptors, panels A3 and D3 show the presence of the respective transcripts in the frontal pole of the *nuclus accumbens.* Most of these $GAD_{65/67}$ mRNA-positive cells (Dig-labeled olligonucleotides) exhibit the presence of the D_1 (panel A3) or D_2 (panel B3) receptor mRNAs. Panels C1 to C6 show representative examples of frequently found associations between unlabeled GABAergic cells (Dig-labeled olligonucleotides) with non-GABAergic (putatively pyramidal) neurons expressing DA D_2 receptors in layer V of the mPFC. Bar size: 20 µm.

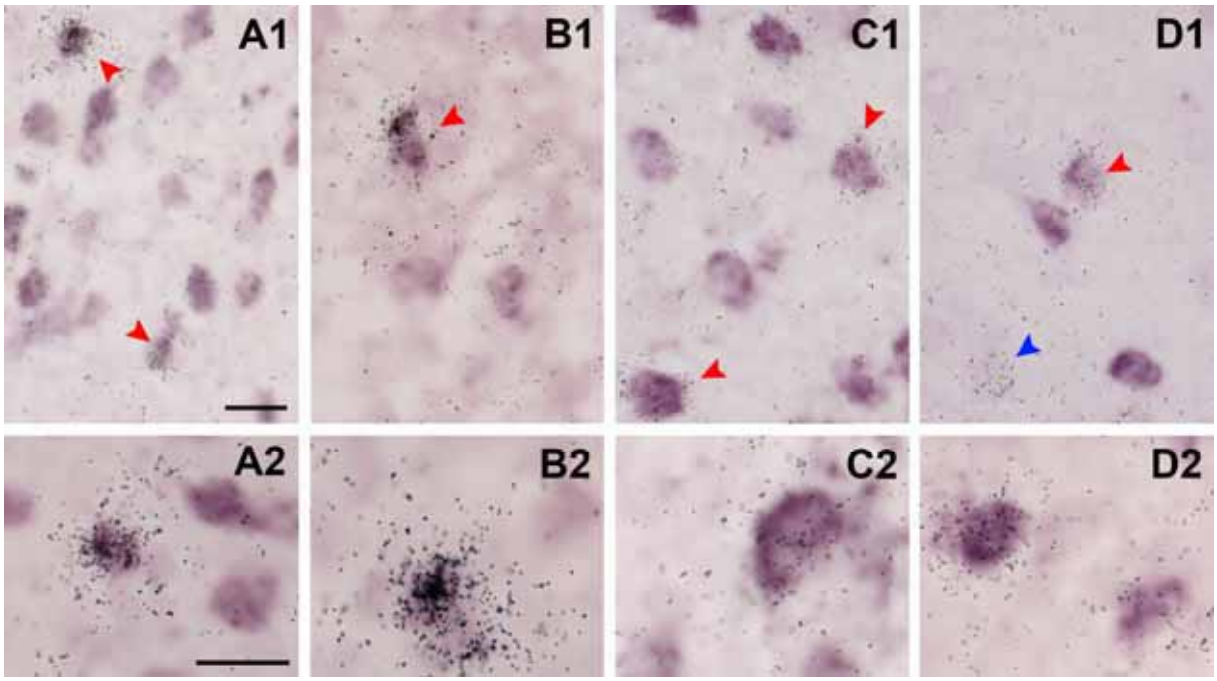

Figure 3. A1, B1. Examples of the differential expression of D_1 receptors in individual cells of mPFC (layer VI). A1 is a . high magnification photomicrograph of layer VI in mPFC showing the presence of some vGluT1 mRNA-positive cells with a standard level of expression of D_1 receptor mRNA together with a cell showing a very high expression of the D_1 receptor transcript (upper left side). Panel A2 shows another vGluT1 mRNA- and D_1 receptor mRNA-positive cell at a higher magnification. B1 and B2 show examples of GABAergic cells (Dig-labeled olligonucleotides) also expressing high levels of D_1 receptor mRNA in the same area. C-D) Contrary to the D_1 receptor, the level of expression of DA D_2 receptors appeared more homogenous, althoguh small differences were also found. C1 and D1 show the presence of pyramdial (C1) and GABAergic (D1) cells with high levles of expression of the D_2 recepror mRNA in layer V (red arrowheads). Bar size: 20 µm.

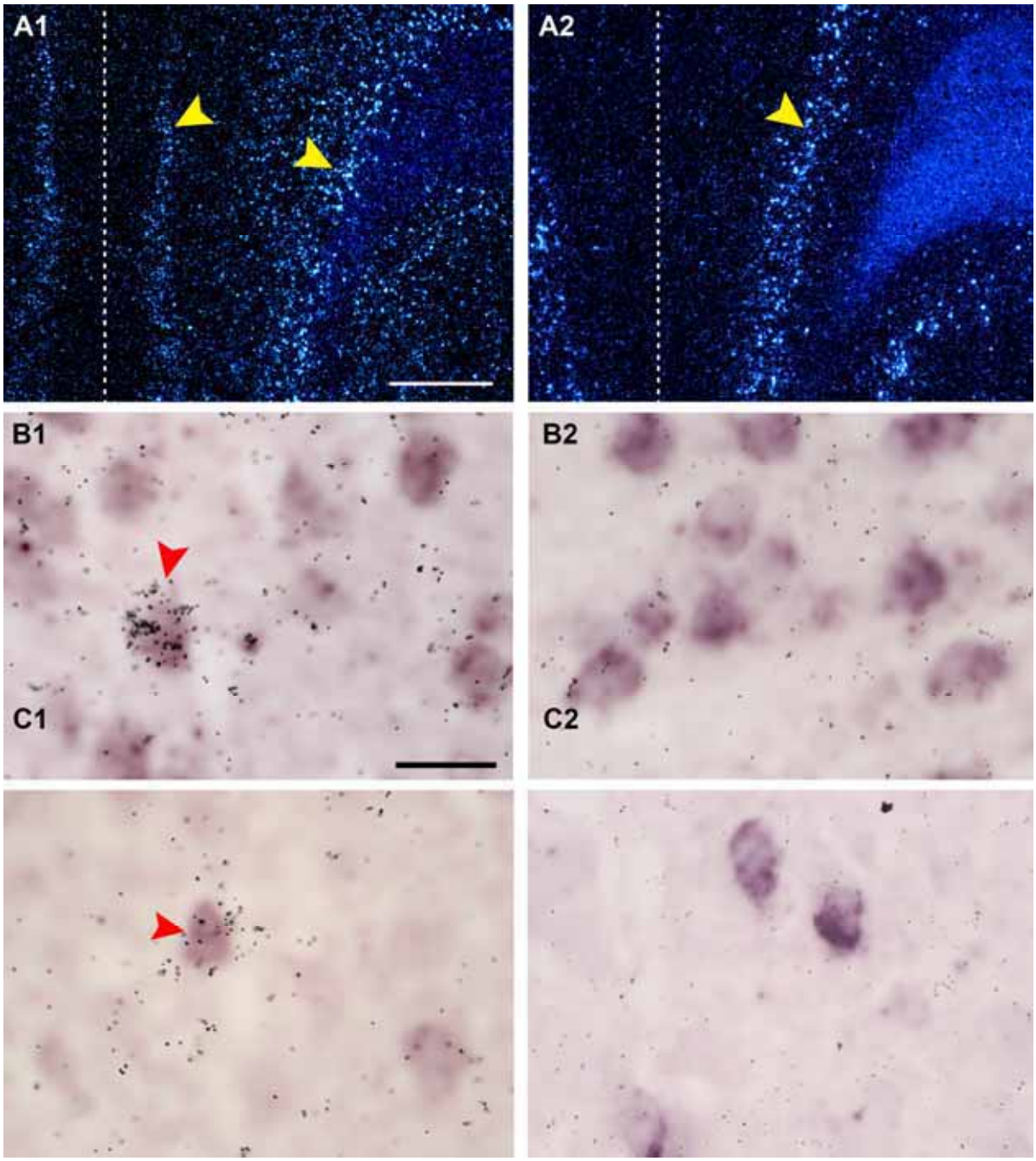

Figure 4. A1-A2. Low magnification dark-field photomicrographs showing the differential localization of DA D_1 (A1) and D_2 (A2) receptor mPNAs in rat mPFC. Cells expressing D_1 receptor mRNA are mainly localized in layers II, V and VI (yellow arrowheads mark layers II and VI in panel A1), Cells expressing D_2 receptors are mainly localized in layer V (yellow arrowhead in panel A2). Th edotted line shows the localization of midline. B-C) High magnification photomicrographs showing the differential cellular expression of D_1 and D_2 receptor mRNAs in layer II of the mPFC. D_1 receptor mRNA in layer II is expressed by pyramidal (vGluT1-positive) and GABAergic (GAD-positive) cells, as shown in panels B1 and C1, respectively. Red arrowheads mark the presence of double-labeled pyramidal and GABAergic cells. Panels B2 and C2 show the presence of pyramidal (B2) and GABAergic (C2) cells in layer II not expressing DA D_2 receptors. Bar size: 0.5 mm in A and 20 µm in B-C.

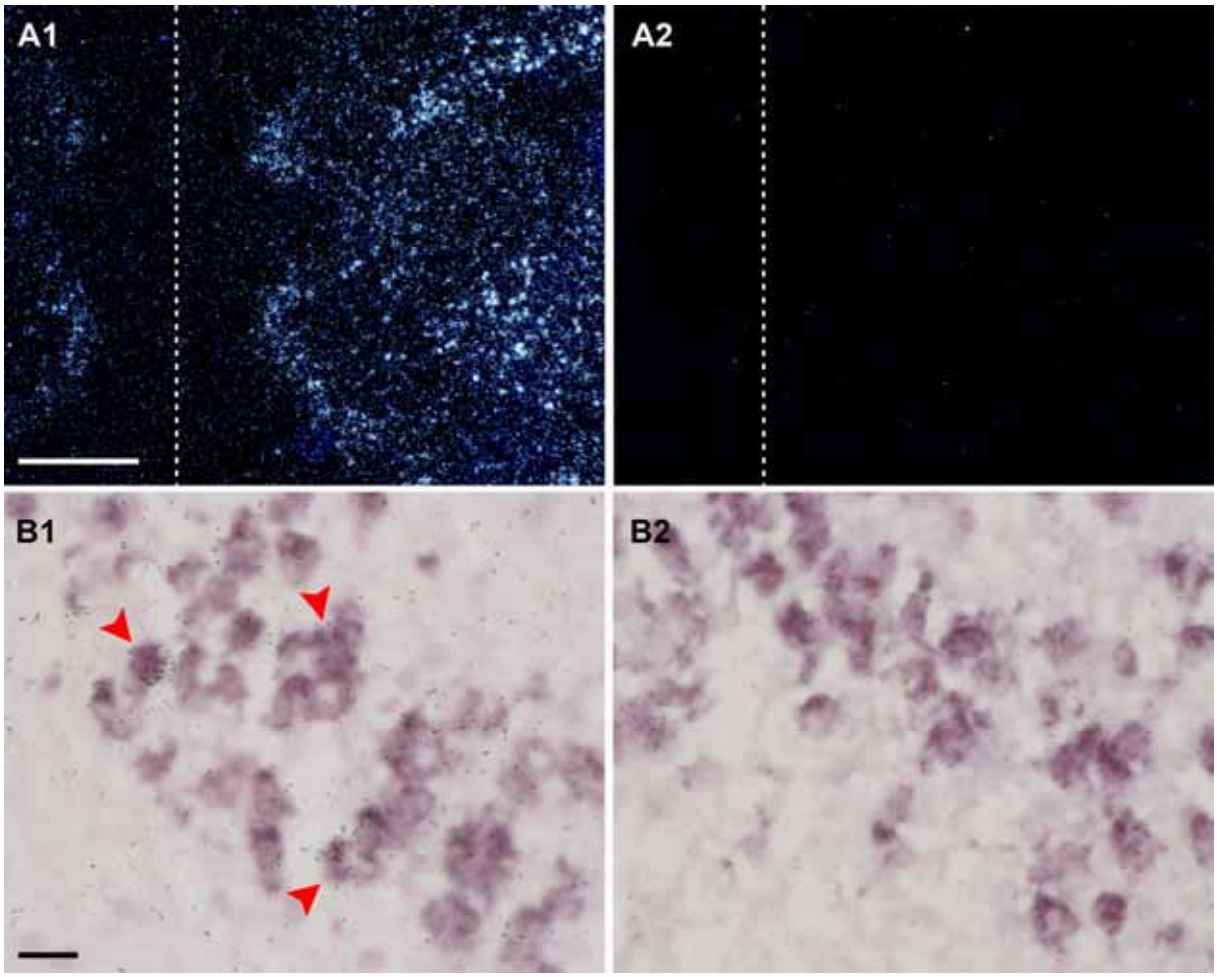

Figure 5. A1-A2. Low magnification ark-field photomicrographs showing the differential localization of DA D_1 (A1) and D_2 (A2) receptor mPNAs in ventromedial aspects of the PFC. Note the abundant presence of cells expressing D_1 receptor mRNA in the tenia tecta and adjacent areas such as the anterior olfactory and endopiriform nuclei in panel A1. These cells do not express D_2 receptor mRNA (panel A2). B1-B2) High magnification photomicrographs showing the differential cellular expression of D_1 and D_2 receptor mRNAs in the tenia tecta. B1 shows a cluster of vGluT1 mRNA-positive cells in the tenia tecta which are positive for D_1 receptor mRNA (some are marked with red arrowheads in panel B1). Note the absence of D_2 receptors in these clusters of vGluT1 mRNA-positive cells Bar size: 0.5 mm in A and 20 µm in B.

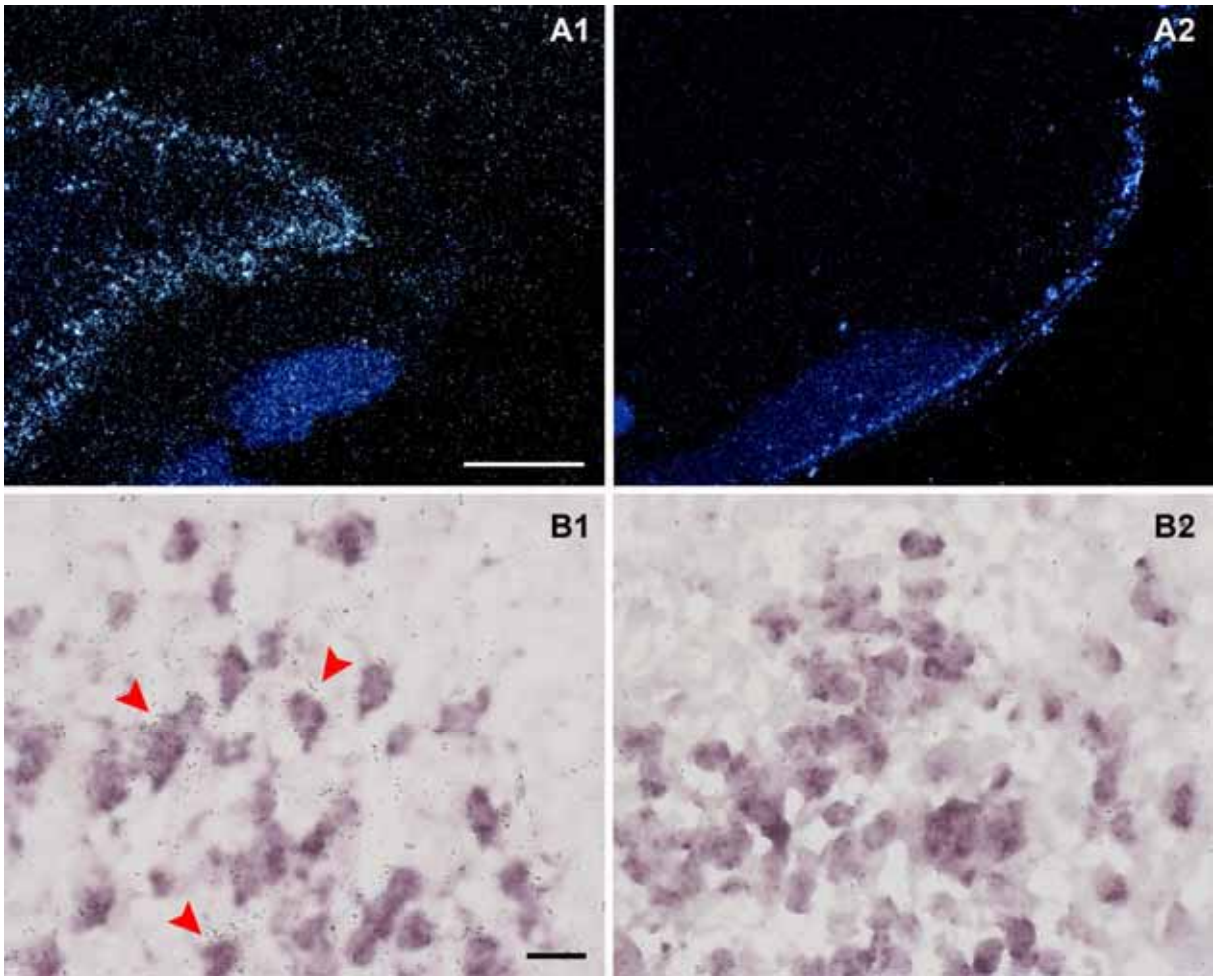

Figure 6. A1-A2. Low magnification ark-field photomicrographs showing the differential localization of DA D_1 (A1) and D_2 (A2) receptor mPNAs in the piriform cortex (ventrolateral PFC). Note the presence of a large number of cells expressing D_1 receptor mRNA in lyaer II of the piriform cortex which do not express D_2 receptors (panel A2). B1-B2) High magnification photomicrographs showing the differential cellular expression of D_1 and D_2 receptor mRNAs in layer II of the piriform cortex. B1 shows a cluster of vGluT1 mRNA-positive cells in the more lateral part of piriform cortex expressing D_1 receptors (some are marked with red arrowheads in panel B1). Note the absence of D_2 receptors in these clusters of vGluT1 mRNA-positive cells. Bar size: 0.5 mm in A and 20 µm in B

Discussion

Despite the major role played by dopaminergic transmission in PFC-dependent higher brain functions and the large number of studies examining the role of DA in the activity of PFC neurons, there were no detailed studies on DA receptor expression in this cortical area. The present study extends previous observations on this topic and provides a detailed examination of the regional and cellular expression of D_1 and D_2 receptor mRNAs in pyramidal and GABAergic cells of the PFC. We devoted a particular attention to their expression in the cingulate, prelimbic and infralimbic areas of the mPFC, where most electrophysiological studies assessing DA function have been carried out.

D_1 and D_2 receptor have been consistently found in rat PFC. As observed herein, D_1 receptor mRNA is present predominantly in deep layers (V-VI) of mPFC as well as in perirhinal areas and piriform cortex (Fremeau et al., 1991;Weiner et al., 1991;Mansour et al., 1991;Mengod et al., 1992;Gaspar et al., 1995) and in layer II (Mansour et al., 1991;Gaspar et al., 1995). D_2 receptor mRNA was localized primarily in layer V of mPFC (Mansour et al., 1990;Weiner et al., 1991;Bouthenet et al., 1991;Gaspar et al., 1995;Le Moine and Gaspar, 1998). Ligand binding studies also show the presence of both receptors in deep layers of mPFC (Mansour et al., 1990;Mansour et al., 1991;Vincent et al., 1993;Davidoff and Benes, 1998).

The preferential localization in deep layers is consistent with the known distribution of mesocortical projections (Thierry et al., 1978;Lindvall et al., 1978;van Eden et al., 1987). However, very few studies have been made to localize the cellular distribution of these two receptors in mPFC. D_1 and D_2 receptors have been found in large and small neuronal subtypes of this cortical area, thought to correspond to pyramidal neurons and GABAergic interneurons, respectively . They have also been identified colocalizing with PV- and CB-positive neurons . However, to our knowledge, this is the first quantitative study examining the cellular distribution of D_1 and D_2 receptors in the two main neuronal subtypes of PFC, both identified with specific markers (vGluT1 and GAD, for glutamatergic and GABAergic cells, respectively).

The main points of the present study are: a) D_1 and D_2 receptor mRNAs are mostly segregated in different neuronal populations, with some overlap in layer V of the mPFC, b) the proportion of each receptor transcript varies largely among PFC areas and cortical layers, c) there was also a great variability in the level of expression of DA D_1 receptor mRNA (and to a lesser extent, D_2 receptor mRNA) with some neurons expressing very high levels (“hot spots”) of the transcripts, and d) local associations of pyramidal and GABAergic cells expressing the same receptor subtype were very infrequently found, yet it was frequent to encounter associations of GABAergic cells not expressing D_2 receptors in close apposition with non-GABAergic -putatively pyramidal- cells expressing DA D_2 receptors.

The above features clearly distinguish the expression of DA D_1 and D_2 receptors in PFC from that serotonergic 5-HT_{1A} and 5-HT_{2A} receptors (Santana et al., 2004;Amargos-Bosch et al., 2004). The latter are expressed in a greater proportion of pyramidal neurons in PFC, with the exception of the 5-HT_{2A} receptor mRNA, which is expressed in a lower proportion in layer VI (e.g., where most DA D_1 receptors are expressed) and in infralimbic cortex. In contrast, the transcript for 5-HT_{1A} receptors is expressed by a relatively larger proportion (5-60 %) of pyramidal neurons in a rather homogenous manner. Likewise, the expression of DA D_1 and D_2 receptors is more restricted than that of α_1-adrenoceptors, which are present in a very large proportion (up to 80 %) of pyramidal and GABAergic neurons in the rat PFC (Santana et al., in preparation).

We have not examined whether D_1 and D_2 receptor mRNAs are co-expressed in the same PFC cells. However, given the very limited overlap between both transcripts, this seems only possible in layer V of the mPFC, where pyramidal and GABAergic cells express one or other receptor. DA has been suggested to modulate the signal/noise ratio of excitatory inputs via the activation of D_1 and D_2 receptors (O'Donnell, 2003). Stimulation of D_1 receptors increased the time in “up” (e.g., more depolarized) states whereas activation of D_2 receptors reduced the firing probability. The present results indicate that this regulatory mechanism can only take lace in layer V of the mPFC, where cells expressing one or other transcript are localized.

The present results may be useful to understand the large variety of electrophysiological data regarding the actions of DA and DA receptor agonists in PFC, which are relevant for the

comprehension of the mechanism of action of antipsychotic drugs. Indeed, may of these studies have often led to non-converging and sometimes opposite conclusions. The reasons are manifold, including the use of different experimental approaches (e.g., *in vivo* vs. *in vitro*) but also may involve the recording of effects in PFC areas and/or cells with differential expression of D_1 and D_2 receptors. Also, given the lack of selectivity of most dopaminergic drugs for receptors within each family (D_1 and D_2) it is also likely that the final effects depend on the presence of D_5 and D_4 receptors, whose expression has not been examined in the present study. However, despite many divergences, some common features of the DA action in PFC have bee proposed (see Seamans and Yang, (2004) for a detailed review). First, DA exerts biphasic effects on PFC cells, at both the temporal (e.g., decreased followed by increased activity) and concentration levels (e.g., excitation at low-moderate concentrations followed by inhibition at higher concentration). Second, DA can activate multiple signaling mechanisms through the same receptor and can exert synapse- and c cell-specific effects, often through a direct interaction with NMDA and GABA receptors. Third, DA effects depend on the membrane potential of the recorded cell and the activity level of local networks and DA can have opposite effects at low and high levels of activity. Finally, DA can exert long-lasting actions that extend beyond the application period. The present study can provide some anatomical and cellular elements to explain the observed divergences and common trends. Hence, the biphasic effects of DA can be likely explained by the presence of D_1 and D_2 receptors in pyramidal and GABAergic cells. Also, the observed associations between non-D_2 GABAergic and D_2-positive pyramidal cells suggest the existence of certain patterns of interaction between both cellular types involving DA actions through D_2 receptors. Moreover, the differential proportion of pyramidal and GABAergic cells expressing each receptor subtype in different cortical layers suggests a very large variability in the physiological effects of DA and a highly specific way of control of selected neuronal populations through D_1 and D_2 receptor stimulation.

Further work is required to examine the possible involvement of DA D_4 and D_5 receptors in the control of the activity of PFC neurons, including their anatomical and cellular localization.

Acknowledgements

Work supported by grant SAF 2004-05525 and Support from the Generalitat de Catalunya (2005SGR00758) and the Spanish Ministry of Health, Instituto de Salud Carlos III, RETICS RD06/0011(REM-TAP Network) is also acknowledged. NS is recipient of a predoctoral fellowship from the Ministry of Science and Education. We thank Judith Ballart for skilful technical assistance

References

Amargos-Bosch M, Bortolozzi A, Puig MV, Serrats J, Adell A, Celada P, Toth M, Mengod G, Artigas F (2004) Co-expression and in vivo interaction of serotonin(1A) and serotonin(2A) receptors in pyramidal neurons of prefrontal cortex. Cerebral Cortex 14: 281-299.

Beaulieu JM, Gainetdinov RR, Caron MG (2007) The Akt-GSK-3 signaling cascade in the actions of dopamine. Trends Pharmacol Sci 28: 166-172.

Bolan EA, Kivell B, Jaligam V, Oz M, Jayanthi LD, Han Y, Sen N, Urizar E, Gomes I, Devi LA, Ramamoorthy S, Javitch JA, Zapata A, Shippenberg TS (2007) D2 receptors regulate dopamine transporter function via an extracellular signal-regulated kinases 1 and 2-dependent and phosphoinositide 3 kinase-independent mechanism. Mol Pharmacol 71: 1222-1232.

Bouthenet ML, Souil E, Martres MP, Sokoloff P, Giros B, Schwartz JC (1991) Localization of Dopamine-D3 Receptor Messenger-Rna in the Rat-Brain Using Insitu Hybridization Histochemistry - Comparison with Dopamine-D2 Receptor Messenger-Rna. Brain Research 564: 203-219.

Castellanos FX, Tannock R (2002) Neuroscience of attention-deficit/hyperactivity disorder: the search for endophenotypes. Nat Rev Neurosci 3: 617-628.

Castner SA, Williams GV, Goldman-Rakic PS (2000) Reversal of antipsychotic-induced working memory deficits by short-term dopamine D1 receptor stimulation. Science 287: 2020-2022.

Dalley JW, Cardinal RN, Robbins TW (2004) Prefrontal executive and cognitive functions in rodents: neural and neurochemical substrates. Neurosci Biobehav Rev 28: 771-784.

Davidoff SA, Benes FM (1998) High-resolution scatchard analysis shows D1 receptor binding on pyramidal and nonpyramidal neurons. Synapse 28: 83-90.

Everitt BJ, Robbins TW (2000) Second-order schedules of drug reinforcement in rats and monkeys: measurement of reinforcing efficacy and drug-seeking behaviour. Psychopharmacology (Berl) 153: 17-30.

Fremeau RT, Duncan GE, Fornaretto MG, Dearry A, Gingrich JA, Breese GR, Caron MG (1991) Localization

of D1 Dopamine Receptor Messenger-Rna in Brain Supports A Role in Cognitive, Affective, and Neuroendocrine Aspects of Dopaminergic Neurotransmission. Proceedings of the National Academy of Sciences of the United States of America 88: 3772-3776.

Gaspar P, Bloch B, Le Moine C (1995) D1 and D2 receptor gene expression in the rat frontal cortex: cellular localization in different classes of efferent neurons. Eur J Neurosci 7: 1050-1063.

Goldman-Rakic PS, Muly EC, III, Williams GV (2000) D(1) receptors in prefrontal cells and circuits. Brain Res Brain Res Rev 31: 295-301.

Grace AA (1991) Phasic versus tonic dopamine release and the modulation of dopamine system responsivity: a hypothesis for the etiology of schizophrenia. Neuroscience 41: 1-24.

Grace AA, Floresco SB, Goto Y, Lodge DJ (2007) Regulation of firing of dopaminergic neurons and control of goal-directed behaviors. Trends Neurosci 30: 220-227.

Graybiel AM, Aosaki T, Flaherty AW, Kimura M (1994) The basal ganglia and adaptive motor control. Science 265: 1826-1831.

Iversen SD, Iversen LL (2007) Dopamine: 50 years in perspective. Trends Neurosci 30: 188-193.

Koob GF, Le Moal M (2001) Drug addiction, dysregulation of reward, and allostasis. Neuropsychopharmacology 24: 97-129.

Landry M, Holmberg K, Zhang X, Hokfelt T (2000) Effect of axotomy on expression of NPY, galanin, and NPY Y1 and Y2 receptors in dorsal root ganglia and the superior cervical ganglion studied with double-labeling in situ hybridization and immunohistochemistry. Exp Neurol 162: 361-384.

Le Moine C, Gaspar P (1998) Subpopulations of cortical GABAergic interneurons differ by their expression of D1 and D2 dopamine receptor subtypes. Brain Res Mol Brain Res 58: 231-236.

Lindvall O, Bjorklund A, Divac I (1978) Organization of catecholamine neurons projecting to the frontal cortex in the rat. Brain Res 142: 1-24.

Mansour A, Meadorwoodruff JH, Bunzow JR, Civelli O, Akil H, Watson SJ (1990) Localization of Dopamine-D2 Receptor Messenger-Rna and D1 and D2 Receptor-Binding in the Rat-Brain and Pituitary - An Insitu Hybridization-Receptor Autoradiographic Analysis. Journal of Neuroscience 10: 2587-2600.

Mansour A, Meadorwoodruff JH, Zhou QY, Civelli O, Akil H, Watson SJ (1991) A Comparison of D1-Receptor Binding and Messenger-Rna in Rat-Brain Using Receptor Autoradiographic and Insitu Hybridization Techniques. Neuroscience 45: 359-371.

Mengod G, Villaro MT, Landwehrmeyer GB, Martinezmir MI, Niznik HB, Sunahara RK, Seeman P, Odowd BF, Probst A, Palacios JM (1992) Visualization of Dopamine D1, D2 and D3 Receptor Messenger-Rnas in Human and Rat-Brain. Neurochemistry International 20: S33-S43.

O'Donnell P (2003) Dopamine gating of forebrain neural ensembles. Eur J Neurosci 17: 429-435.

Paxinos G, Watson C (2005) The Rat Brain in stereotaxic coordinates. San Diego: Elsevier Academic Press.

Pompeiano M, Palacios JM, Mengod G (1992) Distribution and Cellular-Localization of Messenger-Rna Coding for 5-Ht1A Receptor in the Rat-Brain - Correlation with Receptor-Binding. Journal of Neuroscience 12: 440-453.

Santana N, Bortolozzi A, Serrats J, Mengod G, Artigas F (2004) Expression of serotonin1A and serotonin2A receptors in pyramidal and GABAergic neurons of the rat prefrontal cortex. Cereb Cortex 14: 1100-1109.

Schultz W (1998) Predictive reward signal of dopamine neurons. J Neurophysiol 80: 1-27.

Seamans JK, Yang CR (2004) The principal features and mechanisms of dopamine modulation in the prefrontal cortex. Prog Neurobiol 74: 1-58.

Serrats J, Artigas F, Mengod G, Cortes R (2003) GABAB receptor mRNA in the raphe nuclei: co-expression with serotonin transporter and glutamic acid decarboxylase. J Neurochem 84: 743-752.

Svenningsson P, Nishi A, Fisone G, Girault JA, Nairn AC, Greengard P (2004) DARPP-32: an integrator of neurotransmission. Annu Rev Pharmacol Toxicol 44: 269-296.

Thierry AM, Godbout R, Mantz J, Glowinski J (1990) Influence of the ascending monoaminergic systems on the activity of the rat prefrontal cortex. Prog Brain Res 85: 357-364.

Thierry AM, Tassin JP, Blanc G, Glowinski J (1978) Studies on mesocortical dopamine systems. Adv Biochem Psychopharmacol 19: 205-216.

Tomiyama M, Palacios JM, Cortes R, Vilaro MT, Mengod G (1997) Distribution of AMPA receptor subunit mRNAs in the human basal ganglia: an in situ hybridization study. Mol Brain Res 46: 281-289.

van Eden CG, Hoorneman EM, Buijs RM, Matthijssen MA, Geffard M, Uylings HB (1987) Immunocytochemical localization of dopamine in the prefrontal cortex of the rat at the light and electron microscopical level. Neuroscience 22: 849-862.

Vijayraghavan S, Wang M, Birnbaum SG, Williams GV, Arnsten AF (2007) Inverted-U dopamine D1 receptor actions on prefrontal neurons engaged in working memory. Nat Neurosci 10: 376-384.

Vincent SL, Khan Y, Benes FM (1993) Cellular distribution of dopamine D1 and D2 receptors in rat medial prefrontal cortex. J Neurosci 13: 2551-2564.

Weiner DM, Levey AI, Sunahara RK, Niznik HB, Odowd BF, Seeman P, Brann MR (1991) D1 and D2 Dopamine Receptor Messenger-Rna in Rat-Brain. Proceedings of

the National Academy of Sciences of the United States of America 88: 1859-1863.

Williams GV, Goldman-Rakic PS (1995) Modulation of memory fields by dopamine D1 receptors in prefrontal cortex. Nature 376: 572-575.

Willner P, Muscat R, Papp M (1992) Chronic mild stress-induced anhedonia: a realistic animal model of depression. Neurosci Biobehav Rev 16: 525-534.

Trabajo 6:

The NMDA receptor antagonist phencyclidine activates the expresion of *c-fos* in thalamo-cortical circuits. Reversal by clozapine

Noemí Santana, Pau Celada, Guadalupe Mongod and Francesc Artigas.

En preparación

La administración sistémica de fenciclidina produjo un aumento de la expresión del marcador de actividad neuronal *c-fos* en varias áreas corticales y subcorticales, entre ellas, en los núcleos talámicos con una mayor conexión recíproca con la CPF, los núcleos mediodorsal y centromedial. Otras áreas subcorticales aferentes a la CPF, como el hipocampo ventral o la amígdala no aumentaron significativamente su expresión de *c-fos* tras la administración de PCP. Tampoco lo hicieron las interneuronas GABAérgicas del núcleo reticular del tálamo, encargado del control inhibitorio del resto de los núcleos talámicos. El aumento de expresión de *c-fos* en las neuronas glutamatérgicas de las áreas mencionadas fue revertido por la aplicación del antipsicótico atípico clozapina.

The NMDA receptor antagonist phencyclidine activates the expresion of *c-fos* in thalamo-cortical circuits. Reversal by clozapine

Noemí Santana, Pau Celada, Guadalupe Mongod and Francesc Artigas

Department of Neurochemistry and Neuropharmacology
Institut d'Investigacions Biomèdiques de Barcelona (CSIC), IDIBAPS
Rosselló, 161, 6th floor. 08036 Barcelona, Spain.

Corresponding author:
Francesc Artigas, PhD;
Dept. of Neurochemistry and Neuropharmacology,
Institut d'Investigacions Biomèdiques de Barcelona (CSIC), IDIBAPS.
C/ Rosselló, 161, 6th floor, 08036 Barcelona, Spain.
Phone: +3493-363 8315;
Fax: +3493-363 8301;
e-mail: fapnqi@iibb.csic.es

Abstract.

Non-competitive *N*-methyl-D-aspartate (NMDA) receptor antagonists are widely used as pharmacological models of schizophrenia due to their ability to exacerbate schizophrenia symptoms in patients and to elicit psychotomimetic actions in healthy volunteers. Also, these drugs evoke behavioral alterations in experimental animals that resemble schizophrenia symptoms. However, the neurobiological basis of their pharmacological actions are still poorly known yet the prefrontal cortex (PFC) seems to be a key target area for these agents. Here we used the expression of the immediate early gene *c-fos* as an index of neuronal activity to examine the effect of phencyclidine (PCP) in rat brain. PCP markedly enhanced *c-fos* expression in several cortical areas, such as the prefrontal cortex (PFC), secondary motor cortex, retrosplenial and entorhinal cortex. Double *in situ* hybridization experiments revealed that most of the expression in cortical areas (and particularly in PFC) occurred in pyramidal (vGluT1-positive) neurons. PCP also increased markedly *c-fos* expression in glutamatergic neurons of several thalamic nuclei such as the mediodorsal, centromedial and other midline nuclei such as the rhomboid and reuniens nuclei, but not in GABAergic neurons of the reticular nucleus. The expression of *c-fos* in the hippocampal formation was almost unaffected by PCP administration. Only a few neurons in the ventral subiculum showed an increased *c-fos* level. In midbrain, the pontine nuclei showed a marked increase in *c-fos* expression. PCP also enhanced *c-fos* expression to low-moderate levels in the amygdala, periaqueductal grey, dorsal raphe and the superior colliculus. Clozapine (CLZ) produced no effect when administered alone but significantly reduced the PCP-induced *c-fos* expression in most areas examined, particularly in cortical and thalamic areas. These results indicate that PCP may exert its psychotomimetic action by activating thalamocortical circuits. In contrast, the putative role of afferents from other regions which project to PFC, such as the hippocampus or the amygdala appears to be a minor one.

Keywords: antipsychotics · GABAergic interneurons · glutamate · NMDA receptors · prefrontal cortex · pyramidal neurons · thalamus.

Introduction

Non-competitive *N*-methyl-D-aspartate (NMDA) receptor antagonists such as the dissociative anesthetics ketamine and phencyclidine (PCP) and MK-801 (dizocilpine), have been extensively used as pharmacological models of schizophrenia due to their ability to evoke positive and negative symptoms of schizophrenia as well as the cognitive deficits of the illness in humans. These agents induce a potent behavioural syndrome (hyperactivity, ataxia signs, stereotypes), as well as cognitive and sensory deficits in experimental animals that resemble human schizophrenia symptoms (Javitt and Zukin, 1991;Krystal et al., 1994;Malhotra et al., 1997;Newcomer et al., 1999). NMDA receptor antagonists also induce schizophrenia symptoms in healthy subjects and aggravate them in schizophrenic patients (Krystal et al., 2003). Furthermore, the behavioural effects of NMDA receptor antagonists are sensitive to the treatment with antipsychotic drugs that alleviate psychotic symptoms in schizophrenic patients (Geyer et al., 2001;Krystal et al., 2003).

Despite the widespread use of NMDA receptor antagonists as pharmacological models of schizophrenia, their neurobiological basis of action is still poorly known. Neuroimaging studies indicate that a sub-anaesthetic dose of ketamine increases the activity of the prefrontal cortex (PFC) in human volunteers (Breier et al., 1997). In experimental

animals, NMDA receptor antagonists such as MK-801 or PCP have been shown to increase the neuronal activity (Suzuki et al., 2002;Jackson et al., 2004;Kargieman et al., 2007) and to decrease cortical synchrony in the medial prefrontal cortex (mPFC) (Kargieman et al., 2007). Both effects are reversed by classical (haloperidol) and atypical (clozapine) antipsychotic drugs, which suggests a direct relationship to the psychotomimetic actions of PCP (Kargieman et al., 2007).

The disrupted neuronal function in PFC is accompanied by an increased release of various neurotransmitters in this area, such as glutamate (Moghaddam et al., 1997;Adams and Moghaddam, 2001;Lorrain et al., 2003;Lopez-Gil et al., 2007), dopamine (Moghaddam and Adams, 1998;Mathe et al., 1999;Schmidt and Fadayel, 1996), serotonin (Martin et al., 1998;Millan et al., 1999;Adams and Moghaddam, 2001;Amargos-Bosch et al., 2006;Lopez-Gil et al., 2007) and acetylcholine (Nelson et al., 2002).

The disorganized increase in neuronal activity and neurotransmitter release in PFC may likely mediate the deleterious effects of NMDA receptor antagonists on cognitive processes (Krystal et al., 2003;Jackson et al., 2004). Indeed, the PFC is involved in a large number of higher brain functions (Fuster, 1997;Miller and Cohen, 2001), which are altered in schizophrenic patients.

Despite the remarkable effects of NMDA receptor antagonists on PFC function, it is unclear whether they are mediated by a direct action on PFC neuronal elements or other areas are also involved. Hence, it has been suggested that NMDA receptor blockade in local GABAergic interneurons may disinhibit pyramidal neurons resulting in an increased discharged rate (Jackson et al., 2004). However local administration of PCP or MK-801 in mPFC attenuated the spontaneous discharge of PFC neurons (Jodo et al., 2005;Suzuki et al., 2002) and the application of PCP in ventral hippocampus increased the activity of mPFC neurons (Jodo et al., 2005), suggesting that NMDA receptor antagonists may drive the increase in PFC neuronal activity through the enhancement of hippocampal-PFC excitatory inputs. Likewise, systemic -but not intra-PFC- administration of ketamine, PCP and MK-801 increased the release of 5-HT (and of glutamate, when examined) in PFC (Amargos-Bosch et al., 2006;Lopez-Gil et al., 2007).

To provide a deeper insight of the brain areas and neuronal types affected by PCP, we examined the effect of its systemic administration on the expression of the immediate early gene *c-fos* in various cortical and subcortical areas. Using double *in situ* hybridization, we devoted a particular attention to the expression of *c-fos* in glutamatergic (vGluT1-positive) and GABAergic ($GAD_{65/67}$-positive) neurons in order to clarify the neuronal elements affected by PCP. Finally, we also examined the ability of the atypical antipsychotic clozapine to reverse PCP-induced changes.

Materials and methods

Animals and treatments

Adult male Wistar rats (250-300 g) were purchased from Iffa Credo (Lyon, France). Animals were acclimatized to standard laboratory conditions (12 hr light-dark cycle and 22 ± 2 ºC room temperature) with food and water provided *ad libitum*. Animal procedures were performed according to the European Union regulations (O.J. of E.C. L358/1 18/12/1986) for the use of laboratory animals and was approved by the Institutional Animal Care and Use Committee. Rats were administered i.p. with the following treatments: saline + saline, saline + PCP(10 mg/kg), CLZ (5 mg/kg) + saline and CLZ (5 mg/kg) + PCP (10 mg/kg), respectively. Time between injections was 30 min and rats were killed by administration of 0.3 ml of pentobarbital 1 h after the second injection. The rats were immediately decapitated, the brains rapidly removed, frozen on dry ice and stored at -20ºC. Tissue sections, 14-µm thick, were cut using a microtome-cryostat (Microm HM500 OM, Walldorf, Germany), thaw-mounted onto APTS (3-aminopropyltriethoxysilane, Sigma,St Louis, MO, USA)-coated slides and kept at –20ºC until use.

In situ hybridization histochemistry

The oligonucleotide probes used to detect different mRNAs were: *c-fos* complementary to bases 131-178 (GenBank accession number NM_022197.1). For the mRNA coding for the vesicular glutamate transporter vGluT1 mRNA (a glutamatergic cell marker) two oligonucleotides complementary to bases 127-172 and 1756-1800 (GenBank accession number U07609) were used. GABAergic cells were identified by the presence of the enzyme synthesizing GABA, glutamic acid decarboxylase (GAD) that in adult brain exists as two major isoforms, GAD65 and GAD67. Two oligonucleotides for each isoform mRNA were

made: bp 159-213 and 514-558 (GenBank accession number NM_012563) and bp 191-235 and 1600-1653 (GenBank accession number NM_017007). They were synthesized and HPLC purified by Isogen Bioscience BV (Maarsden, The Netherlands). *c-fos* oligonucleotide was labeled at its 3'-end with [^{33}P]-dATP (>2500 Ci/mmol; DuPont-NEN, Boston, MA, USA) with terminal deoxynucleotidyltransferase (TdT, Calbiochem, La Jolla, CA, USA) and purified with ProbeQuant™ G-50 Micro Columns (GE Healthcare UK Limited, Buckinghamshire, UK). vGluT1 and GAD oligonucleotides were individually labeled with Dig-11-dUTP (Boehringer Mannheim) using TdT (Roche Diagnostics GmbH, Mannheim, Germany), and purified as above.

The protocols for single- and double-label *in situ* hybridization were based on previously described procedures (Tomiyama et al., 1997;Landry et al., 2000) as recently described (Santana et al., 2004). Frozen tissue sections were first brought to room temperature, fixed for 20 min at 4°C in 4% paraformaldehyde in phosphate buffered saline (1× PBS: 8 mM Na_2HPO_4, 1.4 mM KH_2PO_4, 136 mM NaCl, 2.6 mM KCl), washed for 5 min in 3× PBS at room temperature, twice for 5 min each in 1× PBS and incubated for 2 min at 21°C in a solution of predigested pronase (Calbiochem, San Diego, CA) at a final concentration of 24 U/ml in 50 mM Tris–HCl pH 7.5, 5 mM EDTA. The enzymatic activity was stopped by immersion for 30 s in 2 mg/ml glycine in 1× PBS. Tissues were finally rinsed in 1× PBS and dehydrated through a graded series of ethanol. For hybridization, the radioactively-labeled and the non-radioactively labeled probes were diluted in a solution containing 50% formamide, 4× SSC (1× SSC: 150 mM NaCl, 15 mM sodium citrate), 1× Denhardt's solution (0.02% Ficoll, 0.02% polyvinylpyrrolidone, 0.02% bovine serum albumin), 10% dextran sulfate, 1% sarkosyl, 20 mM phosphate buffer pH 7.0, 250 µg/ml yeast tRNA and 500 µg/ml salmon sperm DNA. The final concentrations of radioactive and Dig-labeled probes in the hybridization buffer were in the same range (~1.5 nM). Tissue sections were covered with hybridization solution containing the labeled probe(s), overlaid with Nescofilm coverslips (Bando Chemical Ind., Kobe, Japan) and incubated overnight at 42°C in humid boxes. Sections were then washed four times (45 min each) in a buffer containing 0.6 M NaCl and 10 mM Tris-HCl (pH 7.5) at 60°C.

Development of radioactive and non-radioactive hybridization signal

Hybridized sections were treated as described by (Landry et al., 2000). Briefly, after washing, the slides were immersed for 30 min in a buffer containing 0.1 M Tris–HCl pH 7.5, 1 M NaCl, 2 mM $MgCl_2$ and 0.5% bovine serum albumin (Sigma) and incubated overnight at 4°C in the same solution with alkaline-phosphate-conjugated anti-digoxigenin-F(ab) fragments (1:5000; Boehringer Mannheim). Afterwards, they were washed three times (10 min each) in the same buffer (without antibody) and twice in an alkaline buffer containing 0.1 M Tris–HCl pH 9.5, 0.1 M NaCl and 5 mM $MgCl_2$. Alkaline phosphatase activity was developed by incubating the sections with 3.3 mg nitroblue tetrazolium and 3.3 mg bromochloroindolyl phosphate (Gibco BRL, Gaithersburg, MD) diluted in 10 ml of alkaline buffer. The enzymatic reaction was blocked by extensive rinsing in the alkaline buffer containing 1 mM EDTA. The sections were then briefly dipped in 70 and 100% ethanol, air-dried and dipped into Ilford K5 nuclear emulsion (Ilford, Mobberly, Cheshire, UK) diluted 1:1 with distilled water. They were exposed in the dark at 4°C for 5 weeks and finally developed in Kodak D19 (Kodak, Rochester, NY) for 5 min and fixed in Ilford Hypam fixer (Ilford).

Analysis of the results

Tissue sections were examined in bright- and dark-field in a Wild 420 macroscope (Leica, Heerbrugg, Germany) and in a Nikon Eclipse E1000 microscope (Nikon, Tokyo, Japan) equipped with bright- and dark-field condensers for transmitted light and with epi-illumination. Micrography was performed using a digital camera (DXM1200 3.0, Nikon) and analySIS Software (Soft Imaging System GmbH, Germany). Bright-field images were captured with transmitted light. Dark-field images were also captured with Darklite illuminator (Micro Video Instruments, Avon, MA, USA). The figures were prepared for publication using Adobe Photoshop software (Adobe Software, Mountain View, CA, USA).

A semiquantitative measure of the optical densities was conducted for *in situ* hybridization studies with the AIS^R computerized image analysis system (Imaging Research Inc, St Catharines, Ontario, Canada). Individual values of optical densities were calculated as the mean of 2 adjacent sections of 3 rats per treatment group. Statistical analysis was performed using the Statistica package.

Results

The administration of 10 mg/kg i.p. PCP induced a marked increase in the expression of *c-fos* in various brain regions, notably in cortical and thalamic areas. Figure 1 shows dark-field photomicrographs at low magnification depicting the expression of *c-fos* at 4 different AP levels, corresponding approximately to +3.72 mm, -2.52, -3.96 and -6.36 mm from bregma (Paxinos and Watson, 2005). Table 1 shows the approximate level of expression of *c-fos* induced by PCP in the various areas analysed. Maximal levels of expression were observed in several cortical and thalamic areas. In contrast, the various structures of the basal ganglia such as the caudate-putamen or globus pallidus were unaffected by PCP. Likewise, the hippocampus showed a very low level of expression in PCP-treated animals.

Figure 2 shows an estimation of the effect of PCP on various brain areas as assessed by optical densities in films exposed to the hybridized sections. Two-way ANOVA of the optical density data in the 19 regions examined revealed a significant effect of PCP ($F_{1,76}$ = 314.5, $p < 0.00001$), region ($F_{18,76}$ = 22.2, $p < 0.000001$), and a significant interaction between both factors ($F_{18,76}$ = 6.7, $p < 0.00001$). The following sections analyze in more detail the effect of PCP in the various brain areas examined.

Neocortex

PCP (10 mg/kg i.p.) administration induced a very large expression of *c-fos* in the neocortex. This effect was predominant in more rostral cortices, such as the PFC and motor cortex (Fig. 1, panels A2, B2). An intermediate expression was also noted in more caudal cortical areas, including the entorhinal cortex.

PCP increased *c-fos* expression in various fields of the PFC, but mainly in its medial part (layers III-VI) of the cingulate, prelimbic and infralimbic cortices). PCP also increased *c-fos* expression in the piriform cortex, the agranular insular cortex and in a narrow band of cells in the boundary between layers III and V, extending over dorsal and lateral aspects of the PFC (Fig. 1, panel A2).

In the mPFC, the maximal expression of *c-fos* was noted in layers III-V of the prelimbic area (Figs. 1 and 3). Double *in situ* hybridization experiments revealed that *c-fos* expression took place essentially in pyramidal neurons (vGluT1-positive). Panel B2 of figure 3 shows a high-magnification microscopic field illustrating the abundance of vGluT1-positive neurons expressing *c-fos* in the prelimbic area of the mPFC. In contrast, PCP did not increase the expression of *c-fos* in GABAergic interneurons (Figure 3, panel C2). A few GAD-positive neurons showed a low-moderate signal, but this was not different from that observed in saline-treated rats. A more detailed quantitative study of the effect of PCP on pyramidal and GABAergic neurons of the PFC has been reported elsewhere (Kargieman et al., 2007). Briefly, PCP significantly increased the proportion of *c-fos*-positive pyramidal neurons to 280% of control levels. When considering the individual level of expression (as assessed by counting the number of silver cells in positive cells), the effect reached 240% of control values.

In addition to PFC, lateral and dorsal aspects of the neocortex at various AP level also showed a marked expression of *c-fos* in response to PCP administration (Fig. 1, panels B2-D2). There was a remarkable increase in *c-fos* expression by PCP in the retrosplenial cortex at all AP levels examined, which appeared to take place in intermediate layers (II-III). In more lateral aspects of the neocortex, *c-fos* expression increased particularly in layer IV, as well as in deeper layers (VIb), as observed in fig. 1 panels B2-D2.

Figure 4 shows a detailed examination of the effect of PCP in the retrosplenial cortex at AP -2.52. Double *in situ* hybridization analysis revealed that PCP increased the expression of *c-fos* in pyramidal neurons. Panels B2 and D2 show a large number of double-labeled cells in the retrosplenial cortex and in layer IV of the M2 area of the motor cortex. Interestingly, unlike in PFC, PCP also induced a very marked expression of *c-fos* in a substantial proportion of GABAergic neurons of the retrospleanial cortex and layer IV of the motor cortex (panels C2 and E2).

In addition, PCP also increased the expression of *c-fos* in the medial entorhinal cortex, in an area adjacent to the ventral subiculum (Fig. 1, panel D2; see also below, hippocampal formation).

Thalamic nuclei

In addition to the above cortical areas, PCP induced a very marked expression of *c-fos* in various thalamic nuclei, notably in the centromedial (CM) and mediodorsal (MD) nuclei as well in other midline nuclei such as the rhomboid (Rh) and reuniens (Re) nuclei. A more moderate, but still marked effect was noted in the ventromedial nucleus (VM). In contrast, the effects in other nuclei such as the ventral

posteromedial (VPM) and ventral posterolateral (VPL) thalamic nuclei exhibited a much lower level of expression of *c-fos* compared to the mediodorsal or centromedial nuclei (Fig.1, panel B2 and Fig. 5, panels A2 and B2). Fig. 2 shows the increase in optical density produced by PCP in various thalamic nuclei.

Double *in situ* hybridization experiments revealed that the expression of *c-fos* took place in vGluT1-positive relay thalamic neurons. A large proportion of these glutamatergic neurons showed a marked increase of *c-fos* expression in response to PCP administration (fig. 5, panels C2 and E2). In contrast, the GABAergic neurons of the reticular nucleus of the thalamus (Rt) (which provide feedforward inhibitory input to the rest of thalamic nuclei) did not show any increase in *c-fos* expression after PCP administration (figure 5, panel D2).

Hippocampal formation

Due to previous data suggesting an action of NMDA receptor antagonists in hippocampal projection neurons that may later increase PFC neuronal activity via excitatory inputs (Jodo et al., 2005), we payed an special attention to the effect of PCP in various hippocampal fields.

PCP did not increase the expression of *c-fos* in the dorsal hippocampus above control levels (compare panels B1 and B2 in Fig. 1). In the ventral hippocampus, a very moderate increase in the number of cells expressing *c-fos* was observed, which that was far from that observed in cortical or thalamic areas. Very few neurons expressed *c-fos* in response to PCP in the dentate gyrus and CA subfields whereas a moderate population did so in the ventral subiculum (Fig. 6, panel B2). Likewise, a small group of neurons in the medial entorhinal cortex, adjacent to the ventral subiculum showed a marked expression of *c-fos* in PCP-treated rats..

Other areas

PCP also increased the expression of *c-fos* in discrete areas of the forebrain and midbrain. The only exception were the pontine nuclei, which showed a remarkable increase in the expression of *c-fos* in PCP-treated rats. Also, a small group of cells at AP -5.30 in the periaqueductal grey, below the 3rd ventricle (possibly the Edinger-Westphal nucleus) exhibited a marked increase in *c-fos*. Besides these areas, there was a moderate number of cells expressing *c-fos* in the amygdala, the hypothalamus, the superior colliculus and the periaqueductal grey (Fig. 1). Because of its relevance in the function of cortico-limbic circuits, its role in behavioral control and its reciprocal connectivity with the PFC, we examined in more detail the effect of PCP on cells in the amygdaloid complex.

PCP induced a moderate increase of *c-fos* expression in the amygdala (Fig. 7). Double *in situ* hybridization experiments revealed that PCP induced the expression of *c-fos* in principal neurons (vGluT1-positive) as well as in local GABAergic interneurons. Panel B2 shows several vGluT1-positive neurons expressing *c-fos*. However, some cells also expressing *c-fos* which are not glutamatergic are observed in the same microscopic field. Conversely, panel C2 shows GAD- and *c-fos*-positive cells together with some adjacent GAD-negative, *c-fos*-positive cells.

Effect of clozapine on c-fos expression

The administration of CLZ (5 mg/kg i.p.) alone produced very little effects on the basal expression of *c-fos* in the various brain areas examined. However, it markedly attenuated the increase in *c-fos* induced by PCP in a region-dependent manner. Two-way ANOVA of the optical density data in the 19 regions examined (4 treatments: SAL + SAL, SAL + PCP, CLZ + SAL, , CLZ + PCP) indicated a significant effect of the region ($F_{18,152}$ = 31.7, $p < 0.00001$), treatment ($F_{3,\ 152}$ = 178.7, $p < 0.00001$) and a significant interaction between both factors ($F_{18,152}$ = 4.5, $p < 0.00001$). Post-hoc Tukey test revealed significant differences between SAL + PCP and SAL + SAL and between CLZ + PCP and SAL + PCP but not between CLZ + SAL and SAL + SAL.

The antagonism by CLZ of the increased *c-fos* expression induced by PCP was not complete and depended on the region examined. However, CLZ prevented to a large extent the increased *c-fos* in all cortical and thalamic areas (Figs. 1 and 2). CLZ pre-treatment reduced the number of *c-fos*-positive glutamatergic cells, compared with the effect of PCP alone. A detailed analysis of the effect of CLZ on the expression of *c-fos* evoked by PCP in GABAergic neurons is lacking in most brain areas. However, in PFC, the combination of CLZ and PCP induced the expression of *c-fos* in GABAergic neurons, an effect that may be involved in the attenuation of the expression in glutamatergic neurons (Kargieman et al., 2007).

Figure legends

Table 1. *c-fos* mRNA expression in rat brain areas after PCP treatment

Bregma	Brain area	*c-fos* mRNA expression level
	Cortical areas	
(+3.20)	Prelimbic cortex (PL)	+++
(+3.20)	Infralimbic cortex (IL)	+
(+3.20)	Pirifom cortex (Pir), anterior	++
(-2.50)	Pirifom cortex (Pir), posterior	++
(-3.90)	Entorhinal cortex (En), middle	+++
(-6.30)	Entorhinal cortex (En), post	+++
(-2.50)	Retrosplenial granular cx (RSGb), ant	++++
(-2.50)	Retrosplenial agranular cx (RSA), ant	++++
(-6.30)	Retrosplenial granular cx (RSGb), post	++++
(-6.30)	Retrosplenial agranular cx (RSA), post	++++
	Thalamus	
(-2.50)	Laterodorsal th nu, dorsomedial (LDDM)	+++
(-2.50)	Central medial th nu (CM)	+++
(-2.50)	Mediodorsal th nu (MD)	+++
(-2.50)	Paraventricular th nu (PV)	+++
(-3.90)	Lat post th nu, mediorostral (LPMR)	+++
(-3.90)	Mediodorsal th nu, lateral (MDL)	+++
(-3.90)	Paraventricular th nu, posterior (PVP)	+++
(-3.90)	Parafascicular (PF)	+++
(-3.90)	Posterior hypothalamic area (PH)	+++
	Hippocampal formation	
(-6.30)	CA1	+
(-6.30)	Ventral Subiculum (VS)	+
	Amygdaloid complex	
(-2.50)	Basolateral amygdaloid nuclei (BLA, BLP)	+
	Other brain areas	
(-6.30)	Dorsal raphe (DR)	++
(-6.30)	Pontine nuclei (Pn)	+++
(-2.50)	Lateral Habenula (LHb)	+++

Note. A relative score from low (+) to maximal (++++) expression is shown.

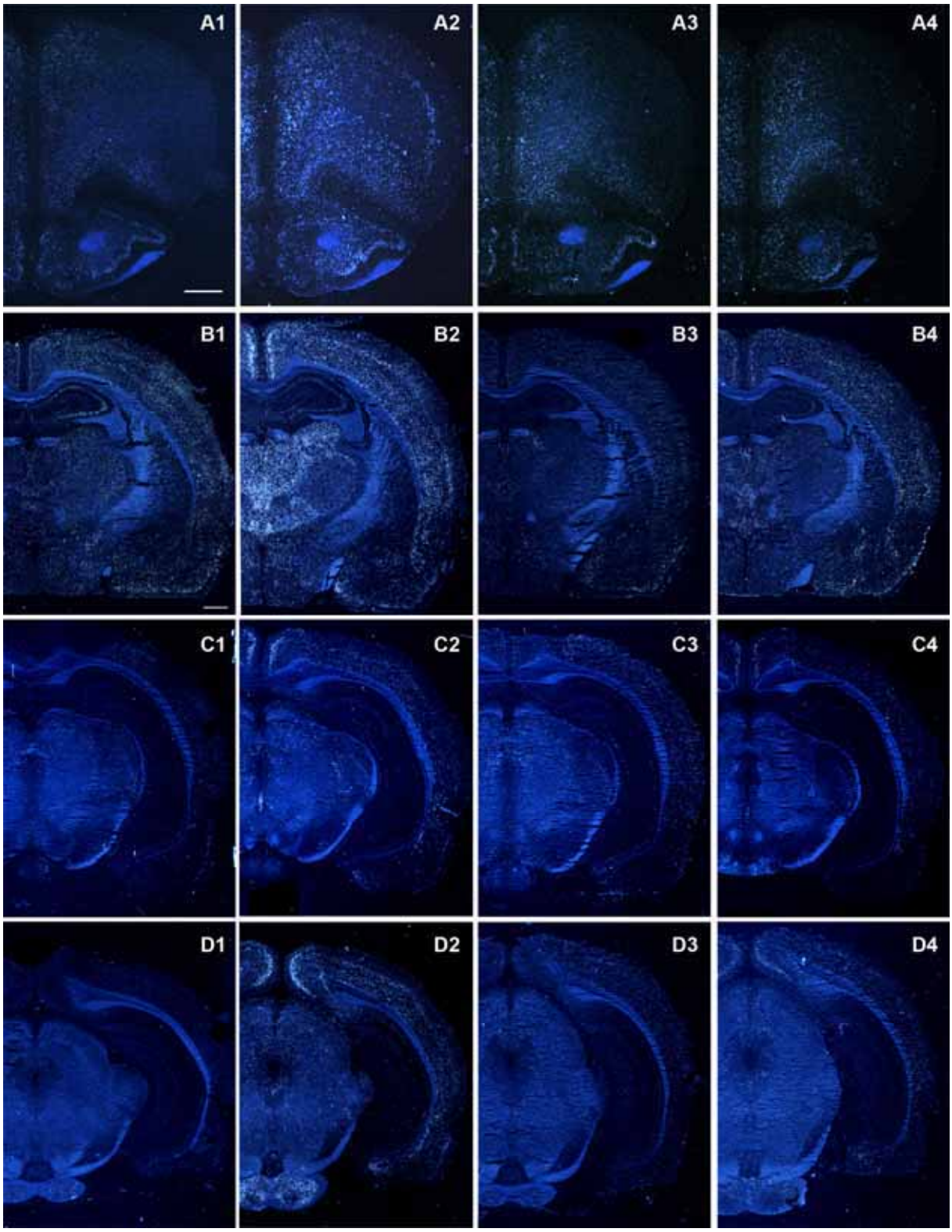

Figure 1. Macroscopic dark-field images from emulsion-dipped coronal sections at four different AP levels from control and treated rats showing the localization of cells expressing *c-fos* mRNA. A) AP level +3.72 mm, B) AP level -2.52 mm; C) AP level -5.28 mm, D) AP level -6.36 mm. Columns correspond to the following treatments: 1) SAL + SAL, 2) SAL + PCP, 3) CLZ + SAL, 4) CLZ + PCP. Note the marked expression of *c-fos* in various cortical and thalamic areas of PCP-treated rats together with the relative absence of a significant increase in hippocampal areas (dentate gyrus, CA1, CA3). In the neocortex, a particularly remarkable increase was observed in the various areas of the PFC (dorsal anterior cingulate, prelimbic, infralimbic), the piriform, retrosplenial, parietal (secondary motor) and lateral (somatosensoy) cortices. Bar: 1 mm.

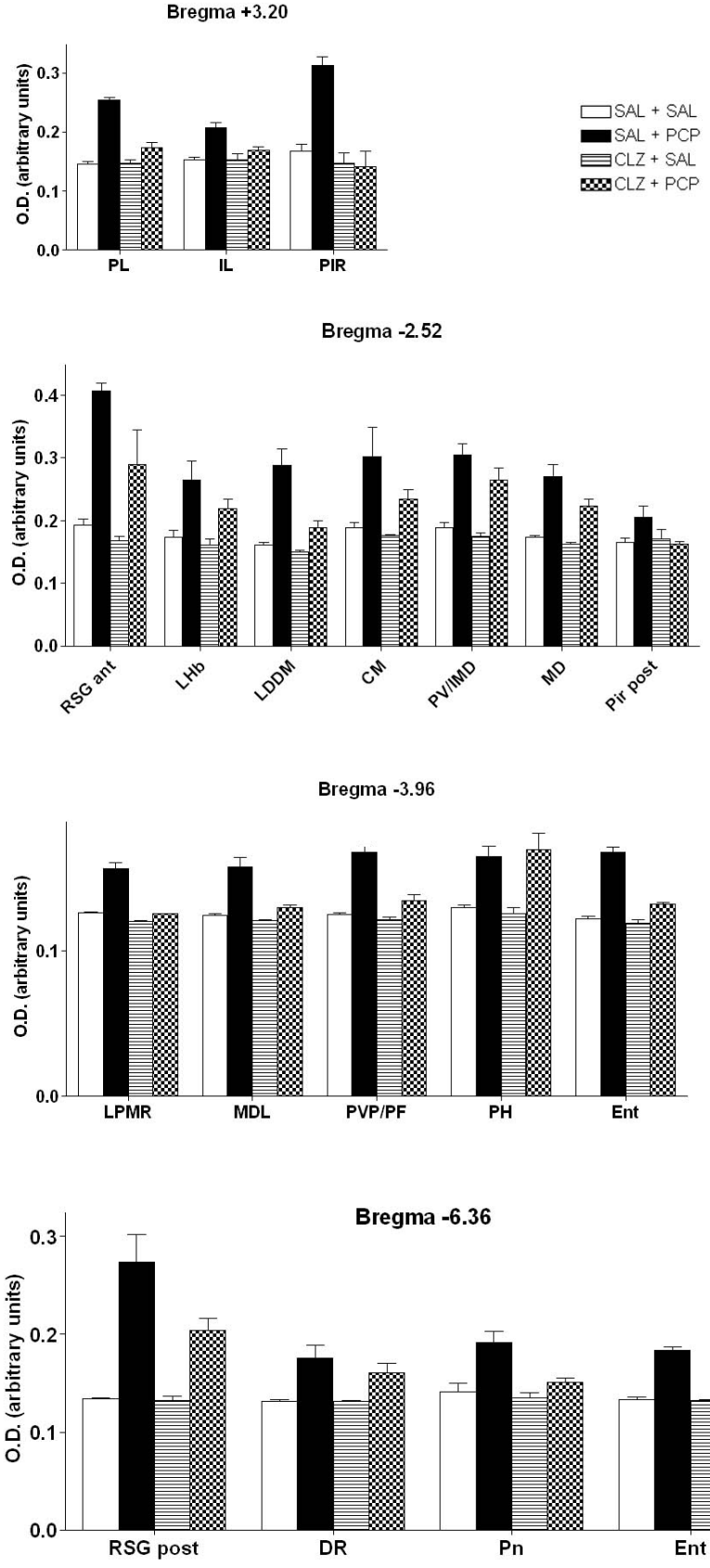
Bregma +3.20
O.D. (arbitrary units)
0.0
0.1
0.2
0.3
PL
IL
PIR
SAL + SAL
SAL + PCP
CLZ + SAL
CLZ + PCP
Bregma -2.52
O.D. (arbitrary units)
0.0
0.1
0.2
0.3
0.4
RSG ant
LHb
LDDM
CM
PV/IMD
MD
Pir post
Bregma -3.96
O.D. (arbitrary units)
0.0
0.1
LPMR
MDL
PVP/PF
PH
Ent
Bregma -6.36
O.D. (arbitrary units)
0.0
0.1
0.2
0.3
RSG post
DR
Pn
Ent

Figure 2. Bar graphs showing the optical density measures in films exposed to hybridized sections of rats treated with SAL + SAL, SAL + PCP, CLZ + SAL and CLZ + PCP. Each graph shows the brain structures with positive *c-fos* expression after PCP treatment at the indicated AP level. Abbreviations: PL, prelimbic cortex, IL infralimbic cortex; PIR, piriform cortex; RSG, retrosplenial granular cortex; LHb, lateral habenula; LDDM, laterodorsal thalamic nucleus, dorsomedial part; CM centromedial th nu; PV, paraventricular th nu; IMD intermediodorsal th nu; MD, mediodorsal th nu; See text for statistical analysis.

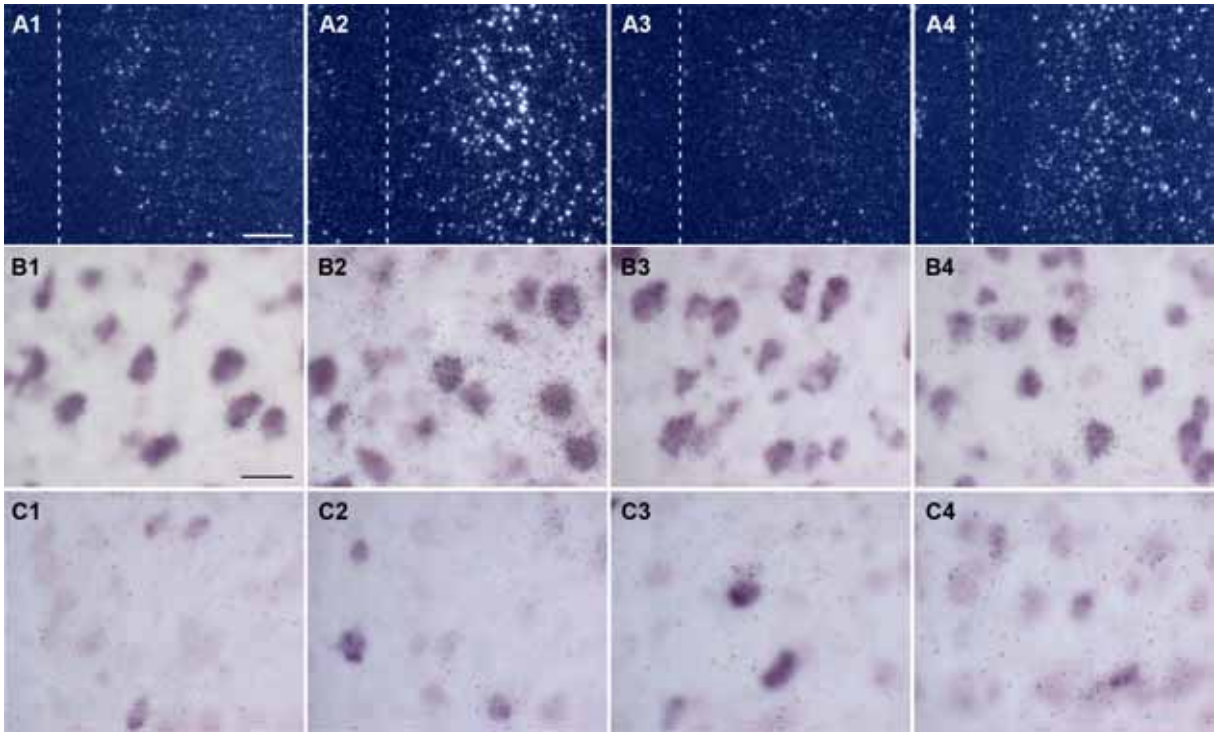

Figure 3. A) Macroscopic dark-field images from emulsion-dipped coronal sections at AP +3.72 mm showing an enlargement of the medial PFC (prelimbic area). The dashed line indicates brain midline. Columns correspond to the following treatments: 1) SAL + SAL, 2) SAL + PCP, 3) CLZ + SAL, 4) CLZ + PCP. Note the occurrence of a large number of *c-fos* positive cells in rats treated with PCP and the reversal elicited by CLZ, which by itself did not increase *c-fos* expression. B) are high magnification photomicrographs showing the detection in mPFC (prelimbic area) of *c-fos* mRNA using ^{33}P-labeled oligonucleotides (silver grains) in pyramidal cells, visualized by hybridization with Dig-labeled oligonucleotides complementary to vGluT1 mRNA (dark precipitates). Note the increase in the number of *c-fos* positive cells and the density of silver grains per cell induced by PCP as well as the CLZ-induced antagonism of this effect. C) High magnification photomicrographs showing the expression of *c-fos* mRNA (silver grains) in GABAergic cells of the prelimbic PFC, visualized by GAD mRNA (dark precipitate). Note the existence of *c-fos* positive cells not expressing GAD mRNA in the SAL + PCP group (C2). Bars: A) 0.15 cm; B,C) 20 μm

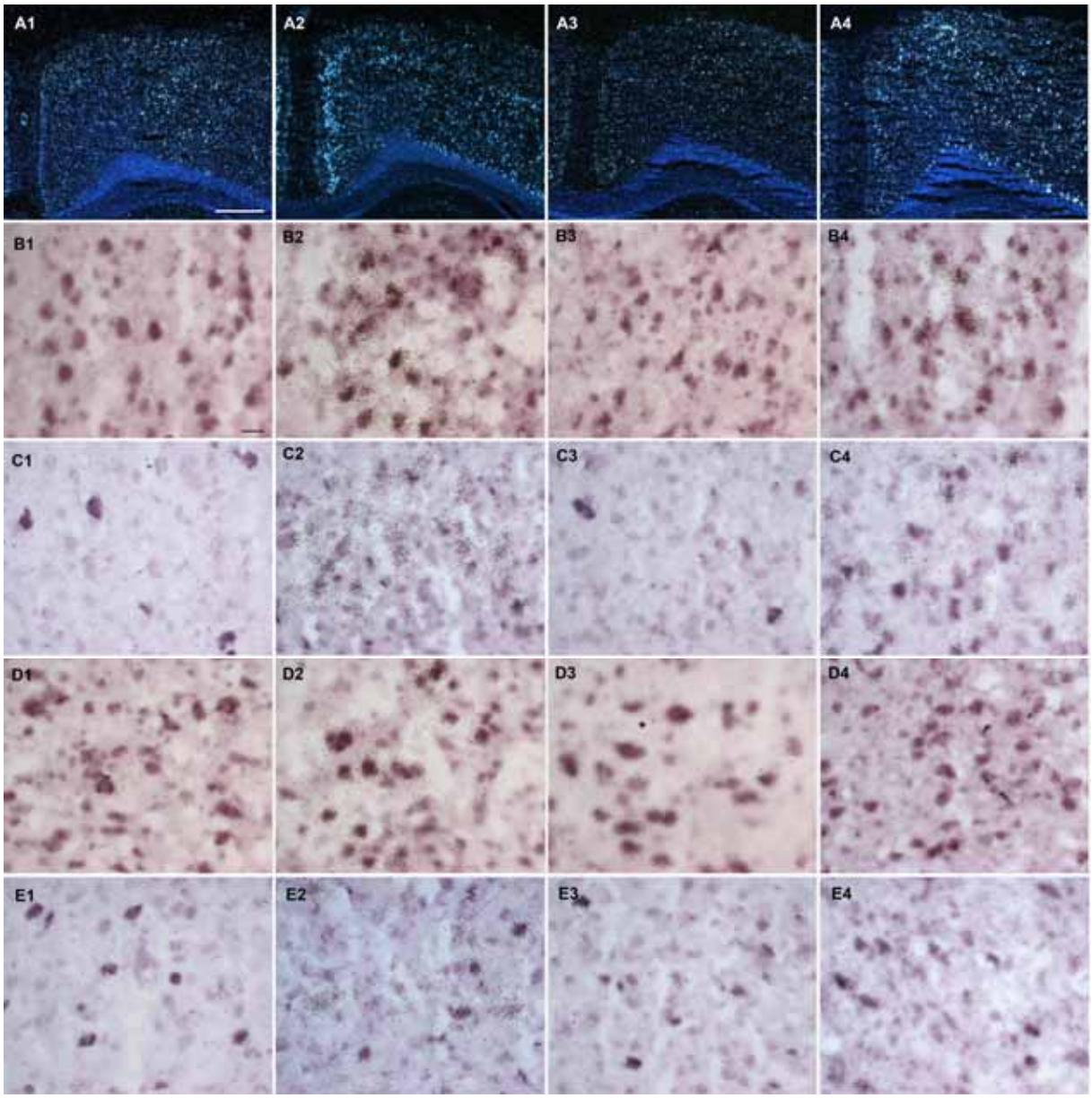

Figure 4. A) Macroscopic dark-field images from emulsion-dipped coronal sections at AP -2.52 mm showing the expression of *c-fos* in retrosplenial cortex. Columns correspond to the following treatments: 1) SAL + SAL, 2) SAL + PCP, 3) CLZ + SAL, 4) CLZ + PCP. Note the occurrence of a large number of *c-fos* positive cells in rats treated with PCP and the partial reversal elicited by CLZ, which by itself did not increase *c-fos* expression. B) and D) are high magnification photomicrographs showing the detection in retrosplenial cortex (B) and layer IV of the parietal cortex (secondary motor area, M2) (D) of *c-fos* mRNA using ^{33}P-labeled oligonucleotides (silver grains) in pyramidal cells, visualized by hybridization with Dig-labeled oligonucleotides complementary to vGluT1 mRNA (dark precipitates). Note the increase in the number of *c-fos* positive cells and the density of silver grains per cell induced by PCP as well as the partial antagonism induced by CLZ. C) and E) are high magnification photomicrographs showing the detection in retrosplenial cortex (C) and layer IV of the parietal cortex (secondary motor area, M2) (E) of *c-fos* mRNA using ^{33}P-labeled oligonucleotides (silver grains) in GABAergic cells, visualized by GAD mRNA (dark precipitate). Note that PCP induced a marked increase of *c-fos* mRNA in non-GABAergic as well as in GABAergic neurons. Bars: A) 0.25 cm; B,C,D,E) 20 μm

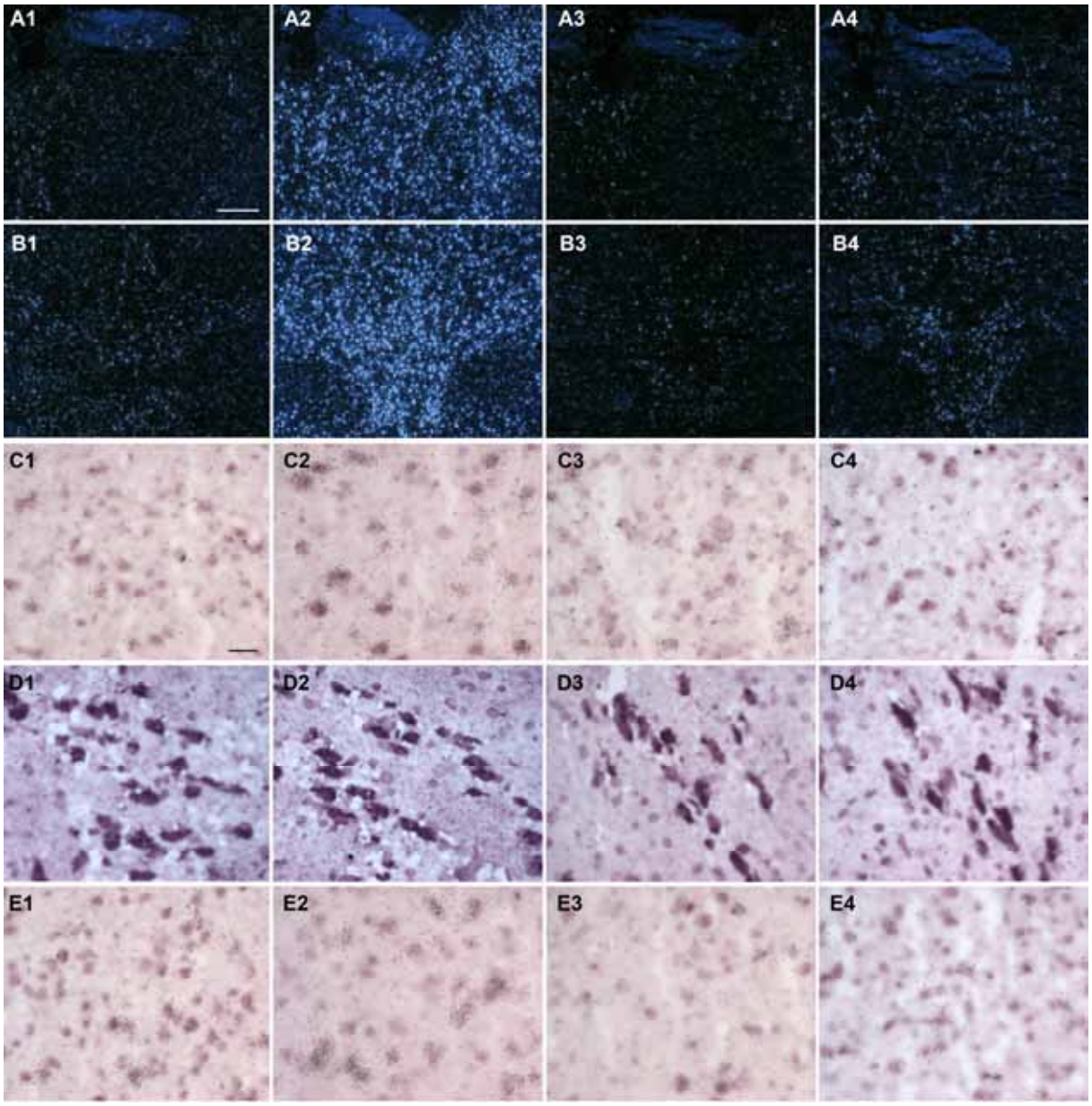

Figure 5. A) and B) Macroscopic dark-field images from emulsion-dipped coronal sections at AP -2.52 mm showing the expression of *c-fos* in the mediodorsal (A) and centromedial (B) thalamic nuclei. Columns correspond to the following treatments: 1) SAL + SAL, 2) SAL + PCP, 3) CLZ + SAL, 4) CLZ + PCP. Note the occurrence of a large number of *c-fos* positive cells in rats treated with PCP and the partial reversal elicited by CLZ, which by itself did not increase *c-fos* expression. C) and E) are high magnification photomicrographs showing the detection in the mediosorsal (C) and centomedial (E) thalamic nuclei of *c-fos* mRNA using ^{33}P-labeled oligonucleotides (silver grains) in thalamic relay cells, visualized by hybridization with Dig-labeled oligonucleotides complementary to vGluT1 mRNA (dark precipitates). Note the large increase in the number of *c-fos* positive cells and the density of silver grains per cell induced by PCP as well as the antagonism induced by CLZ. D) high magnification photomicrographs showing the lack of expression of *c-fos* mRNA using ^{33}P-labeled oligonucleotides (silver grains) in GABAergic cells, of the reticular nucleus of the thalamus, visualized by GAD mRNA (dark precipitate). Bars: A,B) 0.1 cm; C,D,E) 20 μm

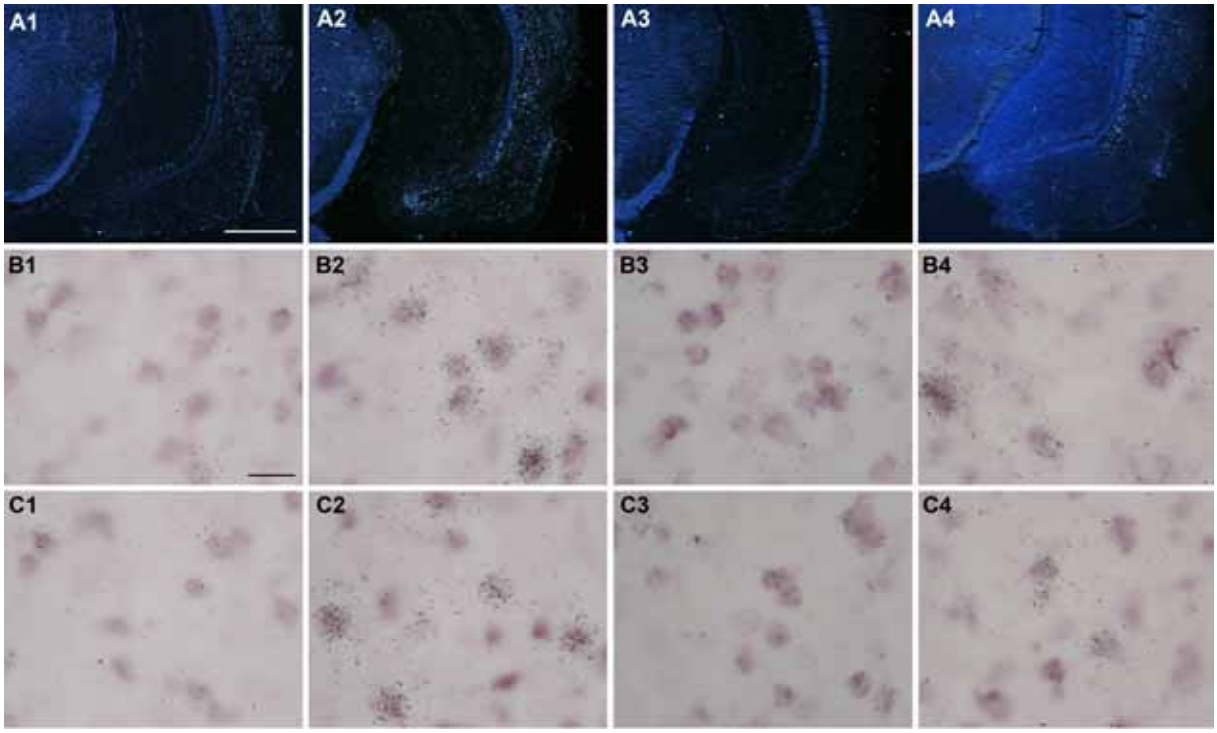

Figure 6. A) Macroscopic dark-field images from emulsion-dipped coronal sections at AP - 6.36 mm showing an enlargement of the ventral hippocampus and medial entorhinal cortex. Columns correspond to the following treatments: 1) SAL + SAL, 2) SAL + PCP, 3) CLZ + SAL, 4) CLZ + PCP. Note the occurrence of a very low number of *c-fos* positive cells in the hippocampus of PCP-treated rats and the presence of groups of cells in the entorhinal cortex, adjacent to the lower part of the corpus callosum. B) and C) are high magnification photomicrographs showing the detection in ventral subiculum (B) and medial entorhinal cortex (C) of *c-fos* mRNA using ^{33}P-labeled oligonucleotides (silver grains) in pyramidal cells, visualized by hybridization with Dig-labeled oligonucleotides complementary to vGluT1 mRNA (dark precipitates). Note the increase in the number of *c-fos* positive cells and the density of silver grains per cell induced by PCP as well as the CLZ-induced antagonism of this effect. Bars: A) 0.5 cm; B,C) 20 µm.

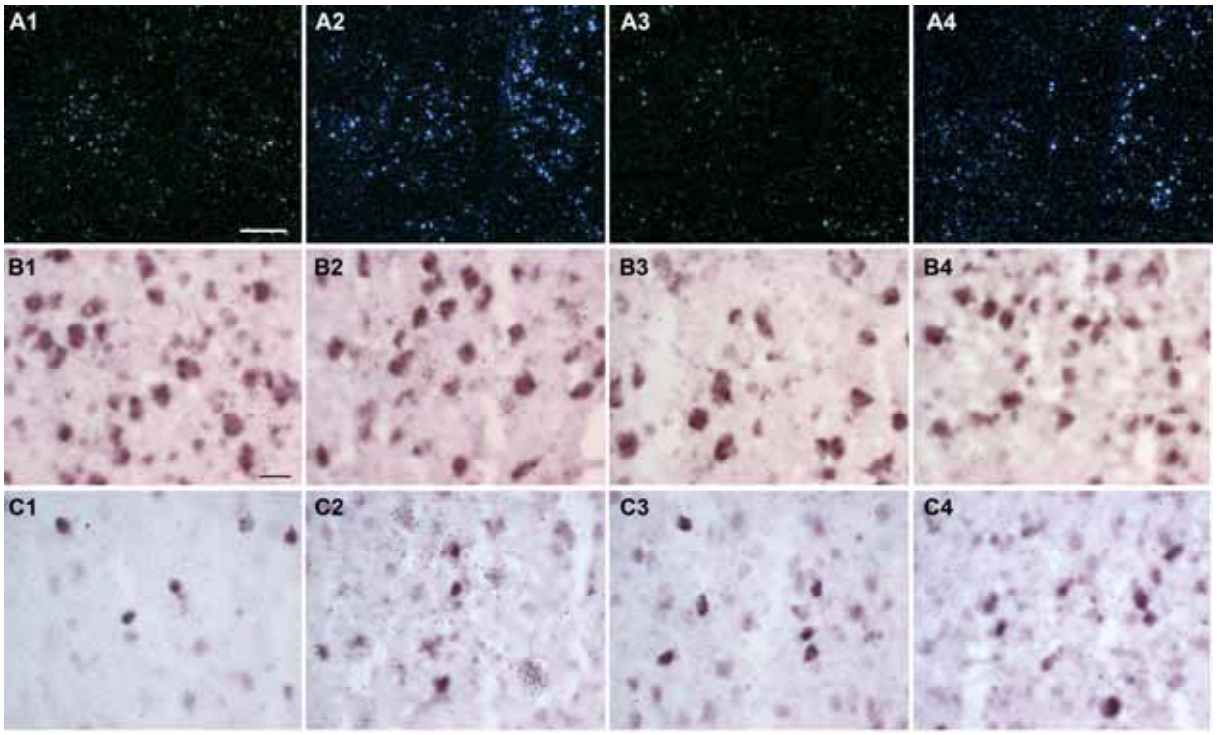

Figure 7. A) Macroscopic dark-field images from emulsion-dipped coronal sections at AP -6.36 mm showing the expression of *c-fos* in the amygdala (left hand side) and entorhinal cortex (right had side). Columns correspond to the following treatments: 1) SAL + SAL, 2) SAL + PCP, 3) CLZ + SAL, 4) CLZ + PCP. PCP induced a moderate increase of the number of *c-fos* positive cells which was partly antagonized by CLZ, which did not increase *c-fos* expression by itself. B) high magnification photomicrographs showing the detection basolateral amygdala *c-fos* mRNA using ^{33}P-labeled oligonucleotides (silver grains) in pyramidal cells, visualized by hybridization with Dig-labeled oligonucleotides complementary to vGluT1 mRNA (dark precipitates). Note the increase in the number of *c-fos* positive cells and the density of silver grains per cell induced by PCP as well as the antagonism induced by CLZ. C) high magnification photomicrographs showing the the detection in the same area of *c-fos* mRNA using ^{33}P-labeled oligonucleotides (silver grains) in GABAergic cells, visualized by GAD mRNA (dark precipitate). Note that PCP induced a marked increase of *c-fos* mRNA in non-GABAergic as well as in GABAergic neurons. Bars: A) 0.1 cm; B,C) 20 µm.

Discussion

The present results indicate that the non-competitive NMDA receptor antagonist PCP increases the expression of *c-fos* in various brain areas, but notably in cortical and thalamic areas that are reciprocally connected. This suggests that PCP markedly alters information processing in thalamocortical and corticothalamic circuits, an effect likely accounting for its psychotomimetic properties. This view is also supported by the antagonism of PCP-induced *c-fos* expression by the atypical antipsychotic clozapine.

c-fos is taken as a cellular marker of increased neuronal activity (Dragunow and Faull, 1989;Konkle and Bielajew, 2004;Panagis et al., 1997). Hence, it can be assumed that cells expressing *c-fos* had an increased discharge rate in response to PCP. This view is supported by a recent study in PFC showing that PCP administration increased discharge rate of pyramidal neurons, identified by antidromic activation from midbrain and *c-fos* expression in the same neuronal types (vGluT1-psotive cells) (Kargieman et al., 2007). Yet, it remains to be established whether other neuronal types (e.g., thalamic relay cells or hippocampal pyramidal neurons) have a parallel increase in activity and *c-fos* expression.

The most marked increase produced by PCP was noted in the PFC, retrosplenial cortex and in layer IV of various motor and sensory cortices (fig 1, panel B2), as well as in the thalamic nuclei that are reciprocally connected with these cortical structures. Hence, the mediodorsal, centromedial, reuniens and rhomboid nuclei of the thalamus project densely to cingulate, prelimbic and infralimbic areas of the PFC (Berendse and Groenewegen, 1991;Kuroda et al., 1998;Vertes et al., 2006). The retrosplenial and secondary motor cortices, which also showed an enhanced *c-fos* response, are also innervated by midline thalamic nuclei (Vertes et al., 2006). In turn, these areas project to the midline thalamic nuclei, thus closing thalamocortical circuits (Groenewegen and Uylings, 2000;Vertes, 2004;McKenna and Vertes, 2004;Gabbott et al., 2005). The increase in firing rate (Suzuki et al., 2002;Kargieman et al., 2007) of PFC neurons and the increased *c-fos* expression in PCP-sensitive neurons is consistent with the increased PFC glutamate output induced by non-competitive NMDA-R blockade (Adams and Moghaddam, 1998;Lopez-Gil et al., 2007). Yet, this is discordant with the fact that NMDA receptor blockade in mPFC does not increase glutamatergic synaptic activity *in vitro* (Aghajanian and Marek, 2000) nor *in vivo* (Suzuki et al., 2002). This further indicates that excitatory effects of PCP on PFC neurons are secondary to NMDA-R blockade in non-pyramidal neurons

Thus, the primary site of action of PCP remains unclear. Two main (yet not exclusive) possibilities remain open. On the one hand, PCP might block tonic NDMA inputs onto GABAergic neurons of the reticular nucleus, which provides inhibitory input to excitatory relay neurons in the rest of thalamic nuclei. Reticular disinhibiton would then result in an increased excitatory input of thalamocortical afferents, thus resulting in the increased *c-fos* expression in cortical areas (e.g., PFC, retrosplenial cortex). This view is supported by the fact that PCP increased *c-fos* expression in glutamatergic relay neurons of the mediodorsal, centromedial, ventromedial, reuniens and rhomboid nuclei, but not in GABAergic neurons of the reticular nucleus. The inability to increase *c-fos* expression in GABAergic neurons of this nucleus does not seem to be due to its neurochemical phenotype since PCP increased *c-fos* in GABAergic neurons of other areas (e.g., motor and retrosplenial cortices, amygdala). Likewise, PCP increased *c-fos* expression in layer IV of secondary motor cortex and in a narrow band of cells between layers III and V in PFC (the latter area lacks layer IV). This cortical layer is the main target for thalamic excitatory inputs in the neocortex (Kuroda et al., 1998). Furthermore, the disinhibition of mediodorsal thalamic afferents to PFC with bicuculine (an effect analogous to the removal of tonic $GABA_A$ inputs from the reticular nucleus) enhances the expression of *c-fos* and the discharge rate of pyramidal neurons in PFC (Bubser et al., 1998;Puig et al., 2003). These experimental evidences suggests that PCP evokes a primary activation of various thalamic nuclei which later results in an increased cortical function via thalamocortical inputs.

However, the opposite is also possible, given the reciprocal connectivity between cortical and thalamic areas. PCP might disinhibit cortical pyramidal neurons in the PFC by blocking NMDA inputs on local GABAergic interneurons (Jackson et al., 2004). This effect would increase the discharge rate of pyramidal neurons in the various areas of the mPFC projecting to a variety of cortical areas and to subcortical structures (Vertes, 2004), thus increasing their activity and, consequently, *c-fos* expression. In support of this possibility is the observation that PCP

and MK-801 increase the firing rate of putative (Suzuki et al., 2002;Jackson et al., 2004) or identified pyramidal neurons in PFC (Kargieman et al., 2007). Also, PCP increased *c-fos* expression in the same neuronal population (Kargieman et al., 2007), this study). Indeed, the present results cannot clarify which area(s) is the primary target for PCP actions nor whether it can act simultaneously on different GABAergic populations to disinhibit principal (glutamatergic) neurons in various cortical and subcortical areas. Further work is required to clarify this issue.

The PFC exerts a top-down control of many other cortical and subcortical areas in the brain including motor and limbic areas with which the PFC is reciprocally connected in most instances (Miller and Cohen, 2001). Pyramidal neurons in the PFC receive a large array of inputs from sensory and associative cortical areas, as well as from the thalamus, the hippocampus and other subcortical structures. In turn, axons of pyramidal neurons project to and modulate neuronal activity in these areas (Fuster, 1997;Groenewegen and Uylings, 2000;Miller and Cohen, 2001). Since NMDA receptor antagonists increase the activity of PFC neurons (Suzuki et al., 2002;Jackson et al., 2004;Kargieman et al., 2007), it may be possible that the behavioural syndrome evoked by these agents results from a PFC-induced activation of cortical and subcortical motor areas secondary to the increase of PFC activity. However, in addition to PFC, the present results suggest that other brain areas are involved in the complex behavioural response induced by PCP and, possibly, other NMDA receptor antagonists. Indeed, there is a striking similarity between the present results and those obtained by (Vaisanen et al., 2004) using MK-801. Despite the latter study did not examine the neurochemical phenotype of *c-fos*-expresing cells, the regional distribution was essentially in the same areas than PCP: medial PFC, piriform, retrosplenial and secondary motor (parietal) cortices, as well as in several thalamic nuclei. This suggests that, despite some behavioral differences between both compounds, the neurobiological basis of their psychotomimetic action is very similar.

Interestingly, neither Vaisanen et al., (2004) nor the present study found an increased activation of hippocampal areas after non-competitive NMDA receptor blockade. Indeed, the hippocampus has been claimed to mediate the increase in PFC activity induced by MK-801 or PCP via the CA1-PFC pathway (Jodo et al., 2005). Here we found only a minor population of vGluT1-positive neurons in the ventral subiculum expressing *c-fos* after PCP treatment, an observation which does not support a major role of hippocampal inputs onto the PFC to account for the increased *c-fos* expression in the latter area.

The reversal by CLZ of the increased *c-fos* expression in most brain areas is a further support for the use of PCP as an experimental model of schizophrenia. Indeed, CLZ -which by itself did not alter *c-fos* expression- markedly attenuated the increase produced by PCP. This agrees with recent findings showing that CLZ was also able to reverse the disruption in cortical activity induced by PCP. More specifically, CLZ markedly attenuated the increase in pyramidal cell firing induced by PCP in the mPFC and reverse the loss in cortical synchrony (Kargieman et al., 2007). Interestingly, CLZ alone did not alter *c-fos* expression in GABAergic neurons yet increased it in animals treated with PCP, suggesting an state-dependent action. This effect occurred in deeper cortical layers, perhaps in large parvalbumin-positive GABAergic interneurons, which are densely expressed in layer V (Grobin et al., 2003) and have been implicated in the pathophysiology of schizophrenia (Lewis et al., 2005). The increased activity of GABAergic cells induced by CLZ + PCP may be related to the normalized pyramidal discharge through enhanced local inhibitory inputs.

In summary, the present study shows a prominent increase of the activity of thalamocortical circuits by PCP, as assessed by *c-fos* expression, that likely accounts for its schizomimetic action. This view is further supported by the antagonism exerted by the atypical antipsychotic CLZ. However, additional work is necessary to clarify the primary site(s) of blockade of NMDA receptors.

Acknowledgements

Work supported by grant SAF 2004-05525. Support from the REMTAP network (IDIBAPS-ISCIII RETIC C03/06) and Generalitat de Catalunya (2005-SGR00758) is also acknowledged. We also thank Judith Ballart for skilful technical assistance.

References

Adams B, Moghaddam B (1998) Corticolimbic dopamine neurotransmission is temporally dissociated from the cognitive and locomotor effects of phencyclidine. J Neurosci 18: 5545-5554.

Adams BW, Moghaddam B (2001) Effect of clozapine, haloperidol, or M100907 on phencyclidine-activated glutamate efflux in the prefrontal cortex. Biol Psychiatry 50: 750-757.

Aghajanian GK, Marek GJ (2000) Serotonin model of schizophrenia: emerging role of glutamate mechanisms. Brain Res Brain Res Rev 31: 302-312.

Amargos-Bosch M, Lopez-Gil X, Artigas F, Adell A (2006) Clozapine and olanzapine, but not haloperidol, suppress serotonin efflux in the medial prefrontal cortex elicited by phencyclidine and ketamine. International Journal of Neuropsychopharmacology 9: 565-573.

Berendse HW, Groenewegen HJ (1991) Restricted cortical termination fields of the midline and intralaminar thalamic nuclei in the rat. Neuroscience 42: 73-102.

Breier A, Malhotra AK, Pinals DA, Weisenfeld NI, Pickar D (1997) Association of ketamine-induced psychosis with focal activation of the prefrontal cortex in healthy volunteers. American Journal of Psychiatry 154: 805-811.

Bubser M, De Brabander JM, Timmerman W, Feenstra MGP, Erdtsieck-Ernste EBHW, Rinkens A, Van Uum JFM, Westerink BHC (1998) Disinhibition of the mediodorsal thalamus induces Fos-like immunoreactivity in both pyramidal and GABA-containing neurons in the medial prefrontal cortex of rats, but does not affect prefrontal extracellular GABA levels. Synapse 30: 156-165.

Dragunow M, Faull R (1989) The use of c-fos as a metabolic marker in neuronal pathway tracing. J Neurosci Methods 29: 261-265.

Fuster JM (1997) The Prefrontal Cortex. Anatomy, Physiology, and Neuropsychology of the Frontal Lobe. Philadelphia-New York: Lipincott-Raven.

Gabbott PL, Warner TA, Jays PR, Salway P, Busby SJ (2005) Prefrontal cortex in the rat: projections to subcortical autonomic, motor, and limbic centers. J Comp Neurol 492: 145-177.

Geyer MA, Krebs-Thomson K, Braff DL, Swerdlow NR (2001) Pharmacological studies of prepulse inhibition models of sensorimotor gating deficits in schizophrenia: a decade in review. Psychopharmacology 156: 117-154.

Grobin AC, Heenan EJ, Lieberman JA, Morrow AL (2003) Perinatal neurosteroid levels influence GABAergic interneuron localization in adult rat prefrontal cortex. J Neurosci 23: 1832-1839.

Groenewegen HJ, Uylings HB (2000) The prefrontal cortex and the integration of sensory, limbic and autonomic information. Prog Brain Res 126: 3-28.

Jackson ME, Homayoun H, Moghaddam B (2004) NMDA receptor hypofunction produces concomitant firing rate potentiation and burst activity reduction in the prefrontal cortex. Proceedings of the National Academy of Sciences of the United States of America 101: 8467-8472.

Javitt DC, Zukin SR (1991) Recent advances in the phencyclidine model of schizophrenia. Am J Psychiatry 148: 1301-1308.

Jodo E, Suzuki Y, Katayama T, Hoshino KY, Takeuchi S, Niwa SI, Kayama Y (2005) Activation of medial prefrontal cortex by phencyclidine is mediated via a hippocampo-prefrontal pathway. Cerebral Cortex 15: 663-669.

Kargieman L, Santana N, Mengod G, Celada P, Artigas F (2007) Antipsychotic drugs reverse the disruption in prefrontal cortex function produced by NMDA receptor blockade with phencyclidine. Proceedings of the National Academy of Sciences of the United States of America .In Press.

Konkle AT, Bielajew C (2004) Tracing the neuroanatomical profiles of reward pathways with markers of neuronal activation. Rev Neurosci 15: 383-414.

Krystal JH, D'Souza DC, Mathalon D, Perry E, Belger A, Hoffman R (2003) NMDA receptor antagonist effects, cortical glutamatergic function, and schizophrenia: toward a paradigm shift in medication development. Psychopharmacology (Berl) 169: 215-233.

Krystal JH, Karper LP, Seibyl JP, Freeman GK, Delaney R, Bremner JD, Heninger GR, Bowers MB, Charney DS (1994) Subanesthetic Effects of the Noncompetitive Nmda Antagonist, Ketamine, in Humans - Psychotomimetic, Perceptual, Cognitive, and Neuroendocrine Responses. Archives of General Psychiatry 51: 199-214.

Kuroda M, Yokofujita J, Murakami K (1998) An ultrastructural study of the neural circuit between the prefrontal cortex and the mediodorsal nucleus of the thalamus. Prog Neurobiol 54: 417-458.

Landry M, Holmberg K, Zhang X, Hokfelt T (2000) Effect of axotomy on expression of NPY, galanin, and NPY Y1 and Y2 receptors in dorsal root ganglia and the superior cervical ganglion studied with double-labeling in situ hybridization and immunohistochemistry. Exp Neurol 162: 361-384.

Lewis DA, Hashimoto T, Volk DW (2005) Cortical inhibitory neurons and schizophrenia. Nat Rev Neurosci 6: 312-324.

Lopez-Gil X, Babot Z, Amargos-Bosch M, Sunol C, Artigas F, Adell A (2007) Clozapine and Haloperidol Differently Suppress the MK-801-Increased Glutamatergic and Serotonergic Transmission in the Medial Prefrontal Cortex of the Rat. Neuropsychopharmacology.

Lorrain DS, Baccei CS, Bristow LJ, Anderson JJ, Varney MA (2003) Effects of ketamine and N-methyl-D-aspartate on glutamate and dopamine release in the rat prefrontal cortex: Modulation by a group II selective metabotropic glutamate receptor agonist LY379268. Neuroscience 117: 697-706.

Malhotra AK, Adler CM, Kennison SD, Elman I, Pickar D, Breier A (1997) Clozapine blunts N-methyl-D-aspartate antagonist-induced psychosis: A study with ketamine. Biological Psychiatry 42: 664-668.

Martin P, Carlsson ML, Hjorth S (1998) Systemic PCP treatment elevates brain extracellular 5-HT: a

microdialysis study in awake rats. Neuroreport 9: 2985-2988.

Mathe JM, Nomikos GG, Blakeman KH, Svensson TH (1999) Differential actions of dizocilpine (MK-801) on the mesolimbic and mesocortical dopamine systems: role of neuronal activity. Neuropharmacology 38: 121-128.

McKenna JT, Vertes RP (2004) Afferent projections to nucleus reuniens of the thalamus. J Comp Neurol 480: 115-142.

Millan MJ, Brocco M, Gobert A, Joly F, Bervoets K, Rivet J, Newman-Tancredi A, Audinot V, Maurel S (1999) Contrasting mechanisms of action and sensitivity to antipsychotics of phencyclidine versus amphetamine: importance of nucleus accumbens 5-HT2A sites for PCP-induced locomotion in the rat. Eur J Neurosci 11: 4419-4432.

Miller EK, Cohen JD (2001) An integrative theory of prefrontal cortex function. Annu Rev Neurosci 24: 167-202.

Moghaddam B, Adams B, Verma A, Daly D (1997) Activation of glutamatergic neurotransmission by ketamine: A novel step in the pathway from NMDA receptor blockade to dopaminergic and cognitive disruptions associated with the prefrontal cortex. Journal of Neuroscience 17: 2921-2927.

Moghaddam B, Adams BW (1998) Reversal of phencyclidine effects by a group II metabotropic glutamate receptor agonist in rats. Science 281: 1349-1352.

Nelson CL, Burk JA, Bruno JP, Sarter M (2002) Effects of acute and repeated systemic administration of ketamine on prefrontal acetylcholine release and sustained attention performance in rats. Psychopharmacology 161: 168-179.

Newcomer JW, Farber NB, Jevtovic-Todorovic V, Selke G, Melson AK, Hershey T, Craft S, Olney JW (1999) Ketamine-induced NMDA receptor hypofunction as a model of memory impairment and psychosis. Neuropsychopharmacology 20: 106-118.

Panagis G, Nomikos GG, Miliaressis E, Chergui K, Kastellakis A, Svensson TH, Spyraki C (1997) Ventral pallidum self-stimulation induces stimulus dependent increase in c-fos expression in reward-related brain regions. Neuroscience 77: 175-186.

Paxinos G, Watson C (2005) The Rat Brain in stereotaxic coordinates. San Diego: Elsevier Academic Press.

Puig MV, Celada P, Diaz-Mataix L, Artigas F (2003) In vivo modulation of the activity of pyramidal neurons in the rat medial prefrontal cortex by 5-HT2A receptors: Relationship to thalamocortical afferents. Cerebral Cortex 13: 870-882.

Santana N, Bortolozzi A, Serrats J, Mengod G, Artigas F (2004) Expression of serotonin1A and serotonin2A receptors in pyramidal and GABAergic neurons of the rat prefrontal cortex. Cereb Cortex 14: 1100-1109.

Schmidt CJ, Fadayel GM (1996) Regional effects of MK-801 on dopamine release: effects of competitive NMDA or 5-HT2A receptor blockade. J Pharmacol Exp Ther 277: 1541-1549.

Suzuki Y, Jodo E, Takeuchi S, Niwa S, Kayama Y (2002) Acute administration of phencyclidine induces tonic activation of medial prefrontal cortex neurons in freely moving rats. Neuroscience 114: 769-779.

Tomiyama M, Palacios JM, Cortes R, Vilaro MT, Mengod G (1997) Distribution of AMPA receptor subunit mRNAs in the human basal ganglia: an in situ hybridization study. Mol Brain Res 46: 281-289.

Vaisanen J, Ihalainen J, Tanila H, Castren E (2004) Effects of NMDA-receptor antagonist treatment on c-fos expression in rat brain areas implicated in schizophrenia. Cell Mol Neurobiol 24: 769-780.

Vertes RP (2004) Differential projections of the infralimbic and prelimbic cortex in the rat. Synapse 51: 32-58.

Vertes RP, Hoover WB, Do Valle AC, Sherman A, Rodriguez JJ (2006) Efferent projections of reuniens and rhomboid nuclei of the thalamus in the rat. Journal of Comparative Neurology 499: 768-796.